<u>AUTOMOBILE FRICTION MATERIALS.</u>

A test instrument and technique for determining dynamic

mechanical properties in relation to brake squeal

by

Roger David Rushton

Submitted for the degree of Ph.D. September 1973.

ii
SUMMARY

This study is primarily concerned with the problem of brake squeal in disc brakes, using moulded organic disc pads. Moulded organic friction materials are complex composites and due to this complexity it was thought that they are unlikely to be of uniform composition. Variation in composition would under certain conditions of the braking system, cause slight changes in its vibrational characteristics thus causing resonance in the high audio-frequency range.

Dynamic mechanical properties appear the most likely parameters to be related to a given composition's tendency to promote squeal. Since it was necessary to test under service conditions a review was made of all the available commercial test instruments but as none were suitable it was necessary to design and develop a new instrument. The final instrument design, based on longitudinal resonance, enabled modulus and damping to be determined over a wide range of temperatures and frequencies. This apparatus has commercial value since it is not restricted to friction material testing.

Both used and unused pads were tested and although the cause of brake squeal was not definitely established, the results enabled formulation of a tentative theory of the possible conditions for brake squeal. The presence of a temperature of minimum damping was indicated which may be of use to braking design engineers.

Some auxillary testing was also performed to establish the effect of water, oil and brake fluid and also to determine the effect of the various components of friction materials.

ACKNOWLEDGMENTS

CONTENTS

INDEX TO FIGURES

INDEX TO TABLES

Definition of Symbols

Where more than one definition exists the definitions are given in order of priority.

A   The static displacement. $A = F_0/k_1'$

Amplitude of vibration during continuous wave propagation.

A number dependent on the setting on the strain divider on the Rheovibron — found from tables.

B   Thickness of the test specimen.

The ratio of working and natural angular velocities $B = \omega/\omega_n$

$B_1 = \omega_1/\omega_n$

$B_2 = \omega_2/\omega_n$

C   The r.m.s. value of the couple on the E.R.D.E. Dynamic Modulus Analyser.

D   Width of the test specimen.

E   Young's Modulus (the ratio of stress to strain) $E = \sigma/\gamma$

E^* Complex Young's Modulus $E^* = E' = iE''$

$|E^*|$ Absolute Young's Modulus $|E^*| = \sigma_o/\gamma_o = \sqrt{(E')^2 + (E'')^2}$

E' Elastic (real) component of complex Young's Modulus $E' = |E^*| \cos\delta$

E'' Viscous (imaginary) component of complex Young's Modulus $E'' = |E^*| \sin\delta$

F   Force.

F_0 Amplitude of sinusoidal force.

F_0^* Complex amplitude of sinusoidal force.

F_0' Real component of amplitude of sinusoidal force.

F_0'' Imaginary component of amplitude of sinusoidal force.

F $= \dot{X} k_1'' \tau$

F $= k_1' X$

G   Shear modulus $G = \tau/\varepsilon$

G^* Complex shear modulus $G^* = G' + iG''$

$|G^*|$ Absolute shear modulus $G^* = \tau_o/\varepsilon_c = \sqrt{(G')^2 + (G'')^2}$

G' Elastic (real) component of complex shear modulus.

G'' Viscous (imaginary) component of complex shear modulus.

I Moment of inertia.

K Bulk Modulus.

The value of the dynamic force on the Rheovibron.

Constant in the torsion pendulum theory.

K_n A constant dependent on the mode number and the method of clamping

on the B&K Complex Modulus Apparatus.

L Length or effective length of test specimen.

Longitudinal modulus.

$|L*|$ Absolute longitudinal modulus.

L_0 Amplitude of elongation on the Rheovibron.

M Mass of test specimen.

N A number dependent on the setting on the balance meter on the

Rheovibron – found from tables.

R R.m.s. displacement on the E.R.D.E. Dynamic Modulus Analyser.

S Elastic coefficient on the E.R.D.E. Dynamic Modulus Analyser.

S_s Torsional elastic coefficient on the E.R.D.E. Dynamic Modulus

Analyser.

T Temperature.

Period of oscillation $T = 1/f$.

V Voltage.

V_0 Amplitude of sinusoidal voltage.

X Displacement.

X_0 Amplitude of sinusoidal displacement .

Z Viscous component on the E.R.D.E. Dynamic Analyser.

Z_s Torsional viscous component on the E.R.D.E. Dynamic Modulus

Analyser.

a Acceleration

Real component of R on the E.R.D.E. Dynamic Modulus Analyser.

a_{ref} Reference acceleration level.

a_n Amplitude of oscillation on the torsion pendulum.

b   Imaginary component of R on the E.R.D.E. Dynamic Modulus Analyser.

d   Damping capacity (mechanical loss factor, damping factor).

d_s Damping in a specimen $d = \tan \delta$

e   Extension in a specimen $e = X$

f   Frequency.

f_o Frequency at peak acceleration or force

f_n Natural frequency (resonance frequency)

f_1 Lower frequency in the bandwidth method for determining damping.

f_2 Upper frequency in the bandwidth method for determining damping.

Δf $= f_2 - f_1$

i $= \sqrt{-1}$

k   Spring constant (force to produce unit extension).

    Error constant in the Rheovibron.

k_s Spring constant of a specimen or model.

$|k_s^*|$ Complex spring constant of a specimen or model.

k_s^* Absolute spring constant of a specimen or model.

k_s' Real component of the complex spring constant of a specimen or model.

k_s'' Imaginary component of the complex spring constant of a specimen or model.

k_m' Spring constant of any spring in a model.

k_m'' Spring constant of any dashpot in a model (if the fluid in the dashpot is Newtonian $k_m'' = \mu_m \omega$

m   Unit of mass of a material.

n   Any number.

    Calibration factor in the Rheovibron.

t   Time.

u   Vibration during continuous wave propagation.

v   Velocity.

v_e Extensional wave velocity of sound in a material $v_e = \sqrt{\dfrac{E^*}{\rho}}$

v_s Shear wave velocity of sound in a material $v_s = \sqrt{\dfrac{G^*}{\rho}}$

v_l Longitudinal wave velocity of sound in a material $v_l = \sqrt{\dfrac{L^*}{\rho}}$

x Distance between vibration source and pick-up during continuous wave propagation.

α Exponential attenuation coefficient during continuous wave propagation

Shape factor in torsion pendulum theory.

γ Normal strain. $= e/L$

γ_o Amplitude of sinusoidal normal strain.

δ Phase lag between stress and strain or force and displacement.

$\triangle$ Logarithmic decrement in torsion pendulum theory.

ϵ Shear strain.

θ Angle of rotation.

Phase difference between vibration source and pick-up during continuous wave propagation.

λ Wavelength.

κ The ratio of phase angle to distance between vibration source and pick-up during continuous wave propagation $= \theta/x$.

μ_m Viscosity of a dashpot.

γ Poisson's ratio.

ρ Specific density of specimen material.

σ Normal stress $= F/BD$.

σ' Component of stress in phase with strain.

σ'' Component of stress 90° out of phase with strain.

σ_o Amplitude of sinusoidal stress.

τ Shear stress.

Relaxation time $\tau = \mu_1/k_1'$

ψ A small frequency difference.

ω Angular velocity.

ω_n Natural angular velocity (resonance angular velocity). $= 2\pi f$.

ω_1 Lower angular velocity in bandwidth method.

ω_2 Upper angular velocity in bandwidth method.

CHAPTER 1

INTRODUCTION

1.1 General Introduction

This thesis is the report of an attempt to correlate the dynamic mechanical properties of moulded organic disc brake pad materials with their tendency to squeal in service.

Brake squeal may be defined as an unpleasant high audio-frequency sound emitted by the braking system during operation under certain, as yet, undefinable conditions. It is thought probable that under certain conditions, irregularities in the composition of individual pad materials could cause slight changes in their vibrational characteristics, thus causing the rotor to resonate in the high audio-frequency range. There is also considerable evidence from the braking system manufacturers that certain friction material compositions show a greater tendency to promote squeal than others. Brake squeal, in common with most other noise, is unwanted sound which can have both physiological and psychological effects on the community and hence may be regarded as a form of environmental pollution. It is now likely that legislation on brake squeal will be brought out in the near future in America which will be operative on the export trade from Britain.

Previous work on the elimination of brake squeal over the past fifty years has been mainly concerned with modifying the mechanical system but although this undoubtedly has some influence on the tendency of squeal, braking system engineers are still a long way from solving the problem and have found little about the basic reasons for it.

Any physical property of the pad material which would indicate its tendency to promote squeal, could be monitored at the development stage in order to design out brake squeal and be of obvious use to a specialised industry.

The dynamic mechanical properties, modulus and mechanical loss factor (damping factor), appeared the most suitable parameters to study as they can be evaluated as a function of composition and uniformity. There are several techniques available for studying these parameters over a wide range of frequencies and temperatures. As no recorded information about this aspect of friction material technology seemed available, dynamic mechanical test methods were carefully reviewed in order to select one which would

i) be related to squeal in terms of frequency and mode
of testing.

ii) take suitable specimens in terms of size and rigidity.

This review appears later but it will suffice to say now that no commercial technique reviewed was suitable and thus a dynamic mechanical test instrument had to be developed.

This instrument was used to test a number of samples of commercial disc pad materials. A general idea of the dynamic mechanical behaviour of these materials was determined by examining a large number of unused pads and an attempt to determine properties relevant to brake squeal was made by examining a number of pads from cars which suffered from brake squeal and a few from cars with no history of brake squeal.

Testing was also performed on some of the component materials of friction materials so as to attempt to determine which of the components had noticeable effects on the dynamic mechanical behaviour of friction materials. The effect of environmental agents, such as engine oil, water and brake fluid, on the dynamic mechanical properties of the friction materials was also determined.

1.2 Literature Review

1.2.1 Braking Systems

1.2.1.1 Definition

The braking of road vehicles has been reviewed in detail by Newcombe and Spurr (1) hence this introduction needs only to summarise the situation in general terms.

The braking system in any vehicle is a device for converting the kinetic energy of the moving vehicle to heat (or occasionally some other form of energy) hence slowing the vehicle or bringing it to rest. In road vehicles, cars, trucks, etc., this is achieved by an assembly consisting of a rotor (disc or drum) and stator (caliper and pad or brake shoe and lining) which are brought into contact by high pressure derived indirectly from the brake pedal operated by the driver. Usually the assembly is at the road wheel and sometimes additionally in the transmission system. As the driver varies the pressure in response to some road hazard the rate of energy conversion and hence the temperature of the friction surface varies. The heat is dissipated by conduction, convection and radiation from the pad or shoe and disc or drum at a fairly slow rate, which increases as the differential between the hot surface and the ambient atmosphere rises, hence the temperature reached in the braking system depends on the number and duration of brake applications.

1.2.1.2 Design Demands

The brake system must withstand frequent exposure to very high temperatures. It has been found (2), (3) that a car descending an alpine slope can give resultant lining temperature of over $700^{\circ}C$ in the lining surface, while aircraft brakes may reach $1500^{\circ}C$. The life of the friction surfaces is related in a complicated way to the temperature reached.

Ergonomics also makes some demands on the braking system. In order for the deceleration on braking to be tolerable, it must be reasonably even and progressive, i.e. related directly to pedal pressure. Mechanical arrangements must be such that the pedal pressure for the maximum possible deceleration must be within the capability of any likely driver.

In most countries, there are legal requirements for a second brake system in addition to the main or primary one. This is often operated by a simple and purely mechanical linkage regardless of the nature of the primary system, and functions additionally as a parking brake. On heavier vehicles the primary system is often operated by servo systems which can be vacuum operated, mechanically operated or for heavy duty the pressure may be applied by compressed air.

Finally, the braking system is required to be free from any vibrations and noise especially the high pitched squeal which tends to arise with some materials or under certain conditions.

1.2.1.3 Drum and Disc Brakes

Originally, all vehicles used drum brakes, but now the trend is to disc brakes although drum brakes are still in considerable use. The main problems concerning drum brakes are as follows (4):-

    i) Distortion of the drum.

    ii) Expansion of the drum.

    iii) Poor heat dissipation.

    iv) Size of drum for high performance cars.

    v) Poor braking stability.

Disc brakes alleviate all these problems but introduce three new ones:

    i) The disc is exposed to water, grit, etc.

ii) Hand brakes present a design problem (which is one of the reasons why disc brakes are often only fitted to the front wheels).

iii) Differential wear occurs in a radial direction.

Disc brakes also have the advantage that they can easily be designed to be self adjusting.

Reference (4) cites six variations on the disc brake:

i) Hydraulic cylinders on either side of the disc.

ii) One cylinder with a floating caliper.

iii) Large single cylinder.

iv) Small multiple ones.

v) Circular linings.

vi) Segmental linings.

1.2.2 Organic Friction Materials

1.2.2.1 Definition and Function

The automotive brake converts the kinetic energy of a moving vehicle to heat, stores the heat temporarily, and eventually dissipates it to the atmosphere. The sliding friction couple in the brake consists of a cast iron rotor (drum or disc) and a stator on which is mounted a friction material consisting of asbestos fibre, an organic resin binder, fillers and property modifiers. Sintered metal linings are becoming popular and on aircraft ceramic based materials are in use but this review is restricted to organic materials.

At high energy absorption rates heat is generated much faster than it can be dissipated, by convection and conduction, so that the temperature at the sliding interface reaches a point where chemical reactions occur rapidly. Thus the chemical nature of the surface is continually changing (5). First, the organic components on the interface begin to convert to volatiles, tar or carbon which is eventually oxidised to carbon dioxide. Secondly, the asbestos wears away more rapidly due to the reduced binder strength and at higher temperatures degrades from its fibrous form to an olivine powder

with little or no reinforcing value. At very high temperatures the friction
material will decompose, oxidise or melt and as a consequence the wear rate
increases and the coefficient of friction may decrease causing fade. In
general fade may be ascribed to the formation of a gaseous, liquid or low
friction solid phase at the interface or to some combination of these
phenomena (6), (7), It is thus important to be able to measure and calculate
the temperatures produced in the friction assembly at the wheel. Considerable
work in the field has been done by Newcombe (1), (8), (9), (10).

1.2.2.2 Required Characteristics (2), (11),(12)

For a moulded organic friction material to be acceptable as an
automotive brake lining the following points must be satisfied:

 i) The coefficient of friction should remain constant under all
  operating conditions. There should be no'early morning
  sharpness'and no severe decrease in friction due to wet
  conditions.

 ii) Wear resistance should be high. This is an economic
  consideration but unfortunately a low wear rate friction
  material gives rise to adverse properties so a compromise
  has to be reached. In general at normal low temperatures
  the wear rate should be minimal, increasing moderately at
  elevated temperatures but returning to the original low wear
  rate when temperatures return to normal. Four possible wear
  mechanisms exist at the sliding interface (11):

  a) Adhesion of the two materials followed by cohesive
   failure of one material as the two slide past each other.

  b) Ploughing or gouging of one material by a fragment of
   another (harder) material.

    c) Thermal or mechanical fatigue or melting which permit

       pieces to become detached from the surface of a solid

       material.

    d) Oxidation and pyrolysis leading to gas formation.

       This mechanism is thought to be the main cause of wear

       (see section 1.2.2.1).

 iii) Mating surface properties are important. The rotor

    should be free from:-

    a) Scoring as this will in turn increase wear of the

       friction material.

    b) Polishing as this will reduce the coefficient of friction.

    c) General wear and abrasion.

    d) Heat spotting as this will promote fade.

    i.e. corrosive or abrasive ingredients should be minimal.

  iv) Thermal swell must be low.

   v) There should be no tendency to produce brake noise.

  vi) There should be sufficient mechanical strength to prevent:-

    a) Cracking.

    b) Shearing from the back plate (or shoe).

 vii) Compressibility should be minimal to reduce ineffective

    pedal movement.

viii) The friction material should be cheap to produce.

The above points are common to both disc and drum brakes. In addition

disc brakes, which lack self-servo help, require high friction coefficients

and high temperature strength. The higher 'peak' temperatures at which disc

brakes operate require, in addition, maximum fade resistance and recovery.

1.2.2.3 Raw Materials

The basis of most organic friction materials is asbestos fibre bound together by a thermosetting phenolic resin with certain fillers and property modifiers as additives.

1.2.2.3.1 Asbestos

This material is almost universally used as the foundation of organic friction materials. The most usual form of asbestos used in friction materials is chrysotile, the principal member of the serpentine group of minerals with the approximate compositional formula, (13)

$$Mg_3 (Si_2 O_5)(OH)_4 \quad or \quad 3MgO.2SiO_2.2H_2O$$
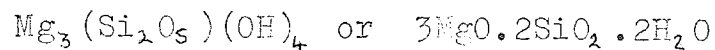
Structurally it is a pseudo hexagonal network of SiO_4 tetrahedra in which three of the apices of each group are linked together in cylindrical lattices involving closed concentric cylinders, spirals and helices on the fourth apex linked to a brucite layer, $Mg(OH)_2$, (See fig.1.)

Key

H Hydrogen
O Oxygen
Magnesium
Silicon
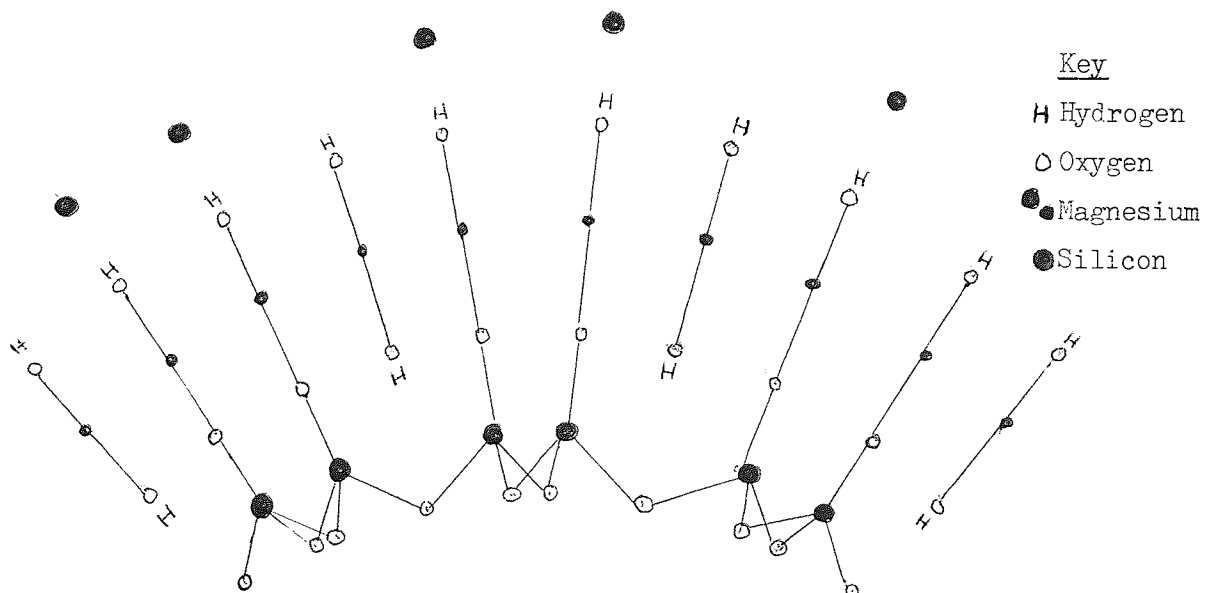
Fig. 1   Schematic structure of chrysotile asbestos (13)

Sheets are continuous in direction of curvature and normal to plane of section as is the fibre axis.

Thermal decomposition of chrysotile asbestos has been established to involve loss of water and formation of forsterite $Mg_2SiO_4(2MgO, SiO_2)$, talc $Mg_3Si_4O_{10}(OH)_2$ $(4SiO_2.3MgO.H_2O)$, enstatite $MgSiO_3(MgOSiO_2)$ and quartz SiO_2 . In the presence of iron (from the rotor) olivine $(Mg,Fe)SiO_4$ and Fayalite Fe_2SiO_4 which are isomorphous with forsterite are also formed (5,13,14,15). Thermal decomposition of asbestos has also been studied by differential thermal analysis (D.T.A.) and thermogravimetric analysis (T.G.A.) (13,16).

The properties of asbestos which make it important as a base for friction materials are as follows:- (12)

    i) It is non combustible.

    ii) It has good thermal stability.

    iii) It has a relatively high coefficient of friction.

    iv) It is fibrous with high mechanical strength giving it excellent reinforcing properties.

    v) It can be readily:-

      a) Moulded.

      b) Corded.

      c) Braided.

      d) Woven.

    vi) Chrysotile asbestos is:-

      a) Cheap.

      b) Abundant.

      c) Does not score the rotor.

Chrysotile asbestos is used in a variety of grades from 7D (dust) to 4R (fairly long fibres) either single or multigrade depending on requirements (2,11,17,18).

    i) Long fibre friction materials:-

        a) are expensive.

        b) have high mechanical strength.

        c) have poor flow properties during moulding.

    ii) Short fibre friction materials:-

        a) are cheaper.

        b) have lower mechanical strength.

        c) have better flow properties during moulding.

1.2.2.3.2 Binders

Historically these were thermoplastic bituminous materials (15,18) e.g. asphalts, pitches and natural resins but with the need for greater thermal stability thermosetting resins are now used. The binders in common use are (11,15,17,18) :-

    i) Phenolic resins.   )
)
    ii) Cresylic resins.   )   formaldehyde or
)   furfural based
    iii) Oil modified phenolic resins.   )

    iv) Copolymers of the above with synthetic rubbers:-

        a) Butadiene/styrene.

        b) Butadiene/acrylonitrile.

Depending on the final manufacturing process involved, the binders are used as powders or as liquids and as such, different physical properties become important (11):-

i) For liquid resins:-

    a) Viscosity - ability to impregnate fibre.

    b) Process time.   )

) solvent evaporation

    c) Temperature requirements.   )

    d) Solids content - uniformity.

    e) Green strength - bonding strength in the

       semi-processed state.

ii) For powdered resins:-

    a) Particle size - coverage, uniform, dispersion and

       part strength.

    b) Flow properties - dispersion and processing.

    c) Cure rate properties.

The chemistry of the resin system is important as this can influence the overall properties of the friction material. Phenolic resins are low polymers formed by polymerising aromatic alcohols with aliphatic aldehydes using a catalyst.

Briefly, the formation of phenol-formaldehyde resins, which are probably the most common resins used in organic friction materials, as they are the cheapest, are as follows (19):-

1.2.2.3.2.1 Novolaks

Phenol and formaldehyde in the approximate ratio 1:0.8 are reacted together under acidic conditions

i) First stage-formation of o- and p-methylol phenols
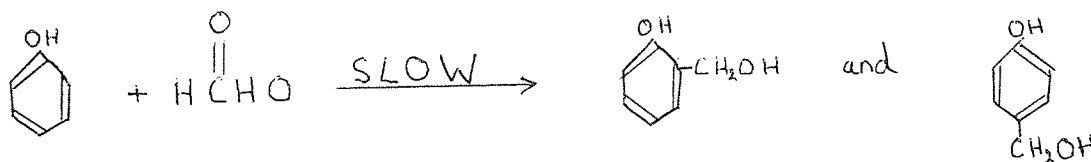
o- and p-methylol phenols

ii) Second stage-condensation with phenol
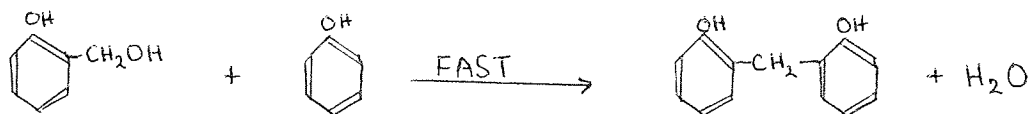
dihydroxydiphenyl methane (d.p.m.)

The three possible isomers occur in proportions dependent on the pH
of the medium. These are equivalent to o-, m- and p- and under usual
conditions m- and p- predominate. These materials react slowly with
further formaldehyde to form their own methylol derivatives which in turn
rapidly react with further phenol to produce higher polynuclear phenols.
Because of the excess of phenol this reaction is terminated when there are
3-6 benzene rings in the novolak unit. Variation of the p-f ratio (20,21)
cause changes in the chemical and physical properties of the resin and
consequential changes in the friction and wear characteristics of the
friction material (2).

Example:
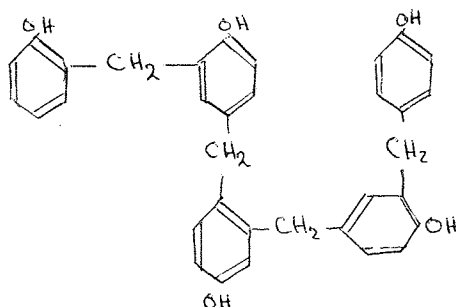
There are no residual methylol groups and there is no cross-linking on heating. If novolaks are mixed with compounds capable of forming methylene bridges, e.g. hexamethylene tetramine or paraformaldehyde they cross-link to give a thermoset network. Modification of the phenol can be used to direct the nature of the final product.

1.2.2.3.2.2 Resoles

Phenol is reacted with an excess of formaldehyde under alkaline conditions. Reaction proceeds rapidly to phenol alcohols but condensation is slow. There is a tendency for low molecular weight polyalcohols to be formed.

e.g.
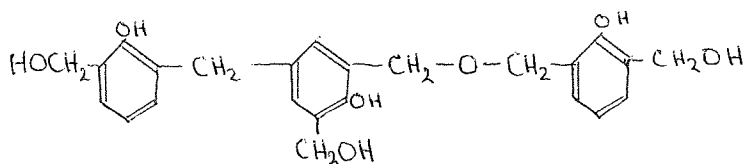
Reactions are more complex and less well defined than for novolaks and as resoles are less used than novolaks they will not be covered in detail here. Heating produces cross-linking via the uncondensed methylol groups or by more complex reactions; no hardener being required.

For both types of resin hardening takes place in three stages:

i) The A stage resin which is low molecular weight, soluble and fusible.

ii) The B stage resin which is rubbery and swollen but relatively insoluble in organic solvents.

iii) The C stage resin which is rigid, hard, insoluble, infusible, cross-linked network.

Below 160°C cross-linking occurs by

a) phenol methylol/phenol methylol condensations to give ether links.
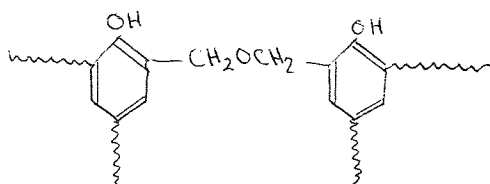
b) phenol methylol/phenol condensations to give methylene links.
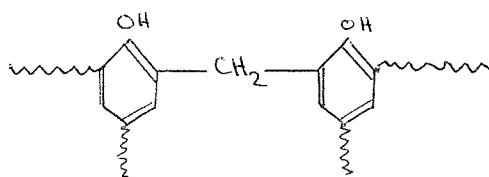
This is probably the normal mode of reaction.

Above 160°C additional cross-linking may occur by condensation of other linkages with phenolic hydroxyl groups to give quinone-methides which are capable of polymerisation and other reactions.

Different resin properties and thus friction material properties can be produced in the following ways:-

    i) Variation of the phenol.

    ii) Variation of the aldehyde e.g. furfural gives better flow properties than formaldehyde.

    iii) Novolak versus resole.

    iv) Variation of the phenol-formaldehyde ratio affects the molecular weight of the A stage resin.

        a) High molecular weight gives poor flow properties and a long cure time.

        b) Low molecular weight gives better flow properties and a shorter cure time.

    v) Increase of the residual volatile content (phenolic bodies) gives a faster cure.

    vi) Variation of the catalyst can influence the direction of linkages and the rate of cure.

1.2.2.3.3 Fillers and Property Modifiers

These two groups are discussed together because many of the materials which are normally used as fillers or extenders in applications other than friction materials, are also property modifiers in friction materials. The property modifiers fall into two groups:

1.2.2.3.3.1 Non abrasive

    i) High friction materials.

        a) Friction dust (larger than 50 mesh). These are cross-linked resinous polymers in granular form often called cardolite dusts. The most frequently used friction dust is derived from cashew nut shell liquid which is a phenol with a long aliphatic side chain capable of being converted into a phenolic resin and cured to a thermoset in the usual way. Friction dusts reduce wear and stabilise the coefficient of friction perhaps by imparting a film on the surface of the lining making it more homogeneous. Unfortunately friction dusts in heavy concentrations cause excessive fade. They also do not appear to be chemically compatible with metal inclusions and this restricts their use.

        b) Other cured resins and polymeric materials which produce similar effects to the above.

        c) Ground rubber (larger than 50 mesh), either natural or synthetic. Care must be taken that solvents used in subsequent processing do not react with the rubber

   ii) Low friction materials (reduce noise and wear)

        In general these are finely powdered carbonaceous materials which act to some extent as lubricants and include:-

        a) Carbon black

        b) Graphite (produces an extremely low wear rate)

        c) Petroleum coke flour

        d) Coal dust

        e) Wood flour

        f) Cork

        g) Waxes

1.2.2.3.3.2 Abrasive

In this section, because of the widely differing accounts given in the literature, the author has attempted to select the most likely properties exhibited by a given additive.

i) Inorganic extenders (reduce friction). These materials are very cheap and abundant and consequently they are used in large proportions but, as they are abrasive, must be very finely powdered to prevent scoring.

a) Alumina   ) e.g. kaolin, kieselghur, colloidal
b) Silicas   ) silica powder, slate powder.

This type of material has a good resistance to fade but tends to promote noise and produce a moderate wear rate.

c) Barytes (barium sulphate)

This is probably the most common extender as it reduces the wear rate considerably. It does, however, promote fade but has almost complete fade recovery.

ii) Metals

Apart from brass and copper, a general rule is that high melting point metals tend to increase wear (probably by producing poor mating surface properties) and low melting point metals tend to decrease wear (probably by acting as high temperature lubricants). Concentrations must be kept low otherwise wear characteristics deteriorate possibly due to mechanical weakening of the working surface. They are usually added to stabilise the coefficient of friction.

a) Zinc - as chips or powder reduces coefficient of friction.

b) Lead - produces wear if used in large quantities.

c) Iron - as filings increases the coefficient of friction.

d) Steel wool - decreases the coefficient of friction.

e) Aluminium.

f) Antimony.

g) Brass.

h) Copper.

Brass and copper are the most common metals found in organic friction materials. Although they have high melting points the wear produced is decreased when other fillers are present indicating that they may act as scavengers to break up undesirable surface films. Their good thermal conductive and capacitative properties tend to improve the dispersion of heat and influence the thermal break down point of the lining.

iii) Metal Oxides

There is little information in the literature on the ratio of the metal oxides used and their function but it is generally thought that they act as reducing agents dispersing any chemical degradation of the binder resin and releasing a metal rich film at the interface relieving the working surface when under severe thermal stress. They tend to raise the friction level.

a) Copper oxide

b) Lead oxide

c) Chrome oxide

Chrome oxide is probably most used, accounting for the green nature of many commercial linings. It gives an increased friction level, an increased mechanical strength, and hence a low wear rate, but lowers fade resistance. Its high thermal stability (it decomposes at $1900^{o}C$) makes it chemically inert.

1.2.2.4 Formulating Techniques

Historically, formulation of friction materials is not a science but more an art closely allied to the trial and error technique employed by chefs in the development of a recipe for a cake mix which will produce a satisfactory cake with the required characteristics. This situation has led to lining materials containing twenty or thirty different ingredients with little understanding of the chemical and physical functions of the various components. Consequently few papers deal with this subject. The attitude of most lining material manufacturers to keep such knowledge as they have as trade secrets has given rise to an expensive formulation technique involving the addition of fresh ingredients to a standard mix without removal of existing ones.

One of the main problems is that most research in tribology, the science of friction, wear and lubrication, has tended to be concentrated on metal-metal friction couples, with a little work on metal-thermoplastic couples but practically none on metal-thermoset couples.

Only recently have publications started to appear on the science of formulation (7,11)

Basically the formulator has five tasks.

1.2.2.4.1 Selection of Required Characteristics

The required characteristics given in section 1.2.2.2, most important for a particular application, must be determined.

Common applications are:-

    i) Railway rolling stock.

    ii) Commercial vehicle.

    iii) Racing car.

    iv) High performance car.

    v) Small private car.

    vi) Industrial machinery.

1.2.2.4.2 Characterisation of Raw Materials

The appropriate properties of the raw materials from section 1.2.2.3 must be determined e.g.:-

    i) Density.

    ii) Compressibility.

    iii) Hardness.

    iv) Degree of polymerisation.

    v) Thermal stability.

    vi) Oxidative stability.

1.2.2.4.3 Selection of Raw Materials

This is based on:

    i) the above chemical and physical properties

    ii) friction and wear data obtained in research type testing of simple friction couples which, as stated previously, are not generally available.

    iii) a set of qualitative formulation rules of which there are basically three relations to general groups of raw materials:

Group (1) promotes

a) low friction

b) low noise

c) low wear rate

d) low fade resistance

These materials are mainly carbonaceous fillers, e.g. graphite. Unfortunately low friction is not desirable for disc brakes.

Group (2) promotes

a) improved fade resistance

b) noise

c) wear

d) poor mating surface properties

These materials are mainly inorganic extenders.

Group (3) promotes

a) high friction

b) noise

c) fade

d) wear

This group is not clearly defined but includes the metal oxides and various other materials.

iv) The most important characteristics required.

1.2.2.4.4 Proportions of Raw Materials

This involves varying the mix and making friction and wear tests on the final lining to determine the optimum composition. The most systematic and economical method of doing this is by the use of a ternary diagram(7). This is a graphical representation of all possible combinations of the three classes of components. Briefly, this is an equilaterial triangular graph with each side of the triangle representing a percentage composition of a particular component. Thus any point within the triangle represents a particular composition. If more than one property modifier is present then for one diagram the ratio of these to each other must remain constant. Wear can be expressed on the diagram by a peg system, wear being proportional to peg height. A typical ternary diagram is shown in fig. 2(7). This technique has enabled some more qualitative rules to be made.

Fig. 2 A typical ternary diagram
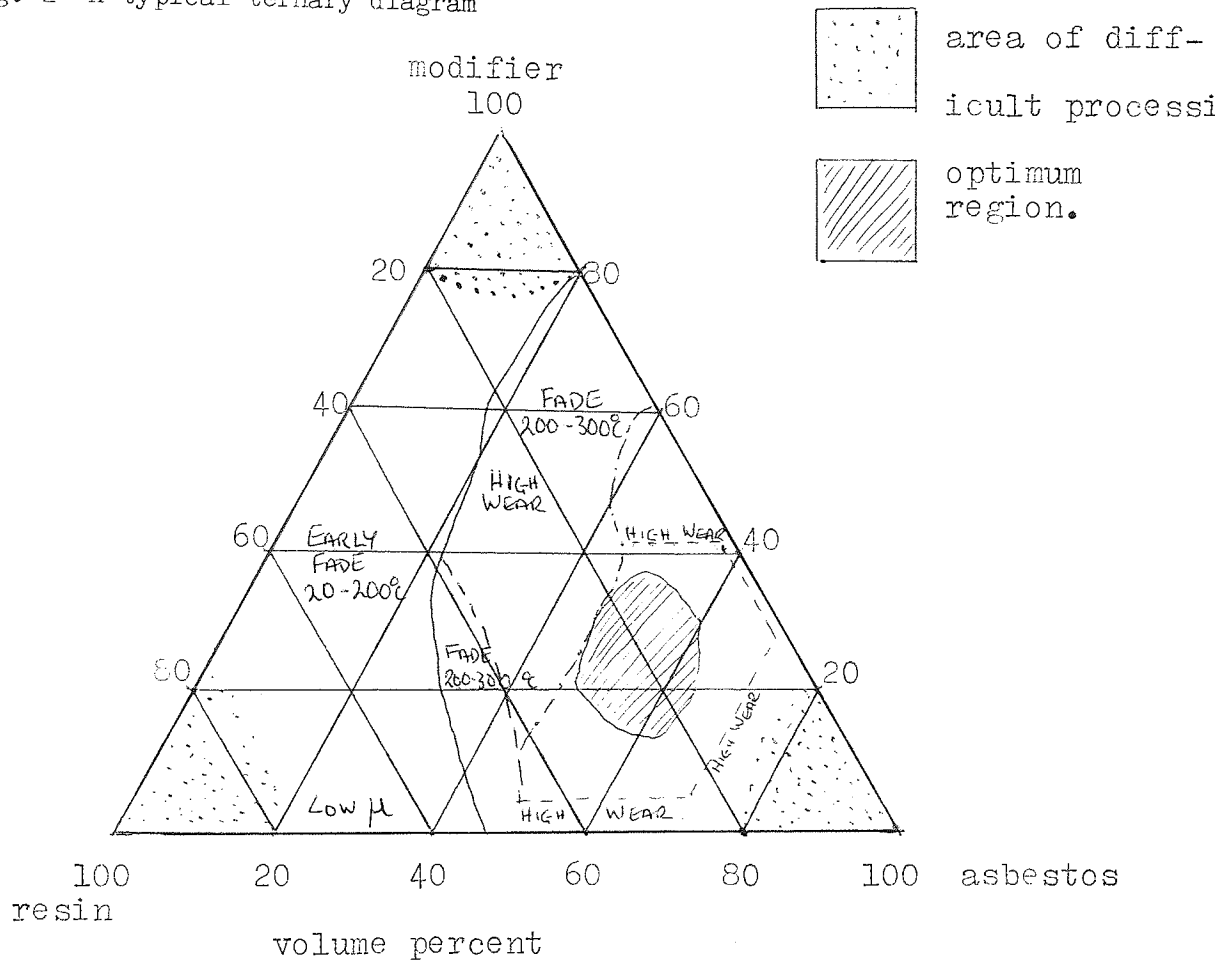
i) Along any constant asbestos-content line, cold friction increases as modifier content increases but hot friction is almost invariable.

ii) Along any constant modifier-content line, cold and hot friction increase as asbestos content increases.

iii) Along any constant resin-content line, cold friction increases only slightly as modifier content increases but hot friction increases as asbestos content increases.

In general, cold friction increases as either modifier or asbestos content increases, but hot friction only increases as a asbestos content increases. Typical formulations showing the changes over the last ten years are shown in table 1.

Table 1   Typical Formulations

Raw Material	Carrol (24) 1962	Ternary Diagram (7) 1966	Private Communication 1972
Asbestos	50 – 70 %	30 – 60 %	50 %
Inorganic Modifier		15 – 40 %	10 – 20 %
Organic Modifier	10 – 30 %	5 – 15 %	5 – 15 %
Resin Binder	10 – 30 %	20 – 30 %	15 – 25 % (drums) 10 – 20 % (discs)

1.2.2.4.5   Selection of the Manufacturing Process

Selection of the manufacturing process to be used depends on the nature, size, shape and degree of aglomeration of the particles in the mix. Some of the processes are described in section 1.2.2.5.

1.2.2.5   Manufacturing Processes

Historically, pre 20th century linings were of leather, wood and iron but around the turn of the century impregnated woven fabrics, mostly of cotton, were introduced as they were more flexible. After the introduction of asbestos as the base material almost every conceivable process for converting it into a woven, wound, moulded, laminated or extruded product seems to have been tried, but the following processes are probably the most important today.

1.2.2.5.1 Resin Impregnation of Woven Asbestos Fabric

Woven linings are made by vacuum impregnation of resin into woven asbestos fabric which is then baked, calendered, die pressed and ground to size. Modifiers cannot be used as these would be filtered out during impregnation but zinc or brass wire or cotton are sometimes woven into the fabric. Expensive long fibre asbestos, poor heat stability and poor property control has led to a gradual decline in the use of woven linings although they do have better flexibility compared to moulded products and are thus still used in low temperature industrial applications.

1.2.2.5.2 Saturation of Millboard

This cheap method can include modifiers but has the disadvantage that only thin linings can be produced and thus apart from production of clutch facings is of little importance. Basically asbestos pulp and modifiers are mixed with size, dried into board and saturated in liquid resin or oil to 100% saturation. After curing the board is cut to size.

1.2.2.5.3 Wet Mix Dough Process

Asbestos, liquid binder and modifiers are mixed with a kerosene type solvent in a z-blade mixer to produce a dough. This can be processed as follows:

    i) By cold extrusion (ram or screw) into strip form which is cut to desired lengths, dried to remove solvent and cured in formers in an oven.

   ii) By shaping in a profile calendering machine and incorporating a wire mesh in the back of the strip. Curing is as above.

iii) By a sheeting process. The mix is fed into the nip
between two rolls, of which one is heated, rotating in
opposite directions. The heated roll picks up a layer of
the mix by evaporation of the solvent and the nip opens
to allow build up of material. At the correct thickness
the sheet is removed from the mill, cut to size, clamped
and cured.

iv) By conventional compression moulding.

1.2.2.5.4 Moulding Processes

The above processes are designed only for production of drum linings.
This review is concerned with disc brakes, which have to be integrally
moulded on to a back plate, and thus moulding, which is applicable to all
types of lining will be described in detail for production of disc pads.
The wet mix process has already been mentioned but preferable is the
dry mix process:

i) The asbestos fibres are opened but by passing through a
hammer mill from which the grinding screen has been removed.

ii) The ingredients are weighed out into a mixer, which has a
tumbling rather than a heating action as this would tend to
reconsolidate the asbestos, and mixed to uniformity.

iii) Using a weighed quantity of mix a cold preform is made to
reduce the volume, ensure uniformity and to reduce the chance
of blistering.

iv) The backing plate is sprayed with a bonding cement, partially
dried and placed in a hot mould which has been lubricated with
a soap-graphite dispersion.

v) The preform is transferred to the hot mould, on top of the
backing plate, and pressure applied.

vi) The mould is periodically 'breathed' to release volatiles
which could cause blistering.

vii) The pad is then post-baked in a ventilated oven to complete the cure.

The moulds used in this process are cheap as they do not need to be of high finish or precision.

1.2.2.6 Finished Product Tests

Many finished product tests are available and most usual are:-

i) Specific gravity - indicates structure and composition (29).

ii) Gogan, Brinell or Rockwell hardness - indicates structure and cure (29).

iii) Loss on ignition - indicates composition, total ash only (29).

iv) Acetone extraction - indicates composition, soluble organics only (29).

v) Cross breaking strength (29).

vi) Shear strength.

vii) Dimensional tests.

viii) Visual inspection for surface defects.

ix) Dynamometer tests:-

a) S.A.E.J.661a.(30). This is based on the Chase dynamometer which is of a constant rubbing nature and is described by Burkman and Highley (31).

b) F.A.S.T. (friction assessment screening test) (32). This is also a constant rubbing machine.

c) Tests made on the Girling test machine (33). This machine is useful because it incorporates a scaled reproduction of the vehicle braking system. Loading is transient, variable, can be programmed and as velocity can be varied the machine is not constant rubbing.

x) Pyrolitic gas chromatography (34,35,36,37).

xi) Infra-red spectroscopy (36).

xii) X-ray radiography (38).

xiii) Optical Resinography (38).

xiv) D.T.A. (38) and T.G.A.

1.2.3 Brake Squeal

1.2.3.1 Introduction

Brake squeal, like any other noise, is unwanted sound and as such can have both physiological and psychological effects on the community. Consequently for several years workers have been trying to establish the nature and cause of squeal and methods of eliminating it. Although this review is concerned with disc brake squeal much of the work on drum brake squeal is still relevant.

There are four main theories of brake squeal:-

i) Slip-stick theory (39.40,41,42,43,44,45). This may account for judder and hum (see below) but is unlikely to cause resonant vibrations.

ii) Sprag-slip theory (46). Here the caliper representation is good but the squeal modes produced are poor.

iii) Geometric coupling theory (47). Here the caliper representation is poor but the squeal modes produced are good.

iv) Single-degree-of-freedom model theory (48). This combines the sprag-slip and geometric coupling theories and demonstrates the importance of non-linear coupling within the combined system.

Theory (iv) is the most recent and the most complete but critical summaries of the other three theories are given by North (49) in his literature survey on brake squeal and by Spurr (50) in his discussion of the occurrence and mechanism of brake squeal.

1.2.3.2 Definition

Brake noise occurs over a wide range of frequencies with frequencies between 3 and 15kHz causing the principal annoyance.

Fosberry and Holubecki (51) classified brake noise into five categories:-

i) Judder (less than 100 Hz)

Very low frequency, non resonant vibrations originating from the wheel and brake assembly acting on the suspension or chassis.

ii) Hum (100-400 Hz)

Resonant sinusoidal vibrations of the brake system on the suspension.

iii) Low frequency squeal (1.3 - 2.6 kHz)

Resonant vibrations probably originating from the back plate.

iv) Drum Squeal (3 - 15 kHz)

High frequency resonant vibrations of the drum.

v) Wire brush (up to 20 kHz)

Very high frequency resonant vibrations of the drum.

In the case of disc brakes, squeal categories (iii) and (iv) merge to give a band of squeal at about 2 - 3 kHz. Disc brake squeal appears to be more predominant than drum brake squeal and the author contends that this is a consequence of the difference in layout of the two systems. If it is assumed that the origin of squeal is at the rotor-lining interface then the disc brake has effectively one and the drum brake two centres of resonant vibration which can either reinforce or interfere with each other. This simple theory accounts for the fact that disc brakes squeal more frequently but with lower intensities. On this reasoning the disc brake should present a less complex vibrating system and the author hopes that by studying disc brake squeal any conclusions will also be applicable to drum brake squeal.

Brake squeal is unique to certain situations and thus it is essential to study the braking system at the wheel as a whole. The author considers that the fundamental problem is one of irregularities in composition, state of cure, moisture content, etc., in individual linings which in particular systems cause slight changes in the vibrational characteristics so that the system resonates in the high audio frequency range. He will try to relate these changes to changes in the dynamic mechanical properties particularly the mechanical damping factor of the friction material.

1.2.3.3 Established Facts on Brake Squeal

The following is a survey of the established facts on squeal.

    i) Squeal is erratic and fugitive and is dependent on a certain condition of temperature, pedal pressure, weather, humidity, state of wear, etc.

    ii) Hard friction materials are more prone to squeal than soft ones.

    iii) Squeal is not directly related to the coefficient of friction but it is found that squeal is more prevalent in materials with a high coefficient of friction (46,52)

    iv) Linings can be graded in their tendency to squeal (49)

    v) Squeal is thought to be due to:

        a) radial vibrations of the rotor (52,53,54,55,56)

        b) torsional vibrations of the lining (57)

        c) bending vibrations of the lining (58)

    vi) Usually there is one main frequency and several harmonics dependent on, but not necessarily the same as, the natural frequency of the rotor (46,54,55)

    vii) The frequency of squeal is independent of rubbing speed (43,52)

viii) Tendency to squeal is related to the manner of contact
(43,46,53,52,59,60) In this context. rotor design
distortion, wear pattern and dust have some relevance.

ix) Squeal is often related to the flexibility in the system
particularly with drum brakes (53,59)

x) During squeal brake torque increases.

1.2.3.4 Approaches to Eliminating the Problem

Several instrumental techniques have been used to study brake squeal
but apart from Gieck's (56) work which involves the use of ultra slow
motion photography most involve a test rig with accelerometers or pickups
placed at strategic points.

In the published work on brake squeal three basic approaches have
been made to eliminate the problem.

i) To remove the source of energy which feeds the vibration.
The source is almost certainly at the interface of the
stator and the rotor.

ii) To keep the frequency out of audible range.

iii) To reduce the amplitude until it is inaudible.

The first two approaches are aimed at designing out brake squeal
and are the main concern of researchers in the field but the third is a
means of removing it when it is already present.

1.2.3.4.1 Cures for Brake Squeal

The following methods for rectifying brake squeal are all examples
of approach (iii) above (39,59,61,62):-

i) By general maintenance of the braking system at the wheel
involving replacement of distorted, worn, faulty or
incorrect components and necessary lubrication and
adjustment of moving parts.

ii) By altering existing components:

    a) Generally stiffening up the mechanical components, i.e. making the system less prone to vibration.

    b) Cutting or chamfering the friction material i.e. altering the manner of contact by influencing the dissipation of wear debris and also the wear pattern.

    c) Replacing the lining with one of a lower coefficient of friction or inserting graphite plugs into the existing lining (this also reduces the coefficient of friction).

    d) Cutting the web of the shoes on drum brakes to make them more flexible so that better contact can be made with the drum.

iii) By fitting external damping devices:

    a) On disc brakes damping shims (63) and springs are commonly used.

    b) On drum brakes damping bands around the circumference of the drum (64) or ring segments against the mouth of the drum (65) are common devices.

It must be stressed that the technique of reducing the amplitude of squeal to an inaudible level is unsatisfactory because only low frequency noise can be successfully damped and eventually the components of the rectified system begin to wear or lose their efficiency and squeal may return.

The technique of designing out squeal is far more satisfactory.

1.2.4 Conclusion

It has been stated that certain friction materials show less tendency to squeal than others and these materials can exist in a very squeal prone braking system without squealing, whereas other materials will squeal in a near perfect system. Thus it is more pertinent to design friction materials with no tendency to squeal than to try to influence a constantly changing mechanical environment.

1.3 Dynamic Mechanical Testing

1.3.1 Definition and Introduction

Materials and structures which are subjected to movement during service conditions do not behave in the same way as when they are static.

In the past materials were tested solely under near static conditions to determine their strength and modulus by such tests as tensile elongation, flexural deformation and torsional deformation. It was often found however, that when these materials were commissioned under dynamic conditions, their behaviour was different from that predicted by the static tests. Thus it became necessary to use such methods as fatigue and dynamic mechanical testing which are both cyclic in nature. Just as fatigue tests will show that a material will fail at a different load to that shown in static tests, dynamic mechanical tests give different moduli to those given by the static tests.

Whereas fatigue testing has long been important in the testing of metals, dynamic mechanical testing has only recently gained importance with polymers although the ideas were first put forward by Alexandrov and Lazurkin in 1939 (66). This is because polymers normally show a considerable degree of viscoelasticity. Viscoelasticity means that materials exhibit elastic behaviour, attributed to bond stretching and bond angle deformation, and viscous behaviour, thought to be due to relative molecular movement involved in uncoiling of chains (which also includes some elastic behaviour) and inter-chain slipping (67). Viscoelastic materials hence exhibit both recoverable elastic deformation and non-recoverable deformation which is related to the mechanical damping in the material. The mechanical energy lost is converted to heat.

A great advantage of dynamic mechanical testing is that it is non-destructive and thus actual service components and even complete structures

may be evaluated using this approach.

1.3.1.1 Basic Dynamic Principles

The mathematical theories regarding the viscoelastic response of a material to dynamic loading are exactly analogous to the theories of dielectric behaviour of material in electrical networks.

Dynamic properties of polymers depend on the movements of segments of molecules when subjected to a stress. If a sinusoidal stress is applied to a material the resultant strain will be sinusoidal but will lag behind the stress (unless the material is purely elastic) in a manner depending on the average time required to move the polymer segments.

Mathematically this can be represented by two techniques.

    i) Using complex notation. This is a more complete method although it is difficult to represent pictorially.

Let the sinusoidal stress and strain be represented respectively by

$$\sigma = \sigma_0 e^{i\omega t}$$

$$\gamma = \gamma_0 e^{i(\omega t - \delta)}$$

where σ is the normal stress.

      σ_0 is the amplitude of normal stress.

      γ is the normal strain.

      γ_0 is the amplitude of normal strain.

      ω is the angular velocity.

      t is time.

      δ is the phase angle between stress and strain.

Dividing stress by strain

$$\frac{\sigma}{\gamma} = \frac{\sigma_0}{\gamma_0} e^{i\delta} = \frac{\sigma_0}{\gamma_0} \cos \delta + i \frac{\sigma_0}{\gamma_0} \sin \delta$$

Let

$$E^* = \frac{\sigma}{\gamma}$$

where E^* is the complex Young's Modulus.

$$E' = \frac{\sigma_o}{\gamma_o} \cos \delta$$

where E' is the elastic (real) component of complex Young's Modulus.

$$E'' = \frac{\sigma_o}{\gamma_o} \sin \delta$$

where E'' is the viscous (imaginary or loss) component of complex

Young's Modulus.

Hence

$$E^* = E' + iE'' \dots\dots\dots\dots\dots \text{eq. 1.3.1.1}$$

From the corresponding Argand Diagram

$$|E^*| = \frac{\sigma_o}{\gamma_o} = \sqrt{(E')^2 + (E'')^2}$$

where $|E^*|$ is the absolute Young's Modulus.

Hence

$$E' = |E^*| \cos \delta$$

$$E'' = |E^*| \sin \delta$$

Dividing E'' by E'

$$\frac{E''}{E'} = \tan \delta = d$$

where d is the mechanical loss factor, damping factor or internal

friction.

Many publications concerning the damping of polymeric materials use the

term '$\tan \delta$' to express the degree of damping in a material but recently

it has become more common to use the more general 'd' since δ is only

actually measured in forced vibration experiments and in other experiments

quantities which are approximately equivalent to $\tan \delta$ are determined.

Equation 1.3.1.1 may now be rewritten as

$$E^* = E'(1 + id)$$

ii)   Using trigonometrical notation. This can be used to
demonstrate the wave relationships vectorially although
mathematically it is incomplete.

Let the sinusoidal stress and strain be represented respectively
by

$$\sigma = \sigma_0 \cos \omega t$$

$$\gamma = \gamma_0 \cos(\omega t - \delta)$$

These may be represented by two vectors length σ_0 and γ_0 moving with
angular velocity ω but separated by a phase angle of δ
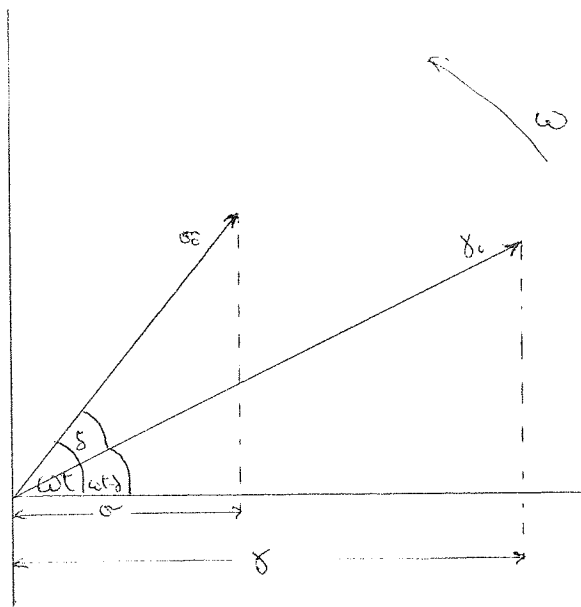
Fig. 3   Vector representation of dynamic stress and strain

The stress vector is resolved into two components, one, σ', in phase with the strain i.e. the elastic component, and the other, σ'', 90° out of phase with the strain i.e. the viscous or loss component.
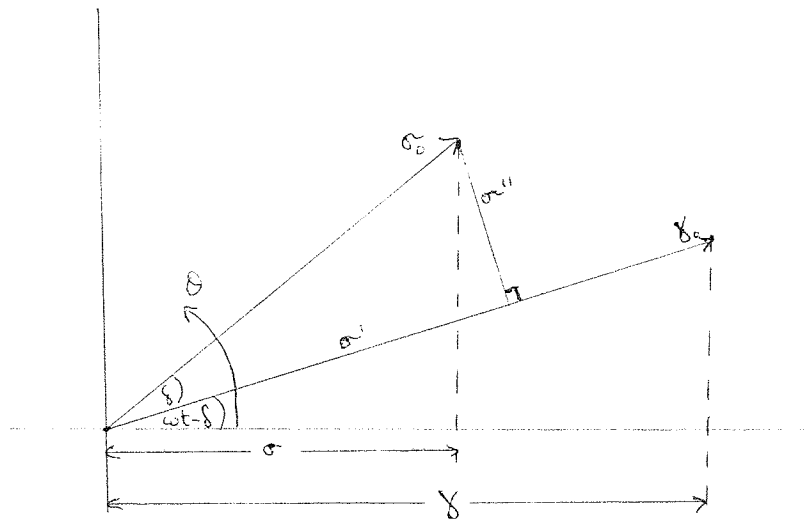
Fig. 4 Vector representation showing the resolution of the stress into two components

From the vector diagram

$$\sigma' = \sigma_0 \cos \delta$$

$$\sigma'' = \sigma_0 \sin \delta$$

Let

$$E' = \frac{\sigma'}{\gamma_0} = |E^*| \cos \delta$$

$$E'' = \frac{\sigma''}{\gamma_0} = |E^*| \sin \delta$$

As before

$$|E^*| = \frac{\sigma_0}{\gamma_0} = \sqrt{(E')^2 + (E'')^2}$$

$$\frac{E''}{E'} = \tan \delta = d$$

If the waveforms of the above equations are produced it can be shown that the loss component of the stress, σ'', is in phase with the rate of change of strain whilst the elastic component, σ', is in phase with the strain itself (see Fig. 5). Hence E' and E", which are based on σ' and σ'' are related to strain and rate of strain respectively.

Classically from static theory the same relationship exists.

Hooke's Law states that

$$\sigma = E\gamma$$

where E is Young's Modulus.

For a Newtonian fluid.

$$\sigma = \eta\dot\gamma$$

where η is material viscosity.

Hence

E' is related to E, a measure of elasticity.

E" is related to η, a measure of viscosity.

The above derivations are applicable to normal type stressing of a material. A completely analogous set of equations exist for shear type stressing of the material giving rise to the dynamic shear moduli G*, |G*| G' and G".

$$G* = G' + iG''$$

$$|G*| = \sqrt{(G')^2 + (G'')^2}$$

$$\frac{G''}{G'} = \tan\delta = d_{shear}$$

Analogous equations also exist for the dynamic longitudinal and bulk moduli L and K.

The dynamic Young's and shear moduli are related by the following equation

$$E = 2G(1 + \nu)$$

39
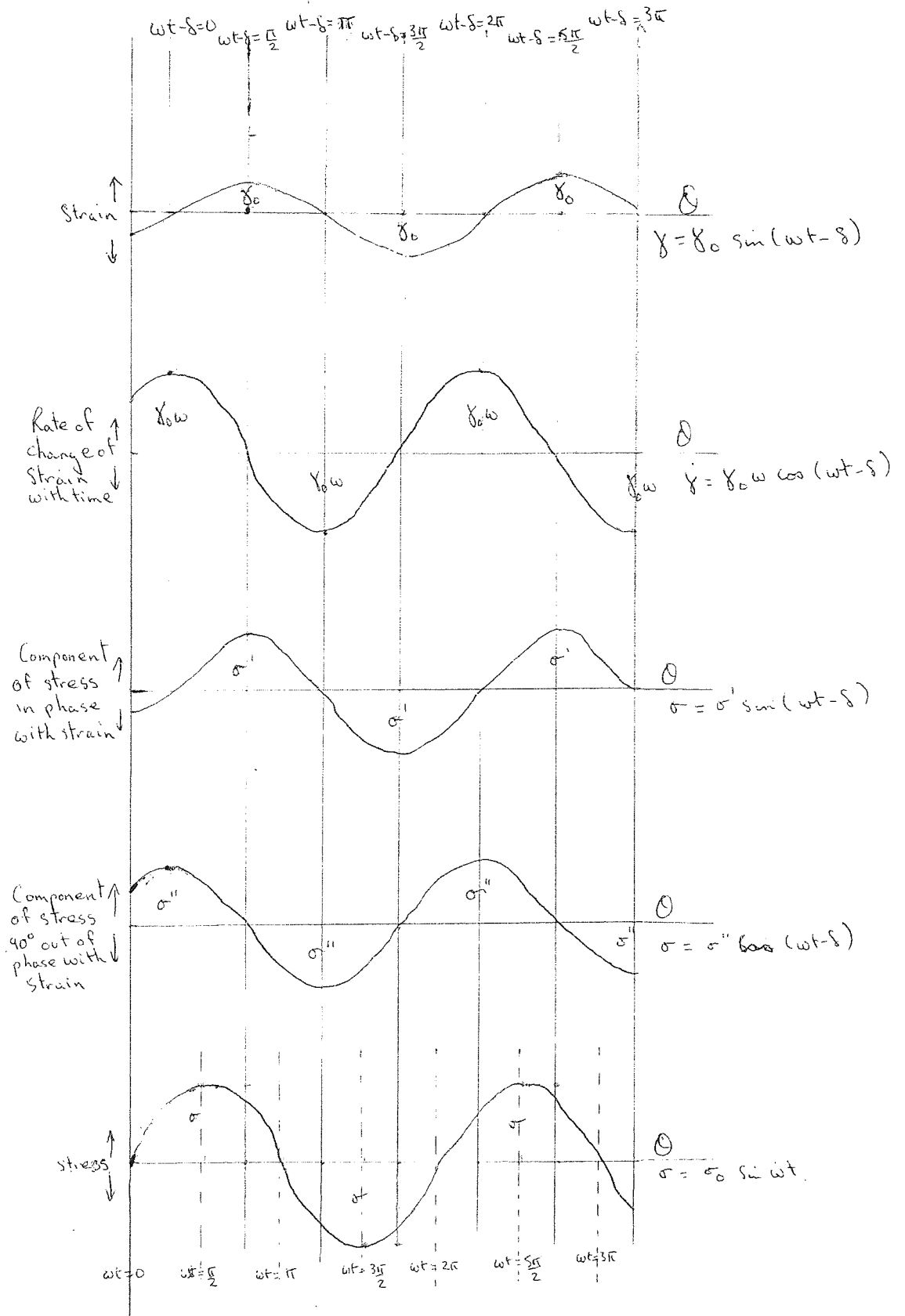
Fig. 5 Stress and Strain Waveforms

where ν is Poisson's ratio.

The most important dynamic mechanical properties of a material are E', G', d and d shear from which E*, G*, $|E*|$, $|G*|$, E" and G" can easily be derived. A variety of methods are available for the determination of these properties (see sect. 2.1).

1.3.1.2 Basic Rheological Equations For Solid Systems

Rheology is defined as the science dealing with deformation and flow of matter (68,69). Deformation is a general term which refers to the alteration of the shape or size of a collection of matter under the application of an external force system. If the deformation is time dependent then the material is said to 'flow'.

Rheology thus encompasses all stress–strain–time properties of solid and liquid materials and material systems in the manner shown in Fig. 6.

F	S	R
ENVIRONMENTAL CONDITIONS e.g. temperature, atmosphere, radiation.	FORCING FUNCTION F – X – t input.	MATERIALS & STRUCTURAL SYSTEM with its rheological properties defined by its Rheological Equation.	RHEOLOGICAL RESPONSE e.g. creep, relaxation, damping.
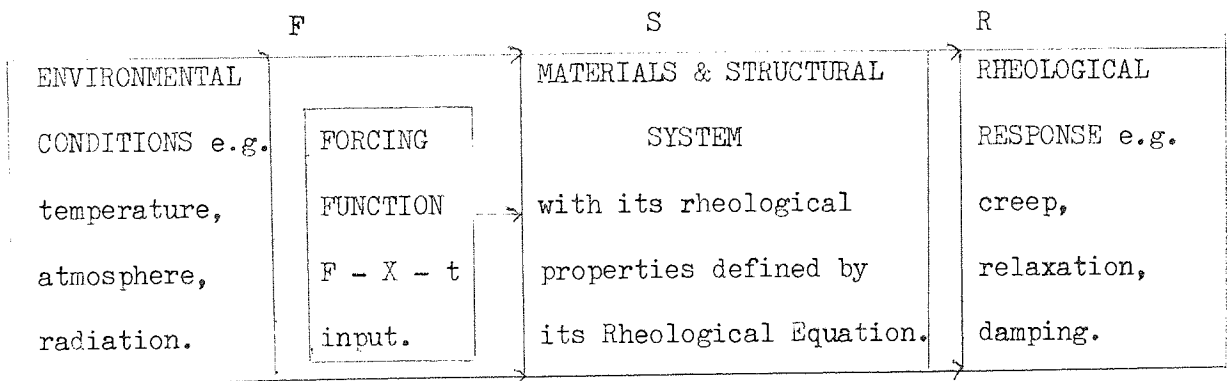
Fig. 6 Role of the system, material or structural, and system properties in defining the relationship between forcing function and response (from ref. 70)

The rheological equations are usually simplified to include only those terms of interest in a given problem, in order to allow a mathematical

analysis and thus there is some degree of approximation. In the field of visco-elasticity only the rheological equations for linear viscoelasticity (71) have provided the mathematical tractability required to solve a significant number of classes of engineering problems.

Testing of materials and structures is dependent on applying a known forcing function, F, observing the rheological response, R, and constructing suitable rheological equations to describe the properties of the system, S. This thesis is primarily concerned with the rheological properties of damping and modulus of solid materials.

There are three basic approaches.

i) The solid state or micromechanistic approach, which involves the study of chain uncoiling, chain slipping, bond stretching etc. (see sect. 1.3.1)

Although this approach may not be able to predict quantitatively the properties of specific engineering materials it is useful for generalising rheological behaviour, in providing a basis for making correlations among different properties and in extending existing data beyond the range of variables studied experimentally.

ii) Ad hoc testing and simulated service evaluation.

Ad hoc or specific purpose tests are intended to provide data for particular materials under special combinations of stress and environmental conditions. The main disadvantage of this technique as applied to this current study is that the property data is not generally extendable, in the absence of a more basic understanding, to problems which involve different combinations of stress and environmental conditions.

iii)   Phenomenological and macroanalytical approach.

This is intermediate between (i) and (ii) and is the engineering approach for defining the properties of materials and relating these properties to structural performance. This approach is used in the current investigations into the dynamic mechanical testing of friction materials. It involves determination of the unit properties of materials (by testing simple specimens under simplified environmental conditions), idealising these properties to ease mathematical manipulation and relating them to the behaviour of part of a structure.

1.3.1.3 Limitations on the Theoretical Treatment

Brake squeal in disc brakes is thought to be due to flexing of the disc around six to fourteen radial nodes (55). The action on the pad material is thus sinusoidal (assuming that the disc flexes in the most natural manner and no harmonics are present) consequently testing will be carried out using sinusoidal vibrations and the theory will be limited to sinusoidal forcing functions of the form

$$F = F_0 \sin \omega t$$

The amplitude of the force is $F_0(N)$, the period $T(s^{-1})$ the frequency of vibration is $f = 1/T(Hz)$ and the angular velocity is $\omega = 2\pi f(\text{rad } s^{-1})$.

Friction materials are complex composites which probably are not very unified but for the purposes of the theoretical treatment they will be regarded as uniform and to behave as linear viscoelastic materials. It is appreciated however, that other mechanisms involved in practice may include an elasticity, dislocation and inhomogeneous plastic slip and flow phenomena. The term 'linear' means that the stress is linearly proportional

to the strain and the term viscoelastic implies that the strain is rate dependent containing both recoverable and nonrecoverable strain.

1.3.2 Material and Member Nomenclature

A member is defined as a specimen of uniform material without joints or interfaces. A particularly property of a member is a function of the corresponding unit property of the material from which it is made (see Table 2).

Consider the system shown in figure 7 which can represent a test specimen or a model.

Rigid support

S

Viscoelastic specimen (without mass)

Exciting force F

M

Rigid mass with zero damping (equivalent to the mass of the specimen)
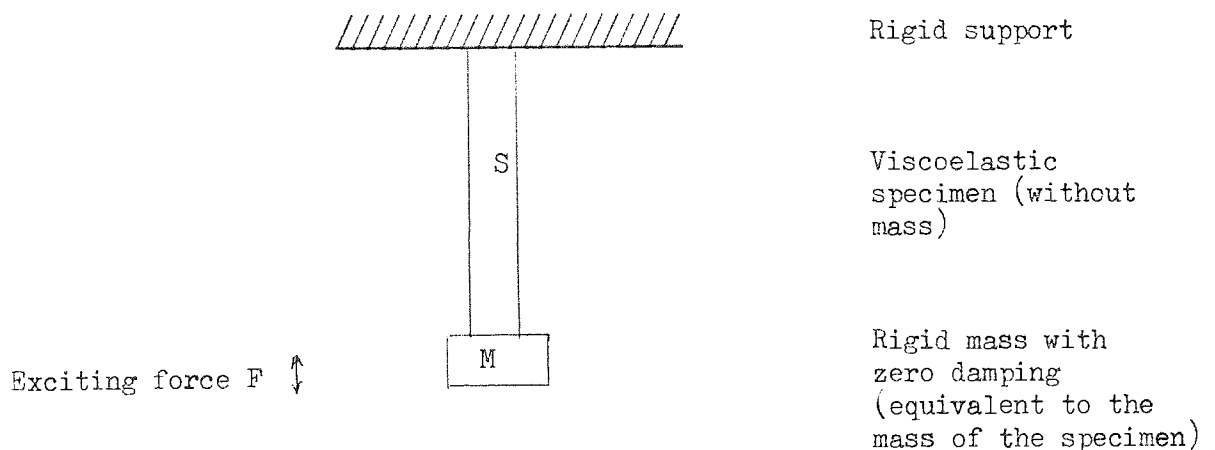
Fig. 7 Single degree of freedom system

Hereafter properties of the specimen will be denoted by the subscript 's'.

For linear viscoelastic materials the complex notation of linear viscoelasticity is the standard nomenclature (72).

The stiffness or spring constant of a linear specimen can be expressed in complex notation as

$$k_s^* = k_s' + ik_s''$$

where k_s^* is the complex stiffness of the specimen.

k_s' is the elastic component of the stiffness.

k_s'' is the viscous component of the stiffness.

If the complex stiffness, k_s^*, of a specimen can be determined under known conditions of loading and stress distribution then the unit complex stiffness properties or moduli can be determined.

Under uniform normal load

$$E = \frac{\sigma}{\gamma}$$

where E is Young's Modulus.

$$\sigma = \frac{F}{BD}$$

where F is the force on the specimen.

B is the width of the specimen.

D is the thickness of the specimen.

$$\gamma = \frac{X}{L}$$

where X is the extension in the specimen.

L is the length of the specimen.

$$E = \frac{FL}{BDX}$$

k_s is the force to produce an extension of unity in the specimen.

$$E = \frac{k_s L}{BD}$$

Thus

$$E^* = k_s^*(L/BD), \quad E' = k_s'(L/BD), \quad E'' = k_s''(L/BD)$$

Hence

$$E^* = E' + iE''$$

where E* is the complex modulus of the material.

 E' is the elastic component of modulus.

 E" is the viscous component of modulus.

Similar equations, in terms of the shear modulus, G, exist for torsional loading.

The damping factors of members and materials are given by the ratios

$$d_s = \frac{k''_s}{k'_s} \text{ , and } d = \frac{E''}{E'}$$

but by substituting for k''_s and k'_s in terms of E" and E'

$$d_s = \frac{E''(BD/L)}{E'(BD/L)} = \frac{E''}{E'} = d$$

Hence for linear materials the damping factor of a specimen is the same as the damping factor of the material of which it is composed irrespective of the dimensions of the specimen.

In general the theory for specimens and materials is the same and table 2 gives the comparability of the two sets of properties.

Terms appropriate for unit properties of uniform materials.	Terms appropriate for properties of the total specimen.
Normal stress σ	Force F
Stress rate $\dfrac{d\sigma}{dt} = \dot{\sigma}$	Force rate $\dfrac{dF}{dt} = \dot{F}$
Normal strain δ	Displacement X
Strain rate $\dfrac{d\delta}{dt} = \dot{\delta}$	Displacement rate (velocity) $\dot{X}$
Second derivative of strain $\dfrac{d^2\delta}{dt^2} = \ddot{\delta}$	Velocity rate (Acceleration) $\ddot{X}$
Mass m	Mass M
Modulus or stiffness E	Stiffness or spring constant k_s
$E^* = E' + iE''$	$k_s^* = k_s' + ik_s''$
$|E^*| = \sqrt{(E')^2 + (E'')^2}$	$|k_s^*| = \sqrt{(k_s')^2 + (k_s'')^2}$
Similarly for other moduli	
Damping factor d	Damping factor d_s $(d_s = d)$

Table 2 Corresponding properties for members and materials

1.3.3 Idealisations and Models for Defining Rheological Properties

In studying dynamic mechanical properties, idealisation of the elastic and viscous properties of solids is the first step to forming workable rheological equations in viscoelasticity, the next step is to design a mechanical model, which behaves in a similar way to real materials and consists of elements of idealised properties linked together. In general the macro-elements of the model, their connections and arrangement bear some similarity mathematically to the micro-constituents and mechanism in the real material.

The force-displacement-time relation of any real linear viscoelastic material can be represented by the general differential equation (73)

$$\left[a_0 + a_1 \, (\partial/\partial t) + a_2 (\partial^2/\partial t^2) + \ldots\ldots + a_n (\partial^n/\partial t^n)\right] F = \text{eq. 1.3.3.1}$$

$$\left[b_0 + b_1 \, (\partial/\partial t) + b_2 (\partial^2/\partial t^2) + \ldots\ldots + b_n (\partial^n/\partial t^n)\right] X$$

where a_i and b_i ($i = 1$ to n) are material constants.

In order to apply a mathematical treatment this equation must be simplified to only a few terms which are found to give a good approximation to the behaviour of real materials. These simplified equations are related to mechanical models composed of perfectly elastic springs, perfectly viscous dashpots and sometimes masses which are regarded as being perfectly rigid.

The properties of these components are defined as follows:-

    i)   For a linearly elastic spring.

        The equation of motion is given by Hooke's Law

$$F = k_1' X$$

        Under sinusoidal loading it can be shown that

$$k_s' = k_1'$$

$$k_s'' = 0$$
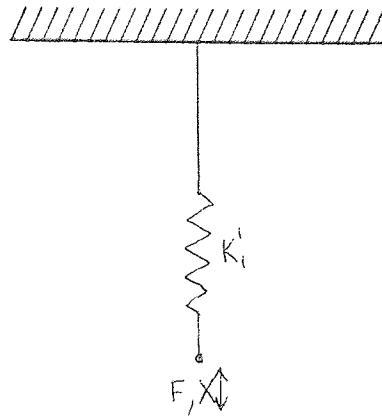
Fig. 8 The Linearly Elastic Spring

ii)   For a linearly viscous dashpot (i.e. one with Newtonian

viscosity

The equation of motion is given by

$$F = \mu_1 \dot{X}$$

Under sinusoidal loading it can be shown that

$$k'_s = 0$$

$$k''_s = k''_1 = \mu_1 \omega$$
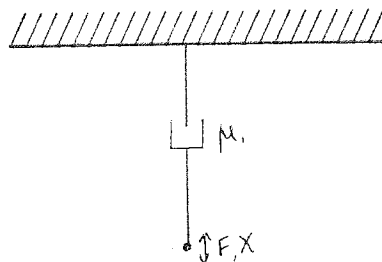
Fig. 9 The Linearly Viscous Dashpot

iii)   For a rigid mass.

The equation of motion is given by Newton's Law.

$$F = M\ddot{X}$$

Under sinusoidal loading it can be shown that

$$k'_s = -M\omega^2$$

$$k''_s = 0$$
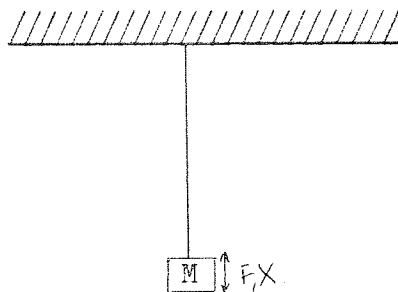
Fig. 10   The Rigid Mass

Models are combinations of any number of these components in series or in parallel and each model can be used to demonstrate a particular type of behaviour characteristic of plastics, rubbers, metals etc.

In general the more components a model has, the better the correlation with real materials but the more complex the mathematical treatment.

For description of viscoelastic materials the Voigt model correlates with the theory already discussed and will be described in detail in section 1.3.4.

The common models and their defining equations will now be summarised without derivation, which can be found in references on the subject (70,71,73,74).

1.3.3.1 Biparameter Models

i) Maxwell-type model (series-biparameter viscoelastic model)

The equation of motion is given by

$$\dot{F} + \frac{k_i'}{\mu_i} F = k_i' \dot{X}$$

Under sinusoidal loading and with a Newtonian fluid in the dashpot, it can be shown that

$$k_s' = \frac{k_i' \left(k_i''\right)^2}{\left(k_i'\right)^2 + \left(k_i''\right)^2}$$

$$k_s'' = \frac{\left(k_i'\right)^2 k_i''}{\left(k_i'\right)^2 + \left(k_i''\right)^2}$$

Hence

$$d_s = \frac{k_s''}{k_s'} = \frac{k_i'}{k_i''}$$

ii) Voigt-type model (parallel-biparameter anelastic model)

The equation of motion is given by

$$F = \mu_i \dot{X} + k_i' X$$

Under sinusoidal loading and with a Newtonian fluid in the dashpot, it can be shown that

$$k_s' = k_i'$$

$$k_s'' = k_i''$$

Hence

$$d_s = \frac{k_i''}{k_i'}$$
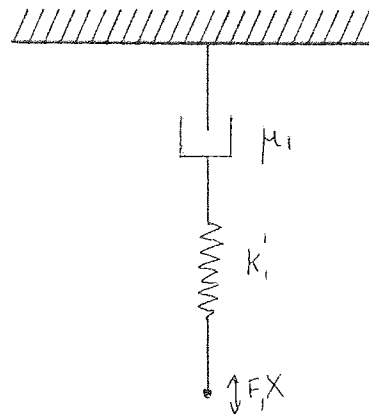
Fig. 11 The Maxwell Model
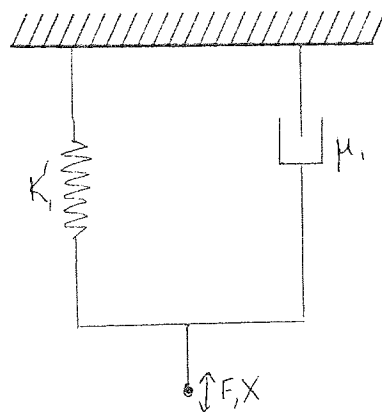
Fig. 12 The Voigt Model

1.3.3.2 Triparameter Models

i) Triparameter anelastic model (two springs – simplest

anelastic model)

The equation of motion is given by

$$F + \frac{\mu_1}{k'} \dot{F} = \ddot{X}k'_2 + \frac{\mu(k'_1 + k'_2)\dot{X}}{k'_1}$$

Under sinusoidal loading and with a Newtonian fluid in the

dashpot, it can be shown that

$$k'_s = k'_2 + \frac{k'_1 (k''_1)^2}{(k'_1)^2 + (k''_1)^2}$$

$$k''_s = \frac{(k'_1)^2 k''_1}{(k'_1)^2 + (k''_1)^2}$$
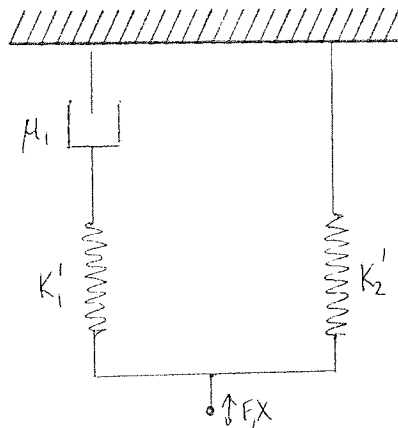
Fig. 13 The Triparameter Anelastic Model

ii) Triparameter viscous model (two dashpots)

The equation of motion is given by

$$F + \frac{\mu_1}{k_1'} \dot{F} = (\mu_1 + \mu_2)\ddot{X} + \frac{\mu_1 \mu_2}{k_1'} X$$

Under sinusoidal loading and with a Newtonian fluid in the dash-pots it can be shown that

$$k_s' = \frac{(k_1'')^2 k_1'}{(k_1')^2 + (k_1'')^2}$$

$$k_s'' = \frac{k_1'' (k_1')^2}{(k_1')^2 + (k_1'')^2} + k_2''$$
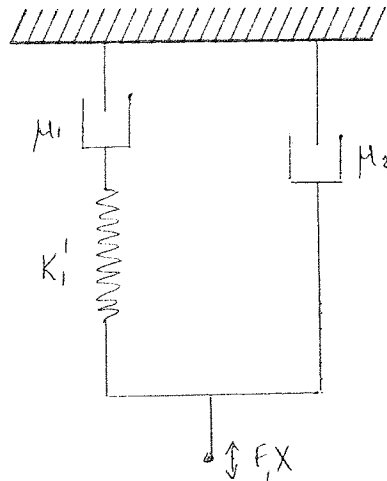
Fig. 14   The Triparameter Viscous Model

1.3.3.3 General Linear Viscoelastic Model

The equation of motion is given by equation 1.3.3.1

Under sinusoidal loading and with a Newtonian fluid

in the dashpots it can be shown that

$$k'_s = \sum_{n=1}^{m} \frac{(k''_n)^2 \, k'_n}{(k'_n)^2 + (k''_n)^2}$$

$$k''_s = \sum_{n=1}^{m} \frac{k''_n \, (k'_n)^2}{(k'_n)^2 + (k''_n)^2}$$
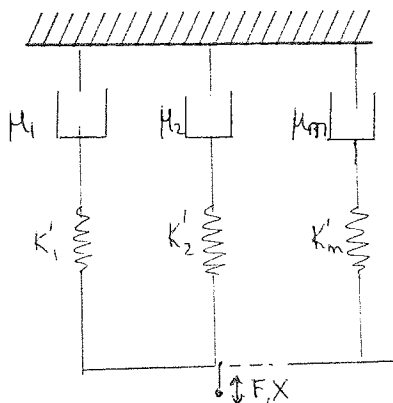
Fig. 15   The General Linear Viscoelastic Model

1.3.4 Voigt-Type Models

1.3.4.1 Simple Voigt Model (no added mass)

Consider a sinusoidal force applied to the model shown in Fig. 16.
As both legs are subjected to the same strain, the total force in the system
is given by the sum of the forces in each leg.

External force
$F = F_0 e^{i\omega t}$

External displacement
$X = X_0 e^{i(\omega t - \delta)}$
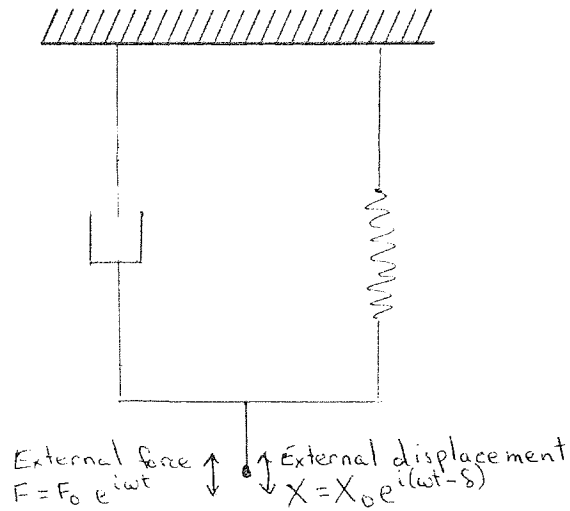
Fig. 16   The Simple Voigt Model (no added mass)

The force in the dashpot, F_d, is given by

$$F_d = \mu_1 \dot{X}$$

The force in the spring, F_s, is given by

$$F_s = k_1' X$$

The total force, F, is thus given by

$$F = \mu_1 \dot{X} + k_1' X \quad \dots\dots\dots\dots\dots\dots\dots\dots\dots \text{eq. 1.3.4.1}$$

If

$$X = X_0 e^{i(\omega t - \delta)}$$

Then

$$\dot{X} = X_0 i\omega e^{i(\omega t - \delta)}$$

$$= i\omega X$$

Substituting in equation 1.3.4.1 for $\dot{X}$

$$F = X(\mu i\omega + k')$$

$$\frac{F}{X} = k_s^* = i\mu\omega + k' \quad \dots\dots\dots\dots\dots\dots\dots\dots \text{eq. 1.3.4.2}$$

But $\quad k^*_s = k'_s + ik''_s$ ....eq. 1.3.4.3

Equating the real parts and the imaginary parts from equations 1.3.4.2 and 1.3.4.3.

$$k'_s = k'_1$$

$$k''_s = \mu_1 \omega$$

If the fluid in the dashpot is Newtonian then

$$k''_1 = \mu_1 \omega$$

Hence

$$k''_s = k''_1$$

Thus the spring provides the real stiffness and the dashpot the imaginary stiffness and the following equations are valid.

$$|k^*_s| = \sqrt{(k'_s)^2 + (k''_s)^2} = \sqrt{(k'_1)^2 + (k''_1)^2} = |k^*_1|$$

$$d_s = \frac{k''_s}{k'_s} = \frac{k''_1}{k'_1} = \tan\delta$$

$$k'_s = |k^*_s| \cos\delta = |k^*_1| \cos\delta$$

$$k''_s = |k^*_s| \sin\delta = |k^*_1| \sin\delta$$

These equations are directly comparable with the equations derived for material properties in section 1.3.1.1.

Although the Voigt model correlates well with the complex notation approach to linear viscoelasticity, its behaviour differs from real linear viscoelastic materials in the following ways:-

    i)   There is no elastic response during load application or release.

    ii)   In the model the creep rate approaches zero with sufficient time.

iii) After sufficient time at zero force, no permanent set

remains in the model irrespective of prior loading history.

iv) There is no condition for a resonant frequency at which X_o

passes through a maximum at constant force F_o.

1.3.4.2 Voigt Model with Added Mass

The theory can be expanded to eliminate this last difference and create

a resonance condition. This is accomplished by addition of a mass, M,

to the bottom of the model.

The equation of motion is given by

$$F = M\ddot{X} + \mu\dot{X} + k_1'X$$

With a Newtonian fluid in the dashpot and applying a similar

analysis to that used in the previous section

$$k_s' = k_1' - M\omega^2$$

$$k_s'' = \omega\mu = k_1''$$

$$d_s = \frac{k_1''}{k_1' - M\omega^2} = \tan\delta \qquad \dots\dots\dots\dots\dots\dots\dots eq.1.3.4.4$$

$$|k_s^*| = \frac{F_o}{X_o} = \sqrt{(k_1' - M\omega^2) + (k_1'')^2} \qquad \dots\dots\dots\dots\dots eq.1.3.4.5$$

External force $F = F_0 e^{i\omega t}$

External displacement $X = X_0 e^{i(\omega t - \delta)}$
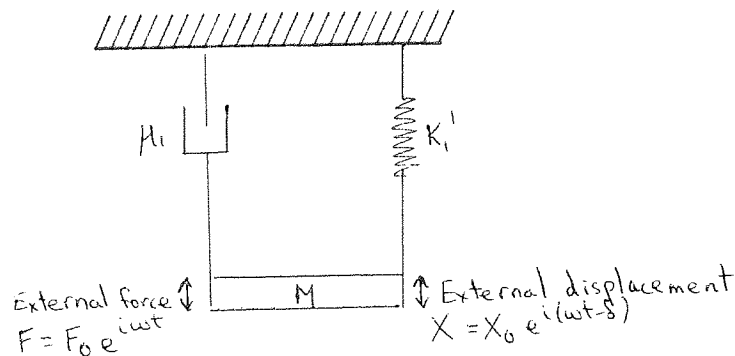
Fig. 17 The Voigt Model with Added Mass

The term $\left(k_1' - M\omega^2\right)^2$ reaches a minimum value when $k_1' = M\omega^2$ and thus when this occurs X_o passes through a maximum at constant force F_o, d_s is infinite and $\delta = 90^\circ$.

From classical mechanical vibration theory

$$\omega_n = \sqrt{\frac{k_1'}{M}}$$

where ω_n is the angular velocity at resonance.

Dividing the right hand side of equation 1.3.4.4 throughout by M

$$d_s = \frac{k''/M}{\omega_n^2 - \omega^2} \qquad \ldots\ldots\ldots\ldots\ldots\ldots\ldots\ldots\ldots\ldots\ldots eq.1.3.4.6$$

when $\omega^2 \gg \omega_n^2$ $\qquad d_s \doteq \frac{k_1''}{\omega^2 M}$

when $\omega^2 \to 0$ $\qquad d_s \doteq \frac{k''}{k_1'}$ $\qquad$ i.e. the model becomes equivalent to
or $M \to 0$ $\qquad\qquad\qquad\qquad\qquad$ the simple Voigt model.

Hence with low masses and frequencies much lower than the resonant frequency the model behaves in the same manner as the simple Voigt model and thus damping may be found from the phase difference between force and displacement.

By examination of equation 1.3.4.6 it can be seen that

i) at low frequencies $d_s = \tan\delta$ is small and positive and thus $\delta \doteq 0^\circ$.

ii) at high frequencies d_s is small and negative and thus $\delta \doteq 180^\circ$.

iii) at $\omega = \omega_n$ d_s is infinite and thus $\delta = 90^\circ$.

Only the rate of change of δ with frequency gives an indication of the damping (a rapid change indicates low damping and a gradual change indicates high damping).

If there were no damping δ would change instantaneously from 0° to 180°

at resonance.

Re-arranging equation 1.3.4.5

$$\left|k_s*\right| = \sqrt{(k'')^2 - M^2 \left(\omega_n^2 - \omega^2\right)^2}$$

at resonance

$$\left|k_s^*\right| = k_1'' = \mu_1\omega_n$$

Again, if ω or M tend to zero the model behaves as the simple Voigt

model.

1.3.4.3 The Bandwidth Technique of Determining Damping as Used

in Resonance Techniques

The bandwidth technique is a commonly accepted technique for determin-

ing damping although its theoretical validity is not easily found in the

literature. The following derivation establishes its validity.

From classical vibration mechanics it can be shown that if the viscosity

of the dashpot is increased a level is reached at which the system will

cease to vibrate. This level is the critical viscosity, μ_c , and it can

be shown that

$$\mu_c = 2\sqrt{k_1'M} = 2\omega_n M \quad \dots\dots\dots\dots\dots\dots\dots\dots\dots\dots\text{eq.1.3.4.7}$$

Equation 1.3.4.4 can be rewritten

$$X_o = \frac{F_o/k'}{\left(1 - (\omega/\omega_n)^2\right)^2 + \left(2\mu_1\omega/\mu_c\omega\right)^2}$$

Let $\omega/\omega_n = B$, $2\mu_1/\mu_c = T$, $F_o/k_1' = A$

$$X_o = \frac{A}{\left(1 - B^2\right)^2 + T^2 B^2} \quad \dots\dots\dots\dots\dots\dots\dots\text{eq.1.3.4.8}$$

At resonance $B = 1$ and $X_0 = X_{res} = A/T$

Consider small angular velocity changes to just above and just below ω_n

i.e. let $B_1 = 1 - \curlyvee$

$B_2 = 1 + \curlyvee$

where $B_1 = \omega_1/\omega_n$, $B_2 = \omega_2/\omega_n$

Because T is a dimensionless number let $\curlyvee = nT$ where n is any number.

$$B_1 = 1 - nT \quad \dots\dots\dots\dots\dots\dots\dots\dots\dots\dots\text{eq.1.3.4.9}$$

$$B_2 = 1 + nT \quad \dots\dots\dots\dots\dots\dots\dots\dots\dots\dots\text{eq.1.3.4.10}$$

Substituting in equation 1.3.4.8

$$X_0 = X_1 = \frac{A}{\sqrt{(1-1 + 2nT - n^2T^2)^2 + (1 - 2nT + n^2T^2)T^2}}$$

$$X_0 = X_2 = \frac{A}{\sqrt{(1-1 - 2nT - n^2T^2) + (1 + 2nT + n^2T^2)T^2}}$$

If T is small T^2 is negligible and all terms under the square root containing a power of T greater than T^2 may be disregarded.

$$X_1 = \frac{A}{\sqrt{4n^2 T^2 + T^2}} = \frac{X_{res}}{\sqrt{4n^2 + 1}}$$

$$X_2 = \frac{A}{\sqrt{4n^2 T^2 + T^2}} = \frac{X_{res}}{\sqrt{4n^2 + 1}}$$

Hence $X_1 = X_2$

Let $X_1 = X_2 = X_0$

$$X_0^2 = \frac{X_{res}^2}{4n^2 + 1}$$

$$(2n)^2 = \frac{X_{res}^2 - X_0^2}{X_0^2}$$

$$1/2n = \sqrt{\frac{X_o^2}{X_{res}^2 - X^2}}$$

From equations 1.3.4.9 and 1.3.4.10

$$B_2 - B_1 = 2nT$$

$$T = \frac{B_2 - B_1}{2n}$$

$$T = B_2 - B_1 \sqrt{\frac{X_o^2}{X_{res}^2 - X_o^2}}$$

$$2\mu_1/\mu_c = \frac{\omega_2 - \omega_1}{\omega_n} \sqrt{\frac{X_o^2}{X_{res}^2 - X_c^2}}$$

$$= \frac{f_2 - f_1}{f_n} \sqrt{\frac{X_o^2}{X_{res}^2 - X_o^2}}$$

From basic theory

$$d_s = \text{Tan } \delta = \frac{k''}{k'} = \frac{\mu_1 \omega}{k'} = \frac{2\mu_1 \omega}{\mu_c \omega_n}$$

At frequencies of and around the natural frequency $\omega/\omega_n = 1$

$$d_s = 2\frac{\mu_1}{\mu_c} \qquad \dots\dots\dots\dots\dots\dots\dots\dots\dots\dots\dots\dots\text{eq.1.3.4.11}$$

$$d_s = \frac{f_2 - f_1}{f_n} \sqrt{\frac{X_o^2}{X_{res}^2 - X_o^2}}$$

If $X_o = \frac{X_{res}}{\sqrt{2}}$

$$d_s = \frac{f_2 - f_1}{f_n}$$

1.3.4.4 Resonance Curves

The theory discussed so far has assumed that the peak of the resonance curve occurs at the resonant frequency. This would always be true if there were no damping but is not always true if damping is present.

The following derivations give the relationship between the peak frequency and the resonant frequency for displacement, velocity and acceleration resonance.

Rewriting equation 1.3.4.5

$$X_o = \frac{F_o}{\sqrt{(\mu_1 \omega)^2 + (k_1' - \omega^2 M)^2}} \quad \dots \dots \dots \dots \text{eq.1.3.4.12}$$

If the displacement is sinusoidal

$$X = \frac{F_o \sin(\omega t - \varsigma)}{\sqrt{(\mu_1 \omega)^2 + (k_1' - \omega^2 M)^2}}$$

Differentiating with respect to time to give velocity

$$\dot{X} = v = \frac{F_o \omega \cos(\omega t - \varsigma)}{\sqrt{(\mu_1 \omega)^2 + (k_1' - \omega^2 M)^2}} \quad \dots \dots \dots \dots \text{eq.1.3.4.13}$$

Dividing the right hand side throughout by ω

$$v = \frac{F_o \cos(\omega t - \varsigma)}{\sqrt{\mu_1^2 + (k'/\omega - \omega M)^2}}$$

Let the amplitude of the velocity be v_o

$$v_o = \frac{F_o}{\sqrt{\mu_1^2 + (k'/\omega - \omega M)^2}} \quad \dots \dots \dots \dots \text{eq.1.3.4.14}$$

Differentiating equation 1.3.4.13 with respect to time to give acceleration and dividing the right hand side throughout by ω^2

$$\dot{v} = a = \frac{-F_o \sin(\omega t - \varsigma)}{\sqrt{(\mu_1/\omega)^2 + (k_1'/\omega^2 - M)^2}}$$

Let the amplitude of the acceleration be a_o

$$a_o = \frac{-F_o}{\sqrt{(\mu_1/\omega)^2 + (k_1'/\omega^2 - M)^2}} \quad \dots \dots \dots \dots \text{eq.1.3.4.15}$$

Differentiating equation 1.3.4.12 with respect to ω and setting $dX_o/d\omega = 0$ to give the frequency, ω_o, at which the maximum displacement occurs

$$2\mu_1^2 \omega_o - 4k'M\omega_o + 4M^2 \omega_o^2 = 0$$

The solutions of this equation are

$$\omega_c = 0$$

or
$$\omega_c^2 = \frac{2k_1'M - \mu_1^2}{2M^2}$$

Rewriting using $\omega_n = \sqrt{k_1'/M}$ and equations 1.3.4.7 and 1.3.4.11

$$\omega_c = \omega_n \sqrt{1 - d_s^2/2}$$

Hence maximum displacement occurs below the natural frequency.

Differentiating equation 1.3.4.14 with respect to ω and setting $dv_0/d\omega = 0$ to give the frequency, ω_c, at which the maximum velocity occurs

$$M^2 \omega_0 - (k_1')^2/\omega_c^3 = 0$$

By similar manipulation to above the important solution is

$$\omega_c = \omega_n$$

Hence maximum velocity occurs at the natural frequency.

Differentiating equation 1.3.4.15 with respect to ω and setting $da_0/d\omega = 0$ to give the frequency, ω_0, at which the maximum acceleration occurs

$$2\frac{\mu_1^2}{\omega_c^3} + 4\frac{(k_1')^2}{\omega_c^5} - 4\frac{Mk_1'}{\omega_c^3} = 0$$

By similar manipulation to above the important solution is

$$\omega_c = \omega_n \sqrt{1/(1 - d_s^2/2)}$$

Hence maximum acceleration occurs above the natural frequency.

1.3.5 Frequency - Temperature Superposition

A dependence that models do not portray is the relation between frequency and temperature. It can be shown that if a viscoelastic property

is plotted against temperature at constant frequency the graph produced is
of the same shape as if the same property was plotted against frequency
at constant temperature. This phenomenon also accounts for the fact that
when testing is carried out using free vibration or resonance techniques
the operating frequency decreases as temperature increases.

Because a logarithmic relationship exists a very wide span of
frequencies is required to simulate the effect of a few degrees rise in
temperature. Most test instruments have a relatively narrow frequency range
and thus testing at constant temperature is unsatisfactory.

A complex mathematical theory has been evolved by Ferry (71) which can
be used to translate temperature changes into frequency changes so that
effects that take place at frequencies out of the rnage of an instrument
may be studied by varying the test temperature.

In the testing of friction materials it was necessary to vary
temperature over a wide range at high frequency in order to simulate service
conditions. Consequently it was felt that a complex mathematical treatment
was rather irrelevant to the problem.

1.4 Programme of work

1.4.1 Objective

To determine dynamic mechanical properties of commercial disc brake
pad materials under high audio-frequency vibratory conditions in tension-
compression over a range of temperatures and frequencies.

1.4.2 Equipment

One of the first decisions to be made in a project of this type is
the nature of the equipment to be used, which in this particular project

was severely limited by cost. There are various commercial dynamic mechanical testing instruments available which if suitable would be the best solution. Hence all published work on dynamic mechanical testing instruments and testing procedures must be carefully scrutinised. If however none are suitable, then new equipment must be designed and developed. Here there are many important considerations.

    i)   Existing mathematical analysis must be carefully vetted so that all the approximations and limitations are known.

    ii)   Knowledge must be gained in the use and availability of electronic equipment.

    iii)   Knowledge must be gained in the problems and limitations of workshop engineering in order to design intricate pieces of equipment. In addition to these there are also the economic and time limitations to be considered.

When all the apparatus has been assembled it must be commissioned using samples of known properties. If it is found that a particular set-up is not suitable then further considerations e.g. linearity, clamping, positions of transducers etc., must be taken into account.

1.4.3 Production of test specimens

Disc brake pads are basically segmental blocks of hard friction material integrally moulded on a steel back-plate. The four main considerations when producing test specimens from the disc pads are as follows:-

i) The nature of the machining operations to be used. Test specimens must be dimensionally accurate but must not have been subjected to any extremes of temperature or stress nor to any coolants which might be irreversibly absorbed.

ii) The nature of the cutting tools to be used. Conventional cutting tools are quickly blunted by the friction material and coolants are a problem.

iii) Method of removal of the back-plate.

iv) Specimen shape and size.

1.4.4 Testing

When the equipment has been assembled and commissioned specimens will be cut from pads made by various friction material manufacturers, which have been:-

i) Unused.

ii) Returned after 500 miles free service because of brake squeal.

iii) Used for 500 miles with no history of brake squeal.

Dynamic mechanical testing of these specimens will be made over a range of frequencies and temperatures and under certain other specified conditions. The results of these tests will be examined to determine whether the disc pads which have had a history of brake squeal exhibit any particular dynamic mechanical property or trend in properties which identifies them from the group with no history of brake squeal. The properties of the used pads will be compared with those of the unused pads to determine the effects due to service.

Some auxiliary testing will also be carried out on specimens prepared from the major components of friction materials in order to determine which components are responsible for certain effects which are of interest. The effect of environmental agents, such as engine oil, water and brake fluid, on the dynamic mechanical properties of friction materials will also be investigated.

CHAPTER 2

EXPERIMENTAL

2.1 Review of Dynamic Mechanical Test Methods

2.1.1 Introduction to Dynamic Mechanical Testing

In order to determine the dynamic mechanical properties of modulus and damping factor a great many tests, known as dynamic mechanical tests, have been evolved, some of which are very specialised.

There are two major modes of testing:-

i) Methods in tension-compression involving 'normal' forces and which determine extensional moduli.

ii) Methods in torsion involving shear forces and which determine shear moduli.

Flexural testing involves a mixture of 'normal' and shear forces but usually the test is arranged so that the shear forces are negligible and thus this mode of testing is included under methods in tension-compression.

Each mode of testing is further subdivided into four basic techniques:-

i) Free vibrations involving the application of an external force to set a specimen into vibration and then removal of the external force so that the vibrations die away naturally. Modulus is found from the frequency of free vibrations and damping factor from the decay rate of the vibrations.

ii) Forced vibrations with resonance involving the instigation of 'standing waves' in the specimen, by forcing vibrations, at the resonant frequency. Modulus is determined from the frequency at resonance and damping factor by means of the band-width of reverberation techniques.

iii) <u>Forced vibrations without resonance</u> involving the setting up
of 'travelling waves' in the specimen. This is the only
technique by which testing can be performed at a selected
frequency irrespective of specimen dimensions and temperature.
It is also the only technique by which $\tan \delta$ can be measured
directly. Modulus is found by an attenuation technique which
determines σ_o and γ_o and hence $|E^*|$ and damping factor
is measured directly as the tangent of the phase angle between
stress and strain.

iv) <u>Propagation of waves and pulses</u> which also involves the setting
up of travelling waves and really is a special case of (iii).
Modulus is determined from the phase velocity of the vibration
and damping from the attenuation of the signal during its
passage through the specimen.

In order to select a suitable method for the evaluation of friction
materials it was necessary to review the test methods available especially
those which were commercially available. In this review of dynamic mechanical
test methods only those methods which involve rigid bar shaped specimens and
sinusoidal vibrations have been considered. At the end of the review is a
comprehensive table showing the nature and limitations of all the methods
reviewed and an assessment of the potential of each method as a means for
evaluating the dynamic mechanical properties of friction materials under
conditions relevant to the service condition of squeal in disc brakes bearing
in mind that specimens would have to be cut from disc pads which had been in
service thus presenting a size limitation.

2.1.2 Methods in Shear

2.1.2.1 Torsion Pendulum

This method, which is amongst the simplest, has been used in various

forms by many different workers (75,76,77,78). Described here is the
commercial version known as the Nonius Pendulum.

In the Nonius Pendulum the specimen, which can be of almost any
dimensions, is held rigidly at the bottom end and the top end is clamped on
to an inertia bar suspended by a nichrome wire and counter-balanced so as not
to induce any normal forces in the specimen. To make measurements the bar is
displaced from the rest position and released. The bar oscillates and the
amplitude of the oscillations decays logarithmically due to the damping in the
specimen. The decay may be recorded by many different methods. In the Nonius
version this is accomplished by means of a needle probe, on one end of the
inertia bar, which arcs on to a rotating drum, held at high potential, round
which wax coated carbonised paper is wrapped. The arc burns out a trace of the
oscillations on the carbonised paper and from this the frequency and logarithmic
decay constant can be found (see Fig. 18).

The shear modulus is found from

$$G' = \frac{KLI}{B^3 \, DT^2\alpha}$$

where L is the effective length

K is a constant

B is the thickness

D is the width

T is the period of oscillation

I is the moment of inertia

α is the shape factor

The shape factor α is a number dependant on the ratio B/D. A comprehensive
list of shape factors is given by Trayer and March (79).

The damping is obtained from the logarithmic decrement, $\triangle$, which is the Naperian logarithm of the ration of two successive amplitudes.

$$d = \frac{4\pi\triangle}{4\pi^2 - \triangle^2}$$

If $\triangle$ is small

$$d \simeq \frac{\triangle}{\pi}$$

The frequency of operation is governed by

    i) The dimensions of the specimen.

   ii) The masses on the inertia bar.

Damping characteristics between $d = 0.01$ and 1.0 may be determined by this method.

Initially this method was considered for use in testing friction materials because of analogy with the disc brake where the wheel rotates at low frequency and causes a shearing action on the pad. An attempt was made to automate measurement by means of a shutter mechanism after Smith et al (80). The shutter is attached to one end of the inertia bar which swings across a light beam focused on a photo-electric cell with its output fed via a logarithmic amplifier into a chart recorder.

Later it was thought that the service condition more relevant to squeal involved high frequency, sinusoidal normal forces and thus work on the torsion pendulum was abandoned.
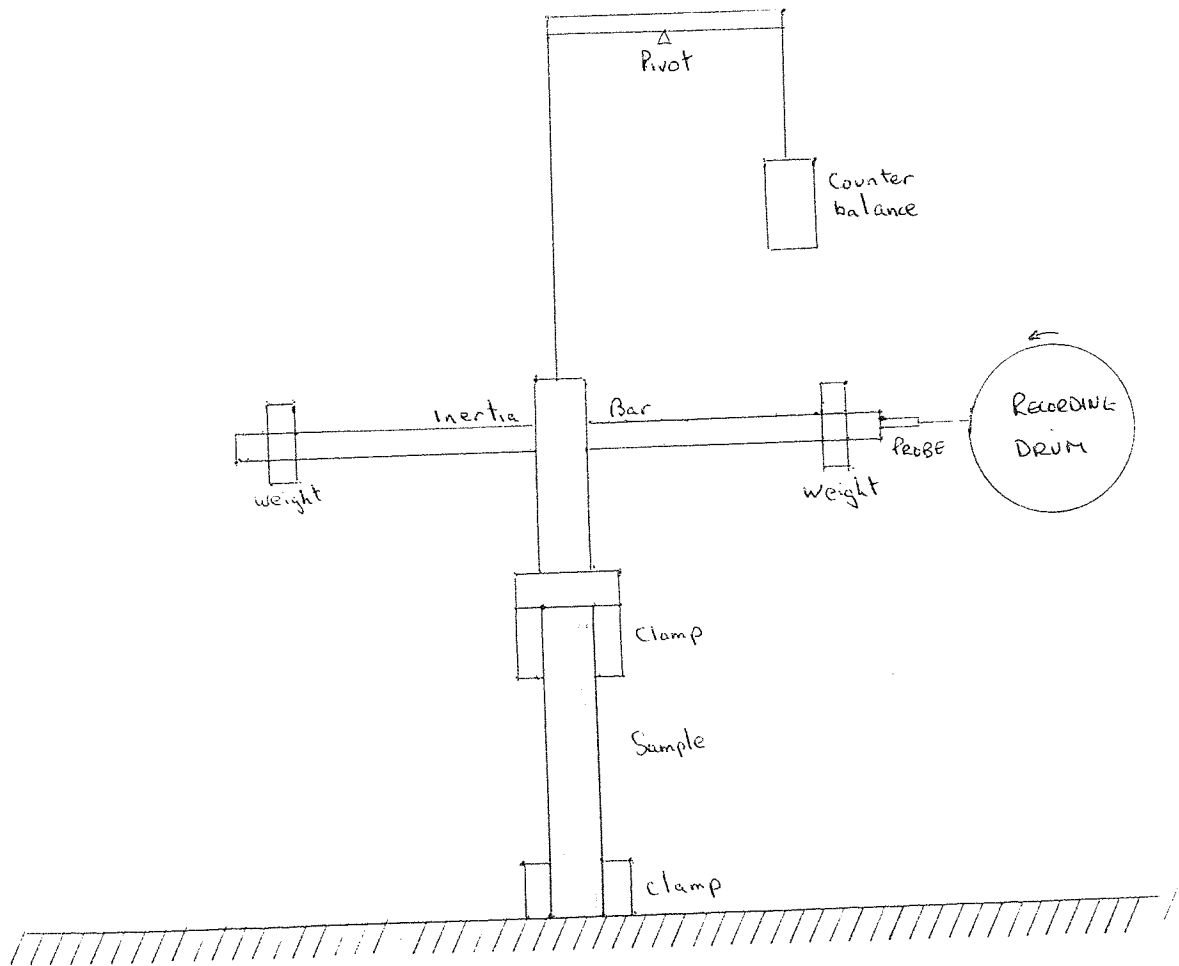
Fig. 18   The Nonius Pendulum

2.1.2.2 Resonant Torsional Vibrations

This electro-dynamic method can be used in the frequency range 100Hz to 10kHz and is described by Barone and Giacomini (81).

A coil of thin wire is fixed round each end of the specimen which is suspended by a fine thread so that each coil is in a magnetic field parallel to the lines of force (see Fig. 19).

An a.c. current is passed through one coil thus exciting the specimen into torsional oscillation which is detected in the second coil by means of the induced a.c. voltage. The shear modulus is determined from the resonant frequency and an analogous equation to that used in longitudinal resonance (see sect. 2.1.3.3). The damping is found by either the bandwidth technique (see sect. 1.3.4.3) or the reverberation technique (see sect. 2.1.3.1).
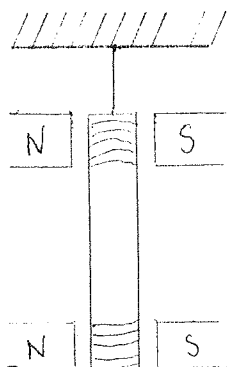
Fig. 19 The torsional resonance test rig

2.1.2.3 Dynamic Modulus Analyser

This test system is unique in that it may be used for both flexural and torsional measurements, hence enabling Poisson's ratio to be determined (see sect. 1.3.1.1).

i) Flexural mode

The digital transfer-function analyser (D.T.F.A.) provides an accurate, sinusoidal output voltage, at preset voltage and frequency. This voltage is used to drive the torque motors, which apply cyclicly varying, equal and opposite couples, $C_{\varepsilon} \sin \omega t$, to the ends of a beam specimen, causing it to flex (see Fig. 20).

Signals proportional to angular displacement are derived from transducers mounted co-axially on the motor shafts. These signals are demodulated and applied to the D.F.T.A., which correlates the demodulation signal to the driving function, removes unwanted noise, and resolves the r.m.s. displacement, R, and phase shift, Θ . These values are displayed, either in polar co-ordinates, as R, Θ , or in the cartesian plane as R = a + ib, where a and b are the real and imaginary components of amplitude R.

Using the classical theory for the equation of motion of the system, it is possible to deduce that the elastic and viscous coefficients respectively are given by:-

$$S = \frac{C\,a}{a^2 + b^2} + I\omega^2$$

$$Z = \frac{C\,b}{a^2 + b^2}$$

where I is an inertia term, and C is the r.m.s. value of the couple.

Since the motors themselves have innate stiffness and frictional characteristics, it is necessary to determine these initially as functions of frequency and temperature, with no specimen present. The values of S and Z so obtained are subtracted from the values of the coefficients determined with a specimen present, so giving the properties S_s and Z_s, of the material alone.

Assuming simple beam theory, then the couples at the ends of the specimen may be equated with bending moment, to give the relationship

$$E^* = \frac{LC}{2I_s R}$$

where I_s second moment of inertia.

L effective length.

Hence

$$E' = \frac{L S_s}{2I_s}$$

$$E'' = \frac{L Z_s}{2I_s}$$

$$d = \frac{Z_s}{S_s}$$

ii) Torsional mode

For torsional testing the electronic system is unchanged from that described above. One end of the specimen is rigidly held and the other is attached axially to the shaft of the torque motor. Thus torsional values of S_s and Z_s may be obtained, and the shear moduli G' and G", may be calculated from

$$G' = \frac{16\ LS_s}{B\ D^3\ \alpha}$$

$$G'' = \frac{16\ L\ Z_s}{B\ D^3 \alpha}$$

where α is a shape factor (see sect. 2.1.2.1).

Provision is made for an environmental chamber so that the effects of temperature may be studied in the range -70°C to $+200^\circ$C.

Frequency may be selected, without regard to specimen dimensions or temperature, over a wide range between 10^{-5}Hz to 10^2Hz.

Test specimens must be made to the dimensions 60mm x 8mm x 1.5mm. Flexural testing may only be performed on rigid materials although testing may be extended to less rigid materials in torsion. No restriction on d is quoted.

The main disadvantage of this method is the cost of the electronic equipment.

A similar method to the torsional test, but based on the Weissenburg Rheogoniometer, was considered for testing friction materials but rejected on the same grounds as for the torsion pendulum.
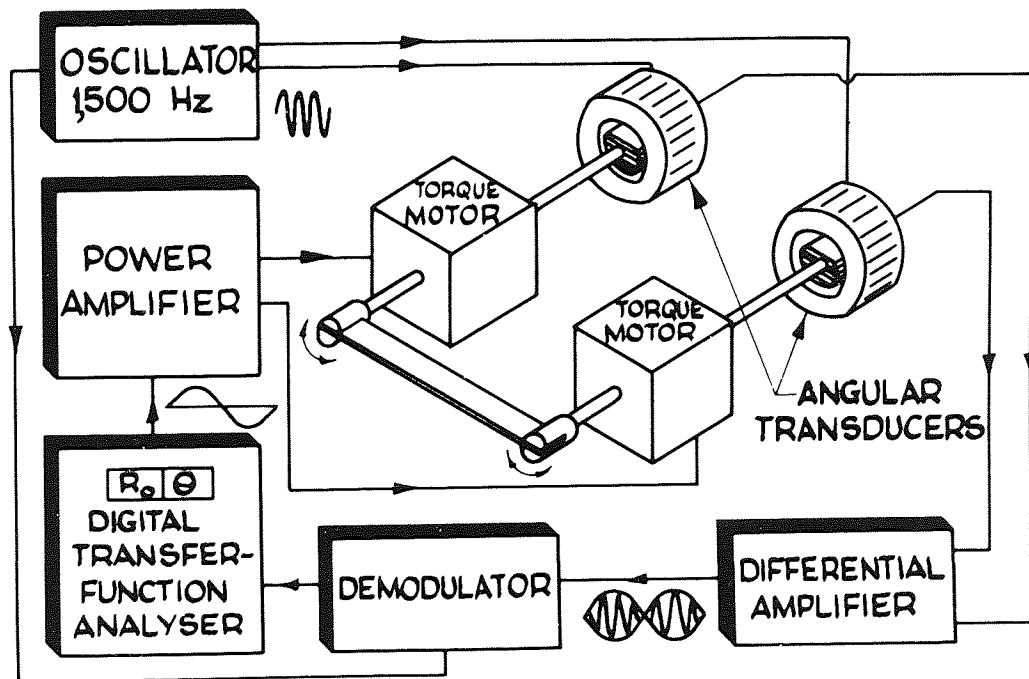
Fig. 20 The dynamic modulus analyser (showing the flexural test mode)

2.1.2.4 Shear Wave Propagation

Both continuous and pulse techniques may be used (see sect. 2.1.3.5), but the main disadvantage is that there is heavy attenuation of shear waves causing many experimental difficulties. A pure shear modulus is, however, determined.

2.1.3 Methods in Tension-Compression

2.1.3.1 Reverberation Method (decay method)

This is a method based on free vibration under normal forces but as it can only be used for determining damping factors it must be used in conjunction with a resonance method. It is of use when testing materials where $d < 0.01$ when the bandwidth method becomes inaccurate.

The test specimen is brought into resonance and then the exciting vibrations stopped. The amplitude of vibration decays in a manner analogous to the torsion pendulum and is recorded either on a chart or by timing a voltage drop on a meter or an oscilloscope.

The logarithmic decrement, $\triangle$, can thus be determined and the damping factor given by

$$d = \frac{\triangle}{\pi}$$

providing that $\triangle$ is small.

2.1.3.2 Resonant Flexural Vibrations

This method is simple in principle, although fairly complex electronic recording apparatus is often required, and has been used and developed by many workers (82,83,84). There are many forms of the test, which is often called the vibrating reed method, based on the same principle but differing in the mode of excitation as well as in the method of recording the resultant vibrations.

A rectangular specimen from the material to be tested is rigidly clamped at one end and brought into transverse vibration over a frequency range encompassing the resonant frequency. The specimen may be driven at the free end or at the clamp and the amplitude of the resultant vibration is plotted against frequency to give a resonance curve.

A commercial apparatus based on this principle is the "Complex Modulus Apparatus Type 3930" made by Bruel & Kjaer. The test jig is shown in Fig. 21. The specimen S under test may be clamped at one end or at both and excited from the side or underneath. The electro-magnetic transducers Pu 1 and Pu 2 can be used either for exciting the bending waves or as pick-ups for the resultant vibrations. The transducers supports K 1 and K 2 can move on a guide pillar L and the transducers can be locked in a given orientation by means of screws Vf 1, Vf 2, Hf 1, Hf 2, Vl 1, Vl 2, A 1, A 2.

Various forms of associated electronic equipment are available for providing the exciting vibration and for measuring and recording the resultant vibrations.

The method is based on the theory of standing waves, of the bending mode type, in straight beams clamped at one or both ends. When the beam is excited with a constant amplitude vibration, as frequency is increased the amplitude of the response vibration will show a series of maxima or resonances. Resonances of several different modes are possible ($n = 1,2,3\ldots\ldots$). The modes differ from each other in the number of nodes along the beam. By measuring the resonant frequency, f_n, and the dimensions of the beam the value of E' can be calculated

$$E' = \frac{48 \kappa \rho L^4 f_n^2}{B^2 K_n^2}$$

where ρ is the density.

L is the effective length.

B is the thickness.

K_n is a constant dependent on the mode number and the method of clamping. A list of values is given in the B&K manual for the apparatus.

Damping is determined by either the bandwidth method (see sect. 1.3.4.3) or the reverberation technique (see sect. 2.1.3.1) and can be measured between $d = 0.001$ and 0.2 although this may be extended to $d = 1$ if coated steel strips are used.

Determination may be made at frequencies up to 2kHz but above this

    i) the higher resonances merge into one another.

    ii) modes of vibration other than bending may be excited.

    iii) specimen lengths become so small as to be non-representative.

Several resonance peaks may be measured on one specimen at a given temperature to give up to about ten values of the dynamic properties which does to some extent alleviate the problem of the resonant frequencies being temperature dependent.

The main disadvantage of the B&K method is that for non-magnetic materials ferromagnetic masses must be attached to the specimen at the transducer points. An advantage is that it can be modified to measure fibres and films.
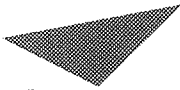
Fig. 21   The B&K Complex Modulus Apparatus Type 3930

2.1.3.3 Resonant Longitudinal Vibrations

This method is the most usual for studies at high frequencies (85,86). A commercial instrument based on this principle is the Dynamic Materials Tester marketed by Dawe Instruments Limited which is described here.

The basic instrument consists of a power oscillator, a test rig and an oscilloscope. The test rig provides central clamping of the specimen on needle points and two electrostatic transducers each mounted on a slider, one at each end of the specimen (see Fig. 22). One transducer is driven by the oscillator and serves as the driving transducer which excites the specimen into vibration which is detected by the pick-up transducer at the other end of the specimen. The signal from the pick-up transducer is amplified and fed into one channel of the oscilloscope and a direct signal from the oscillator is fed into the other channel. A d.c. bias is applied to both electrodes to prevent polarity changes at the drive electrode that would give rise to a double cycle vibration, and to provide a polarising voltage at the pick-up electrode which functions as a electro-static microphone.

Additional facilities available are a check facility for ensuring fundamental resonance by displaying a Lissajou's figure on the oscilloscope, provision for a frequency meter and a pulse producing circuit to pulse drive the specimen at a pulse rate of approximately one second with a multi-vibrator circuit to trigger the oscilloscope time base at each pulse thus enabling signal decay to be studied.

The tuner on the oscillator is manually varied until resonance is detected. The elastic components of modulus is calculated from the resonant frequency as follows:-

Velocity of sound in the specimen material, v, is given by

$$v = \sqrt{\frac{|E^*|}{\rho}} = f_n \lambda$$

where ρ is the density of the specimen material.

λ is the wavelength of the vibration.

At fundamental resonance

$$\lambda = 2L$$

hence

$$|E*| = (2f_n L)^2 \rho$$

Damping is found on the basic instrument by the bandwidth technique (see sect. 1.3.4.3). If the pulsing and multi-vibrator circuits are available the signal decay method (see sect. 2.1.3.1) may be utilised. This is achieved by means of a specially calibrated oscilloscope graticule which enables the time for the signal amplitude to drop to 1/e of its original value to be calibrated from the oscilloscope settings. The pulsing technique enables the decay to be continuously displayed due to the resilience of the oscilloscope.

Although this instrument with all the additional facilities enables measurements to be made over a wide range of frequencies (20Hz to 20kHz) over a wide range of damping ($d = 10^{-2}$ to 10^{-4}) it suffers several disadvantages.

i) All measurements are based on the oscilloscope, the calibration of which may easily become inaccurate after continual use. The thickness of the trace may also lead to inaccuracies.

ii) Calculation of the elastic modulus is based on the theoretical fundamental resonant frequency but the measured resonance is somewhat different (see sect. 1.3.4.4).

iii) No facilities are available for temperature variation.

iv) Central suspension could possibly modify the nature of the vibrations in the specimen.

v) Specimens are restricted to a cylindrical shape with dimensions between 280 mm long x 15 mm diameter and 150 mm long and 6 mm diameter. The electro-static transducers require either an electrical conducting specimen or one which has been coated with an electrical conductor at its ends and at the suspension point.
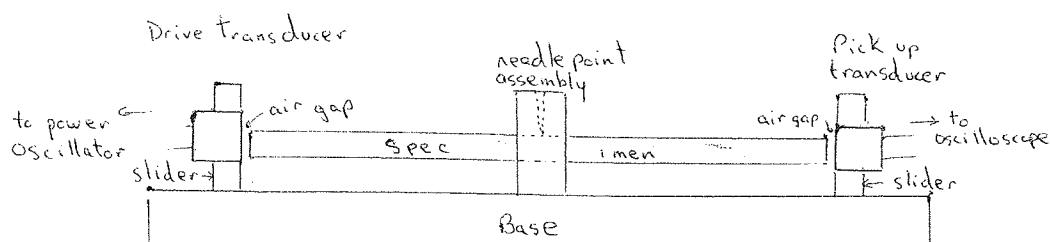
Fig. 22 The layout of the Dynamic Materials Tester test rig

2.1.3.4 Rheovibron (Mode 1 DDV II (B option)

This is a relatively new instrument developed in Japan by Professor

Motowa Takayanagi and marketed in this country by Sangamo Controls Limited.

It employs an electromagnetic vibrator to vibrate the specimen which is held

between two clamps which can be adjusted so as to tension the specimen.

Between the vibrator and the first clamp is a strain measuring transducer and

the second clamp is coupled to a stress measuring transducer. Both

transducers are based on strain gauges in bridge networks and for balancing

purposes a potential divider is connected to the output from each network.

For the strain network this comprises four fixed resistances and for the

stress network there is a calibrated variable potentiometer. There is also

a seven point divider on the input to the balancing meter.

In order to make a measurement the electrical output from the bridge

networks is balanced by means of these dividers. $\tan \delta$ = d is read directly

from the meter and from the settings on the dividers σ_o , γ_o and hence

$|E^*|$ may be calculated.

$$E^* = \frac{\sigma_c}{\gamma_c} = \frac{F_c L}{B\, D\, X_c}$$

where F_c is the amplitude of the force.

      L is the effective length.

      X is the amplitude of elongation.

also

$$F_c = \frac{N\, m}{K}$$

where N is a number which is dependent on the settings on the divider on the balancing meter; it is found from tables.

      K is a number found from the setting on the dynamic force potentiometric divider.

      m is a calibration factor $= 10^2\, N$

$$X_o = nAN$$

where A is a number dependent on the setting on the strain divider; it is found from tables.

      n is a calibration factor $= 5 \times 10^{-5}\, m$

$$|E^*| = \frac{2L}{AKBD} \times 10^6\, Nm^{-2}$$

For extreme accuracy an error constant, k, which accounts for displacement in the drive shafts, must be determined.

$$|E^*| = \frac{2L}{A(K - k)BD} \times 10^6\, Nm^{-2}$$

From $|E^*|$ and d, E' and E'' are easily calculated (see sect. 1.3.1.1).

The instrument is equipped with an environmental chamber and provision is made to vary measurements over four set frequencies: 3.5, 11, 35, and 110 Hz.

The outstanding advantage of this instrument is the fact that $\tan\delta$ may be read directly. There are, however, disadvantages:-

i) The cross sectional area of the specimen has to be within a given range for a certain modulus. This presents a problem with temperature scanning because as the modulus changes the cross sectional area may go out of the range of the instrument.

ii) The thickness of the specimens must not be greater than 1 mm, thus limiting measurements to fibres and films.

iii) Only four frequencies are available.

iv) The reading of $\tan\delta$ can be in error due to instrumental effects (e.g. resonance) and external effects (e.g. exterior vibrations).

2.1.3.5 Wave Propagation

If measurements are required at ultrasonic frequencies or for materials of high damping at high audio frequencies, wave propagation techniques must be used. There are two types of wave propagation commonly used.

i) Continuous

ii) Pulse

2.1.3.5.1 Continuous Wave Propagation

This method has been used by many workers (87,88) and involves determining the phase velocity, v_e, and the attenuation α of a sinusoidal stress wave travelling down a filament or rod of material. The basic layout of the apparatus is shown in Fig. 23.

The vibration source can be a piezoelectric crystal, a magnetostrictive rod or an electro magnetic vibrator depending on the frequency and power required. The vibration source propagates longitudinal waves down the specimen and the pick-up transducer, which is a low mass piezoelectric crystal probe, is moved along the rod to detect the nature of the vibration at various distances from the vibration source. The detected vibration is compared in amplitude and phase with the input vibration.

It is found that the amplitude decreases exponentially and the phase difference δ, increases linearly with the distance, x, between the vibration source and the pick-up transducer.
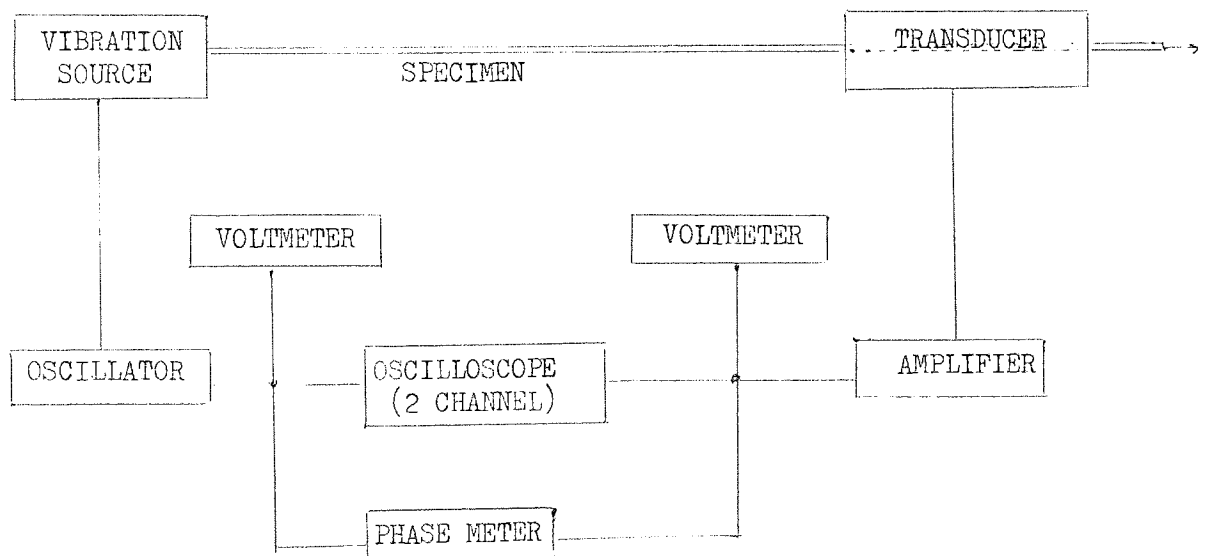
Fig. 23 Layout of continuous wave propagation apparatus

It is found that

$$K = \frac{\theta}{x} = \frac{2\pi}{fv_e}$$

where v_e is the phase velocity.

$$\alpha = \frac{\pi fd}{v_e}$$

where α is the exponential attenuation coefficient.

at $x = 0$ the vibration is characterised by

$$u = A \cos \omega t$$

after travelling a distance x

$$u = Ae^{-\alpha x} \cos \omega (t - x/v_e)$$

For damping

$$v_e = \sqrt{\frac{|E^*|}{\rho}}$$

where $|E^*| = \sqrt{(E')^2 + (E'')^2}$

By determining κ and α, E' and d may be determined for a range of frequencies.

The theory can be extended to account for reflections at the detector. Although this method is fairly simple there are limitations.

  i)   Fairly long specimens are required.

 ii)   Ultra-sonic equipment is expensive.

iii)   The upper frequency limit is approximately 50 kHz, because the wavelengths become too small for measurements to be made.

 iv)   At frequencies approaching 50 kHz there is the problem of velocity dispersion, which arises when the wavelength becomes comparable with the diameter of the specimen. This condition tends to produce an appreciable amount of shear waves with a velocity, v_s

$$v_s = \sqrt{\frac{|G*|}{\rho}}$$

where $|G*| = \sqrt{(G')^2 + (G'')^2}$

because $G < E$, $v_s < v_e$ and a low value is obtained for the modulus.

Thus to determine the pure extensional modulus at high frequencies only thin films or fibres can be used.

Alternatively large diatmeter specimens may be used and the longitudinal modulus, L, determined.

The longitudinal velocity, v_l, assumes ideal velocity dispersion and is given by

$$v_l = \sqrt{\frac{|L*|}{\rho}}$$

where $|L*| = \sqrt{(L')^2 + (L'')^2}$

If Poisson's ratio, ν , is known from other sources the extensional modulus can be calculated using

$$L = \frac{E(1 - \nu)}{(1 + \nu)(1 - 2\nu)}$$

2.1.3.5.2 Pulse Propagation

Above 50kHz the most usual methods involve ultrasonic pulse techniques, which have been used by several workers (89,90) at frequencies up to several megahertz.

High frequency wave-packets are transmitted through the bulk material and the time of transit and the attenuation of the pulse used to determine modulus and damping.

Disadvantages are three-fold:-

i)   The modulus determined is the longitudinal modulus.

ii)   A wave packet contains a narrow band of frequencies and

thus there is a group velocity different from the phase

velocity. As viscoelastic materials attenuate and disperse

vibrations there is some doubt as to the significance of the

transit time.

Table 3. The nature, limitations and potential for testing friction materials, of the most commonly used dynamic mechanical test techniques which employ sinusoidal stressing of rigid, bar shaped specimens (mention is made if the technique has wider applications).

N.B. Although all the shear testing techniques are rejected for testing friction materials, on the grounds that testing is performed on the wrong mode, the methods are still included since initially shear testing was considered suitable (see sect. 2.1.2.1.).

*   Where a commercial instrument is cited the information is applicable to that instrument and not to the method in general.

**   The potential for testing friction materials – where a method is not suitable, only the most significant reason is given although there may be others.

Free Vibration Techniques

	Torsion Pendulum (Nonius Pendulum)*
Testing mode	Shear
Nature of Specimens	Most solids
	20mm x 10mm x 200mm (max.)
	50mm long fibres (min.)
Frequency range	0.1Hz – 5Hz
Range of d	0.01 – 1.0
Other limitations	None
Potential**	Not suitable – wrong test mode

Table 3 (cont.)

Free Vibration Techniques (cont.)

Reverberation

Testing mode	Shear, flexural or tension - compression
Nature of Specimens	Most solids (shear)
	Rigid solids (flexural or tension - compression)
Frequency range	100Hz - 20kHz
Range of d	0.1 - 0.001
Other limitations	Requires a multivibrator - pulsing circuit for accurate work
Potential**	Suitable

Resonant Vibration Techniques

Barone & Giacomini's Apparatus

Testing mode	Shear
Nature of Specimens	Most solids
Frequency range	100Hz - 10kHz
Range of d	0.1 - 0.001
Other limitations	None
Potential**	Not suitable - wrong test mode

Vibrating Reed (B&K Complex Modulus Apparatus)*

Testing mode	Flexural
Nature of Specimens	Most solids including films, fibres and coatings

Table 3 (cont.)

Resonant Vibration Techniques (cont.)

	220mm x 12mm x 12mm (max.)
	75mm long fibres (min.)
Frequency range	10Hz - 2kHz
Range of d	0.1 - 0.001
	coating enables higher damping materials to be studied
Other limitations	Non-magnetic materials require ferro-magnetic masses
Potential**	Principle could be used but would not be very satisfactory because of frequency limitations

Longitudinal Resonance (Dawe Dynamic Materials Tester)*

Testing mode	Tension - compression
Nature of Specimens	Rigid solids
	280mm long x 15mm diameter (max.)
	150mm long x 6mm diameter (min.)
Frequency range	20Hz - 20kHz
Range of d	0.1 - 0.0001
Other limitations	i) Poor instrumentation
	ii) Specimens which are not electrical conductors require coating with a conductor
	iii) No facilities for temperature variation

Table 3 (cont.)

Resonant Vibration Techniques (cont.)

Longitudinal Resonance (Dawe Dynamic Materials Tester)* (cont.)

Potential**	This instrument could not be used because specimens of the required minimum length could not be produced, however the principle was suitable

Forced Vibration Techniques Without Resonance

E.R.D.E. Dynamic Materials Analyser*

Testing mode	Flexure or shear
Nature of Specimens	Fairly rigid solids (torsion test)
	Rigid solids (flexure test)
	One size 60mm x 8mm x 1.5mm
Frequency range	10 Hz – 100Hz
Range of d	Restrictions on d are not quoted
Other limitations	Cost of equipment
Potential**	Not suitable – maximum frequency too low

Rheovibron DDV II (B option)*

Testing mode	Tension – compression
Nature of Specimens	Fibres, films and very thin bars
	5mm x 1mm x 60mm (max.)
Frequency range	Four set frequencies: 3.5,11,35,110Hz
Range of d	0.001 – 1.7

<u>Table 3 (cont.)</u>   Forced Vibration Techniques Without
                              Resonance (cont.)

<u>Rheovibron DDV II (B option)*(cont.)</u>

Other limitations   i)   Errors may be caused by

                          instrumental and external effects

                    ii)   The permitted cross sectional

                          area of the specimen depends on

                          the modulus

Potential**   Instrument not suitable – maximum

                          frequency too low, but the principle

                          was thought suitable

Wave Propagation Techniques

<u>Continuous Wave Propagation</u>

Testing mode   Shear or tension – compression

Nature of Specimens Most solids (torsion test)

                     Long, thin specimens (tension –

                     compression test)

Frequency range   1kHz – 50kHz

Range of d   0.001 – 0.01

Other limitations   Problem of velocity dispersion at

                     high frequencies

Potential**   Not suitable – wrong test mode

                     (torsion test) and specimens

                     impossible to produce (tension –

                     compression test)

Table 3 (cont.)

<u>Wave Propagation Techniques (cont.)</u>

	<u>Pulse Propagation</u>
Testing mode	Shear or tension – compression
Nature of Specimens	Bulk material
Frequency range	20kHz – 10MHz
Range of d	0.001 – 0.01
Other limitations	i) Vacuum testing
	ii) Wave packets are not a single frequency pulse
	iii) In the tension compression test the modulus produced is the longitudinal modulus
Potential**	Not suitable – minimum frequency too high

2.2 The Design and Development of Equipment

2.2.1 The Need for a New Instrument

As previously explained the phenomenon of squeal in disc brakes involves radial flexing of the disc indicating that during a squealing braking operation the disc pad undergoes normal sinusoidal vibration in compression. The sound which is heard emanates from the disc and is most noticeable at frequencies between 3kHz and 15kHz.

In order to determine the dynamic mechanical properties of friction materials under relevant service conditions it is necessary to operate at a frequency between 3kHz and 15kHz, and to use a method which involves normal forces.

As indicated in the previous section all existing commercial test methods are unsuitable for one or more of the following reasons:-

i)   Mode of testing is in shear.

ii) Range of testing frequencies does not extend into the frequency band 3kHz to 15kHz.

iii) Method involves specimens which are

a) too long or too thick to be machined from a disc brake pad

b) too thin so as to be non representative of the friction material

c) made of non rigid material

It thus became necessary to design a test method which would satisfy the conditions for the mode and frequency of operation and take representative specimens machined from a disc brake pad. Ideally the test method should also be simple in operation, not require any elaborate setting up and be cheap in cost.

2.2.2 Selection of a Suitable Technique

If the squealing action at the pad is considered in detail, it will be realised that the pad is subjected to vibrations parallel to the circumference of the disc and which will be termed 'pressure bending waves' (see fig. 24).

From the review of test methods the most relevant techniques are:-

    i) Forced flexural vibrations without resonance (E.R.D.E. Dynamic Modulus Analyser).

    ii) Forced flexural vibrations with resonance (B&K Complex Modulus Apparatus).

    iii) Forced longitudinal vibrations without resonance (Rheovibron).

    iv) Forced longitudinal vibrations with resonance (Dawe Dynamic Materials Tester).

The flexural techniques initially were thought the most applicable but unfortunately were the most difficult to analyse precisely due to the degree of shear waves present. The forced flexural vibration without resonance technique had been discarded because the maximum operating frequency was too low with little chance of sufficiently increasing it. The resonant flexural technique also had been discarded because the maximum operating frequency for accurate results was only about 1kHz.

This left the longitudinal tests. If a longitudinal (pressure) wave passes down a bar shaped specimen, the specimen undergoes a sinusoidal pressure distribution down its length in a similar way to the pressure bending waves on the surface of the pad, but acting on both sides instead of one side as with pressure bending waves.

Longitudinal testing is thus justified. Flexural, longitudinal and pressure bending vibrations are shown in fig. 24.

Fig. 24   The Different Modes

of Vibration Indicating the

Pressure Distributions

i) Flexural Vibrations
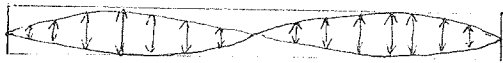
ii) Longitudinal (pressure) vibrations
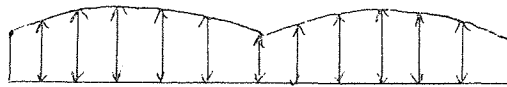
iii) Pressure bending vibrations on the surface

of a disc brake pad. (In practice there would

be only one anti-node at any instant in time)

Of the longitudinal vibration techniques the forced longitudinal

vibration without resonance was selected as the most suitable since

i) it is the most 'pure' technique from the theoretical point

of view because force, displacement and phase angle are all

measured directly.

ii) it is the easier technique to analyse and hence automate.

2.2.3 Development of a Forced Longitudinal Vibration

Without Resonance Technique

2.2.3.1 The Basic Concept

It was decided that the simplest approach to the problem was to build the testing rig in such a way that the specimen functioned as an inverted simple Voigt Model (see fig. 25). The Voigt Model theory should still hold however.
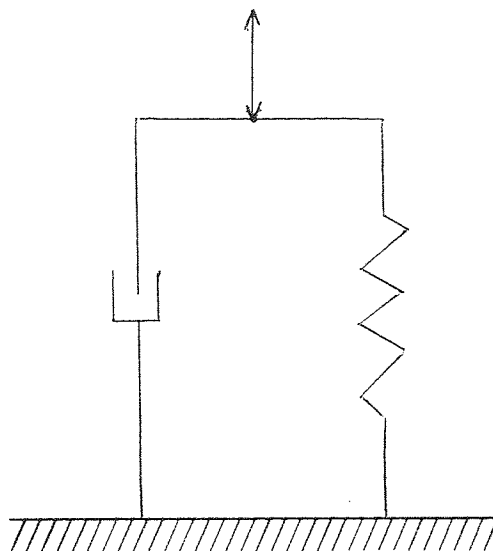
Fig. 25 The Inverted Voigt Model

The specimen would be clamped rigidly at the bottom end and clamped to the drive spindle of a vibrator at the top end. Thus in common with all forced vibration without resonance techniques the specimen was required to be clamped at both ends. It was also necessary to incorporate some method for measuring the force and displacement in the specimen.

     i) Measurement of force.

Initially it was thought that the driving force from the vibrator could be calculated from its power consumption but this proved rather unsatisfactory as it was realised that there would be considerable mechanical and electrical power losses between the electrical input and the mechanical output.

Next it was decided to clamp the bottom end of the specimen to a cantilever to which strain gauges were attached and which had been calibrated

statically by weights to give force readings. This proved rather tedious as the cantilever had to be rigidly secured but also isolated from external vibration. The cantilever itself also had to be very rigid so as to provide an earth for the bottom of the specimen, however this meant that the strain gauges produced readings indistinguishable from the inherent noise level of the strain gauge measuring bridge. Finally it was decided that a piezoelectric dynamic force transducer should be acquired and this proved the most suitable method of measuring force in the system since it was very small with a low mass.

ii) Measurement of displacement.

It was immediately realised that the best method for measuring displacement was by measuring acceleration by using a piezoelectric accelerometer and converting to displacement by integration.

The position and electrical circuitry associated with these transducers will be discussed later but it was hoped that with this system force and displacement could be measured directly and the phase difference between the signals from the force and displacement transducers also measured directly. Hence F_o, X_o and δ could be found giving

$$\sigma_o = \frac{F_o}{BD}$$

$$\gamma_o = \frac{X_o}{L}$$

$$\frac{\sigma_o}{\gamma_o} = |E^*|$$

$$E' = |E^*| \cos\delta$$

$$E'' = |E^*| \sin\delta$$

$$d = \tan\delta$$

2.2.3.2 Transducers

2.2.3.2.1 Piezoelectric Transducers

Vibration is usually measured by an indirect method using a calibrated system, generally consisting of a transducer, a signal conditioning stage and some form of display.

Most modern dynamic force and acceleration transducers are based on piezoelectric materials which generate an electrical output when subjected to mechanical stress. Piezoelectricity is a natural property of some monocrystalline materials such as Rochelle salt, tourmaline and quartz but these have been superseded by polycrystalline, artificially polarised ceramics like barium titanate, lead zirconium titanate and lead metaniobate.

The quality of peizoelectric transducers is dependent on the performance of the ceramic used for the sensing elements. The important factors are Curie point (the temperature at which the ceramic changes its crystal structure and loses its polarization), piezoelectric constant (sensitivity) and temperature stability.

There are several piezoelectric modes which can be used in transducer design but the most common is termed 'thickness expansion'. This provides high sensitivities, and a rugged transducer because the system is mechanically clamped. Force transducers which are designed to work in tension and compression are pre-compressed so as to produce a signal during tensioning.

Piezoelectric transducers produce signals which are a voltage across a high capacitative impedance which generates a charge. The signal can be processed by using either an impedance converter, together with a voltage amplifier, or a charge amplifier.

2.2.3.2.2 The Accelerometer

Accelerometers are the best method for determining displacement because of the following relationship.

The sinusoidal displacement equation is

$$X = X_0 e^{i\omega t}$$

Differentiating with respect to time

$$v = \dot{X} = X_0 i\omega e^{i\omega t}$$

where v is velocity.

Differentiating with respect to time

$$a = \ddot{X} = X_0 i^2 \omega^2 e^{i\omega t} = -X\omega^2 = 4\pi^2 X f^2 \simeq 40 X f^2$$

where a is acceleration.

Hence at 10kHz a very small displacement of 10^{-8} m which would be almost impossible to measure directly, gives an acceleration of approximately $40ms^{-2}$ which can easily be measured.

An accelerometer functions in the following manner. The transducing element consists of two piezoelectric discs on which rests a heavy mass. The mass is preloaded by a stiff spring and the whole assembly is mounted in a metal housing with a thick base. When the accelerometer is subjected to vibration the mass exerts a variable force on the piezoelectric discs. The force is exactly proportional to the acceleration of the mass. Due to the piezoelectric effect a variable potential will be developed across the two discs, which is proportional to the force and therefore to the acceleration of the mass. For frequencies much lower than the resonant frequency of the transducer, the acceleration of the mass will be virtually the same as the acceleration of the whole transducer, and the potential produced will therefore be proportional to the acceleration to which the transducer is subjected. This potential can be detected at the output terminals of the accelerometer and used for determination of the vibration amplitude, waveform and frequency.

From fig. 26 it can be seen that the stiff spring supported by the housing provides the force which preloads the mass. The isolating spring is designed to be slightly more flexible than the housing walls and thus the walls will have no influence on the operation of the accelerometer under normal conditions.
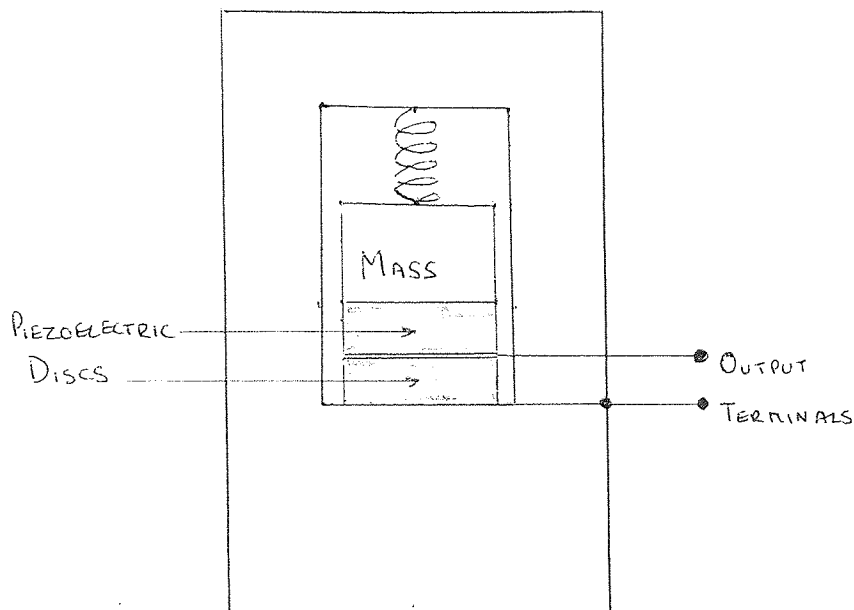
Fig. 26   Schematic Drawing of
an Accelerometer

The accelerometer selected for use in this study was Bruel & Kjaer type 4344, a lightweight mini-accelerometer with a low sensitivity to unwanted environmental excitations. Its low mass of only 2 grammes makes it suited to measurements on small specimens. It can be used to make measurements at temperatures up to $260^{o}C$, has a voltage sensitivity of $2.17mVg^{-1}$ (where g is the acceleration due to gravity) and has high accuracy at frequencies up to 14kHz.

2.2.3.2.3 The Force Transducer

The force transducer operates by simple application of the piezoelectric effect. The force transducer selected for use in this study was Vibrometer type 6QL 25 which again was a mini-transducer with a mass of 1.6 grammes and a sensitivity of $2,800$mVg^{-1}

2.2.3.3 The Electrical Circuit

The electrical components fall into two categories.

    i) Components concerned with the production of vibrations.

    ii) Components concerned with the measurement of vibrations.

2.2.3.3.1 Components Concerned with the Production of Vibrations

    i) The power oscillator

The power oscillator available was the Pye-Ling (now Ling Dynamic Systems) type P.O.5VA which is now obsolete, (names and addresses of suppliers will be found in appendix 1). It provides five watts of power over a frequency range of 5Hz to 20kHz and consists of an oscillator and a power amplifier combined. The signal produced is sinusoidal and frequencies are selected from four bands with fine tuning supplied by a slow motion drive.

A conventional full wave rectifier feeding a capacitive input filter with resistance smoothing provides the power supply common to both oscillator and amplifier.

The oscillator circuit is a Wien Bridge incorporating a thermistor for amplitude control.

The amplifier circuit consists of a double triode feeding a pair of tetrodes.

In addition to the main output, a socket was provided which was used to feed a constant amplitude signal directly into a frequency counter.

The only modification made to this instrument was the addition of

two potentiometers to provide very fine frequency and amplitude

controls.

ii) The frequency counter

It was realised that the calibrated dial on the power oscillator

would not be sufficiently accurate to enable frequency to be measured

from it, and thus a frequency counter was required. The frequency

counter available was the Venner Digital Counter type TSA 6636/2M, a

six digit counter with a store facility so that when the frequency controls

on the power oscillator are stationary the operating frequency is

continuously displayed.

iii) The vibration generator

The vibration generator selected was the Ling Dynamic Systems type 201

an electromagnetic vibrator, which cost £35.

The vibration generator functions by the interaction between a steady

magnetic field, produced by a permanent magnet; and an oscillating current

flowing in a moving coil. From Fleming's Left Hand Rule the force is

generated at right angles to the lines of flux and to the conductor carrying

the current. This force is the product of the instantaneous current and the

magnetic flux density.

The drive is derived from the output from the power oscillator. The

frequency of the movement of the drive spindle is the same as the frequency

of the oscillator signal while the amplitude of motion is proportional to

the signal amplitude.

The maximum frequency at which the vibrator will operate purely

sinusoidally is 10kHz.

2.2.3.3.2 Components Concerned with the Measurement of Vibrations

i) The amplification system

With piezoelectric transducers, as stated previously, amplification can be achieved in two ways

a) by using a charge amplifier

b) by using an impedance converter in conjunction with a voltage amplifier.

For extremely accurate measurements charge amplifiers are preferable because the capacitive effect of the cable from the transducer has no influence, whereas with impedance converters it must be taken into account. Unfortunately from the economic point of view approximately £350 for a two channel charge amplifier proved rather too expensive. Thus it was decided to invest in an impedance converter-voltage amplifier system for the two piezoelectric transducers and to allow for the capacitance of the cables in the calculations.

Since the phase difference between the two signals would ultimately be measured, it was imperative that there should be no phase shift in the amplifying system. Thus components should be either two channel devices or duplicated exactly for each channel.

Two identical impedance converters were supplied by K.F.L. Lansdowne & Company Limited at a cost of £21 each. These were F.E.T. pre-amplifiers which had an inherent gain of 9.9 dB and a maximum output level of 4.5 volts peak to peak. The only modification to these devices was the replacement of the electrolytic d.c. blocking capacitors by polyester capacitors which do not leak, although because of their reduced value the bandwidth of the devices was slightly reduced.

Voltage amplification was originally provided by two Levell 40dB amplifiers but unfortunately the maximum output from these devices was found to cut off at about 2 volts which was rather too low. Enquiries indicated that in order to obtain a reasonable output from a fairly simple system integrated circuits must be used. An examination of the literature on current ranges of two channel, high output amplifiers indicated that most amplifiers were too sophisticated, in that they were multi-range instruments, and the price was correspondingly high at £100 or above.

It was thus decided to build a two channel voltage amplifier and this was achieved, using integrated circuits, at a total cost of about £30. The circuit is shown in fig. 27. The integrated circuits used were R.S Components type 741 OPA a dual-in-line operational amplifier with a peak to peak output voltage of approximately 13 volts. The 741 operational amplifier has a high impedance input and a low impedance output and provides internal frequency compensation.

The amplifier circuit was designed so as to be non-inverting in each channel and phase difference between the two channels was adjusted so as to be as small as possible below 10kHz. Amplification was fixed at a gain of 100 below 10kHz in the amplifier giving a total gain of about 300 in the complete amplification system. Both phase difference and gain were monitored as a function of frequency for the complete amplification system see graphs 1 and 2.

The output from each channel was fed into a two channel oscilloscope, a milli-voltmeter and a phasemeter (see fig. 28).

ii) Voltage measurement

In order to determine the magnitude of the force and acceleration signals two Farnell type TM2 transistorised a.c./d.c. millivoltmeters were bought at a cost of £68 each. These millivoltmeters provide 12 d.c. and 12 a.c. voltage ranges from 1mV to 300V f.s.d. in a 1-3-10 sequence.
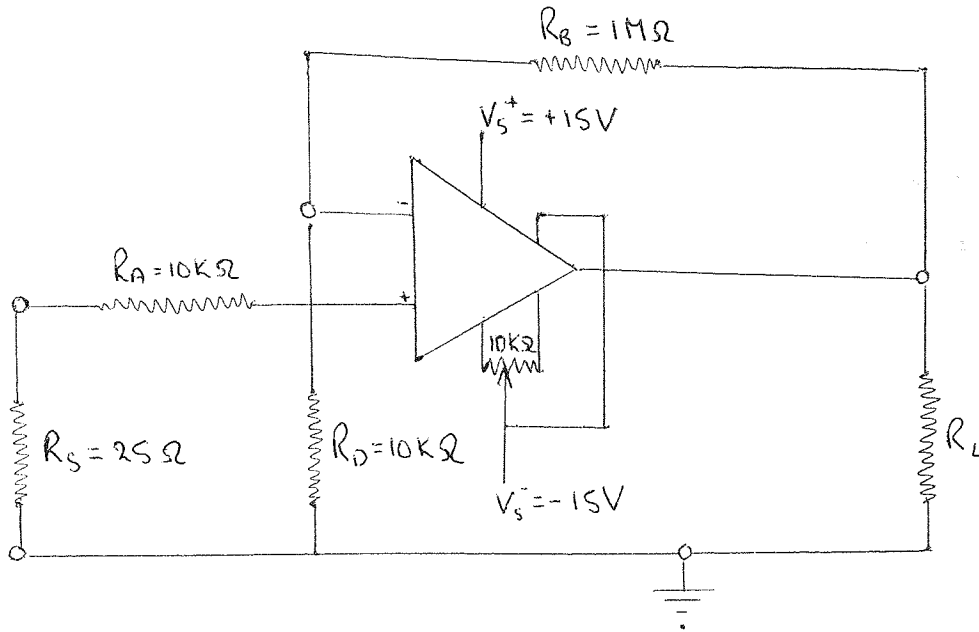
Fig. 27   Circuit for each channel of the amplifier to give a gain of 100
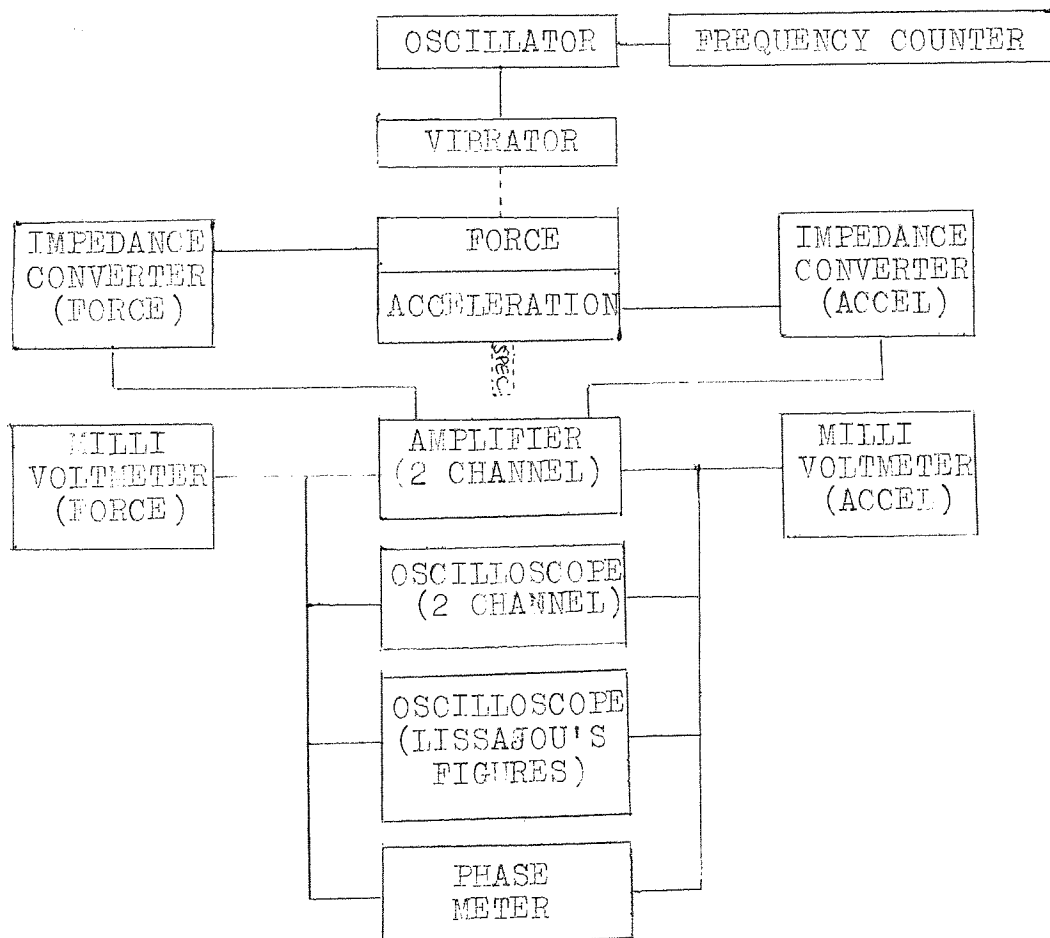
Fig. 28   Block diagram of electrical components in circuit

The a.c. scales are calibrated in volts r.m.s. for sinusoidal inputs, however, the instruments are mean rectified reading instruments. They can be used to measure a.c. signals at frequencies between 10Hz and 5MHz.

iii) Phase measurement

In order to measure the phase difference between the force and acceleration signals a Dawe type 632A phasemeter was purchased at a cost of £231. This instrument is a transistorised phasemeter which will measure the phase difference between two signal sources with frequencies between 50Hz and 100kHz and at amplitudes between 10mV and 10V. Direct reading of phase angle are given on four quadrant ranges (0°-90°,90°-180°,180°-270° and 270°-360°) and auxiliary ranges of 0°-360° or 180°-0°-180°. Each channel has a fully compensated input attenuator giving six voltage ranges from 30mV to 10V f.s.d., in a 1-3-10 sequence, as monitored on a panel voltmeter which can be switched to either channel.

iv) Oscilloscope display

It was decided that visual display of the signals should be in two forms. Firstly the waveforms should be displayed normally on a two channel oscilloscope so that any distortion could be observed. This was achieved by using a Telequipment type 43R oscilloscope.

Secondly the two signals should be fed into an oscilloscope, one on the x-axis and one on the y-axis so that a Lissajou's figure might be displayed. The only available oscilloscope was a two channel Telequipment oscilloscope type 43A with a time base circuit giving very limited x facilities. Inspection of the circuitry of this oscilloscope indicated that the connections on the cathode ray tube between the time base and one of the y-axes could be reversed. This was done so that the original two equivalent y channel amplifier circuits could be used to control the x- and y-axes over extensive ranges.

The advantage of being able to examine the Lissajou's figure is that it gives a quick indication of the phase changes over a wide frequency band as opposed to the phase meter which requires adjustment of the voltage selector before a reading is valid.

2.2.3.4 Design of the Test Rig

2.2.3.4.1 Principle

In common with all forced vibration without resonance techniques the test rig would involve travelling vibrations from the vibrator, passing down the specimen which would be clamped in position at both ends.

It was decided that the rig should be mounted in a frame-work, with the vibrator at the top end, and designed on the basis that vibrations from the vibrator drive spindle should be transmitted via a drive shaft to the top clamp, through the specimen to the bottom clamp and out via a second shaft to a dissipator block to absorb the vibrations. The measuring transducers could then be interposed between the top clamp and the drive shaft or between the bottom clamp and the lower shaft. It was also convenient to provide some kind of adjustment of the distance between the clamps in order that the apparatus might accept different size specimens.

2.2.3.4.2 Design of the Framework and the Dissipator

Initial attempts at constructing a framework were made using Dexion perforated angle but as this is relatively flimsy it was found that it gave rise to many spurious resonant vibrations. It was decided that a heavy rigid frame was required so as to have a single very low resonant frequency. This was constructed by bolting two lengths of 43mm. $\left(1\frac{5}{8}"\right)$ diameter pipe between two lengths of 105mm. $\left(4"\right)$ channel in the manner shown in fig. 29.

The vibrator was supplied in a swing mounting and the mounting was rigidly bolted centrally on the upper channel using "Nyloc" anti-vibration nuts.

The dissipator was simply a 76mm. (3") diameter steel block 51mm. (2") thick mounted on the bottom channel via three adjustable feet so as to provide a facility for levelling the block.

2.2.3.4.3 Design of the Clamps and Drive Shafts

The first requirement of the clamps was that they should be simple and be so constructed that a specimen could be inserted without disturbing the rest of the test rig. It was decided (see sect. 2.3.1.2) that specimens should be 6mm.x3mm. ($\frac{1}{4}$"x$\frac{1}{8}$") in cross section.

The first attempt at constructing a pair of clamps was as follows. The stationary part of each clamp was machined from a piece of 9.5mm. ($\frac{3}{8}$") diameter brass rod. 9.5mm. ($\frac{3}{8}$") of its length was turned down to 8mm. (5/16") and a 3mm. ($\frac{1}{8}$") slot cut through this turned down section. Thus an end of a specimen would slide into the slot with the forks down each side. Two rings 9.5mm. ($\frac{3}{8}$") deep were machined from brass with an internal diameter of 8mm. (5/16") and a piece of tube welded at right-angles to the side of each ring. The tubes and the side of each ring were sawn through and one half of each tube tapped with a 2BA thread. The rings could thus be slid on to the specimen which would be inserted between the forks, the rings pushed over the forks and tightened using a 2BA bolt.

Unfortunately it was found that this method of clamping added inbalance to the system and gave poor uneven clamping if a specimen was undersize.

In order to remedy these faults it was decided to replace the clamping rings with 9.5mm. ($\frac{3}{8}$") deep tubes of 8mm.(5/16") internal diameter with a 6BA threaded hole tapped in each side. Thus these tubes could be pushed up over the forks and 6BA screws tightened on to them.
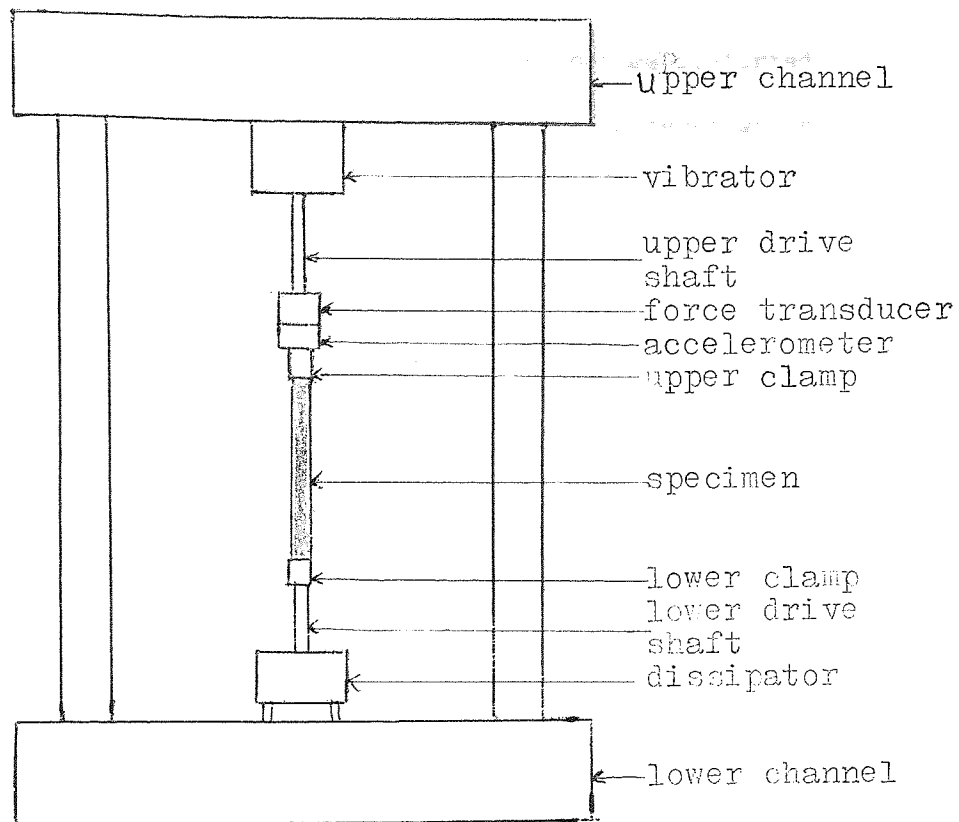
Fig. 29   Forced vibration without resonance test rig (schematic)
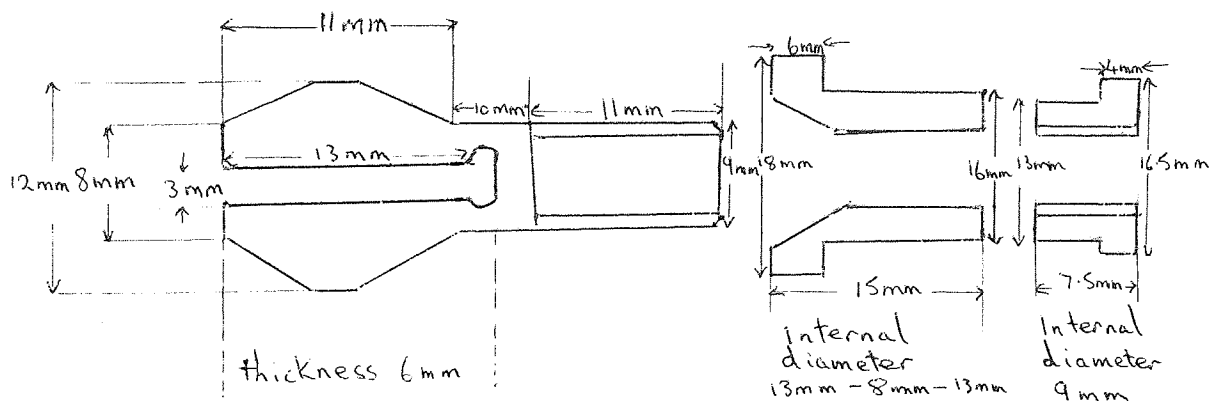
Fig. 30   Final clamp design

These clamps suffered the problem that the forks became distorted giving uneven clamping thus setting up localised stress patterns which could influence results. The degree of clamping force was also found to influence results.

A third type of clamp was devised using spring loading to give uniform and constant clamping forces but this was abandoned almost immediately because it was too heavy and cumbersome.

The final clamp design was made from Dural for lightness and involved a tapered fork and a sheath which could be pushed up the taper, by means of a knurled ring on a thread, so that the forks closed on the specimen (see fig.30).

This type of clamp gave even clamping forces with no distortion and because only finger tightness was used the clamping force was fairly constant.

The drive shafts are devices to transmit vibrations from one part of the test rig to another.

The vibrator had a 2BA hole tapped in the end of the drive spindle and the top drive shaft was a length of 9.5mm. ($\frac{3}{8}$") diameter brass rod, turned down and threaded with a 2BA die at the end.

It was decided that the lower drive shaft should be included in the clamp adjustment assembly. This was manufactured by drilling a 16mm. ($\frac{5}{8}$") diameter hole through the centre of the dissipator block and inserting 105mm. (4") of 16mm. ($\frac{5}{8}$") diameter steel rod down this hole. The top and bottom 38mm. ($1\frac{1}{2}$") of the rod were threaded and lock nuts fitted so that the rod could be held in position in the block with variable lengths protruding.

2.2.3.4.4 Position and Mounting of the Transducers

The first idea was to have the accelerometer at the top end of the specimen and the force transducer at the bottom end.

The end of the upper drive shaft was drilled out and the accelerometer pushed into it so that the accelerometer housing was a tight fit inside it. The accelerometer had a 6BA hole tapped in the base and this was mounted to the top clamp by means of a 6BA stud welded to the top of the clamp.

The force transducer had two undesirable features:-

    i) There were no threaded mounting points, only a flange round the housing.

    ii) The output socket was at the bottom of the transducer unlike the accelerometer which had a side output socket.

In order to mount the force transducer on the top of the lower shaft, the shaft was drilled out to take the base of the transducer and a hole drilled right through the shaft to take the output lead. A nut was manufactured with an internal flange at the top so that it could be screwed on the shaft and tightened down on the force transducer flange.

A brass stud was soldered to the load bearing face and screwed to the bottom clamp.

Unfortunately this system proved unsatisfactory because spurious resonances were produced making measurement of phase angle impossible. It was also thought that the force transducer signal might be shifted in phase relative to the accelerometer signal by effects not due to the specimen.

It was hoped that moving the force transducer to above the accelerometer might remove the spurious phase shifts and an attempt was made to stiffen up the system to reduce the chance of resonance.

Mounting the force transducer above the accelerometer was fraught with difficulties. The force transducer was enclosed in a sheath and clamped as before by screwing down a nut on to the flange on the transducer housing. A hole was drilled in the side of the sheath to take the output lead.

The accelerometer housing was pressed into the bottom end of the sheath.

The accelerometer was mounted on the top clamp as before and the force transducer soldered to a remade drive shaft without the end drilled out. The bottom clamp was mounted on the lower shaft by means of a flange welded on the underside of the clamp so that the flange fitted under the lock nut which originally held the force transducer.

This arrangement (see fig. 29) still gave rise to spurious resonances especially in the region 1kHz to 10kHz which was of particular interest. Unfortunately every time a resonance occurs phase angles and amplitudes are meaningless for the determination of dynamic mechanical properties.

It was decided that it would be impossible to remove all the spurious resonances in the region of interest unless considerable simplification and stiffening of the transducer and clamping systems could be made. This was not possible as transducers with threaded end mountings were required and these were not available. Consequently the forced vibration without resonance technique was abandoned.

2.2.4 Development of a Forced Longitudinal Vibration with Resonance Technique Using Two End Clamping and Separate Force and Acceleration Transducers.

2.2.4.1 The Basic Concept

It was decided that in view of the failure of the forced vibration without resonance technique because of spurious resonances the forced vibration with resonance technique would have a better chance of success.

It was thought that the best approach to the problem was to keep the test rig the same as before, apart from the addition of mass to the upper clamp, so that the mass of the upper clamp, the transducers and the added mass together with the specimen functioned as an inverted Voigt model with added mass (see fig. 31).
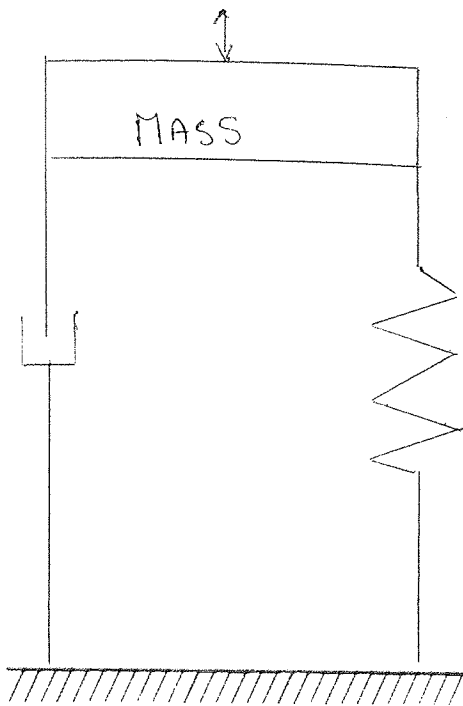
MASS

Fig. 31 The inverted Voigt model with added

mass

Determination of dynamic mechanical properties from the

fundamental resonance of a specimen involves examination of the shape

and position of the resonance peak produced by measuring acceleration

amplitude at constant force amplitude over the relevant frequency range.

For a linear material the resonance peak is Gaussian in shape and the

degree of damping in a material can be determined by using the bandwidth

technique (see sect. 1.3.4.3). The bandwidth technique in its simplest

mathematical form involves plotting the resonance peak under constant

force conditions. From this plot the maximum acceleration amplitude

$(a_0 max)$ is measured and $a_0 r.m.s. = a_0 max/\sqrt{2}$ calculated. The frequency

of maximum acceleration (f_0) and the frequencies at which $a_0 = a_0 r.m.s.$

$(f_2$ and $f_1)$ are found from the plot of the resonance peak and the damping

factor is given by $(f_2 - f_1)/f_0$. As indicated measurement of damping

using the bandwidth technique does not require knowledge of displacement

and thus no integration of the acceleration signal is required.

Obviously if each determination of damping involved manual plotting

of the resonance peak this would be a very time consuming technique.

Automatic plotting on a chart recorder is possible, but a feedback from

the force transducer to a compressor circuit which controls the amplifier

on the oscillator must be used to keep the force amplitude at a constant

level. The compressor circuit acts in such a way that if the amplitude

of the force signal increases from a reference level, the amplitude of

vibrations is instantly reduced until the amplitude of the force signal

has fallen to the reference level and if the amplitude of the force signal

falls the reverse happens.

As the introduction of a compressor circuit would involve severe

modification to the power oscillator it was felt that it would be wiser

to try to find another way of avoiding manual plotting until such time

as the method was firmly established.

Because the signal voltage from each transducer can be measured

on the two millivoltmeters it is possible to determine the frequency

at which a given ratio of acceleration amplitude to force amplitude is

obtained. It will be appreciated that the ratio of amplitudes is exactly

the same as the ratio of the measured r.m.s. voltages from the voltmeters.

For the sake of brevity in the following dissertation the term 'voltage'

will be used to mean r.m.s. voltage and from the theoretical point of view

to indicate the magnitude of the actual force or acceleration amplitude.

Effectively it is the force required to keep a vibration at a given

level which drops to a minimum at resonance so that under constant force

conditions a maximum value of acceleration amplitude is achieved. Thus if

the oscillator tuner is scanned through the resonance frequency

(indicated by the phase of the two signals changing from approximately

180° out of phase through 90° to approximately in phase or vice versa)

the needle of the voltmeter measuring the force voltage will pass through

a minimum and the frequency at which this occurs is f_o (note that f_o is

not the frequency at which the phase difference between the two signals is 90° which is f_{n}, see sect. 1.3.4.4). If the force voltage is now set to a reference value F_{ref}, a_{max} $(\equiv a_{o\ max})$ can be read from the voltmeter measuring acceleration voltage. The value of $a_{r.m.s.} = a_{max}/\sqrt{2}$ $(\equiv a_{o\ r.m.s.})$ can be found from previously constructed tables. By tuning to frequencies above and below f_{o} the frequencies at which the force voltage is F_{ref} when the acceleration voltage is $a_{r.m.s.}$ can be determined (f_{2} and f_{1}). Hence damping may be found from the relation $(f_{2} - f_{1})/f_{o}$ (see fig. 32).
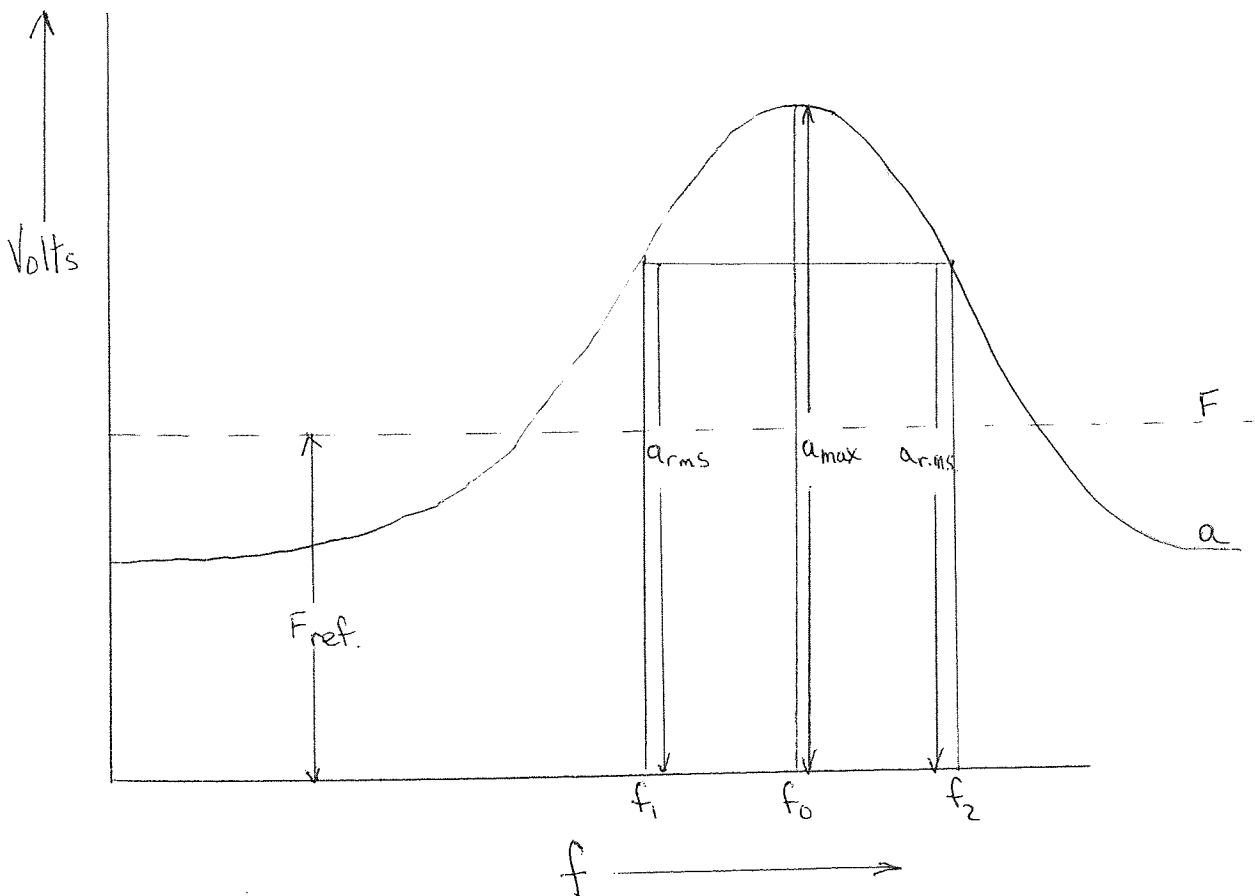
Fig. 32   Diagramatic representation of the measurements made when employing the bandwidth method

The elastic component of the extensional modulus is found from a knowledge of the dimensions of the specimen, the mass above it and the position of the true resonant frequency f_n (the frequency at which the phase difference between the two signals is 90°). The relationship between these properties is derived in the following ways:-

Extensional modulus is given by

$$E' = \frac{\sigma}{\delta} = \frac{FL}{BDX}$$

If k' is the force to produce unit displacement then

$$E' = \frac{k'L}{BD} \qquad \dots\dots\dots\dots\dots\dots\dots\dots\text{eq. 2.2.4.1.1}$$

However

$$f_n = \frac{1}{2\pi}\sqrt{\frac{k'}{M}} \qquad \dots\dots\dots\dots\dots\dots\dots\text{eq. 2.2.4.1.2}$$

Substituting in equation 2.2.4.1.1 for k

$$E' = \frac{4\pi^2 f_n^2 M L}{BD}$$

where M is the added mass.

This relationship holds well if the mass of the specimen is negligible compared with the added mass.

Because the added masses in the test rig were comparable to the mass of the specimen equation 2.2.4.1.2 has to be modified to one third of the mass of the specimen (91).

$$f_n = \frac{1}{2\pi}\sqrt{\frac{k'}{M + \frac{1}{3}M_s}}$$

where M_s is the mass of the specimen.

Substituting in equation 2.2.4.1.1.

$$E' = \frac{4\pi^2 f_n^2 L(M + \frac{1}{3}M_s)}{BD}$$

Hence

    i) If the values of k, M_s, L, B and D remain constant, f_n decreases with increase in M and $f_n(M + \frac{1}{3}M_s)$ has a constant value.

ii) If the values of k, $(M + \frac{1}{3}M_s)$, Band D remain constant, f_n decreases with increase in L and $f_n L$ has a constant value.

iii) If the values of k, $(M + \frac{1}{3}M_s)$, and L remain constant, f_n decreases with decrease in B.D and f_n/BD has a constant value.

Hence the position of the true resonance can be altered by either changing the dimensions of the specimen or by adding or subtracting from the added mass. Obviously changing the dimensions of the specimen is undesirable as it is an irreversible process. However, the technique of adding or subtracting from the added mass provides a useful method of testing the same specimen over a range of frequencies.

2.2.4.2 Design of the Test Rig

As previously stated the test rig was unaltered apart from the addition of mass to the upper clamp. It was felt that it would be better if the complete test rig assembly could be left intact during changing of the added mass in case disturbing the assembly should affect the results.

The most convenient method of achieving this was to manufacture the added masses as semi circular shells so that they clamped round the sheath on the upper clamp. These were constructed from different diameter brass rods by drilling out a 9.5mm($\frac{3}{8}$") diameter hole through the centre of each rod and cutting 9.5 mm ($\frac{3}{8}$") and 6 mm ($\frac{1}{4}$") lengths of each rod. Each annulus was then sawn in half along a diameter and 1.5 mm(1/16") brass tabs welded on each shell on the saw cuts so that they protruded each side of each shell. The protrusions were drilled through and tapped with a 6BA thread. Thus the shells could be placed each side of the sheath and clamped into position using 6BA screws.

A further modification was required when the first measurements were taken. It was found that there was too much interference from

external vibrations in the laboratory. The vibrations, which caused

oscilloscope traces to be poorly defined and meter needles to be

unstable, were transmitted in two ways:-

    i) Through the bench of the test rig.

    ii) Through the air as pressure waves to the test rig.

The first idea to combat these external vibrations was to mount the

test rig on rubber antivibration mountings but this removed only the

larger vibrations. The second idea was to hang the test rig from an

overhead beam. This was accomplished by making two slings from rubber

tubing to fit around the upper channel of the test rig and suspending

these slings from an overhead beam by thick string. This method worked

very well as it provided complete isolation from bench vibrations and the

rubber slings helped to dampen any air-transmitted vibrations which

reached the framework. The final assembly with an added mass in

position is shown in fig. 33.
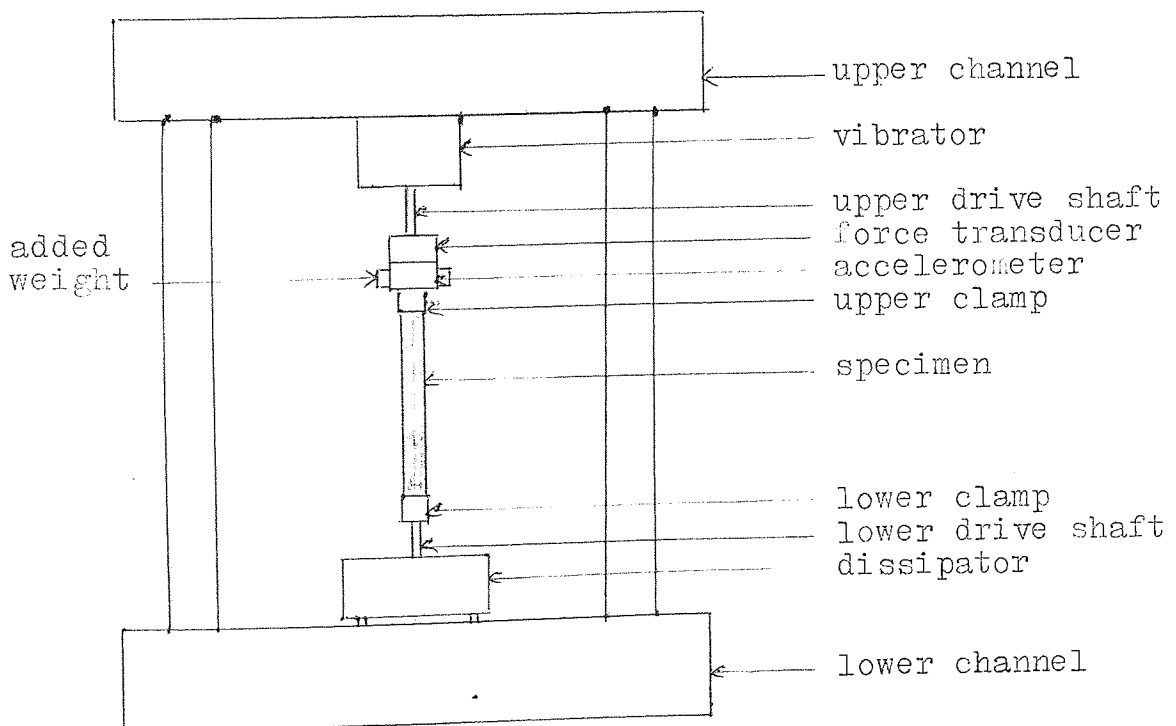
Fig. 33   Forced vibration with resonance, using two end clamping, test

rig (schematic)

2.2.4.3 Commissioning Experiments

The mass above the specimen was found to be 20.5g and it was found that specimens measuring 70mm x 6mm x 3mm ($2\frac{3}{4}$" x $\frac{1}{4}$" x $\frac{1}{8}$") gave resonances at frequencies of about 5kHz i.e. in the middle of the required frequency range.

Weights were added and it was found that the relation $f_n^2 \left(M + \frac{1}{3}M_s\right)$ remained constant as expected.

However, it was found that during mounting of specimens in the clamps, the soldered joint between the force transducer face and drive shaft was prone to breakage and when this was repaired the position and shape of the resonance peak were liable to change. This change was attributed to a change in linearity in the system but it was almost impossible to maintain the same degree of linearity each time breakage occurred. It was also realised that any air gap in the soldered joint would increase the damping in the system.

A second source of error was the fact that there was a lack of rigidity in the system and if a specimen was removed from the clamps and then replaced a change in the results was sometimes noted and this was attributed to a degree of twist in the sample caused by the clamp jaws being misaligned during the screwing down of the thumb screw on the clamp.

A third problem was that of spurious resonances. It was found that with some added masses the fundamental resonance occurred at a frequency near that of a spurious resonance and when this occurred the fundamental resonance peak became very distorted from the ideal Gaussian shape causing damping measurements to be meaningless.

For these three reasons it was decided to abandon this method.

N.B. If the assembly had remained intact and in the same configuration throughout all possible testing any nonlinearity effects would have remained

constant and although the results would be in error relative to other methods comparison between specimens tested on this equipment would have been valid.

2.2.5 Development of a Forced Longitudinal Vibration With Resonance Technique Using One End Clamping and an Impedance Head Transducer

2.2.5.1 The Basic Concept

It was thought that the problems of nonlinearity and rigidity using a two end clamping technique could be overcome if only one end of the specimen was clamped and the other end allowed to take up its own configuration.

It was thought that the best approach to the problem was to redesign the test rig completely by inverting the force and accelerometer transducer assembly and removing the lower clamp and dissipator together with the adjusting device. In this manner measurement of force could be made as close to the upper end of the specimen as possible so that there was a minimum of mass between the force measuring face and the end of the specimen which would contribute to the force measured. Additional masses could be attached to the lower end of the specimen so that the specimen and added mass would function as a Voigt model with added mass. However, because the vibration source and the transducer were at the suspension instead of at the free end, some modification of the theory was required (see sect. 2.2.5.2).

During the formulation of ideas regarding this technique information was received regarding a new transducer marketed by Bruel & Kjaer, known as an impedance head, which had just become available. This transducer was a combined accelerometer and force transducer, mounted in one housing with screwed mounting points at each end and output sockets at the side.

Obviously this was the ideal transducer for use in the test rig!!

The impedance head cost £114 and is described in detail in section
2.2.5.3.

2.2.5.2   Theory of Operation

Consider a Voigt model with added mass being driven at its point
of suspension so that the point of suspension is moving with a
displacement $j = j_0 \sin \omega t$.   This imparts a displacement X, at the bottom
of the model (see fig. 34).
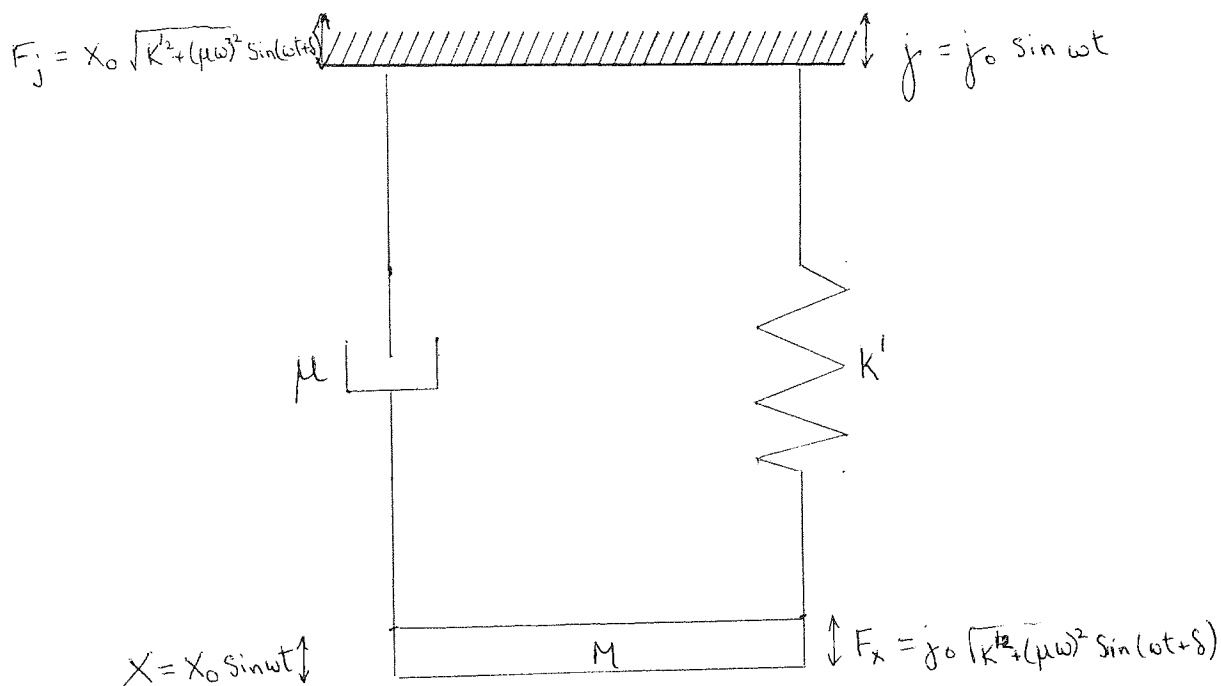
Fig. 34   Forces and displacements at the extremities of a Voigt model
with added mass, vibrated at the point of suspension

The actual displacement, y, of the lower end of the model with
respect to a fixed point is the difference in the displacements at
the bottom of the model and at the suspension.

$$y = X - j$$

The actual velocity, $\dot{y}$, of the lower end of the model with respect to a fixed point is the difference in the velocities at the bottom of the model at the suspension.

$$\dot{y} = \dot{X} - \dot{j}$$

The actual acceleration, $\dot{y}^{\bullet}$, of the lower end of the model with respect to a fixed point is the acceleration imparted to the bottom of the model.

$$\dot{y}^{\bullet} = \dot{X}^{\bullet}$$

From classical vibration theory

$$M\dot{y}^{\bullet} + \mu\dot{y} + ky = F_y \quad \dots\dots\dots\dots\dots\dots\dots\text{eq. 2.2.5.2.1}$$

where F_y is the external force which in this case is zero.

$$M\dot{X}^{\bullet} + \mu(\dot{X} - \dot{j}) + k(X - j) = 0$$

Rearranging

$$M\dot{X}^{\bullet} + \mu\dot{X} + kX = \mu\dot{j} + kj$$

$$= j_0(\mu\omega\cos\omega t + k\sin\omega t)$$

$$= j_0\sqrt{k^2 + (\mu\omega)^2}\sin(\omega t + \delta)$$

Comparing with equation 2.2.5.2.1

$$j_0\sqrt{k^2 + (\mu\omega)^2}\sin(\omega t + \delta) = F_x$$

Hence the magnitude of F_x, the force at the lower end of the specimen is governed by the magnitude of j_0.

Considering the suspension point in a similar manner the actual displacement, w, the actual velocity, $\dot{w}$, and the actual acceleration $\ddot{w}$ relative to a fixed point are given by the following equations:-

$$w = j - X$$

$$\dot{w} = \dot{j} - \dot{X}$$

$$\dot{w}^{\bullet} = \dot{j}^{\bullet}$$

The equation of motion is

$$M\dot{j}^{\bullet} + \mu\dot{j} + kj = X_0\sqrt{k^2 + (\mu\omega)^2}\sin(\omega t + \delta) = F_j$$

Hence the magnitude of F_j, the force at the suspension point, is governed by the magnitude of X_0.

At resonance at the lower end of the model, X_o is at a maximum and F_{xo} is at a minimum (from the theory of the Voigt model with added mass) but at the suspension F_{jo} is at a maximum because X_o is at a maximum and j_o is at a minimum because F_{xo} is at a minimum. Also the phase angle between j and F_j is the same as between X and F_x.

A further effect of vibrating and measuring at the suspension point is that the effect of damping causes f_o to occur at a lower instead of higher frequency than f_n when measuring accelerations.

Fig. 35   The construction of the impedance head

Since the measurement of force and acceleration is made at the suspension point, the acceleration voltage is kept at a reference level (a_{ref}) and F_{max}, f_o, f_λ and f_1 determined from the variation in force voltage in a similar way as for the two end clamping method.

2.2.5.3 The Impedance Head

The impedance head selected was the B&K type 8001 consisting of an accelerometer and a force gauge built together in a common titanium housing. An important feature of the construction is that the force gauge is located very close to the driving point. To achieve a very high stiffness and a low mass below the force gauge the driving platform is made from beryllium. The driving end is sealed with silicone rubber so that the impedance head can be used at any humidity. The output sockets are side mounted and accept the standard B&K mini coaxial cables. At both the mounting end and at the driving end there is a 2BA threaded hole.

The accelerometer has a voltage sensitivity of $25Vg^{-1}$ (where g is the acceleration due to gravity) and the force gauge has a voltage sensitivity of $330mVN^{-1}$. The impedance head may be used at frequencies up to 15kHz; above this frequency the natural resonance of the impedance head complicates measurements. The maximum temperature quoted in B&K literature at which the impedance head may be used is $260^\circ C$ although a private communication with B&K indicated that temperatures up to $300^\circ C$ could be used with little risk. The total mass of the transducer is 28g but the mass below the force gauge is only 1.0g. The construction of the impedance head is shown in fig. 35.

2.2.5.4 Basic Design of the Test Rig

In redesigning the test rig the intention was to have as few components as possible giving the minimum number of joints at which spurious resonances might occur.

The upper drive shaft was eliminated and the mounting end of the impedance head linked to the vibrator via a stainless steel coupling with a 2BA thread at each end. The driving end of the impedance head was connected to the clamp by use of a similar coupling. The dissipator block, the drive shaft and the lower clamp were removed completely so that the specimen could be suspended from the clamp without hindrance at the lower end.

Initial tests indicated that with a clamp and coupling 44mm $\left(1\frac{3}{4}"\right)$ long and mass 11gm holding a specimen 70mm $\left(2\frac{3}{4}"\right)$ long and mass 3gm, the results obtained would be considerably influenced by the properties of the clamp and coupling. It would be very difficult to design an effective clamp which could be regarded as negligible in mass and length compared to the specimens and thus it was decided to abandon the clamp in favour of mounting studs which could be glued on the end of each specimen and screwed directly into the impedance head. The mounting studs chosen were 6mm $\left(\frac{1}{4}"\right)$ 2BA brass countersunk screws which weighed approximately 1.01g. The specimens were glued on the screw head using standard Araldite (the mounting operation is described in section 2.3.3.3).

Even using mounting studs introduces some error because with 6mm of brass and 70mm of specimen the resonant frequency is approximately 92% due to the specimen and 8% due to the brass stud but providing the specimen length is reasonably constant the error in the modulus is reasonably constant. Brass is almost totally elastic and thus the energy lost will be almost totally due to the specimen so that the measured damping factor will be fairly accurate.

The mass below the force gauge not due to the specimen is 2.01g with 1.0g due to the driving platform and 1.01g due to the mounting stud. This is clearly significant compared with a specimen of mass 3gm and so a device which would compensate for the mass not due to the specimen had to be connected into the electrical circuit. The mass compensation device is described in the following section.

N.B. With some materials it would be possible to machine a 2BA thread directly on to the end of the specimen and so eliminate nearly all of the errors. The friction materials used were so brittle that there would have been considerable risk of specimens breaking off inside the transducer.

2.2.5.5 The Mass Compensation Device

The resonant frequency of the impedance head with only the mounting stud in position is well above the required experimental range. Below resonance this assembly will produce two signals which are 180° out of phase. Therefore a compensation voltage can be obtained by passing a signal from the accelerometer through a variable voltage divider and adjusting the divider until the voltage obtained is equal to the voltage from the force gauge. When this compensation voltage is then added to the force voltage the resultant is zero because the two signals are 180° out of phase. Any force signal obtained when a specimen is in position is now solely due to the specimen.

The mass not due to the specimen below the force gauge is somewhat frequency dependent. It becomes more and more influenced by the mass of the piezoelectric discs as frequency increases and so a variable voltage divider is required to optimise compensation at a given frequency (see graph 3).

The mass compensation unit was built in the laboratory and its circuit is shown in fig. 36. A revised block diagram of the layout of the electrical components is shown in fig. 37 and a photograph of the instrumentation is shown in fig. 38.

2.2.5.6 Temperature Variation

Because the disc pad surface in contact with the disc may reach $600^{\circ}C$ under adverse conditions (2), it is important to determine the effect of elevated temperatures on the dynamic mechanical properties of friction materials.

Initially this was accomplished by carrying out testing in an environmental cabinet. Because the testing compartment had no facility for suspension of the test rig, a frame was built from 25mm (1") square tube (see fig. 39) so that the test rig could be suspended from it and the whole assembly fitted in the testing compartment.

The environmental cabinet offered facilities for testing at temperatures between $-20^{\circ}C$ and $+80^{\circ}C$ and at humidities from 0% to 100%. There were however, two drawbacks:-

i) The maximum temperature attainable was far too low but in any case it was realised that the vibrator would most certainly be damaged by higher temperatures.

ii) The effects of a high water content in the air at elevated temperatures was found to be detrimental to the equipment and also produced errors in the results if condensation occurred on the specimen. It was decided that testing at various humidities should be abandoned and instead the effect of absorbed water in the friction material would be investigated.
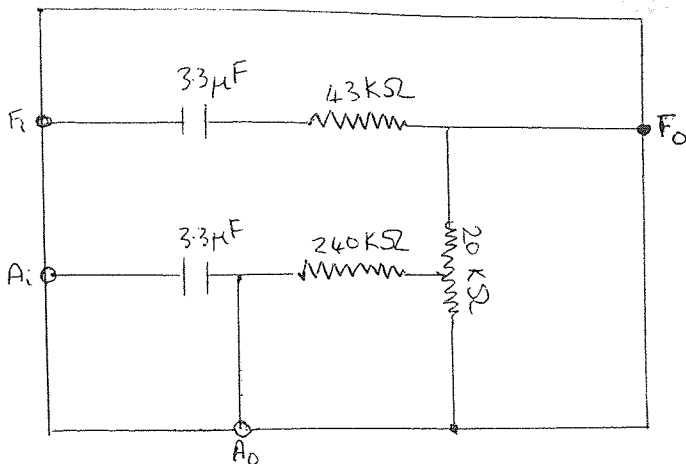
Fig. 36   The mass compensation device
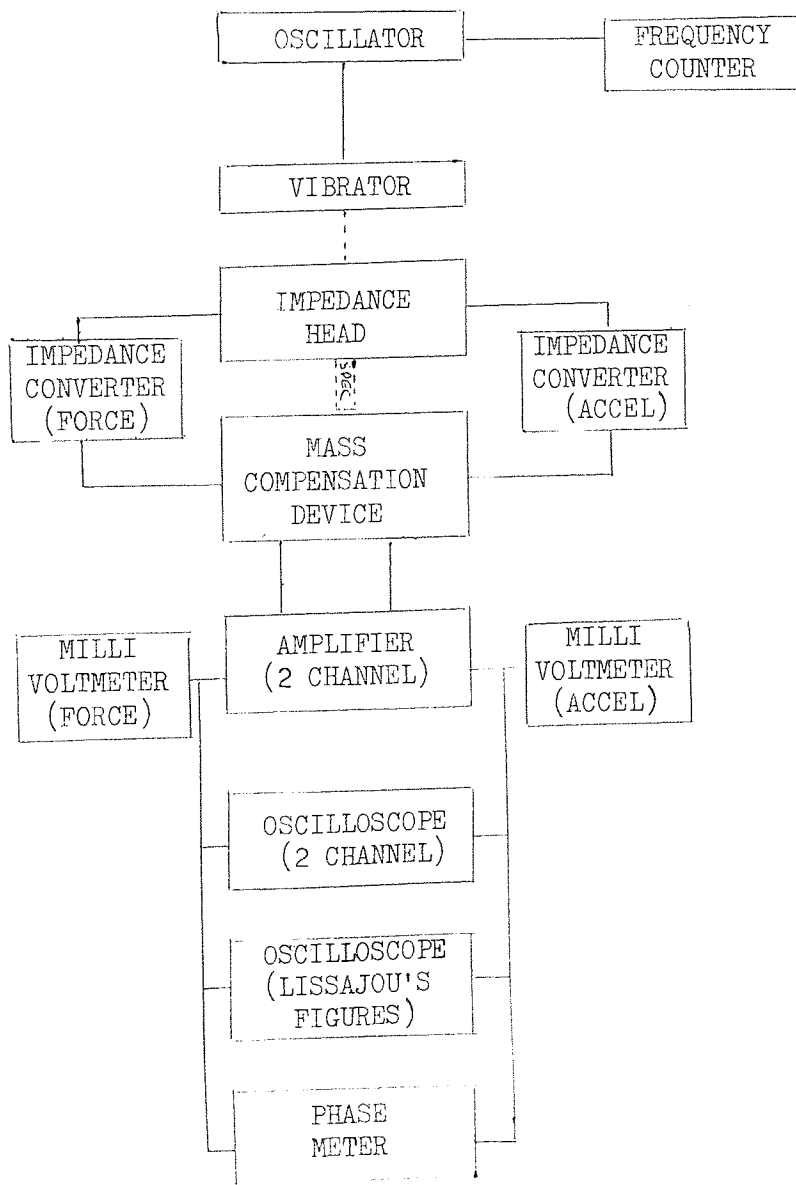
Fig. 37   Block diagram of electrical components in circuit (final)
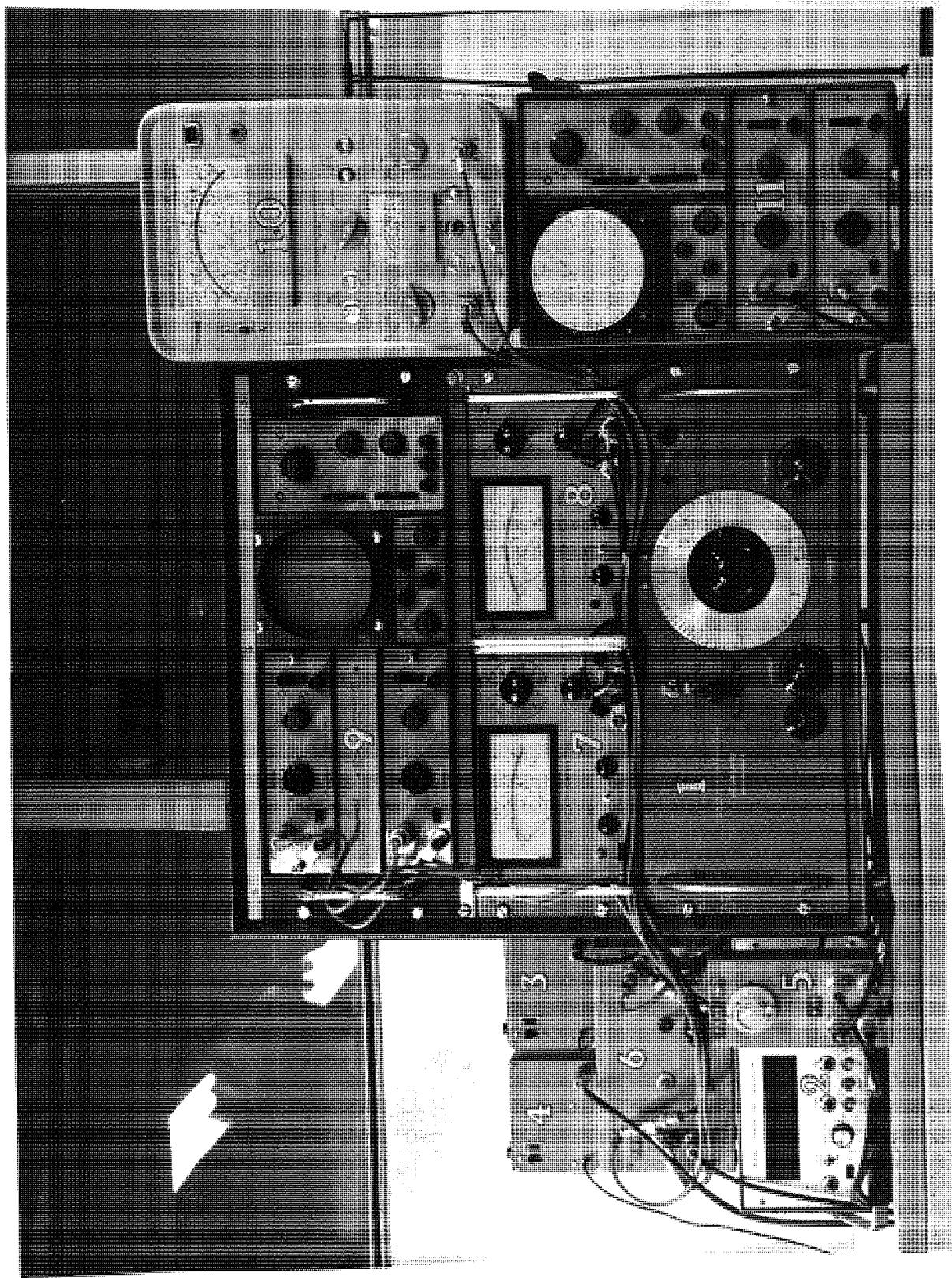
Fig. 38   The test instrumentation in its final form

Key to Fig. 38

1. Power oscillator

2. Frequency counter

3. Impedance converter (force)

4. Impedance converter (acceleration)

5. Mass compensation device

6. Amplifier (2 channel)

7. Millivoltmeter (acceleration)

8. Millivoltmeter (force)

9. Oscilloscope (2 channel)

10. Phase meter

11. Oscilloscope for the production of Lissajou's figures
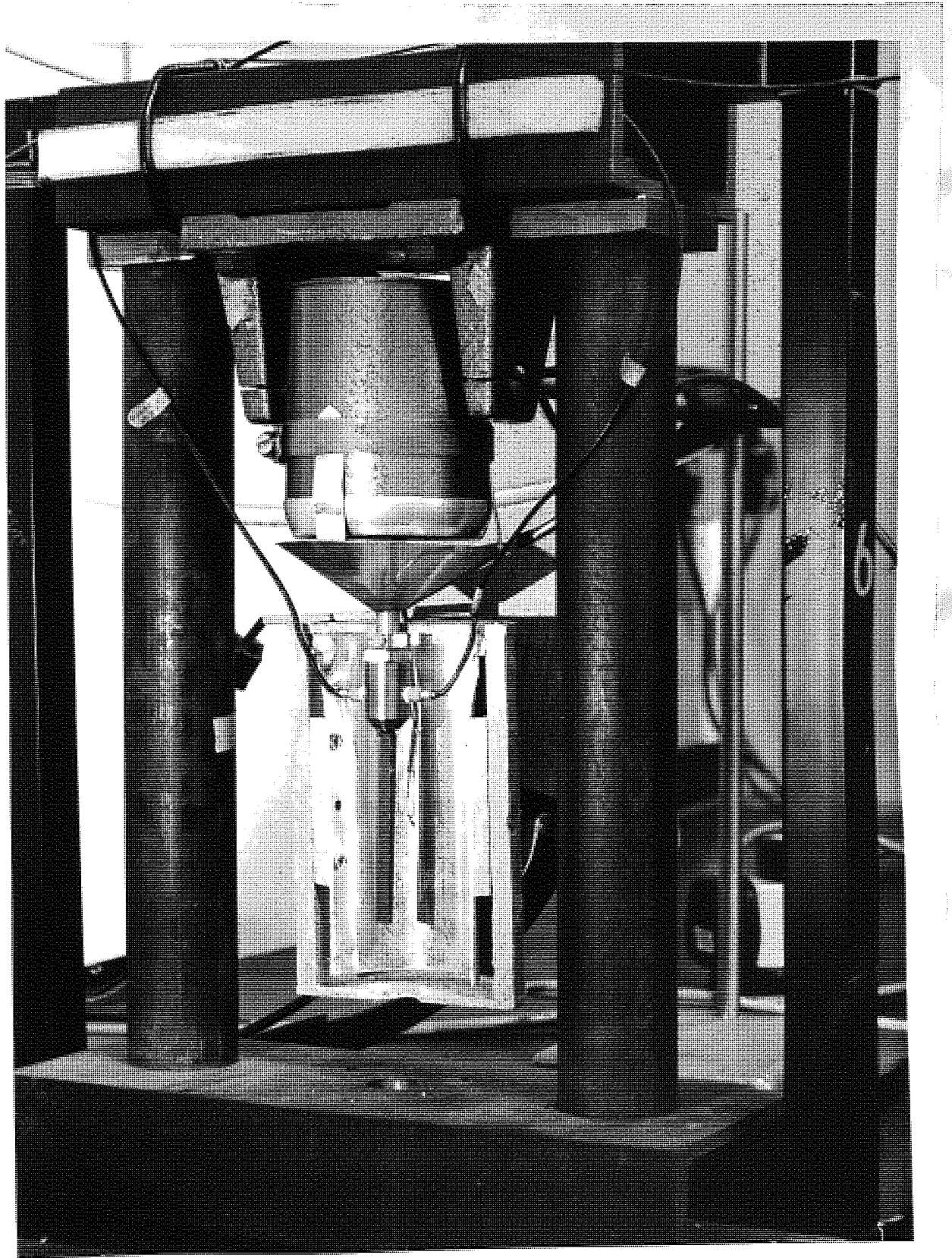
Fig. 39 The final test rig with half the oven in place, suspended from the 25mm (1") square tube framework Working from top to bottom on the test rig are: vibrator, heat shield, drive shaft, impedance head,

The environmental cabinet was consequently abandoned as a method for investigating the effect of elevated temperatures.

The next idea was to make an oven in two halves to enclose just the specimen and to blow hot air into the oven. The oven was constructed as follows.

A length of 75mm (3") diameter asbestos sewer pipe was purchased and a 125mm (5") length cut from it. Two 75mm (3") diameter discs were cut from 3mm ($\frac{1}{8}$") thick "sindanyo" sheet and screwed on each end of the pipe. A 13mm ($\frac{1}{2}$") hole was drilled in the centre of one end (the top) and the whole assembly sawn in two along a diameter. An inner chamber for each half was constructed from 1.5mm (1/16") aluminium sheet so that there was a 6mm ($\frac{1}{4}$") air gap between the aluminium and the asbestos, a 9.5mm ($\frac{3}{8}$") gap between the aluminium and the "sindanyo" at the bottom end and no gap between the aluminium and the sindanyo at the top end.

Each half of the oven had a 19mm ($\frac{3}{4}$") hole drilled in the asbestos near the top and a 19mm ($\frac{3}{4}$") threaded ferrule inserted in each hole. Two supports were made from retort stands and aluminium rod and the two halves of the oven mounted on them so that they met exactly at such a height that the top of the oven just coincided with the bottom of the impedance head on the test rig.

The hot air supply was obtained by passing compressed air through a sindanyo tube with a 220mm (9") 1kW electric fire element inside it. The hot air was fed via a 19mm ($\frac{3}{4}$") T-piece and two 308mm (12") lengths of flexible 19mm ($\frac{3}{4}$") conduit to each half of the oven. The electric fire element was powered by a variable voltage transformer so that the temperature in the oven could be controlled by both varying the setting on the transformer or by varying the air pressure.

Unfortunately the heat losses in the conduit were too great, even when it was lagged with asbestos string, and only 120°C could be attained in the oven.

It was not practical to shorten the conduit and so it was decided that each half of the oven should have its own heater mounted on the side. There would then be no need to have any flexible conduit as ordinary compressed air tubing could be used to carry the cold air via a T-piece to each heater.

Clearly, to have 220mm (9") electric fire elements at each side would be rather clumsy and so it was decided to use heating rods which could be coiled up and mounted inside compact "sindanyo" boxes.

The heating rods supplied by Hedin Limited were 308mm (12") long and rated at 500W. Each rod was coiled into a 50mm (2") diameter coil and mounted inside 50mm (2") of the 75mm (3") asbestos sewer pipe. A portion of the asbestos was cut away from each pipe and two pieces of "sindanyo" mounted at right angles to each other in the gaps (see fig. 40). Two end pieces were cut from 3mm ($\frac{1}{8}$") "sindanyo" for each heater box and a hole drilled in the centre of one end of each box so that a 19mm ($\frac{3}{4}$") threaded ferrule could be inserted.

A fitting to take the compressed air supply was mounted in the "sindanyo", tangentially to the asbestos pipe, on each box (see fig. 40) and a 50mm (2") length of 25mm (1") brass pipe with holes drilled all over it, to form a grid, inserted down the centre of each coil. Asbestos sheathed leads were taken from the ends of each coil to a variable voltage transformer via holes in the "sindanyo" and finally 38mm ($1\frac{1}{2}$") long pieces of 19mm ($\frac{3}{4}$") conduit was connected between the ferrules on the sides of the oven and the heater boxes.

138

asbestos sheathed leads
cold compressed air inlet
grid
heater coil
sindanyo housing
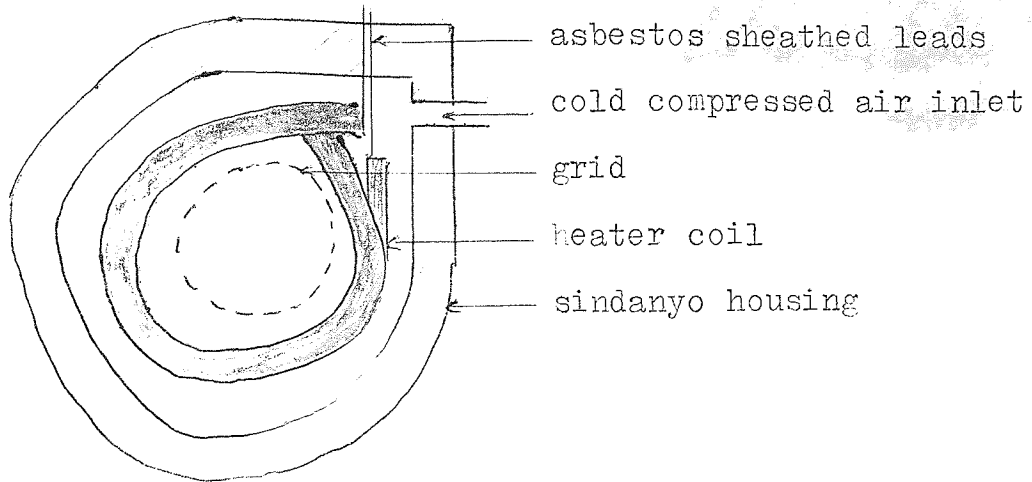
Fig. 40 The construction of a heating box

heater coil

heater coil

grid

grid

grid

grid

thermocouple

cold air
inlet

cold air
inlet

oven inner chamber
(aluminium)

oven outer chamber
(asbestos)
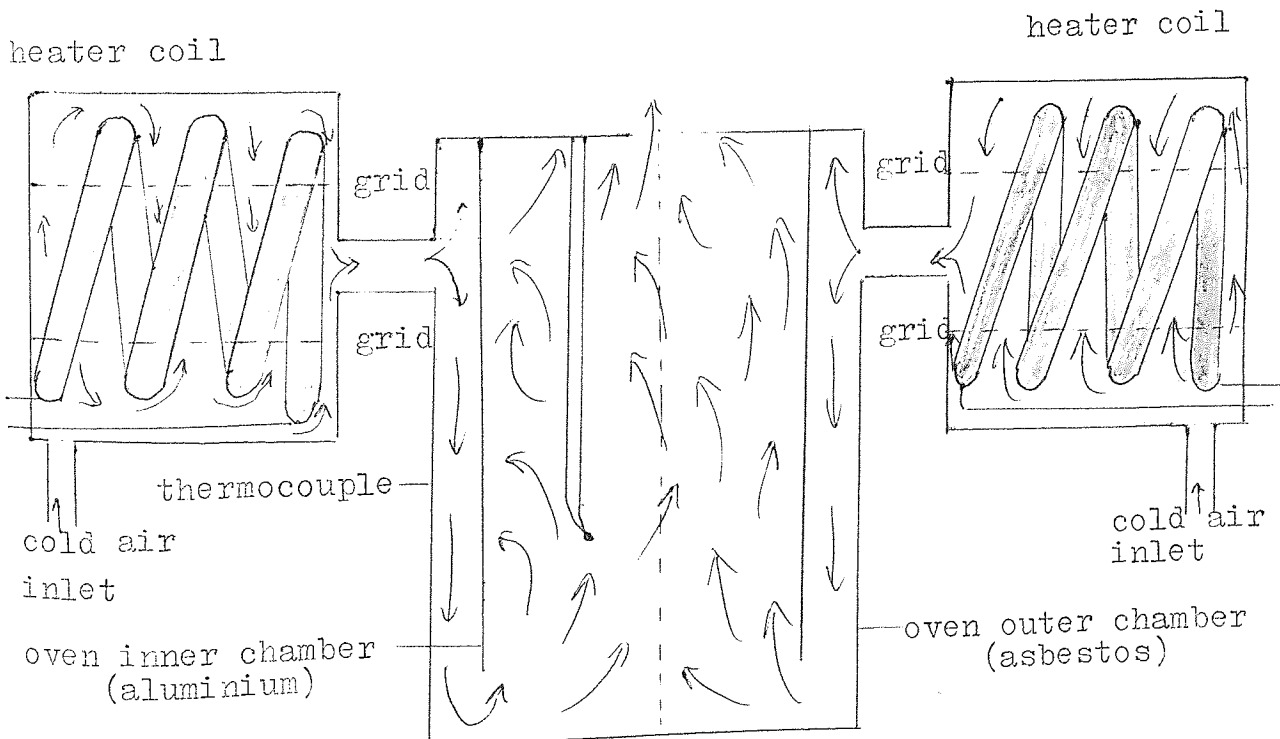
Fig. 41 The construction and operation of the oven and heaters

With this arrangement cold compressed air entered each heating box tangentially, passed round the coil, through the grid and out axially into the oven. In this manner there was sufficient obstruction to ensure effective heating of the air. When the hot air reached the oven it passed down between the two chambers into the centre of the oven and out through the top. Again the obstruction to natural air flow was sufficient to cause enough turbulence to produce an even temperature around the specimen. (see fig. 41).

The next problem was the provision of temperature measurement and control facilities. A direct reading technique was preferable for the measurement of temperature and the most common approaches involve use of either:-

     i) A thermometer.

    ii) A thermocouple coupled to a direct reading pyrometer.

The thermometer approach proved unsatisfactory because there were mounting difficulties because of its length and also temperature control facilities were difficult to arrange.

A thermocouple coupled to a direct reading pyrometer had the following advantages:-

     i) Positioning the thermocouple at the side of the centre of the specimen was easy.

    ii) Mounting provided no difficulties because the leads were flexible.

   iii) The temperature could clearly be read from the meter.

    iv) Provision could easily be made for temperature control.

An Ether type 990 indicating temperature controller was available. This was galvanometer based and could be used for measuring temperatures up to $250^{\circ}C$.

Unfortunately this controller could not be used with inductive loads (e.g. a variable voltage transformer) and thus a solenoid contact breaker had to be built into the circuit. An ammeter was also provided to measure the current to the heaters. The circuits for temperature indication, temperature control and heating supply are shown in fig. 42.

———— live
— — — neutral
.... thermocouple
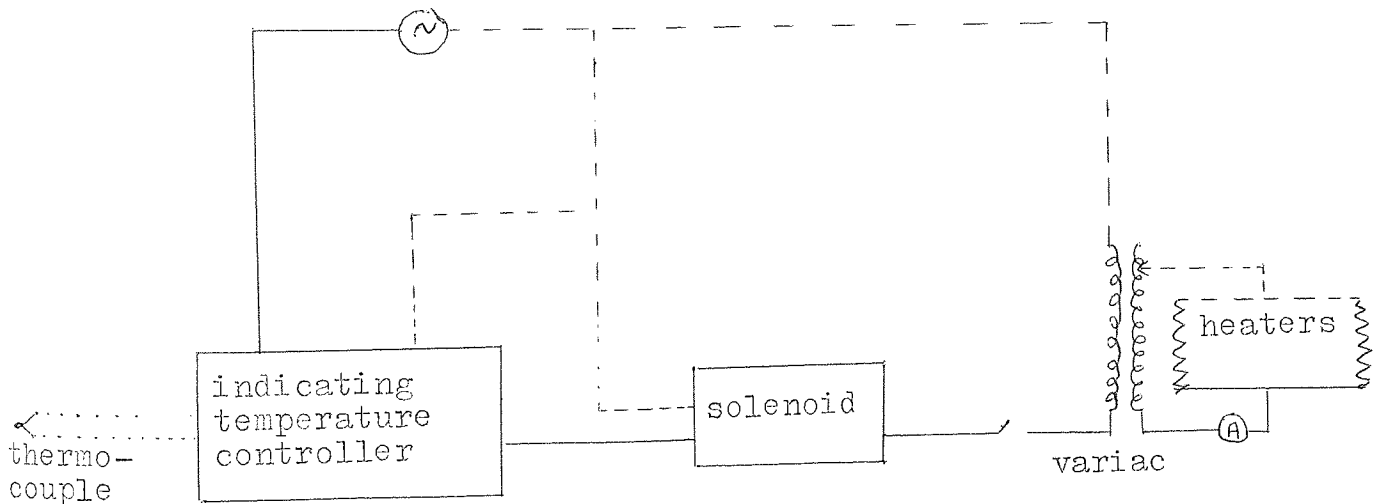
Fig. 42   Temperature indication and control circuits

The temperature indicator was carefully calibrated and the temperature distribution down the axis of the oven investigated to make sure that there was no appreciable variation. It was found that the variation was $1^{\circ}C$ over the specimen length and this was considered satisfactory.

Testing at elevated temperatures was performed using the following technique.

The specimen to be tested was attached to the transducer and the oven placed in position around the specimen. Readings were made at room temperature in the normal manner. Then the compressed air supply turned full on, the variable voltage transformer set to a suitable value from table 4 and the indicating temperature controller set to the required temperature. When the required temperature was reached (announced by the very loud sound of the solenoid opening) the compressed air supply was turned off or reduced (see table 4) so that the temperature was maintained at the required temperature long enough for all readings to be made (about one minute). It was found to be very important to keep the temperature constant within $\frac{1}{2}^{O}C$ to avoid errors due to the resonant frequency changing between readings since the resonant frequency is very dependent on temperature (see sect. 1.3.5).

Setting on the Variac (V)	Flow rate of air in oven during testing	Approximate temperature required (^{O}C)
0	None	Room temperature
160	None	50
180	None	85
200	V. low	120
220	V. low	155
240	medium	185
260	medium	215
270	high	245

Table 4 Variac settings to give the approximate temperature required

Although this technique depends very much on the skill of the operator to adjust the controls in order to maintain a steady temperature whilst taking readings, it has one distinct advantage over most sophisticated systems giving precise temperature control. The more sophisticated temperature control systems nearly always involve continual circulation of air and a continuous rush of air causes vibrations which would be picked up by the impedance head causing distortion of the wave forms and instability of the needles on the meters. The only solution to this problem is to build expensive filters into the electrical circuit to remove the unwanted noise. The technique or reducing the air supply is an economical way of removing the problem.

After a few specimens have been tested it was found that at temperatures above $200^{\circ}C$ the F.E.T. transistor in the force signal impedance matching device was prone to failure. No reasin for this was apparent until it was realised that because the impedance head was outside the oven and just above it, one end was being heated whilst the other end was at room temperature. This caused thermal gradients to be set up in the transducer causing stresses to be set up due to differential expansion. These stresses in turn were causing the signals produced to have spikes on them and particularly large spikes were destroying the F.E.T. transistors. Since the force gauge was nearest the oven it was affected more by this phenomenon than the accelerometer.

The solution to this problem was to place the entire transducer inside the oven so that it was subjected to a more even temperature distribution. However, it was clearly not advisable to have air at $250^{\circ}C$ coming out of the oven and impinging on the rubber mounting surrounding the vibrator drive spindle. It was thus necessary to use a drive shaft to lower the transducer from the vibrator. This was made from a 38mm ($1\frac{1}{2}$") length of 9.5mm ($\frac{3}{8}$") diameter brass rod.
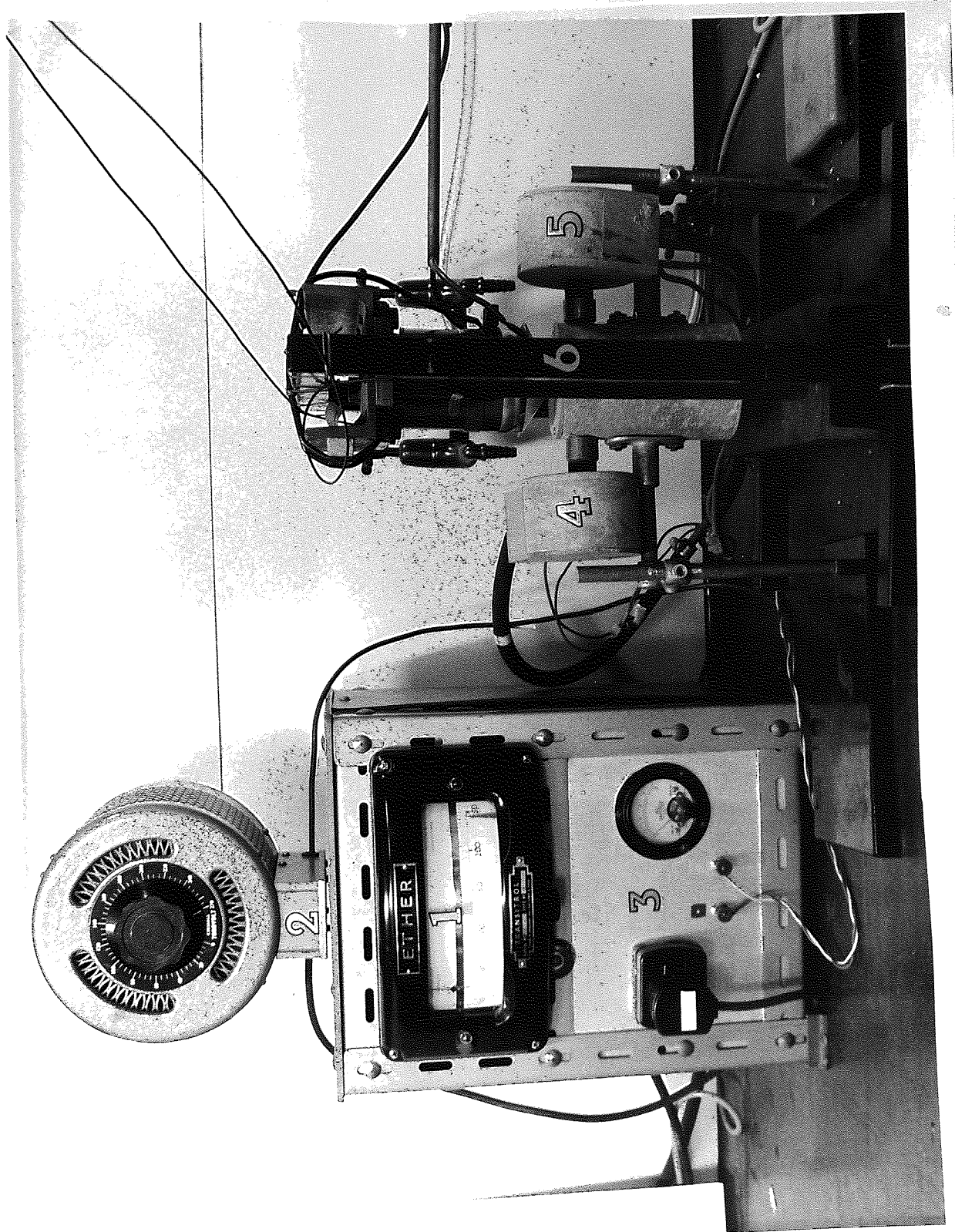
Fig. 45 The test rig and temperature indication and control equipment

Key

1. Temperature indicating controller

2. Variac for controlling the heaters

3. Box containing the solenoid

4.& 5. Heater Boxes

6. Framework supporting the test rig

A 2BA thread was machined on one end and a hole tapped to 2BA at the other. The top of the drive shaft was screwed directly into the vibrator and the stainless steel coupling used to link the impedance head to the drive shaft. It was decided that a heat deflector should also be used to deflect the hot air from the front of the vibrator. This was made from a cone of tin plate with a hole in the centre and three mounting tabs at the side. The tabs were clamped round the side of the vibrator by use of a jubilee clip and the drive shaft passed through the hole in the centre (see fig. 39). A final precaution was a horseshoe shaped piece of 6mm ($\frac{1}{4}$") copper tubing with the ends flattened out, fed with cold compressed air at low pressure and directed down the cone. This had the effect of cooling any air passing through the hole in the cone.

A final modification was the replacement of the leads from the impedance head by B&K type AO 0038 high temperature leads (max. temp. 260°C) This was the final test rig design and is shown in figs. 39 and 43.

A further problem was that of specimens demounting during testing at elevated temperatures. In order to overcome this Araldite was replaced by Redux 64 for glueing the specimens to the mounting studs. Redux 64 is an adhesive used in the brake lining industry for bonding linings to the shoes and will withstand the high temperatures involved in the braking operation. It was also decided to use steel instead of brass mounting studs since this produced fewer mounting problems.

2.2.5.7 Commissioning Experiments

In order to demonstrate that the equipment was operating in the correct manner it was necessary to commission the equipment by testing the specimens made from a material which had established dynamic mechanical properties.

The material selected for these experiments was polypropylene grade G.W.M. 22 manufactured by I.C.I. and filled with 7% glass fibre.

It was decided that the following tests should be made:-

i) Tests of reproducibility to be made under various conditions at room temperature.

ii) Tests to be made on one specimen with various added weights over a temperature range, to determine the effects of altering the testing frequency.

iii) Tests made at room temperature on one specimen which was continuously shortened, so that the validity of the equations governing modulus and damping could be examined over a wide range of dimensions.

2.2.7.1 Reproducibility Tests

These tests were made on a bar machined from polypropylene to the dimensions 6.05mm x 5.44mm x 3.05mm (0.238" x 0.214" x 0.120").
A mounting stud was glued to each end so that weights could be added to the free end. In this manner the specimen could be reversed to determine whether dimensional or structural defects in the specimen had had differing effects depending on which end of the specimen was vibrated.

During the whole series of reproducibility tests an 8.305gm weight was screwed in position on the lower end of the specimen giving a total added mass of 9.317gm.

Tests made were as follows:-

i) The specimen was attached to the transducer in the normal manner. Readings (of f_o, f_n, F_{max}, f_λ and f_1) were taken immediately and after 3,6,9,15,30 and 40 minutes.

ii) Without disturbing the specimen, the oscillator was switched off for 25 minutes and then switched on. Readings were taken immediately and after 6 minutes.

iii) The weight was removed and replaced 6 minutes later.
Readings were taken immediately and after 5 minutes.

iv) The specimen was reversed and the weight reattached.
Readings were taken immediately and after one hour.

v) The specimen was reversed to its original configuration
and readings taken immediately.

vi) The specimen was left undisturbed and all the equipment
switched off over night. Next morning the equipment
was switched on and readings taken immediately.

vii) The specimen was removed and replaced and readings taken
after 10 minutes.

viii) The cross sectional area of the specimen was reduced from
5.44mm x 3.05mm (0.214" x 0.120") to 5.38mm x 3.00mm
(0.212" x 0.118") and readings taken after 20 minutes.

ix) A deep notch was cut in the specimen and readings taken
after 20 minutes.

The results of these experiments are shown in table 5 (see appendix 2)

2.2.5.7.2 Tests Made Over a Temperature Range With Different

Added Weights

The specimen used in the tests on reproducibility was tested over a
temperature range from approximately $6^{o}C$ to approximately $77^{o}C$ in the
environmental cabinet. The environmental cabinet was used so that
testing could be performed at temperatures below room temperature.
Testing was performed with the following added masses:-

i) No added mass so that the frequency of testing was
approximately 9kHz at room temperature.

ii) Added mass of 4.012g so that the frequency of testing
was approximately 2.85kHz at room temperature.

iii) Added mass of 9.317g so that the frequency of testing was
approximately 1.8kHz at room temperature.

iv) Added mass of 20.912g so that the frequency of testing
was approximately 1.25kHz at room temperature.

The results of these experiments are shown in graphs 4,5,6,7.

2.2.5.7.3 Continually Shortened Specimen Tests

A rod of polypropylene was machined to the dimensions
219mm x 6.27mm x 2.97mm (8.62" x 0.247" x 0.117") and mounted on a stud.
Readings were taken in the normal manner. The rod was then reduced
progressively in length and readings taken at each length in the normal
manner. The lengths at which readings were taken were 219mm (8.62"),
167mm (6.58"), 139mm (5.47"), 108mm (4.25"), 76mm (2.99") and 58mm (2.28").

The results of these experiments are shown in table 6. (see appendix 2)

2.3 Preparation of Friction Material Specimens

2.3.1 Shape Considerations

2.3.1.1 The Disc Pad

As indicated in section 1.2.1.3 disc pads come in various shapes
and sizes and the ones that were used in this study are shown in fig.
The majority of samples selected for testing were segmental in shape and
were mounted on a rectangular back-plate. Disc pad designs used in this
study are shown in fig. 44.
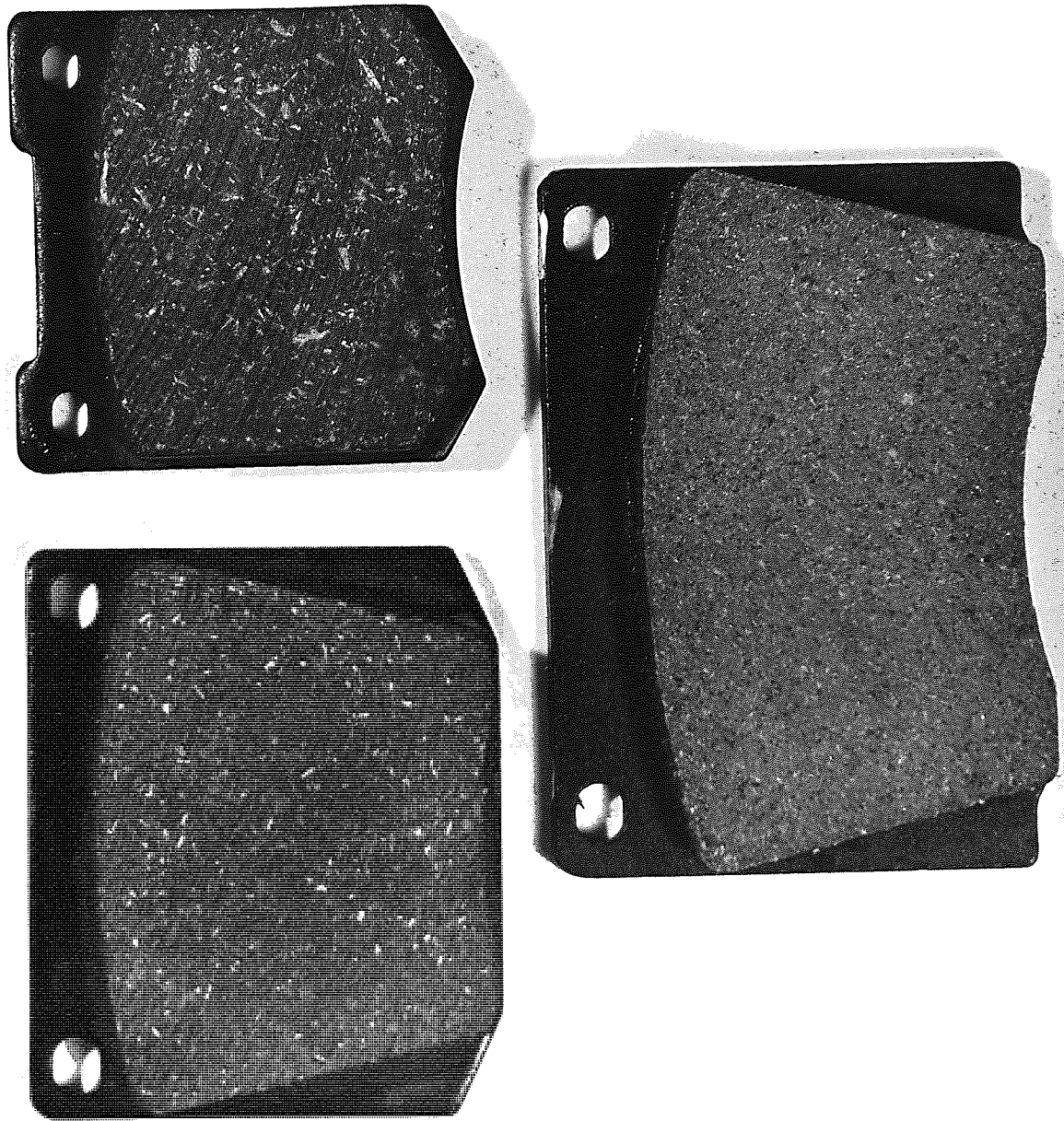
Fig. 44 Disc pad designs used

2.3.1.2 The Friction Material Specimen

In order that the theory discussed in section 2.2.2 may hold,
specimens should be cut parallel to the circumference of the disc.
This however, would not give suitable specimens as they would be curved.
Consequently it was decided to approximate to straight specimens cut
perpendicular to a radius.

It was decided that the specimens should be made as large as
possible so that any localised nonuniformity effects would be averaged
out. Hence it was decided to cut specimens from the longest side of the
pad. Because some of the testing would be performed on used pads with
a reduced thickness it was decided to make the width of the specimens
6mm ($\frac{1}{4}$"). 3mm ($\frac{1}{8}$") was selected for the thickness of the specimens so
that several specimens could be cut with reasonable length since the pad
reduces in width from top to bottom down the face.

It was found that the specimens produced gave resonances in the range
5kHz to 10kHz and so no further dimensional changes were required when
resonance testing was introduced.

2.3.2 Machining Considerations

2.3.2.1 Machining Problems

Friction materials present many machining problems because, as the
name implies, they present high friction to any tools employed for
machining purposes thus tending to blunt them. A further problem arose
when machines required a lubricant/coolant on the cutting surface.
Soluble oil, which is usual for this purpose, could not be used incase
it was irreversibly absorbed into the friction material thus making test
results invalid. A third problem was that the friction materials,
particularly used samples, are fairly brittle materials and thus any

violent machining operations tend to damage the specimens.

Machining operations fell into four categories:-

    i)   Removal of the back-plate.

    ii)   Reduction of a portion of the disc pad to a constant thickness of approximately 6mm ($\frac{1}{4}$").

    iii)   Cutting of specimens 3mm ($\frac{1}{8}$") wide from the reduced portion of the pad.

    iv)   Trimming the specimens to accurate dimensions.

2.3.2.2 Removal of the Back-plate

The first method attempted involved use of a continuous blade hacksaw. The disc pad was held in position by a magnetic chuck acting on the steel back-plate. A new blade was put in the saw but before the back-plate on the first pad was removed the saw had become so blunt that it would not cut anymore! From this experience it was realised that no conventional sawing operation could be used to cut the friction material.

The second method involved shearing the back-plates off in a press by means of a simple shearing jig. The shearing jig was constructed by loosely bolting together two pieces of 76mm (3") angle iron with a piece of 25mm (1") wide, 16mm ($\frac{5}{8}$") thick steel plate between them (see fig. 45). The pad was put in the jig so that the pad edge rested on the side of the steel strip and the edge of the back-plate lay in between the steel strip and the side of the angle iron (see fig. 45). The jig and sample were put in a press which was just closed on the edge of the back-plate thus shearing it off. Care was taken not to close the press on to the edge of the pad material. This method was very quick and only damaged a few of the unused pads but when this method was applied to used samples many pads split and disintegrated.
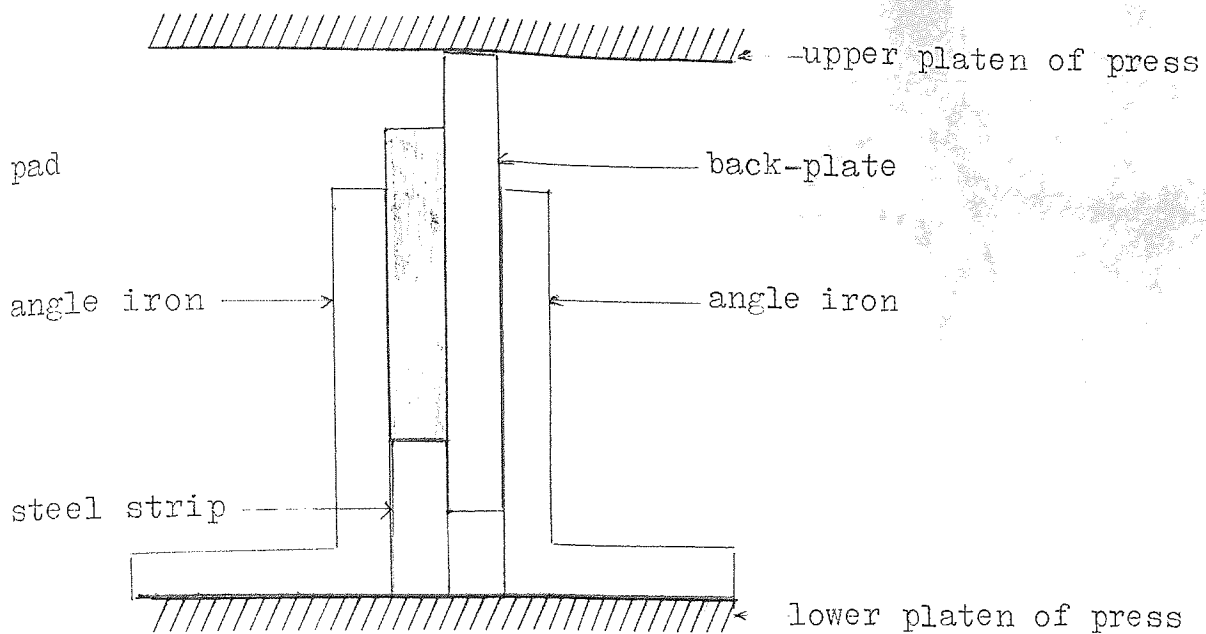
Fig. 45 The shearing jig

The third method tried involved cutting off the back-plate on a shaper. This brought no machinery problems, since it was the steel which was cut, but it was rather a tedious method as at least two traverses were required to cut through 5mm (3/16") of mild steel. In order to remove some of the tediousness a large shaper was used with a long stroke so that five back-plates could be removed at once. Only half the back-plate was removed since only three specimens were required from each pad. (see fig. 46)

2.3.2.3 Reduction of a Portion of the Disc Pad to a Constant Thickness

This was achieved by shaping the pads on a small shaper. From previous comments on the machining of friction materials it will be realised that ordinary hardened steel tipped tools would quickly blunt and so it was necessary to use carbide tipped tools which are expensive and difficult to sharpen. Simple tests showed that friction materials machined in a similar way to cast iron and thus fairly deep cuts with a positive rake tool were required. The tool purchased for this operation was a Camlock 55° positive rake tool which had a disposable tip with eight cutting surfaces.
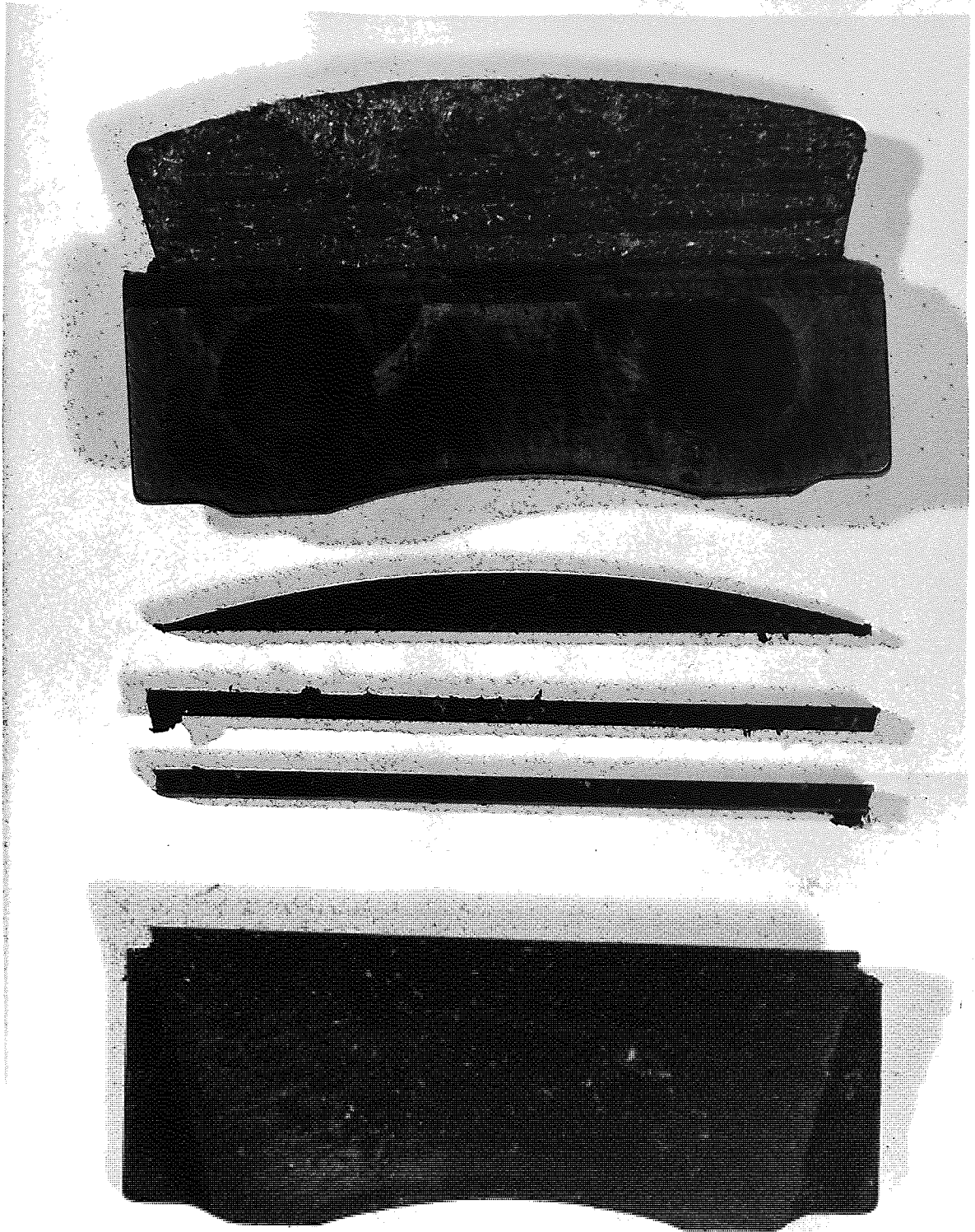
Fig. 46 Stages in the production of specimens from a disc pad

Top: pad with the backplate shaped off.

Centre: two rough specimens and the off cut.

Bottom: the unused portion of the pad.

The tip was made from tungsten carbide. A 254mm (10") stroke and a 0.25mm ($\frac{10}{1000}$") feed on the shaper gave a very good surface finish.

2.3.2.4 Cutting Specimens from the Reduced Portion of the Pad

This was achieved by means of a diamond impregnated cutting wheel on machinery used for cutting rock samples which had a facility for moving the wheel to an accuracy of 0.025mm ($\frac{1}{1000}$"). Some form of coolant had to be used to prevent distortion in the wheel due to overheating. Since soluble oil could not be used the equipment was modified for water cooling. After use the wheel, which was made of copper, was washed with a 0.01% solution of benzotriazole to prevent corrosion.

Two or three specimens were cut from each sample by means of three of four cuts. The first cut gave a setting for the wheel and removed the curved end of the pad. (see fig. 46)

2.3.2.5 Trimming the Specimens to Accurate Dimensions

This involved two operations. The first involved machining flat, square ends on the specimens and the second involved machining the thickness and width to an accuracy of $\pm$0.025mm ($\pm \frac{1}{1000}$"), since it was found that the shaping and cutting operations often produced specimens with dimensions which changed along the length. On the shaped surface this occurred when the shaper tool became blunt causing the cutting action to become irregular. On the cut surfaces this was due to high concentrations of hard components in the friction material deflecting the cutting blade.

Both trimming operations were performed on a linishing machine which is effectively a continuous band of emery paper rotated over a flat bed. The action is thus a light grinding action.

The trimming of the ends was performed with the help of a small jig. This was a rectangular block of hardened steel with a 3.3mm ($\frac{130}{1000}$") wide slot cut to a depth of 6mm ($\frac{1}{4}$") in the top. A plate was then screwed over the slot. (see fig. 47) Thus a specimen of approximate dimensions 3mm x 6mm ($\frac{1}{8}$" x $\frac{1}{4}$") could be clamped so that one end just protruded from one end of the block. This protrusion was then linished flush with the surface of the end of the block. The specimen was then pushed through so that the other end of the specimen protruded from the other end of the block and the process repeated.

The second operation involved checking along the length with a micrometer for variations in width and thickness and lightly linishing down any high spots so that the specimens had sides which were parallel. N.B. Although the nominal cross section for the specimens was 3mm x 6mm ($\frac{1}{8}$" x $\frac{1}{4}$") it was not essential for them to have exactly these dimensions. The main criteria is that specimens should be rectangular bars with parallel sides and square ends. Every attempt was made, however, to keep the dimensions as near as possible to the nominal values so that the resonant frequencies fell in a small range.

2.3.3 Mounting Considerations

2.3.3.1 The Use of Araldite as a Bonding Agent

Initial bonding of the specimens to the mounting studs was made using Araldite standard adhesive. Araldite is an epoxy resin based adhesive which when cured gives a rigid elastic bond. Araldite was suitable for use at temperatures below 100°C but above this temperature the bond degrades and eventually breaks completely. Consultation of the literature pertaining to Araldite indicated that it does not form as good a bond with brass as it does with mild steel.
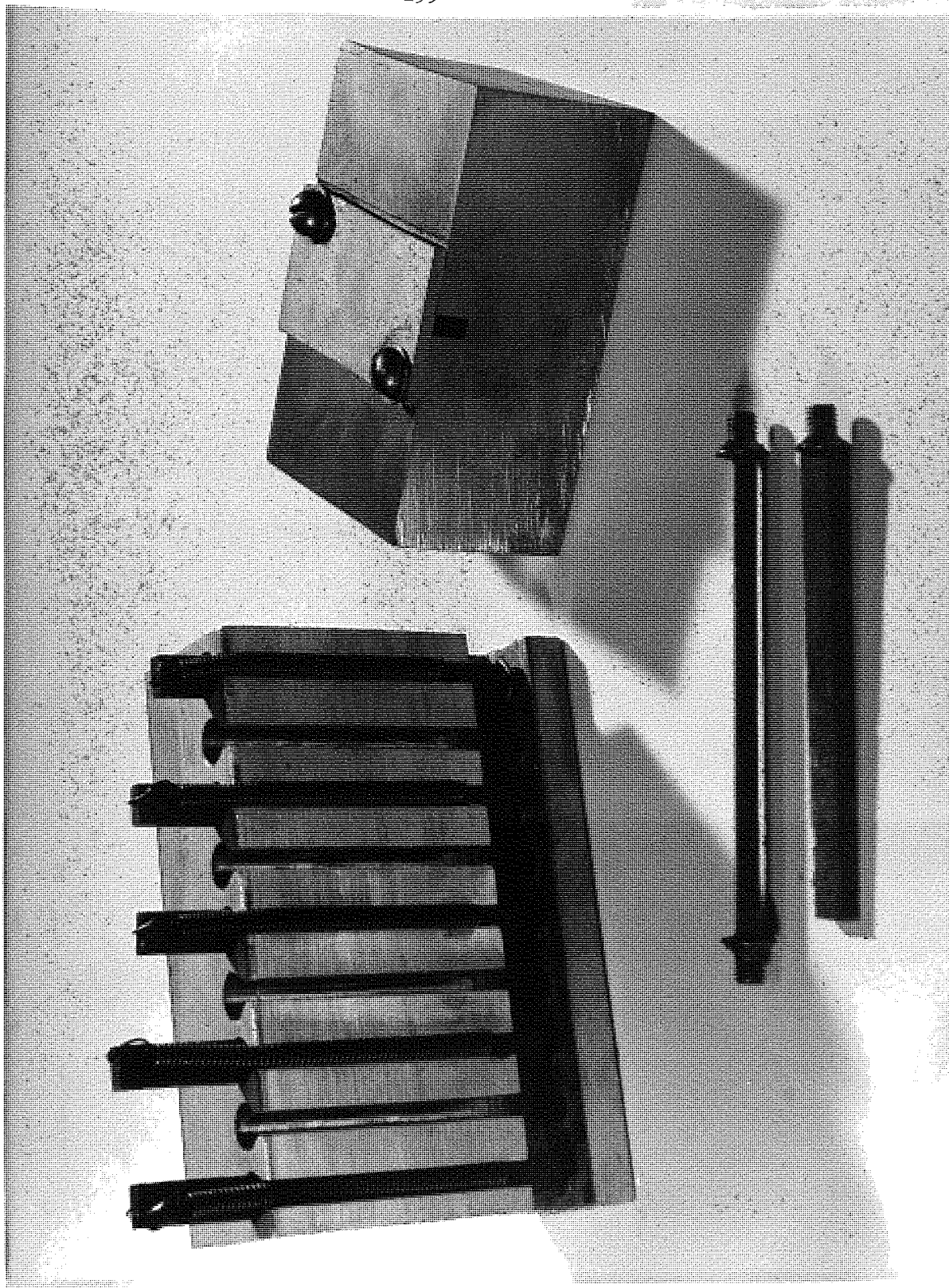
Fig. 47 Trimming and mounting specimens

When viewing the photograph in the normal manner. Top left: the gluing
rig with various size specimens in position. Top right: the jig used
for linishing square ends on the specimens. Centre: specimens with one
and two mounting studs.

Consequently a change was made to mild steel mounting studs.

The main advantages of Araldite is that it cures without the need for heating or clamping.

2.3.3.2 The Use of Redux 64 as a Bonding Agent

Several alternative bonding agents were tried but most failed on the grounds that either the bond formed added damping to the system or it degraded below 250°C.

The most successful bonding agent tried was Redux 64 which is a brake bonding adhesive designed to withstand temperatures up to 250°C for short periods. The adhesive is phenolic resin based and when cured gives a rigid elastic bond.

The only problem with this adhesive is that pressure must be applied to the bonding surfaces during curing, which requires heating to at least 130°C, to prevent the formation of bubbles in the bond.

2.3.3.3 The Mounting Technique

In order to mount the end of the specimen perpendicular to the surface of the mounting stud a gluing jig was made. The jig was made from a rectangular block of aluminium 50mm (2") wide. Nine holes were drilled along the length of the block to a depth of 38mm (1½"). The diameter of these holes was 7mm (0.29") so that the specimens would be a close fit in the holes. The remaining (bottom) 13mm (½") was drilled to a diameter of 5mm (0.2") so that a 2BA screw would rest in the hole. A slot 7.6mm (0.3") wide was cut across the line of holes 5mm (0.2") up from the bottom of the block so that the different diameter holes were now separate. Finally a 3.3mm (0.130") wide slot was cut into each of the upper row of holes. The complete gluing jig with specimens in position is shown in fig. 47.

The mounting operation adopted when using Redux 64 as a bonding agent was as follows:-

i) The head of a 2BA screw was linished and the screw was placed in one of the lower holes in the jig.

ii) A specimen was pushed into an adjacent upper hole.

iii) The top end of the specimen and the top of the 2BA screw were coated with a thin film of adhesive.

iv) The jig was placed in an oven at 75°C for half an hour.

v) The jig was removed from the oven and the specimen from its hole.

vi) The specimen was pushed down the hole above the 2BA screw so that it was in contact with the screw head with the slot in the screw head perpendicular to the width of the specimen which was parallel to the front of the jig.

vii) A light spring was hooked over the end of the specimen and extended down so that the other end hooked in the slot across the jig (see fig. 46)

viii) The jig was put in an oven at 180°C for half an hour.

ix) The jig was removed from the oven and the specimen removed by releasing the spring, pulling the specimen and 2BA screw upwards until the 2BA screw was free from its hole, twisting the specimen through 90° and pulling the specimen through the slot in the front of the jig.

x) The specimen was put in a desiccator to cool.

In practice more than one specimen was mounted at one time.

When Araldite was used for mounting, operations ii), iv), v) and vii) were not required and the temperature in operation viii) was changed to 130°C. Specimens with mounting studs are shown in fig. 47.

2.4 The Testing of Friction Material and Related Specimens

2.4.1 The Testing Programme

2.4.1.1 Sampling

All specimens of disc pads were provided by Girling Limited.

The testing programme was split into two sections:-

i) The testing of specimens cut from pads which had not been used.

ii) The testing of specimens cut from pads which had been used for a nominal 500 miles.

The used pads were mainly from cars which had a history of brake squeal from new. At the 500 mile free service all the pads (usually four as most cars only have disc brakes on the front wheels) from these cars were removed by the garages concerned and sent to Girling Limited without details as to which pads were the offending ones.

A few of the used pads came from Girling test driver's cars which had no history of brake squeal.

The pad materials tested were:-

i) Ferodo type FER 2430.

ii) Mintex type M 78.

iii) Mintex type M 108.

All three specimens were tested from the unused pads but only two were tested from the used pads. Some auxiliary tests were also performed.

2.4.1.2 Friction Material Testing Aims

The unused pads were tested for the following reasons:-

i) To determine the magnitude of the variation of test results between samples of pads made from the same material and between specimens from the same pad.

ii) To determine whether test results from particular pads were significantly different from the majority of pads from the same material, thus suggesting possible squeal prone pads.

iii) To compare with the used pad samples.

The used pads, from cars with a history of squeal, were tested for the following reasons:—

i) To determine whether a particular pad or pair of pads gave significantly different test results to the other pads from the same car. If this were so some correlation with squeal and a particular test result could be made.

ii) To determine any points where the damping fell to a minimum value as a function of temperature.

The used pads from cars with no history of squeal were tested as a control against the other used pads.

2.4.2 The Testing Procedure

2.4.2.1 Pre-treatment of Specimens

The procedure adopted for pre-treatment of the specimens was as follows:—

i) To avoid any changes in the dynamic mechanical properties, during testing at elevated temperatures, being due to chemical changes or degradation in the specimens, all specimens were placed overnight (16 hours) in an oven at $250^{\circ}C$.

ii) The specimens were placed in a desiccator to cool.

iii) The specimens were checked for dimensional accuracy and if necessary linished to size (see sect. 2.3.2.5)

iv) The specimens were measured for width and thickness using a micrometer which measured in inches to the nearest one thousandth of an inch and hence all metric measurements quoted are converted from the British units.

v) The specimens were measured for length using vernier calipers which measured in centimeters to the nearest 1/20mm.

vi) The specimens were weighed to an accuracy of four decimal places on a single pan balance.

vii) The specimens were bonded to mounting studs in the manner described in sect. 2.3.3.3.

The specimens were now ready for testing.

2.4.2.2 Dynamic Mechanical Testing of Specimens

The procedure adopted for the dynamic mechanical testing of the specimens was as follows:-

i) The specimen was screwed into the transducer and the oscillator tuned to the frequency when the phasemeter read 90°.

ii) The specimen was removed and replaced and a light tightening given to the mounting stud by a pair of pliers. If the true resonant frequency moved to a higher frequency or remained at the same frequency, the mounting stud was correctly bedded in. If the true resonant frequency moved to a lower value the specimen was removed and replaced again until a higher or the same true resonant frequency was obtained.

iii) The equipment was left for about 15 minutes and the oscillator again tuned to give a phase reading of 90°.

iv) If after five minutes there was no further movement of the needle on the phase meter then the specimen was ready for testing. If there was still a movement the needle was reset to 90° and checked and reset every five minutes until there was no movement.

v) The first readings were taken at room temperature according to the procedure outlined in appendix 4.

vi) Seven more readings were taken at approximately $30^{\circ}C$ increments up to $250^{\circ}C$.

2.4.3 Auxiliary Testing

2.4.3.1 Tests made to Examine the Effects of External Agents on the Dynamic Mechanical Properties of Friction Materials

Because some people have suggested that brake squeal may be influenced by the presence of external agents such as water, brake fluid and engine oil, it was decided to examine the effects on the dynamic mechanical properties of friction material, when these three liquids were absorbed into friction material specimens which had been previously tested.

Three specimens of Mintex 108 and three specimens of Ferodo 2430 were tested with each external agent using the following technique:-

i) Each specimen was left mounted in the normal manner from its previous testing so that no change in mounting conditions was possible.

ii)   The specimen was immersed in the external agent for 15 minutes.

iii)   The specimen was superficially dried using absorbent tissue.

iv)   Testing was performed in the normal manner except that at temperatures near the boiling point of the external agent, an interval was allowed before testing whilst the rapid evaporation took place.

v)   After testing to 250°C the specimen was allowed to cool down and was retested at room temperature to assess the degree of recovery.

The external agents used were:-

i)   Ordinary tap water (although perhaps rain water would have been more applicable).

ii)   Castrol 10-30 engine oil suspended in tap water since this is the most likely manner in which engine oil would make contact with the disc pad.

iii)   Castrol-Girling brake fluid.

2.4.3.2 The Testing and Preparation of Friction Material Component Specimens

In order to investigate the influence of certain friction material components on the dynamic mechanical properties of the complete friction material, a number of specimens were prepared from friction material components and tested in the normal manner. This series of experiments was only intended as ground-work for a more comprehensive investigation, using moulds and conditions more closely allied to the preparation of disc brake pads, which time did not allow.

Specimens were prepared with the following combinations of materials:-

   i) Cured phenolic resin with no additives except hexamine

       (the cross-linking agent).

  ii) Cured phenolic resin and asbestos in varying percentages.

 iii) Cured phenolic resin, asbestos and barytes.

  iv) Cured phenolic resin, asbestos and metals (in powder and

       chip form).

   v) Cured phenolic resin, asbestos and friction dust.

The reason for including asbestos in the last three combinations was that the cured phenolic resin specimens were very difficult to prepare whilst when asbestos was included specimen preparation was much easier and thus it was felt that it would probably help with specimen preparation if a phenolic/asbestos base was used.

All specimens were prepared in a three plate mould (see fig. 48) which had four cavities.

2.4.3.2.1 Preparation of Cured Phenolic Resin Specimens

Extreme difficulty was experienced in the preparation of specimens containing nothing else except cured phenolic resin because of foaming due to formation of ammonia, during the curing process. In order to avoid this problem the following procedure was adopted:-

   i) A quantity of novolak resin was mixed with $12\frac{1}{2}\%$ hexamine

       by weight and heated in an oven at $150^{\circ}C$ for 15 minutes

       in flat trays.

  ii) The resulting foam was granulated and powdered using a

       Moulinex coffee grinder.

 iii) The powder was sieved and the finer pale yellow powder

       discarded leaving the darker coarse material which was used

       in the moulding powder.
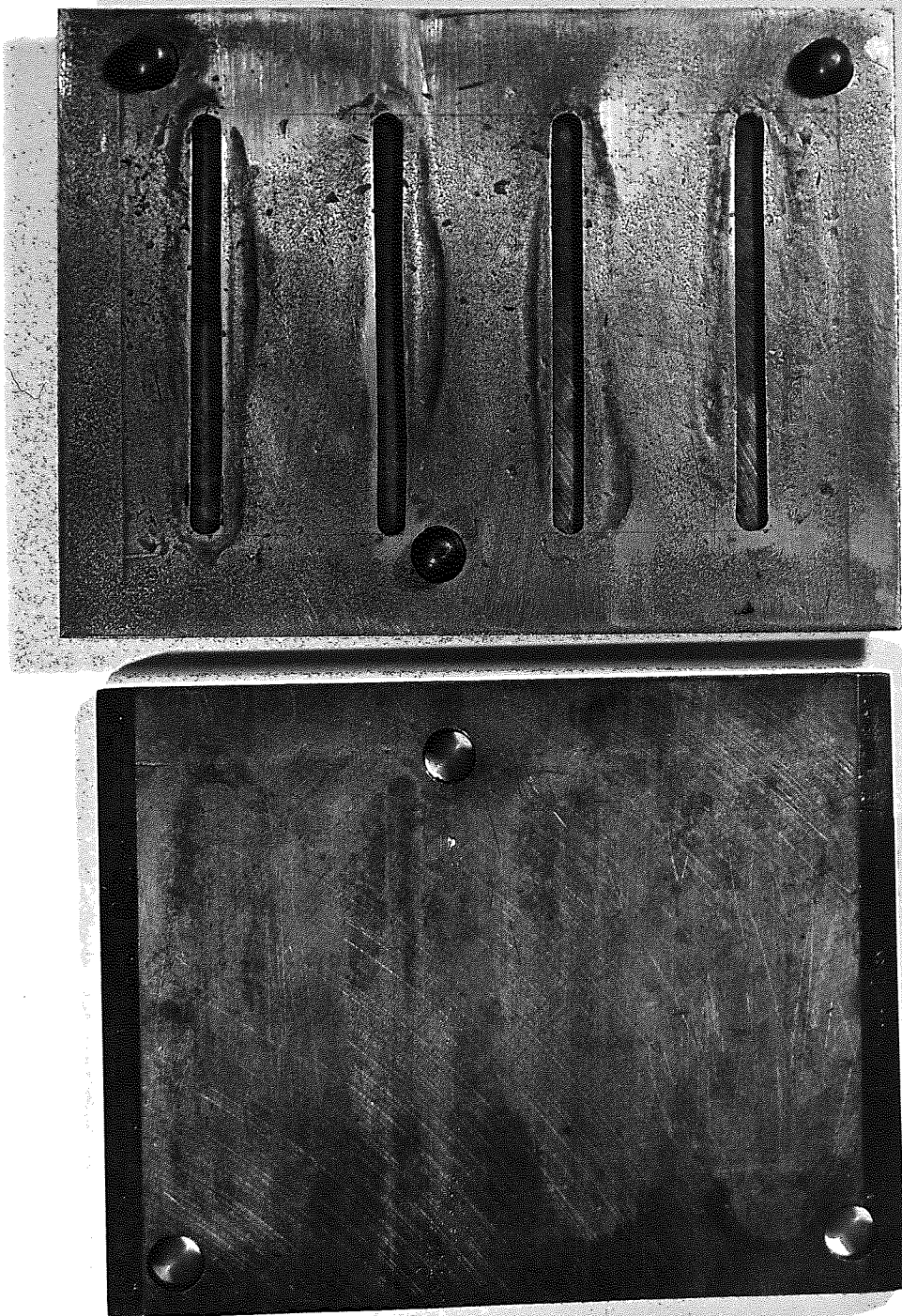
Fig. 48 The mould used when producing specimens from friction material components (shown with the top plate removed)

iv) The moulding powder which had the composition 75% cured
resin, 22% powdered novolak resin, 3% hexamine, was shaken
for 20 minutes on a sieve shaker.

v) 4g of the moulding powder was compressed into each cavity
of the mould and the mould closed.

vi) The mould was placed in a compression moulding press at a
temperature of $160^{\circ}C$ and at a pressure of $16MNm^{-2}$ for
40 minutes.

vii) The specimens formed were translucent and light brown in
colour but as they were quite brittle they were left in
the mould for the next stage.

viii) The specimens in the mould, which was held closed by a weight
to prevent distortion, were put in an oven at $250^{\circ}C$ overnight
(16 hours) to post-cure the specimens.

ix) The specimens, which had turned dark brown/black and were
tougher, were ejected from the mould by removing the top
and bottom plates and carefully pressing out the specimens
from the central plate by means of a press.

x) The specimens were trimmed to shape and mounted on mounting
studs in the normal manner.

2.4.3.2.2 Preparation of Cured Phenolic Resin Specimens
Containing Various Proportions of Asbestos

As asbestos is the major component of friction materials it was
decided to make specimens with varying proportions of asbestos.

The first specimens were made with the composition 50% multigrade
chrysotile asbestos, 44% novolak 6% hexamine. It was then decided that
more representative specimens should be made using 5R chrysotile asbestos
which is commonly used in the brake lining industry.

Unfortunately, with the type of mould used it proved impossible to manufacture specimens with higher than 57% asbestos. Using 5R chrysotile asbestos three moulding powders were made with the compositions given in table 7.

Ref.	Asbestos	Novolak	Hexamine
1	57.0%	37.5%	5.5%
2	43.0%	50.0%	7.0%
3	28.5%	62.5%	9.0%

Table 7   Phenolic/asbestos moulding powder compositions

The following procedure was adopted for the preparation of specimens:-

i) The materials were mixed in the required proportions and shaken and rolled to integrally mix them.

ii) The mixture was then milled for 2 minutes on a two roll mill and the resulting skin removed.

iii) The skin was granulated and powdered.

iv) Specimens were moulded and prepared for testing in the same manner as for the cured phenolic resin only specimens.

2.4.3.2.3 Preparation of Cured Phenolic Resin/Asbestos Specimens Containing Various Fillers and Property Modifiers

Specimens were prepared with the compositions given in table 8 using the same technique outlined for the phenolic/asbestos specimens.

Ref.	Asbestos	Novolak	Hexamine	Filler/property modifier
1	30.0%	35.0%	5.0%	Barytes 15.0%
2	29.0%	34.0%	5.0%	Copper 19.0%
				Zinc 7.5%
				Brass (chips) 5.5%
3	37.5%	44.0%	6.0%	Friction dust 12.5%

Table 8 Composition of Phenolic/Asbestos/Filler Moulding Powders

CHAPTER 3

DISCUSSION

3.1 The Problems of Designing a Suitable Instrument for Measuring the Dynamic Mechanical Properties of Friction Materials

3.1.1 The Problems of Selecting a Suitable Technique

Three different techniques were studied:-

    i) Forced vibrations without resonance.

    ii) Forced vibrations with resonance using two end clamping.

    iii) Forced vibrations with resonance using one end clamping.

In all three cases the electrical measuring equipment was essentially the same. The test rig was where the difference between the techniques existed. Although only the third technique was suitable for testing friction materials the other two techniques had already been established in similar equipment which is commercially available.

    i) The forced vibrations with resonance technique using longitudinal vibrations has been established at low frequencies by the Rheovibron (see sect. 2.1.3.4).

    ii) Forced vibrations with resonance using two end clamping has been established using flexural vibrations and electrostatic transducers by the B&K complex modulus apparatus (see sect. 2.1.3.2).

3.1.1.1 The Rheovibron versus the Experimental Forced Vibration without Resonance Technique

The main reasons why the Rheovibron succeeded while the experimental testing rig failed are as follows:-

i) The Rheovibron apparatus operates at frequencies below
110Hz which is two orders below the frequency at which the
experimental rig was operated. At low frequencies there
is little problem with spurious resonances because only
heavy masses or low stiffness materials have resonances
at these frequencies. At high frequencies spurious
resonances arising from clamps, drive shafts etc., occur
making measurement of phase angle, force, amplitude and
displacement (acceleration) amplitude invalid. At even
higher frequencies there are more spurious resonances and
also harmonics of the lower spurious resonances which occur
at such close intervals that they run into each other so
that there is virtually no flat portion where measurements
can be made.

ii) The Rheovibron can be only used for thin flexible specimens
and so there are few problems with alignment. On the
experimental rig however the friction material specimens
were rigid and thick so that alignment had to be extremely
accurate to avoid setting up unwanted stresses.

iii) Because the specimens used on the Rheovibron are thin
the clamps could be light and simple, whereas on the
experimental rig the thicker samples required more
substantial clamps which added further problems of
resonance etc.

3.1.1.2 The B&K Complex Modulus Apparatus Versus the Experimental Forced Vibration with Resonance Technique Using Two End Clamping

The main reason why the B&K complex modulus apparatus succeeded and the experimental rig failed are as follows:-

i) On the complex modulus apparatus the mode of testing flexual and as the clamping is across the line of vibrations the mode of clamping has little effect on the test results. On the experimental rig the longitudinal vibrations must pass down the line of the clamps thus making the results highly dependent on the nature of the clamps.

ii) Also because it utilises flexual vibrations the complex modulus apparatus can use clamping from the side of the specimen and thus alignment is not a problem. On the experimental rig clamping must be in line with the vibrations so that the specimen and clamps present a continuous medium for the vibrations. Clamping at the side would give an unbalanced system. Alignment was thus still a problem for the experimental rig.

3.1.1.3 The Success of the Forced Vibration with Resonance Technique Using One End Clamping

The success of the forced vibration with resonance technique using one end clamping was due to the following:-

i) The fact that the specimens were only attached at one end meant that there were no alignment problems.

ii) The use of the impedance head meant that the apparatus could be kept simple and thus relatively free from spurious resonances.

iii) The use of mounting studs rather than clamps reduced clamping problems to a minimum.

3.1.2 Transducers

3.1.2.1 Piezoelectric Transducers

Piezoelectric transducers were used in all three techniques as it was realised at an early stage that these transducers were the best suited for use in the test rig. Their advantages are as follows:-

i) They are robust.

ii) They are sealed units and thus can be used under adverse conditions of humidity etc.

iii) They may be used at temperatures up to $250^{\circ}C$.

iv) They do not require complex electronic equipment to convert the signals to meaningful values (the use of a strain gauge network would require a dynamic strain bridge to analyse the signals obtained).

3.1.2.2 The Impedance Head Versus Separate Force and Displacement Transducers

Many of the commercial dynamic mechanical test rigs involve separate force and displacement transducers but this is because measurements are made at different places on the equipment. From the theory given in section 2.2.5.2 determination of dynamic mechanical properties can be made by measuring:-

i) Force and displacement (acceleration) at the top of the specimen.

ii) Force and displacement (acceleration) at the bottom of the specimen.

iii) Force at the top and at the bottom of the specimen.

iv) Displacement at the top and bottom of the specimen.

For the final experimental rig it would have been difficult and complicated to mount transducers on the end of the specimen and thus measurement of force displacement (acceleration) at the top end was selected. This has the advantage that the two transducers are subjected to the same localised stresses and temperature variations.

The impedance head, which was a combined force and acceleration transducer, had obvious advantages over separate force and acceleration transducers:-

i) As the impedance head was a combined unit there was no need for external connections between the force and accelerometer components. During development work with separate transducers it was found that the external connections between the transducers gave rise to many problems of alignment, rigidity and spurious resonances.

ii) The impedance head was built so that the signals from the two transducers were exactly 180° out of phase under perfectly elastic conditions below resonance. This was found impossible to achieve using separate force and acceleration transducers.

3.1.3 The Electrical Circuit

3.1.3.1 The Vibration Generator

The vibrator selected was quite suitable for use in the measurement of the dynamic mechanical properties of friction materials. However, if it were desirable to test other materials at lower frequencies then a more

powerful vibrator would be required since the vibrations below about 500Hz were rather distorted due to the heavy mass of the impedance head (28g). Most of the larger vibrators, however, have a lower maximum operating frequency than 10kHz.

3.1.3.2 The Power Oscillator

The Pye-Ling power oscillator type P.O.5VA is now obsolete. Although it was useful in the development work, if further money were available it would be the first part to be improved. On the market are power oscillators with compressor circuits built in (e.g. B&K Beat frequency oscillator type 1013). A feed-back from the accelerometer to the compressor circuit produces a d.c. signal which controls the amplifier. The compressor circuit acts in such a way that if the amplitude of the acceleration signal increases from a pre-determined reference level, the amplitude of the vibrations is instantly reduced until the amplitude of the acceleration signal has fallen to the reference level and if the amplitude of the acceleration signal decreases the reverse happens.

If a compressor circuit were incorporated only one voltmeter would be required (this is built into the B&K type 1013) and considerable time would be saved in making measurements.

3.1.3.3 The Frequency Counter

This was completely satisfactory but a simpler version would have been adequate. Digital display was a very useful feature.

3.1.3.4 The Mass Compensation Device

This was simple and efficient.

3.1.3.5 The Amplifier System

The system comprising impedance converters and voltage amplifier worked satisfactorily. A possible improvement would be to build a two channel voltage amplifier with F.E.T. transistors on the inputs so that the unit was self-contained.

3.1.3.6 Oscilloscope Display

Since the oscilloscopes were only used for examining the waveforms and Lissajou's figures without any measurements being made from them, simpler instruments could have been used. The oscilloscope which gave the Lissajou's figures could be eliminated altogether since location of the fundamental resonance could be obtained from the phasemeter and the other oscilloscope.

3.1.3.7 Voltmeter Display

The voltmeters were entirely suited for the measurement of the signal voltages produced. As previously mentioned in section 3.1.3.2, if the power oscillator had a compressor circuit built in, only one voltmeter would be required.

3.1.3.8 The Phasemeter

The phasemeter was far more sophisticated than was required since the only measurement made was the location of the 90° phase difference. Considerable simplification could be made.

3.1.4 The Test Rig

3.1.4.1 Spurious Resonances

With all three methods there were problems with spurious resonances. It is impossible to design a system which gave no spurious resonances

since this would require a one component system. When designing a system, with the minimum of spurious resonances, it is important to keep the number of components in the system to a minimum and to operate at the lowest convenient frequency.

With the final, successful technique the problem of spurious resonances arose to a limited extent when they occurred at frequencies in the middle of those encountered during temperature scans when a section of the results was rendered inaccurate.

A further cause of spurious resonances arose from the nature of the friction material specimens. Spurious resonances due to components and joints in the system should remain reasonably constant at given frequencies but occasionally a spurious resonance occurred at a frequency where with previous specimens no problem had arisen. The only explanation for these extra spurious resonances is that they are due to voids and flaws in the specimens.

The following indications of the presence of interfering resonances, even when they were too small to be noticed immediately, were established during the testing programme:-

i) $f_o > f_n$

ii) $f_2 - f_o \not\approx f_o - f_1$

iii) Phase changes around 90° are not smooth and involve stops or reversals.

iv) Two frequencies exist at which the phase difference is 90°.

v) Two minimums exist in the accelerometer voltage between f_2 and f_1.

Not all these points are apparent every time but the presence of only one is indicative of an error in the measurements.

3.1.4.2 Clamping

Several methods of clamping (including mounting using adhesive since this is a method of rigidity holding the specimen) were examined. None of the experimental clamps was successful but from these experimental clamps the following conditions were established for the design of the ideal clamp:-

i) It must be negligible in mass and length compared to the specimen unless compensation is applied.

ii) It must be approximately symmetrical about the longitudinal axis of the specimen.

iii) It must not distort under continual use.

iv) It must not distort the specimen so that unwanted localised stress patterns are set up in the specimen.

v) It must give a constant clamping pressure every time it is used so that any stressing of the specimen is constant.

vi) It must not give a clamping pressure in excess of requirements.

vii) It must be simple in construction in order to keep the number of spurious resonances to a minimum.

viii) It must be easy to operate so as to eliminate the possibility of damaging the specimen, the transducer or the vibrator etc., during the clamping operation.

The technique of mounting the specimens on 2BA screws satisfied all these criteria but introduced a few other problems:-

i) It is difficult to determine whether or not the specimen has been successfully mounted because a poor bond may be satisfactory at room temperature but fail at high temperatures.

ii) Some materials will not bond easily.

iii) It is possible for air bubbles to form in the bond causing high damping values.

iv) The main disadvantage of the technique is that the mounting operation is time consuming whereas normal clamping is not.

3.1.4.3 Alignment

For accurate measurements to be made it is essential that the vibrations emitted by the vibrator pass in a straight line through any drive shafts, transducers, clamps, mounting studs and the specimen.

On the first two dynamic mechanical test techniques studied, alignment was a problem because:-

i) The specimen was clamped at each end.

ii) Some components were soldered face to face.

On the successful technique there was little problem with alignment because clamping was only at one end and all components except the specimen were screwed to each other.

Alignment of the specimen with the mounting stud was not difficult using the mounting jig.

3.1.4.4 Mounting components

From sections 3.1.4.1 and 3.1.4.3 it will be realised that the manner in which components are linked to one another has a direct bearing on the magnitude of the problems of spurious resonance and alignment.

The first two dynamic mechanical test techniques involved separate force and acceleration transducers and because of the lack of suitable mounting points an elaborate system of sheaths and lock nuts had to be devised.

A further problem was the fact that, because the force gauge had no mounting point on its load bearing face, the face had to be soldered to the drive shaft. Problems with spurious resonances and alignment were consequentially rife. The introduction of the impedance head with its threaded mounting points and side mounted output sockets helped with both these problems.

Ideally all components should be screw mounted and as mentioned in section 2.2.5.4 if the specimen material is not brittle the ideal method of attaching it to the transducer would be to machine a 2BA thread on the end of the specimen so that it could be screwed directly into the base of the transducer.

3.1.4.5 Rigidity

In order for accurate measurements to be made, the joints between components below the upper transducer must be rigid and elastic. The first two dynamic mechanical test methods suffered more from problems of non-rigidity than the third because there were more components involved.

In the final method the only rigidity problem was with the nature of the bonding adhesive. Rubber based adhesives were found unsuitable because the cured adhesive was flexible but epoxy resin and phenolic resin adhesives which gave a rigid, elastic bond were satisfactory.

3.1.5 Temperature Variation

3.1.5.1 Oven and Heater Design

The final oven and heater design proved very suitable. The oven was easily installed round the specimen and it was possible to reach $250^{\circ}C$ from room temperature in about twenty minutes with an instantaneous temperature variation of only $\pm 1^{\circ}C$ over the length of the specimen.

The only limitation was that specimens longer than 85mm $(3.4")$ could not be accommodated in the oven without modification.

3.1.5.2 Temperature Indication and Control

Although temperature indication was satisfactory, temperature control was the weakest point in the design of the entire equipment. Throughout the development stages every attempt was made to make the equipment as cheap as possible and in the main this approach was very successful. However the simple method of a solenoid cut-out proved rather unsatisfactory for temperature control because of problems of over-shoot. The idea of reducing the air supply when the required temperature was reached worked well at temperatures up to $100^{\circ}C$ but above this temperature it was difficult to judge the control settings required to maintain a steady temperature. These problems arose because variations in the mains voltage made it impossible to have a set of standard settings.

The best system of temperature control is based on a potentiometric controller which reduces the amount of heat applied as the temperature reaches the required level. There would then be no need to reduce the air supply and thus a filter system would be required to remove the noise from the air supply from the transducer signals.

3.1.6 Further Development

At present the Scientific Instrument Research Association (S.I.R.A.) is examining the equipment and its principles with a view to fully automating the test procedure so that it could be used as a push-button test by inexperienced operators.

3.2 Problems in the Preparation of Friction Material Specimens

3.2.1 Shape Considerations

Bar shaped specimens were the easiest to produce and mount using the equipment available. However, from a commercial point of view it would be easier to grind accurate cylindrical specimens using a specially designed grinding apparatus. Cylindrical specimens would require no modification to the apparatus since no clamping is used but a different design mounting jig would be required.

3.2.2 Machining Considerations

As indicated in section 3.2.2 the only suitable machining operations are those involving:-

    i) Machining on a shaper or lathe using carbide tipped tools.

    ii) Sawing using friction cutting discs.

    iii) Grinding.

As indicated in section 3.2.1, a one operation grinding process would probably be the most suitable from the commercial point of view.

3.2.3 Mounting Considerations

The mounting technique adopted was satisfactory. The only possible improvement would be to standardise weights of adhesive and clamping pressures used.

3.3 Discussion of Test Results

3.3.1 Commissioning Experiments

3.3.1.1 Reproducibility Tests

The following dissertation refers to the results of table 5 (see appendix 2) references given pertain to the test numbers in table 5.

Refs. 1 to 7 show the gradual shift of the resonant frequency to higher frequency followed by a stabilisation. Consequently the value of E' follows a similar pattern. It should however be realised that neglecting reference 1 as the rate of change of frequency is so great that the readings are meaningless, that the change in frequency is only about 1% which is the order of experimental error. Apart from ref. 1, the Δ f, F_{max} and d values are fairly constant suggesting that the entire resonance peak is shifting to a higher frequency without any significant change of size or shape although the slight increase in the Δ f values of refs. 5,6 and 7 may indicate a tendency to maintain a steady damping value even though the position of the peak has changed. The readings taken in ref. 1 may be ignored since the rate of change of the peak to higher frequency was so great that there had been appreciable change in the position of the peak between the measurement of f_2 and f_1 , hence giving a low damping value.

Refs. 8 and 9 indicate that the shift in the position of the peak is not due to time being required for the specimen to react to the presence of vibrations.

Refs. 10 and 11 indicate that removing and re-attaching the weight has little significance and the slight peak shift is possibly due to the unavoidable disturbance of the end of the specimen at the transducer during the removal and re-attaching operation.

Refs. 12 and 13 show that the peak shift occurs in the same manner irrespective of the end at which the specimen is excited into vibration and the modulus and damping values obtained are also independent of the end of excitation.

Ref. 14 serves to reiterate the fact that the peak shift occurs every time the specimen is attached to the transducer.

Ref. 15 shows that the peak shift occurs independently of the presence of vibrations. It also indicates that the peak shift continues to occur over much longer periods than the 40 minutes allowed in ref. 7.

Ref. 16 reiterates the fact that the peak shift takes place every time the specimen is removed and re-attached irrespective of the circumstances involved.

Ref. 17 shows that the slight reduction in cross sectional area gives the expected reduction in the resonant frequency although the same values for damping and modulus are retained.

Ref. 18 shows that the presence of a deep notch does not affect the damping value but may increase the modulus value.

From the above discussion the following points are noted:-

i) Every time a specimen is attached to the transducer a shift in the position of the resonance peak is detected.

ii) The size and shape of the resonance peak remains more or less constant during the peak shift.

iii) Damping values remain fairly constant under all conditions (when readings are taken immediately after attaching the specimen to the transducer, the error in measurement of damping is probably due to the peak shifting significantly between measurement of f_2 and f_1).

The reason for the peak shift is not definitely known but it is probably due to a settling of the threads on the transducer mounting point with the threads on the mounting stud due to the vibrations combined with stress relaxation effects.

Since damping values were thought to be more significant than modulus values in the testing of friction materials it was decided that readings should be taken as soon as the position of the resonance peak had remained constant over a period of five minutes so that the rate of change of position of the peak had no influence on the measurement of damping. The modulus values thus obtained are consequently slightly lower than the true values although they will still be comparable with each other.

3.3.1.2 Tests Made over a Temperature Range with Different Added Weights

Table 9 together with graphs 4,5,6,7 summarise all the information gathered from the four temperature scans using a specimen with different added weights attached to the lower end.

Temperature Scan	1	2	3	4
Weight added, M, (g)	None	4.012	9.317	20.912
Value of f_n at $20^{\circ}C$ (Hz)	9390	2893	1837	1270
Range of f_n between $8^{\circ}C$ and $76^{\circ}C$, Δf_n, (Hz)	3201	971	584	433
$\sqrt{(M + M_s/3)}\ f_n$	–	5794	5608	5808
$\sqrt{(M + M_s/3)}\ \Delta f_n$	–	1945	1782	1980
Value of E' at $20^{\circ}C$ $(GN\,m^{-2})$4.09	4.09	4.82	4.23	4.60
Range of E' between $8^{\circ}C$ and $76^{\circ}C$ $(GN\,m^{-2})$	2.59	1.83	2.45	1.83
Temperature of β peak damping $(^{\circ}C)$	27	20	16	15
Value of f_n at β peak damping (Hz)	8767	2893	1887	1312
Value of d at β peak	0.0800	0.0746	0.0694	0.0669
Value of E' at β peak damping $(GN\,m^{-2})$	3.74	4.82	4.44	4.88

Table 9   Tests made over a temperature range with different added weights

From examination of table 9 and graphs 4,5,6,7 the following features are noted:-

   i) Addition of only a small weight reduces the resonant frequency considerably at constant temperature.

ii) Because of the square root relationship of mass with frequency further additions of weight have progressively less effect.

iii) On the basis of the three runs with added mass the relationship $(M + M_s/3)$ f_n = constant, holds to a $\pm 2.3\%$ accuracy.

iv) The same effects occur when considering the range of resonant frequencies, Δf_n, but here the relationship $(M + M_s/3) \Delta f_n$ = constant is only obeyed to a $\pm 6\%$ accuracy presumably because there are more variables present. It is interesting to note however that the values of $(M + M_s/3) \Delta f_n$ follow the same pattern as the values of $(M + M_s/3) f_n$ a fundamental error may be present.

v) The value of E' determined at 20°C over the four runs is accurate to $\pm 9\%$ which is reasonable considering that adding weights will have appreciable effects on the dimensions of the system (theoretically the added masses should have no volume) making calculation of E' in error. Far more sophisticated equations would have to be developed to take into account the geometry of the added weights and the modulus of their material.

vi) It should be noted that the values of E' in temperature scan 1 are lower than the other three temperature scans and this is to be expected since the addition of weights made from steel which has a modulus of $2.1 \times 10^2 GNm^{-2}$ i.e. two orders of magnitude greater than that of the polypropylene under test.

vii)   The difference in the ranges of E' are quite significant but far more data would be required to make any statement as to the reason for this. It is possible that over a frequency range of 1kHz to 10kHz some inherent change in the dynamic modulus may occur.

viii) It should be noted that all four plots of E' against temperature depict the expected change in gradient from steep, at temperatures at and near the peak, to shallow at temperatures away from the peak.

ix)   Variation of the frequency of test demonstrates the typical change of shape and movement of peaks in curves produced by plotting damping values against temperature over different frequency ranges. (92) As frequency increases:-

a) the height of the peak increases i.e. the peak damping increases.

b) the peak becomes broader.

c) the peak shifts to a higher temperature.

This peak is known as the β peak of polypropylene.

There is also some indication that the overall damping recorded increases at higher frequencies.

It will be noticed that on temperature scans 2, 3 and 4 there are few readings between 40 and 60°C this is because of considerable harmonic distortion in the acceleration signal at and near the resonant frequency. The effects of this are more marked at lower frequencies where the Δf values are smaller. The distortion is such that the voltage measured is smaller than the true value thus causing the value of F_{max} to be determined too high which in turn causes a low value of Δf to be determined causing low damping.

This harmonic distortion appeared to a much lesser extent in the testing of friction materials and although attempts were made to prevent it no cure was found. It appears to be a problem associated with relatively low damping materials tested at high frequencies and is probably due to some kind of 'rattling' in the system caused by mismatched joints or flaws in the specimen.

3.3.1.3 Continually Shortened Specimen Tests

The results from the continually shortened specimen tests are shown in table 6. (see appendix 2) From examination of table 6 the following points are important:-

i) f_n increases linearly with decreasing length of specimen. The relationship, $f_n L$ = constant, holds to an accuracy of $\pm 0.63\%$.

ii) f_n increases linearly with decreasing mass of specimen. The relationship $f_n M_s$ = constant, holds to an amazing accuracy of 0.29%

iii) The relationship $f_n^2 L M_s$ = constant, holds to an accuracy of $\pm 0.56\%$.

iv) The relationship, $f_o^2 L M_s$ = constant, only holds to an accuracy of $\pm 1.7\%$ indicating that modulus values are less accurately determined if f_o is taken as the basis for calculations.

v) The relationship, $|E^*| = 4 f_n^2 L^2 \rho$ (see sect. 2.1.3.3) where $|E^*| = E'$ because the damping is small, produces an average value for E' as $1.18. \pm 0.85\%$ GNm^{-2}. This value although determined to a high degree of accuracy, is low compared to the expected value of 3.68 GNm^{-2} (see appendix 3).

vi) The relationship, $E' = \dfrac{4f_n^2 \pi^2 LM_s}{3BD}$, produces an average

value of E' as 3.88 ± 0.75 GNm^{-2}. This value is in

reasonable agreement with the expected value of 3.68 GNm^{-2}

(see appendix 3)

vii) The variation in the values of ρ determined from the

relationship, $\rho = \dfrac{M_s}{BDL}$, is a real variation since if an

average value for ρ is taken the value of $E' = 4f_n^2 L^2 \rho$

would be less accurate than the values given.

viii) Although E' values are maintained constant, the stiffness

values obtained from the relationship, $k'_s = 4\pi^2 f_n^2 M_s$

$\left(\omega = 2\pi f_n = \sqrt{\dfrac{k'_s}{M_s}} \right)$, increase as the length is reduced.

ix) Because the frequency increases as the length decreases,

operating at constant acceleration means that the

strain is kept nearly constant.

$$\gamma = \frac{X}{L}$$

$$X = \frac{a}{4\pi^2 f_n^2} \quad m$$

$$a = \frac{9.81\, a_{ref}}{25} \quad ms^{-2}$$

Hence

$$= \frac{9.81 \times 10^{-2}\, a_{ref}}{\pi^2 f_n^2 L}$$

Over frequency range 2.532kHz to 9.247kHz, encountered

during testing the strain only varies from 7.68×10^{-9}

to 1.67×10^{-8}

If the values of a_{ref}, required for constant strain,
were predetermined it would be possible to operate the
equipment at these values of a_{ref} and hence obtain dynamic
mechnaical properties at constant strain (because of the
dependence of frequency each value of d is determined
over a small range of strain levels). By use of integrator
networks with facility for single or double integration
it would be possible to work at constant velocity (the
strain level remains constant as the length varies but each
value of d is still determined over a small range of
strain levels) or at constant displacement (the strain
level varies with length but each value of d is determined
at a single strain level). This control over strain level,
which is sometimes important for corellation with deter-
minations made by other methods, would not be possible with
the usual resonance technique where force is kept constant.

x) The average value of d is 0.0860 which is in reasonable
agreement with the expected value of 0.085 (see appendix 3)

xi) In order to maintain a constant value of d the value of
F_{max}, at a constant value of a_{ref}, must decrease as
frequency increases.

The reason for the low value given by the relationship,

$E' = 4f_n^2 L^2 \rho$, is that at the fundamental resonance the value of f_n is
always low. If harmonics are examined the relationship, f_i/i, is used
instead of f_n, where i is the mode number of the harmonic $(f_n = f_{i=1})$.
The relationship, f_i/i, should be approximately constant but there are
indications that this is only true for $i \geqslant 4$ and when $i = 1, 2,$ or 3 the
relationship has a value lower than the constant value.

It should be realised that unless modulus is completely independent

of frequency, even above i = 3 there will always be some variation

in the value of f_i/i but this is usually slight in comparison with the

deviation of f_n.

These facts are not generally stated in the literature and so it

was decided to perform a single experiment to investigate this

theory. Graph 8 and table 10 demonstrate that over a series of four

modes the value of f_i/i increases exponentially to a near constant value

as i increases. Because of distortion in the waveforms due to violation

of the upper frequency limits of many of the electrical components no

attempt has been made to calculate values of E' and d.

Mode Number i	f_i (Hz)	f_i/i (Hz)	f_0 (Hz)	F_{max} (V) (@ a_{ref} = 1V)
1	2801	2801	2751	4.8
2	8614	4307	8004	0.76
3	14260	4565	13380	0.54
4	19630	4907	18729	0.42

Table 10 The Significance of the ratio f_i/i

Table 10 suggests that if f_n is used to calculate modulus values

from $E' = 4f_n^2 L^2 \rho$ the answers will be a factor of $(2801/4907)^2 = 1/3.1$

too low. Examination of the relationship, $E' = 4 \pi^2 f_n^2 \, LM_s/3BD$, indicates

that it should produce moduli which are a factor $\pi^2/3 = 3.3$ larger

than the moduli produced from the relationship, $E' = 4f_n^2 L^2 \rho$ and thus

it is not surprising that the values calculated from this latter

relationship are in better agreement with literature values produced

from other methods. The relationship, $E' = 4\pi^2 f_n^2 L(M + M_s/3)/BD$

has thus been used in all calculations of E'.

N.B. If harmonics are examined $E' = 4\pi^2 f_i^2 LM_s/3BDi^2$ should not be used.

3.3.2 The Testing of Friction Material and Related Specimens

3.3.2.1 The Dynamic Mechanical Properties of Unused Disc Pads

Twenty four*unused pads finally were tested. Twelve pads were Mintex type 108 taken from batch number MNTX108GHD44BQ and their dynamic mechanical test results are depicted by the graphs in the BK series. Twelve pads were Ferodo type 2430. Four pads came from each of the following batch numbers FER2430FFF458, FER2430F FF454 and FER2430F FF and their dynamic mechanical test results are depicted by the graphs in the BK+, B+ and B series respectively. For simplicity the graphs have been reduced in size so that their shapes and magnitudes can be easily compared see figs. 49 and 50 (see appendix 2) but the salient points are summarised in tables 11 and 12. From the results given in these tables, graphs 9 and 10 have been constructed so as to represent the average and range of damping profiles exhibited by the various types and batches of pads.

From the graphs it can be seen that pads of a given type exhibit similar damping profiles but there is considerable variation in the actual values even with specimens from the same batch.

*   All the specimens were prepared and coded before any test work was commenced but during the development of the test rig many specimens were permanently damaged and consequently the numerical order of the pad samples finally tested is incomplete. For ease of reference the coding was not revised for the purpose of this thesis.

Ref.	Density* (Mgm^{-1})	$E'(GNm^{-2})$** $0°C-250°C$	$0°C$	DAMPING*** Max.	Min.	$250°C$
18BK	2.02	9.0–6.0	0.0125	0.0175(80°C)	0.0125(160°C)	0.0225
16BK	1.99	9.0–6.0	0.0125	0.0200(80°C)	0.0175(150°C)	0.0300
15BK	1.95	7.5–5.5	0.0150	0.0200(90°C)	0.0150(150°C)	0.0200
14BK	2.03	9.0–6.0	0.0150	0.0200(90°C)	0.0175(160°C)	0.0300
13BK	1.97	8.0–5.5	0.0125	0.0150(90°C)	0.0125(160°C)	0.0225
12BK	1.98	8.5–5.5	0.0125	0.0175(70°C)	0.0150(170°C)	0.0225
11BK	1.98	8.0–6.0	0.0100	0.0150(70°C)	0.0125(160°C)	0.0250
10BK	1.93	7.5–5.5	0.0125	0.0150(80°C)	0.0125(160°C)	0.0200
9BK	2.03	9.0–6.0	0.0100	0.0200(120°C)	0.0150(170°C)	0.0225
8BK	1.99	8.0–6.0	0.0125	0.0150(80°C)	0.0125(160°C)	0.0250
4BK	1.98	8.0–6.0	0.0125	0.0175(80°C)	0.0125(150°C)	0.0200
1BK	1.95	7.5–5.5	0.0125	0.0150(90°C)	0.0125(160°C)	0.0250
AVERAGE			0.0125	0.0175(80°C)	0.0150(160°C)	0.0250

Table 11 The dynamic mechanical properties of unused Mintex M108 pads from batch MNTX108GHD44BQ

Ref.	Density* (Mgm)	$E'(GNm^{-2})$ $0°C-250°C$	$0°C$	DAMPING*** Min.	$250°C$
11B+	2.50	11.0–10.0	0.0100	0.0075(140°C)	0.0150
10B+	2.46	10.0–9.0	0.0125	0.0075(130°C)	0.0200
9B+	2.56	11.5–10.5	0.0125	0.0100(130°C)	0.0200
8B+	2.45	9.0–8.0	0.0125	0.0075(130°C)	0.0200
AVERAGE			0.0125	0.0075(130°C)	0.0200

Table 12.1 The dynamic mechanical properties of unused Ferodo 2430 pads from batch FER2430F FF454

Ref.	Density* (Mgm^{-3})	$E'(GNm^{-2})$** $0^{o}C\text{-}250^{o}C$	$0^{o}C$	D A M P I N G***		$250^{o}C$
					Min.	
11BK+	2.62	11.0–10.0	0.0100	$0.0075(130^{o}C)$		0.0275
10BK+	2.55	11.0–10.0	0.0125	$0.0100(130^{o}C)$		0.0250
9BK+	2.61	12.0–11.0	0.0100	$0.0075(130^{o}C)$		0.0325
3BK+	2.54	12.0–11.0	0.0125	$0.0075(120^{o}C)$		0.0325
	AVERAGE		0.0100	$0.0075(120^{o}C)$		0.0275

Table 12.2 The dynamic mechanical properties of unused Ferodo 2430 pads from batch FER2430F FF458

Ref.	Density* (Mgm^{-3})	$E'(GNm^{-2})$** $0^{o}C\text{-}250^{o}C$	$0^{o}C$	D A M P I N G***		$250^{o}C$
					Min.	
5B	2.55	11.0–10.0	0.0100	$0.0075(130^{o}C$		0.0300
4B	2.54	10.0–9.0	0.0100	$0.0075(130^{o}C)$		0.0250
3B	2.49	8.0–7.0	0.0100	$0.0075(130^{o}C)$		0.0300
2B	2.48	8.0–7.0	0.0100	$0.0075(130^{o}C)$		0.0250
	AVERAGE		0.0100	$0.0075(130^{o}C)$		0.0275

Table 12.3 The dynamic mechanical properties of unused Ferodo 2430 pads from batch FER2430F FF

* Average density over three specimens

** Average elastic modulus over three specimens to the nearest $0.5GNm^{-2}$

*** Average damping over three specimens to the nearest 0.0025

Indeed if the individual graphs of figs. 49,50 are studied it will be seen that even within a given pad there is considerable variation in the damping profiles obtained from the three specimens. Although it is thought that some of the more extreme and irregular variations are due to spurious effects during testing, in general the variations are due to the non-uniformity of the friction materials and not experimental error since in comparison the experimental specimens of section 3.3.2.6 which should be more uniform in their manufacture, give test results with much less variation under the same testing conditions. Also particular specimens were retested some time later and the results were found to be reproducible.

In most cases the modulus values show the trend of following the density because in general the more dense materials (e.g. metals) are more elastic than the lower density materials (e.g. asbestos). There is far less variation between modulus curves of specimens from the same Mintex pad than from the same Ferodo pad and this is borne out by the more consistent density exhibited by the Mintex pads. This is surprising since visual inspection of the Ferodo 2430 pads show them to be much finer grain pad than the Mintex 108 pads which would suggest that in a small specimen the larger particles of the Mintex pads would give rise to greater density variations. This unexpected result may indicate that there are many more components in the Ferodo 2430 pads and that these are not so well mixed as in the Mintex 108 pads.

There does not appear to be any correlation between variation of the modulus profile with variation of the damping profile for either friction material and in many cases the modulus profile for the three specimens from a single pad vary markedly whilst the damping profiles are almost identical.

3.3.2.2 The Dynamic Mechanical Properties of Used Disc Pads From Cars with a History of Brake Squeal

Sixteen* sets of pads finally were tested with each set comprising of the four pads from the front wheels of a car with a history of disc brake squeal. No information was available as to which were the offending pair or which pads were paired together on the same wheel. Seven sets of pads were from cars using Ferodo type 2430 pads, six sets of pads were from cars using Mintex type M78 pads and three sets of pads were from cars using Mintex type M108 pads. No batch numbers were recorded since in many cases the same set of pads contained a mixture of batch numbers and in other cases the batch numbers were absent or illegible.

The dynamic mechanical test results for these pads are shown in the graphs in figures 51 and 52 (see appendix 2) which are again reduced in size for ease of comparison. Again the salient points are summarised in tables 13, 14 and 15 and graphs 11, 12 and 13 constructed to represent the average and range of damping profiles exhibited by the various types of pads.

* The sets of pads were coded by the prefix letter used by Girling Limited when the pads were supplied but because many of the pads were worn too thin for specimens to be prepared, the letters do not follow an alphabetical sequence.

Ref.	Density* (Mgm^{-2})	$E'(GNm^{-2})$** $0°C-250°C$	$0°C$	DAMPING*** Min.	$200°C$	$250°C$
FA	2.52	10.0–8.0	0.0125	0.0075(130°C)	0.0100	0.0250
FG	2.54	12.0–9.0	0.0125	0.0075(100°C)	0.0300	0.0500+
FM	2.52	11.0–9.0	0.0100	0.0075(70°C)	0.0500	0.0500+
FP	2.56	10.0–8.0	0.0125	0.0075(90°C)	0.0250	0.0500+
FU	2.50	11.0–9.0	0.0125	0.0075(90°C)	0.0300	0.0500
FV	2.55	12.0–10.0	0.0125	0.0075(110°C)	0.0150	0.0400
FW	2.54	11.0–8.0	0.0125	0.0075(120°C)	0.0200	0.0500+
		AVERAGE	0.0125	0.0075(100°C)	0.0250	0.0500+
SF	2.41	7.0–5.5	0.0150	0.0075(100°C)	0.0250	0.0500+

Table 13   The dynamic mechanical properties of used Ferodo 2430 pads

Ref.	Density* (Mgm^{-2})	$E'(GNm^{-2})$** $0°C-250°C$	$0°C$	DAMPING*** Min.	$200°C$	$250°C$
MB	2.05	7.0–6.0	0.0125	0.0100(110°C)	0.0200	0.0500
MD	1.92	7.0–6.0	0.0150	0.0075(110°C)	0.0150	0.0250
ME	2.00	7.0–6.0	0.0100	0.0075(120°C)	0.0100	0.0300
MF	2.00	7.0–6.0	0.0150	0.0100(120°C)	0.0300	0.0500+
MG	1.98	7.0–6.0	0.0100	0.0075(110°C)	0.0200	0.0500
MH	1.99	7.0–6.0	0.0175	0.0075(100°C)	0.0200	0.0500
		AVERAGE	0.0125	0.0075(110°C)	0.0200	0.0450

Table 14   The dynamic mechanical properties of used Mintex M78 pads

Ref.	Density* (Mgm^{-2})	$E'(GNm^{-2})$** $0°C-250°C$	$0°C$	DAMPING*** Min.		$200°C$	$250°C$
MA	2.46	10.0-8.0	0.0125	0.0075(110°C)		0.0300	0.0500+
MB	2.62	15.0-12.0	0.0125	0.0100(100°C)		0.0500	0.0500+
MC	2.61	12.0-9.0	0.0150	0.0100(100°C)		0.0500	0.0500+
		AVERAGE	0.0125	0.0100(100°C)		0.0400	0.0500+
SF	1.81	6.0-4.0	0.0150	0.0075(110°C)		0.0250	0.0500

Table 15   The dynamic mechanical properties of used Mintex M108 pads

* Average density over eight specimens.

** Average elastic modulus over eight specimens to the nearest $0.5GNm^{-2}$.

*** Average damping over eight specimens to the nearest 0.0025.

SF denotes pads from cars with no history of disc brake squeal (all other pads are from cars with a history of disc brake squeal.

As with the unused pads the shapes of the damping profiles are the same for pads made from the same type of friction material. Since the service history of each set of pads is different and pads from different batches are involved, the range over which the damping profiles extend is greater than for the unused pads. The most interesting effect, however is the change in the average damping profiles from those exhibited by the unused materials. In the case of the Ferodo pads the shape of the profiles is the same as for the unused pads but the position of the minimum has shifted from 130°C to 100°C and the damping values increase more rapidly as the temperature increases such that on average the damping at 250°C is twice that for the unused pads. In the case of the Mintex pads M108 and M78, which for the purposes of this investigation are regarded as

being essentially the same material since investigations performed by

Girling Limited have shown this to be the case, the changes are more

dramatic. The maximum at $80^{\circ}C$ has vanished, the minimum has shifted from

$160^{\circ}C$ to $100^{\circ}C - 110^{\circ}C$ and has reduced in value from 0.0150 to 0.0075

and again the damping value at $250^{\circ}C$ has doubled. These changes mean that

whereas the damping profiles of unused Ferodo and Mintex pads are

recognisably different, after use the damping profiles are indistinguishable.

This statement is supported by the fact that some of the profiles in

figures 51 and 52 are intermediate between the damping profiles of the average

used and unused pads indicating that some of the pads are only slightly

used.

The modulus values for the Ferodo 2430 pads are little altered

from the values for the unused pads which was expected since the density

values were similar. However, although the used Mintex M78 pads have

similar densities and moduli to the unused Mintex pads, the used Mintex

M108 pads have higher densities and thus higher moduli than the unused

pads. This indicates that since the basic materials are the same and

assuming that no serious degradation has taken place, the increase in

density of the Mintex M108 material must be due to compression during use.

This is supported by physical inspection of the materials which suggests

that the Mintex materials would be more compressible than the Ferodo

materials.

The foregoing discussion has made no attempt to suggest any fundamental

differences between the four pads in each set in order to define a

condition for break squeal. Since there are two pads per disc it would

seem likely that it is a combination of two pads which gives rise to a

squeal condition and because only two pairs of pads for each car were

available it was not possible to even guess which were the offending pairs from their dynamic mechanical test results. Furthermore it should be recognised that in many cases the two specimens from a given pad had very different dynamic mechanical test results indicating that the pad was not uniform. This means that in order to gain meaningful results the dynamic mechanical properties of the complete pad must be established. Unfortunately the scope of this project did not permit investigations of this nature since a completely new technique is involved.

3.3.2.3 The Dynamic Mechanical Properties of Used Disc Pads
From Cars With No History of Brake Squeal

Because of the difficulty in obtaining only slightly used disc pads which were free from complaint, Girling Limited were only able to supply one set of Ferodo 2430 pads and one set of Mintex M108 pads which had no history of squeal. The dynamic mechanical properties of these pads are shown in tables 13 and 15. It can be seen that the damping properties of these pads are essentially the same as their counterparts from cars with a history of squeal.

The density and moduli values are more interesting since both are lower than the average for the unused pads. The only explanation for this is that the pads from cars with no history of squeal, although made from the same material, were smaller than the unused pads and may have been moulded with less pressure causing the material to have a lower density.

3.3.2.4 The Effect of External Agents on the Dynamic Mechanical
Properties of Friction Materials

The dynamic mechanical test results from the external agent tests are shown in graphs 14,15,16,17,18,19 and these should be compared with graphs 20,21,22,23 which show results for the same specimens but with no external agents added.

At elevated temperatures the external agents vaporise causing the weight of the specimens to vary and because this variation cannot be satisfactorily monitored, determination of modulus is not possible. On certain of the test runs, near the boiling point of the external agent, vaporisation was so great that the position of the resonance frequency changed too rapidly for accurate damping measurements to be made. In such instances a five minute delay was taken to allow for stabilisation and this is shown on the graphs where appropriate.

3.3.2.4.1 The Effect of Immersion in Tap Water

Three specimens from pad sample 9+BK (Ferodo type FER2430F FF458) and three specimens from pad sample 15BK (Mintex type MNTXM108GHD44BQ) were tested. Table 16 gives some information obtained from the relevant graphs.

	15BK		9+BK	
	Approx. temp. of min. damping (^{o}C)	Approx. value of min. damping	Approx. temp. of min. damping (^{o}C)	Approx. value of min. damping.
No water added	150	0.0135	110	0.0065
Water added	160	0.0155	140	0.0075

Table 16   The effect of water on the damping minima

Below about 100°C the effect of the water was to increase the damping considerably and for each material the increase was approximately proportional to the water lost as determined by weighing the specimens before and after testing (see table 17).

Water lost (g)	Specimen		
	1	2	3
15BK	0.1026	0.0805	0.0793
9+BK	0.1191	0.1618	0.1888

Table 17   Weights of water lost during testing

Between 100°C and 160°C rapid changes take place as the water is lost.

Above 160°C the results for specimens with and without water added are similar indicating that most of the water had been lost. This was confirmed when the specimens were retested at room temperature and found to give approximately the same results as when no water was added.

From these observations the following conclusions are drawn:-

i) The damping below $100^{\circ}C$ is approximately proportional to the amount of water in a given disc pad.

ii) The minimum damping value is only slightly increased by the presence of water but the temperature of minimum damping can change considerably especially if under dry conditions the temperature of minimum damping is well below $160^{\circ}C$.

iii) The effect of adding water to a disc pad is reversible and all water appears to be lost above $160^{\circ}C$.

3.3.2.4.2 The Effect of Immersion in an Oil-Water Suspension

Since tap water did not give lasting changes in the specimens it was decided to use the same specimens again. Table 18 gives some information obtained from the relevant graphs.

	15BK		9+BK	
	Approx. temp. of min. damping ($^{\circ}C$)	Approx. value of min. damping.	Approx. temp. of min. damping ($^{\circ}C$)	Approx. value of min. damping
No suspension added	150	0.0135	110	0.0065
Suspension added	180	0.0155	150	0.0075

Table 18   The effect of an oil-water suspension on the damping minima

Again the damping below $100^{\circ}C$ is approximately proportional to the amount of water and oil present (see table 19).

Weight lost (g)		Specimen	
	1	2	3
15BK	0.1095	0.0888	0.0913
9+BK	0.0543	0.1103	0.2003

Table 19   Weights of suspension lost during testing

Between $100^\circ C$ and $180^\circ C$ rapid changes take place as the suspension vaporises.

Above $180^\circ C$ all effects of the suspension have disappeared which is confirmed by retesting at room temperature.

The conclusions drawn are the same as those for the effect of adding only water except that the recovery temperature is $180^\circ C$ instead of $160^\circ C$ which is probably caused by oil having a higher boiling point than water.

3.3.2.4.3   The Effect of Immersion in Brake Fluid

Although there were no apparent lasting changes caused by immersion in an oil-water suspension it was decided to use different specimens in case minute traces of oil were still present. The specimens chosen for testing were from pads with the same type and batch number as before but designated 11+BK and 14BK for test purposes. Tables 20 and 21 give some information obtained from the relevant graphs.

	14BK		11+BK	
	Approx. temp. of min. damping (^{O}C)	Approx. value of min. damping.	Approx. temp. of min. damping (^{O}C)	Approx. value of min. damping.
No brake fluid added	150	0.0165	110	0.0075
Brake fluid added	180	0.0200	160-200	0.0165

Table 20   The effect of brake fluid on the damping minima

The Mintex friction material 14BK gives a distinct damping maximum and the effect of brake fluid on this maximum is shown in table 21 .

14BK	Approx. temp. of max. damping (^{O}C)	Approx. value of max. damping
No brake fluid added	80	0.0200
Brake fluid added	90	0.0270

Table 21   The effect of brake fluid on the damping maxima

Again the damping below 100°C is approximately proportional to the amount of brake fluid present (see table 22).

Weight lost (g)	Specimen		
	1	2	3
14BK	0.0592	0.0496	0.0623
11+BK	0.1469	0.1443	0.1328

Table 22   Weights of brake fluid lost during testing

Although the shape of the damping profiles revert to those of the untreated specimens above $200^{o}C$, an overall increase in damping is observed. This is confirmed by retesting at room temperature when results indicate an overall increase of approximately 0.0025 in the damping.

From these observations the following conclusions are drawn:-

i) The damping below $100^{o}C$ is approximately proportional to the amount of brake fluid in a given pad.

ii) Throughout the complete damping profiles the effect of adding brake fluid is to increase the damping substantially. The positions of maxima and minima are also shifted to higher temperatures.

iii) The effect of adding brake fluid to a disc pad is not reversible as the damping of the friction material is permanently increased.

3.3.2.4.4 Conclusions

From the experiments made with the external agents water, oil-water suspension and brake fluid, the following conclusions are drawn:-

i) The damping below $100^{o}C$ is approximately proportional to the amount of external agent taken up by a given disc pad. The Ferodo pads tend to take up more of the external agents than the Mintex pads and thus the effects are greater.

ii) The damping maximum values and minimum values are increased by the external agents and the positions of maxima and minima are shifted to higher temperatures.

iii) The effect of water and oil-water suspension on the damping

properties of a disc brake pad are reversible but the effect

of brake fluid is not.

3.3.2.5 The Significance of Various Components of Friction Materials

As was pointed out in section 2.4.3.2 this work was only intended to
be a preliminary investigation and is by no means complete. Graphs 24,25,
26,27,28,29,30,31 show the variation of the dynamic mechanical properties
over a temperature range from room temperature to about $250^{o}C$. In all
the experiments similar specimen dimensions to friction material specimens
were used and it was found that the resonant frequencies all fell within
the required frequency range i.e. 1kHz - 10kHz.

In each experiment at least two specimens of the same composition
were made and tested and the damping profiles of each specimen in a given
experiment were found to be the same within the limits of experimental
error. However, as usual if in a given experiment the density of one
specimen was slightly higher than the others then the modulus profile,
although having the same shape, occurred at a higher range of values.
It proved impossible to control density accurately using a three plate
mould since the quantity of flash could not be controlled. If a commercial
disc pad mould had been available for use control of flash would have been
possible.

Since the moduli curves all followed the predicted trend (i.e. a
gradual decrease with increasing temperature when the damping is not
changing rapidly and a rapid decrease when the damping is changing rapidly)

they will not be discussed further, only the value at an intermediate temperature of $130^{o}C$ will be quoted for comparison purposes. The damping curves are more interesting and are discussed below:-

i) Cured phenolic resin only

Within the temperature range studied the damping followed an exponential profile which has no maximums or minimums. Between $20^{o}C$ and $150^{o}C$ the damping value only increased from about 0.01 to 0.02 whereas from $150^{o}C$ to $250^{o}C$ the increase was from about 0.02 to 0.15. The modulus at $130^{o}C$ was approximately 3.5 GNm^{-2}.

ii) Cured phenolic resin with multigrade asbestos

The effect of adding 50% asbestos was to reduce the exponential trend so that between $20^{o}C$ and $200^{o}C$ the damping value varied between 0.01 and 0.02 and only rose to approximately 0.045 at $250^{o}C$. There was also some indication of a maximum at $50^{o}C$ and a miminum at $120^{o}C$ which is characteristic of some friction materials. The modulus at $130^{o}C$ was approximately trebled to 9.5 GNm^{-2} by the addition of the asbestos.

iii) Cured phenolic resin with 5R asbestos

Unexpectedly the effect of adding 28% asbestos suppressed the exponential nature of the damping profile more than adding 43% of asbestos which in turn was more effective than adding 57% of asbestos. Between $20^{o}C$ and $150^{o}C$ all three damping curves showed a profile similar to that of cured phenolic resin only specimens in varying between 0.01 and 0.02 but between $150^{o}C$ and $250^{o}C$ the damping increased to 0.04 (28.5%)asbestos, 0.065 (43%) and 0.082 (57%). There was some indication

of a maximum at 60°C and a minimum at 110°C on the profile for 57%

asbestos but this was not observed on the other profiles. As expected

as the amounts of asbestos were increased the modulus at 130°C increased

from 7.2 GNm^{-2}(28.5% asbestos) to 8.7 GNm^{-2}(43%) and 11.5 GNm^{-2}(57%).

iv)   <u>Cured phenolic resin with asbestos and metal</u>

The damping profile was observed to follow the damping profile of

phenolic with 28% 5R asbestos very closely. Because the introduction of

metal was not expected to affect the damping, the indication is that the

percentage of asbestos in the specimen (in this case 29%) governs the

damping and not the phenolic/asbestos ratio as would be indicated by a

damping profile similar to that of phenolic with 43% 5R asbestos. As

expected modulus was high at an average value of 9.9 GNm^{-2} at 130°C.

v)   <u>Cured phenolic resin with asbestos and barytes</u>

Again the damping profile followed the profile of phenolic with 28%

asbestos but there were quite definite indications of a maximum at 50°C

and a minimum at 110°C. Modulus was high at an average value of 10.25 GNm^{-2}

at 130°C.

vi)   <u>Cured phenolic resin with asbestos and friction dust</u>

Here both the modulus and the damping profiles were very similar to

those for phenolic with 28.5% asbestos. The modulus was 7.2 GNm^{-2} at

130°C.

As a result of these observations the following conclusions are drawn:—

i) The damping profile of a friction material is basically the exponential profile of cured phenolic resin suppressed by the asbestos and modified by the property modifiers present.

ii) The modulus profiles of the experimental profiles follow the usual trends and serve only to indicate density variations within a group of specimens with allegedly the same composition.

iii) The effect of varying the asbestos concentration is unclear and needs further investigation particularly since small concentrations of asbestos have more effect than large concentrations. The three component specimens indicate that it is the percentage of asbestos in a friction material which governs the damping profile rather than the phenolic/asbestos ratio.

iv) Some evidence of a damping maximum at $50^\circ C$-$60^\circ C$ and a damping minimum at $110^\circ C$-$120^\circ C$ exists with certain types of asbestos in particular concentrations and when barytes is added but more work is required to establish the causes of this effect which occurs in the damping profiles of most friction material specimens.

v) Friction dust and metal inclusions appear to have little or no effect on the damping profile of friction materials although metals appear to increase modulus values.

3.4 Correlation With Brake Squeal

3.4.1 Compilation of the Information Gained from this Study on the Dynamic Mechanical Properties of Friction Materials

Although no direct indications as to the cause of or the conditions for brake squeal were established, this study has produced useful insight into the dynamic mechanical properties of friction materials which may be of future use to braking system design engineers.

Each friction material has its own characteristic damping profile both in the used and in the unused condition but there may be considerable differences between the two conditions. The unused Mintex pads have very different damping profiles to the Ferodo 2430 pads but after use the damping profiles are very similar. After use both materials have a distinct minimum at about $105^{\circ}C$ but the actual position of this minimum may vary between $70^{\circ}C$ and $120^{\circ}C$. The damping value at this minimum also varies and may be as low as 0.005 or as high as 0.015.

There were no obvious differences between pads involved in squeal and those not, although a more precise testing programme (see sect. 3.4.2) may have exposed slight differences. This situation is not helped by the fact that non-uniformity is always present. Specimens from the same pad may have different composition and thus different properties and density is affected by compressibility and moulding pressures. Mintex M108 is more compressible than Ferodo 2430.

The effects of oil, water and brake fluid are as follows:-

    i)   Damping below $100^{\circ}C$ is increased in proportion to the amount of external agent absorbed.

    ii) The temperatures and values of any maxima and minima in the damping profile are increased.

These effects are reversible in the case of water and oil but not in the case of brake fluid. Ferodo 2430 pads tend to absorb more of the external agents than the Mintex M108 pads and thus the effects are greater.

From the tests on experimental linings the following conclusions are drawn.

i) The damping profile of a friction material is basically the exponential profile of cured phenolic resin suppressed by the asbestos and modified by the property modifiers present.

ii) The effect of varying the asbestos concentration is unclear. The indications are that smaller concentrations have more effect and that it is the percentage of asbestos in a friction material which governs the damping profile.

iii) Some evidence of a damping maximum at $50^{\circ}-60^{\circ}C$ and a damping minimum at $110-120^{\circ}C$ exists with certain types of asbestos in particular concentrations and when barytes is added but the results are not conclusive.

iv) Friction dust and metal inclusions appear to have little or no effect on the damping profile although metals appear to increase modulus values.

Throughout the testing programme variation in modulus was found to indicate variation in density.

3.4.2 The Problems of Correlating Data

During this project it was found that there were several deficiencies in the testing programme which led to restrictions on the degree of correlation.

i) In order to make comparisons between different specimens the readings should be subjected to a standard technique for discarding results where slight inaccuracies occur. During this project only a simple visual assessment was made of the distortion in the waveforms and the effect of spurious resonances. Hence some results may be more in error than others. With a fully automated instrument a built in rejection mechanism could be used to keep the results within certain defined limits of experimental error.

ii) Because temperature control was not good and considerable time was required to complete a set of readings at a given temperature, some results for damping may be in error due to the temperature changing between taking the readings of f_o, f_2 and f_1 . With an automated system temperature control would be better and also a set of readings would be completed much more quickly than by hand, making errors in damping values even smaller.

iii) Detailed examination of pads which had a history of squeal was not possible because no indication was given as to which pads were involved on the squealing brake. More information about squeal might be obtained if information was also available regarding :-

a) The car involved.

b) The age and state of the braking system.

c) The type of brake involved.

3.4.3 A Tentative Theory of How Dynamic Mechanical Properties May Be Related to Brake Squeal

As stated in section 3.4.1 the used friction materials studied showed distinct minima in the plots of damping against temperature. The minimum value of damping varied from sample to sample with the same basic friction material and the position of the minimum varied over a range of $50^{o}C$. The variations are probably due to slight variations in the quantities of asbestos and barytes in the particular specimen under test.

Based on the assumption (ref. 48) that low damping in the disc pad is a contributing factor in making the disc susceptible to vibration i.e. in causing brake squeal, two further assumptions are possible:-

i) When the pad is at the temperature at which the damping

is at a minimum the system is most prone to brake squeal.

ii) The lower the minimum value the more prone the system is to

brake squeal.

In order for this theory to be viable it must account for the relevant features of brake squeal listed in section 1.2.3.3.

Assumption (i) above means that the incidence of brake squeal is a function of the operating temperature of a given disc brake pad. Hence:-

a) Brake squeal will be erratic and fugitive since the

temperature of minimum damping will only be realised

under certain conditions and will vary from pad to pad.

b) Under standard conditions of driver, road, traffic and speed the temperature of the disc pad will be a function of external temperature, pedal pressure, weather and humidity.

c) Because wear can change the average composition of the pad the position of the minimum damping may vary.

d) As indicated above the driver can influence the operating temperature of a brake solely by the frequency and degree of his braking operations. Thus a driver who makes frequent violent applications of the brake will operate the pad at a much higher temperature than the driver who makes few gentle applications with the same car under similar conditions. Thus one driver may experience brake squeal and the other may not, a situation which in practice is not uncommon.

e) Because the nature of the road and the intensity of traffic affect the frequency and degree of the braking operations, the temperature of the pad will also vary, which could account for the erratic and fugitive nature of brake squeal. On a test run made by Girling Limited (94) between Tyseley, Birmingham and Borth, Cardiganshire via the Cambrian Mountains in a 1964 Mark 3 Ford Zephyr 6 fitted with Girling type 16 FS front calipers, a thermocouple in one of the front disc pads indicated a variation between room temperature and $320^{\circ}C$ although once the car was under way and a few applications of the brake had been made the temperature never fell below $100^{\circ}C$. An analysis of part of this run is shown in graph 32.

From assumption (ii) above:-

    a) If the average composition of the pad is changed by wear then the minimum damping value may vary so that over a period of time squeal may disappear and re-appear.

    b) Hard materials are usually low damping materials (e.g. metals) whereas soft materials usually have high damping (e.g. rubber). Thus it is reasonable to expect that hard friction materials will have a lower minimum damping and thus be more prone to squeal.

If the damping provided by the pad does prevent disc squeal then the effective damping will be reduced if the contact between the disc and the pad is reduced. Hence squeal is more likely if contact is reduced by disc distortion wear pattern or dust.

In the foregoing discussion reference is made to "the disc pad" but it should be realised that since there are two pads per disc it is the combined effect of both pads which is thought to give rise to squeal. If this is correct, a change of only one pad could be sufficient to cure a case of brake squeal and this is often the case in practice.

Although this theory is not disproved by any of the established facts regarding disc brake squeal only trials using normal production vehicles fitted with thermocouples in the disc pads can be used to give weight to the theory. At the time of this present study no facility was available for vehicle trials.

Finally, it is felt that if the mechanical system at the brake is very

squeal prone then a much higher minimum damping will be required to eliminate brake squeal whereas a near perfect system will tolerate a lower minimum damping without giving rise to brake squeal.

3.5 Suggestions for Future Work

Although this study has indicated that there may be correlation between the dynamic mechanical properties of friction materials and the incidence of brake squeal, the results are far from conclusive and thus more work is required. Most of these suggestions for future work have been mentioned previously but to summarise they may be considered under three headings:-

 i) Modifications to the testing equipment.

 ii) More detailed study of individual disc pads with a well defined history.

 iii) More thorough investigation into the effect of various friction material components on the dynamic mechanical properties of friction materials.

3.5.1 Modifications to the Equipment

As indicated in section 3.1.6 the most desirable feature would be complete automation of the equipment. If this is not possible then improvement of the temperature control system and provision of filter units to reduce waveform distortion should have priority. A device to measure the degree of waveform distortion would be a useful addition to maintain results within certain defined limits of experimental error.

3.5.2 Individual Disc Pad Study

As indicated in section 3.4.2 before detailed examination of disc
pads with a history of squeal can be made, information is required
regarding:-

     i)   The car involved.

    ii)   The age and state of the braking system.

   iii)   The type of brake involved.

If pads with this information are not available then experiments should be
made on various vehicles with various pads in an attempt to find a squeal
prone pad which has a well documented history. Once this has been achieved
experiments should be made to determine the composition, uniformity and
surface wear pattern of squeal prone pads.

If it is possible to experiment with a car which has squealing brakes
then determination of the temperatures at which squeal occurs could be
used to prove or disprove the theory of section 3.4.3 by later comparison
with the temperatures of minimum damping determined when the pads are cut
up and tested.

3.5.3 The Effect of Various Friction Material Components

Some preliminary work along these lines has already been carried out
see section 2.4.3.2. This work indicated that the resin-asbestos-barytes
ratio was important in determining the damping/temperature profile of a
given disc pad. More relevant information may be obtained, however, if
various composition experimental disc pads were made using typical pressures
and temperatures. These experimental pads could then be cut up and tested
in the normal manner.

Attempts could then be made to design a pad which had desirable friction material properties and a low tendancy to squeal in service.

3.5.4 The Ideal Test Technique

The previous suggestions are all along the lines of this present study but as mentioned in section 3.3.2.3 ideally a completely new technique is required to give the most accurate information. Because of problems of non-uniformity the ideal test method would determine the dynamic mechanical properties of complete pads including the back-plate. This would have the added advantage that the pads would be re-usable thus enabling such phenomena as changes due to wear to be studied in detail.

CHAPTER 4

CONCLUSION

This study has yielded the following:-

i) An apparatus to determine the dynamic mechanical properties
of damping and modulus over a wide range of frequencies and
temperatures. This apparatus has commercial value in that
it is not restricted to friction material testing and covers
a frequency range which is covered by few commercial
instruments.

ii) Information regarding the dynamic mechanical properties of
disc pad materials a field where no similar information is
readily available. This information indicates the presence
of a temperature of minimum damping, a feature which is not
generally taken into account by braking system engineers.

iii) A tentative theory of how dynamic mechanical properties of
friction materials may be related to brake squeal which,
if proved, may give rise to the design of disc pads with
little or no tendency to squeal in service.

APPENDIX 1

Names and Addresses of Suppliers

Frequency Counter.

Venner Electronics Ltd,

Kingston By-Pass,

New Malden,

Surrey.

Oscillator.

Ling Altec,

Baldock Rd,

Royston,

Herts.

Vibrator.

Ling Altec (address as above)

Impedance Head.

Bruel & Kjaer Laboratories Ltd,

Cross Lances Rd,

Hounslow,

Middlesex.

Charge Matching Devices.

K.F.L. Lansdowne & Co.,

44, Weatherall Rd,

SmallField,

Horley,

Surrey.

Mass Compensation Device.

Bruel & Kjaer Laboratories Ltd,

(address as above)

Phase Meter.

Dawe Instruments Ltd,

Concord Rd,

Western Ave,

London W.3.

Voltmeters.

Farnell Instruments Ltd,

Sandbeck Way,

Wetherby,

Yorkshire.

Oscilloscope.

Telequipment Ltd,

313, Chase Rd,

Southgate,

London.

APPENDIX 2

Results.

This appendix contains all the graphs refered to in the main body
of the thesis together with tables which represent directly recorded
results.

Test No.	Temp. °C	f_n Hz	f_o Hz	f_λ Hz	f_1 Hz	Δf Hz	F_{max} V	$F_{r.m.s}$ V	d	E' GNm^{-2}
1	21.0	1800	1785	1863	1752	111	6.00	4.24	0.0622	4.07
2	21.0	1831	1817	1884	1761	123	5.80	4.10	0.0677	4.20
3	21.0	1841	1828	1888	1765	123	5.80	4.10	0.0673	4.25
4	21.0	1845	1827	1890	1767	123	5.80	4.10	0.0673	4.27
5	21.0	1848	1831	1893	1769	124	5.80	4.10	0.0677	4.28
6	21.0	1852	1843	1896	1772	124	5.80	4.10	0.0673	4.30
7	21.0	1851	1842	1897	1773	124	5.80	4.10	0.0673	4.29
8	21.5	1848	1830	1897	1771	126	5.90	4.17	0.0689	4.28
9	21.5	1848	1838	1897	1771	126	5.90	4.17	0.0686	4.28
10	21.5	1846	1836	1890	1767	123	6.00	4.24	0.0670	4.27
11	21.5	1847	1839	1895	1771	124	6.00	4.24	0.0674	4.28
12	21.5	1821	1818	1875	1758	113	5.70	4.03	0.0622	4.17
13	22.0	1855	1838	1896	1772	124	5.60	3.96	0.0675	4.31
14	23.0	1810	1796	1869	1752	117	6.00	4.24	0.0651	4.11
15	21.0	1878	1864	1917	1793	124	5.60	3.96	0.0658	4.40
16	21.0	1865	1843	1898	1776	122	5.40	3.82	0.0662	4.35
17	21.0	1838	1820	1880	1757	123	5.60	3.96	0.0676	4.34
18	22.0	1859	1840	1901	1777	124	5.70	4.03	0.0674	4.45

Table 5 Reproducibility Test Results

Key. (see sect. 2.2.7.1) (The reference numbers in brackets refer to the test numbers from the table.)

    i) Specimen attached to transducer and readings taken immediately (1) and after 3(2), 6(3), 9(4), 15(5), 30(6) and 40(7) minutes.

    ii) Oscillator switched off for 25 minutes, switched on and readings taken immediatly (8) and after 6 (9) minutes.

iii) Weight removed and replaced 6 minutes later and readings taken immediately (10) and after 5 (11) minutes.

iv) Specimen and weight reversed and readings taken immediately (12) and after one hour (13).

v) Specimen reversed to its original configuration and readings taken immediately (14).

vi) Equipment switched off over night and readings taken next morning (15) immediately after switching on.

vii) Specimen removed and replaced and readings taken after 10 minutes (16).

viii) Specimen cross sectional area reduced and readings taken after 20 minutes (17).

ix) Deep notch cut in specimen and readings taken after 20 minutes (18).

Test No	Temp. $^\circ$C	Length L mm	Weight M_s g	f_n Hz	f_o Hz	f_2 Hz	f_1 Hz	Δf Hz	f_{max} V	$F_{r.m.s}$ V
1	21.9	212	4.0190	2532	2505	2606	2408	198	6.20	4.38
2	21.9	167	3.1667	3222	3150	3320	3039	281	4.70	3.32
3	22.0	139	2.6132	3894	3865	4004	3687	317	3.95	2.79
4	22.0	108	2.0291	5020	4975	5148	4707	441	3.00	2.12
5	22.2	76	1.4383	7081	6959	7242	6631	611	2.40	1.70
6	22.3	58	1.1053	9247	9077	9422	8613	809	2.00	1.41

continued

Test No.	a_{ref} V	$f_n M_s$ kgs^{-1}	$f_n L$ ms^{-1}	$f_n^2 LM_s$ MN	$4\pi^2 f_n^2 M_s$ MNm^{-1}	$f_o^2 LM_s$ MN	ρ Mgm^{-3}	$4f_n^2 L^2 \rho$ GNm^{-2}	$\dfrac{4\pi^2 Lf_n M_s}{3BD^2}$ GNm^{-2}	d
1	3.15	10.18	536.7	5.462	1.017	5.342	1.017	1.17	3.85	0.0790
2	3.15	10.20	538.1	5.493	1.298	5.248	1.017	1.18	3.88	0.0892
3	3.15	10.18	541.3	5.507	1.564	5.426	1.009	1.18	3.88	0.0820
4	3.15	10.19	542.1	5.522	2.018	5.424	1.008	1.19	3.91	0.0886
5	3.15	10.19	538.1	5.480	2.846	5.294	1.016	1.18	3.88	0.0878
6	3.15	10.22	536.3	5.480	3.730	5.279	1.022	1.18	3.88	0.0891

Table 6 Results of the Continually Shortened Specimen Tests.

Explanation of the Graphs in Figures 49, 50, 51 and 52.

For ease of comparison the graphs of figures 49, 50, 51 and 52 have been simplified as much as possible. In each the scale of the vertical axis for the damping curve is 0.01, 0.02, 0.03, 0.04 as indicated in the key. Hence the damping curves are all directly comparable. Since the modulus values differ significantly from specimen to specimen, the vertical axis scale is shown on each graph, the units being GNm^{-1}. The modulus curves can easily be easily recognised since they always follow a steady reduction as temperature increases. The horizontal axis represents temperature and the divisions marked represent $100^{\circ}C$ and $200^{\circ}C$ (see key).

A list of specimen densities is given in table 23.
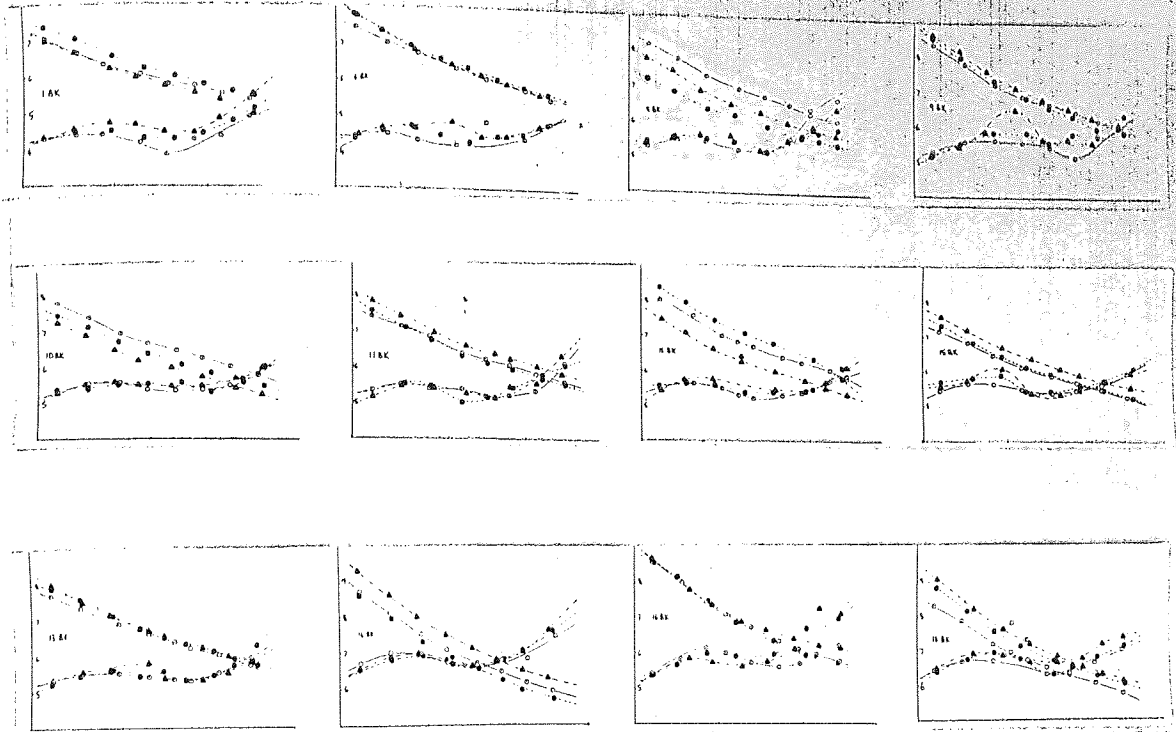
Fig. 49 Dynamic mechanical properties of unused Mintex 108 pads.
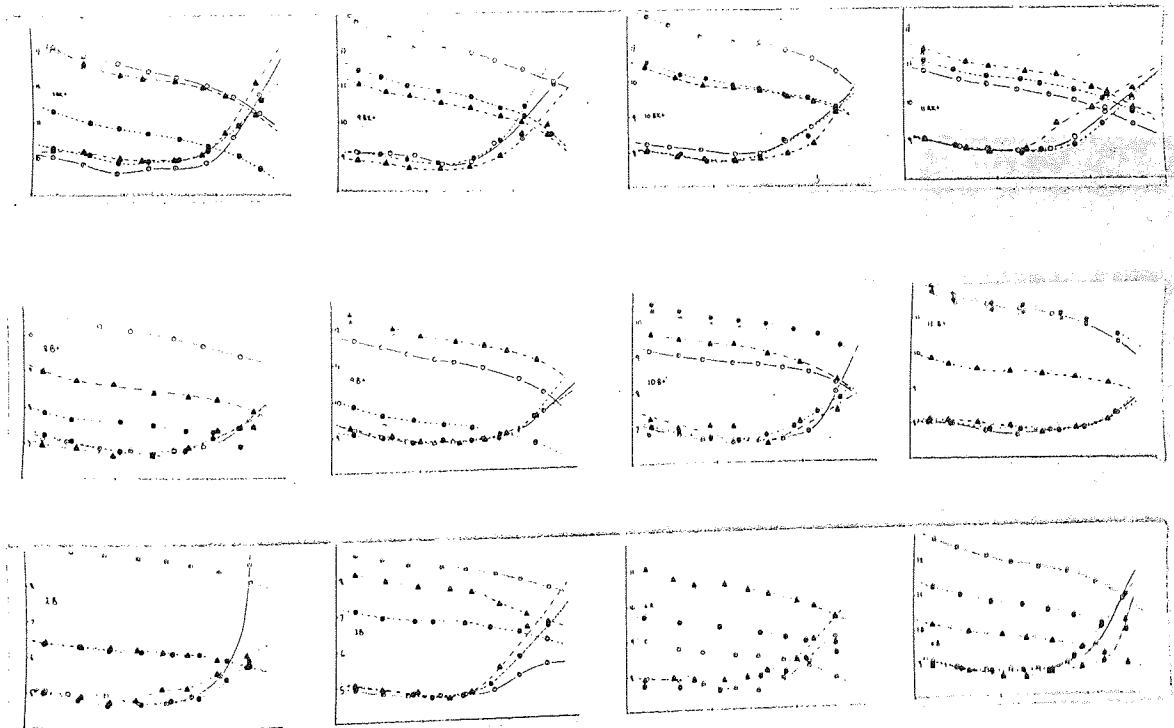
Fig. 50 Dynamic mechanical properties of unused Ferodo 2430 pads.

M108
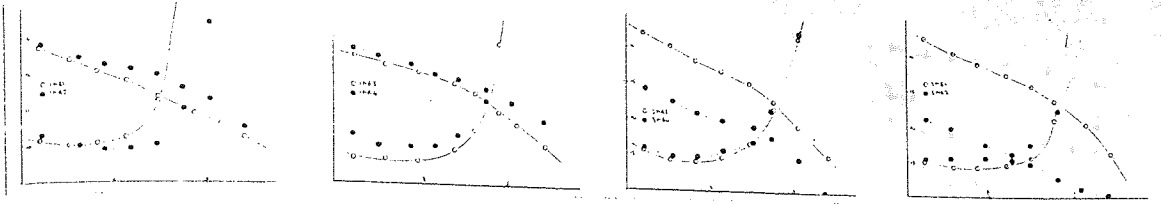
M108
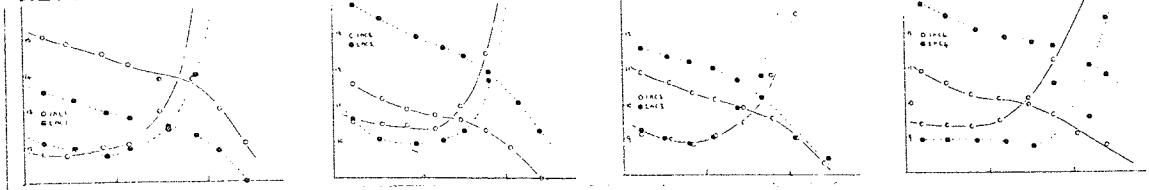
M108
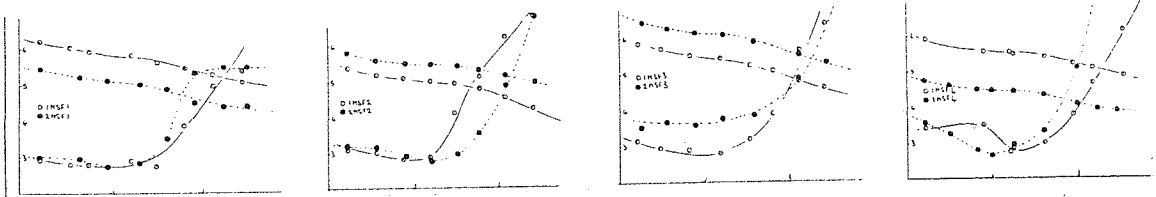
M108
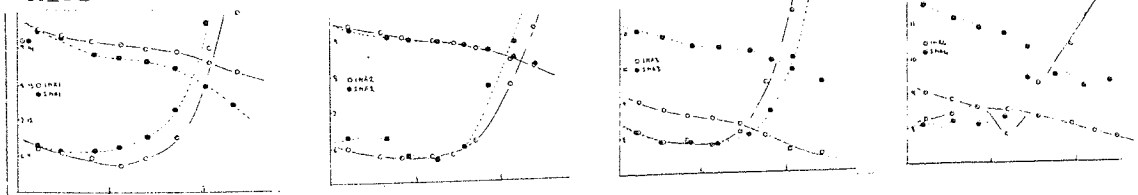
M78
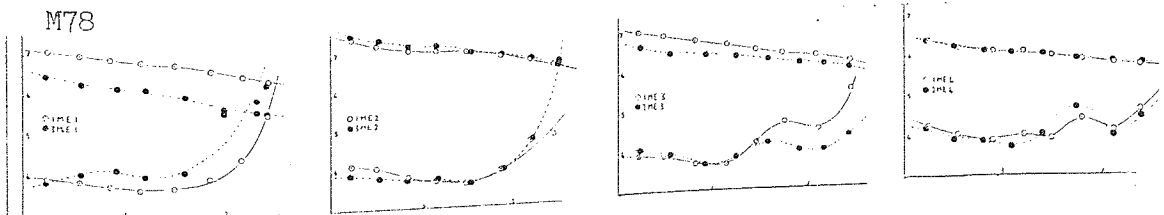
Fig. 51 Dynamic mechanical properties of used Mintex 108 and 78 pads.

M78

M78

M78

M78

M78
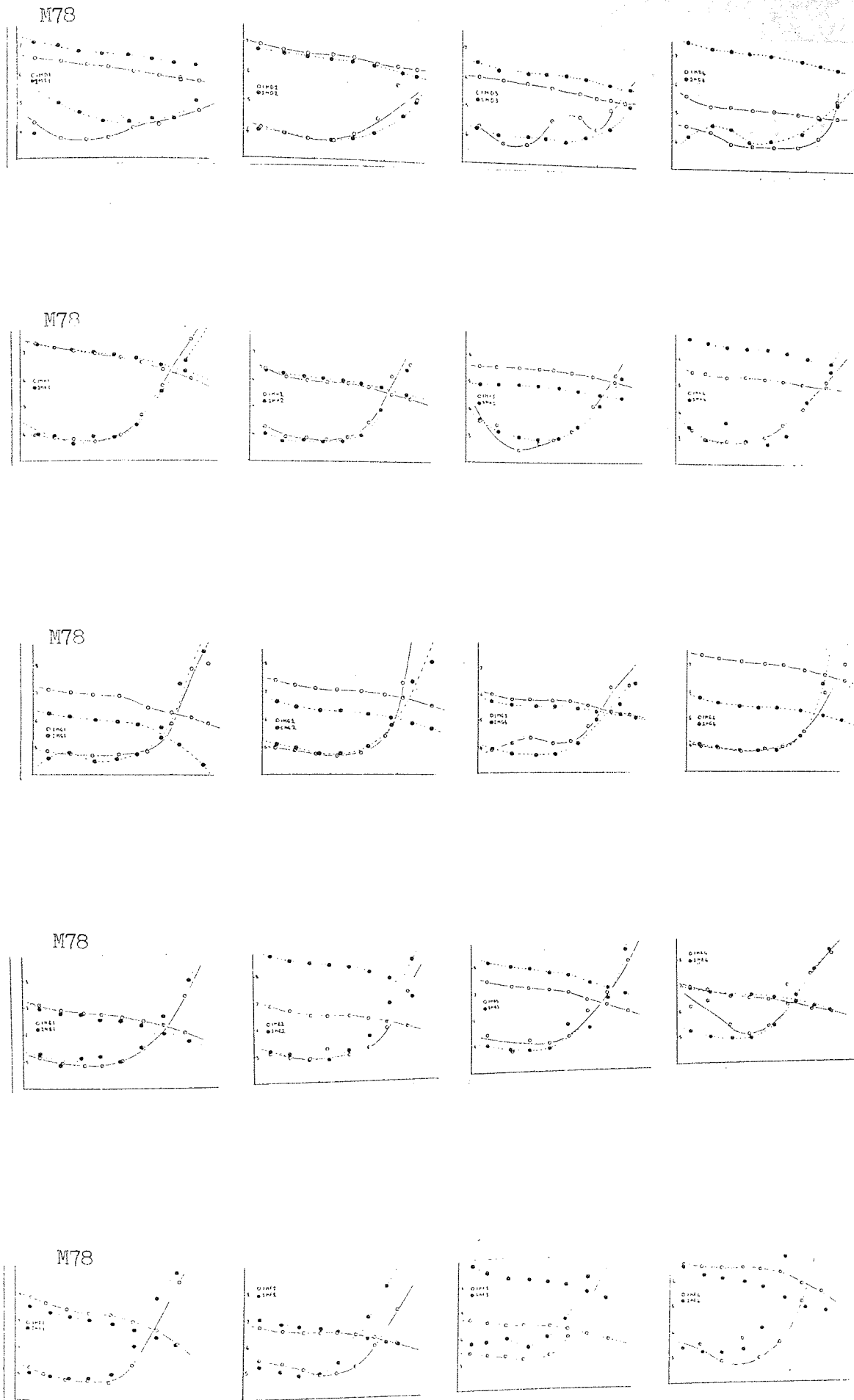
Fig. 51 Continued.

Fig. 52 Continued.

KEY

⊙ ——— SPECIMEN 1

● - - - - SPECIMEN 2

▲ - · - · - SPECIMEN 3

$\dot{E}$ (GNm⁻²)

[VALUES GIVEN]

0.04

0.03

α

0.02

0.01

0

100   200

TEMP (°C) →
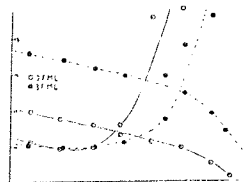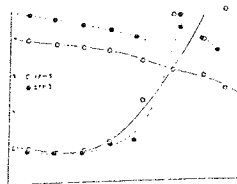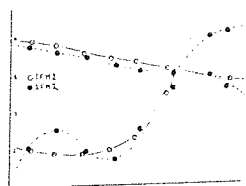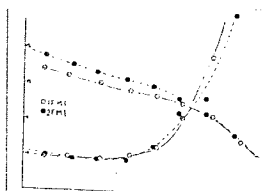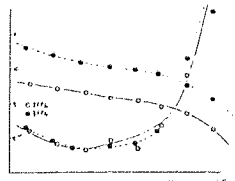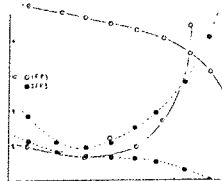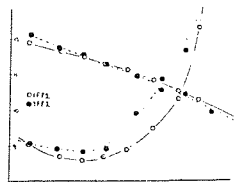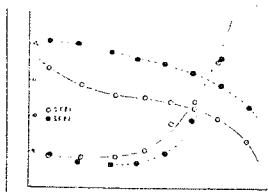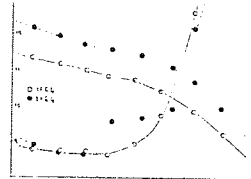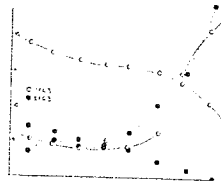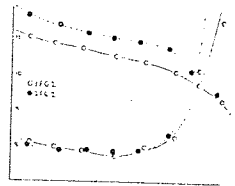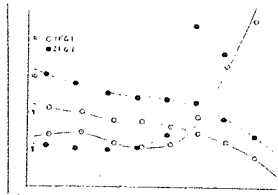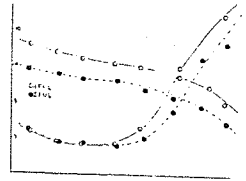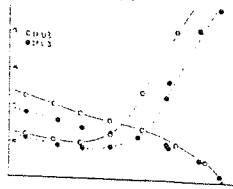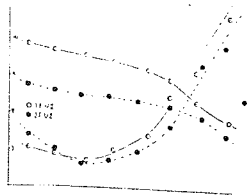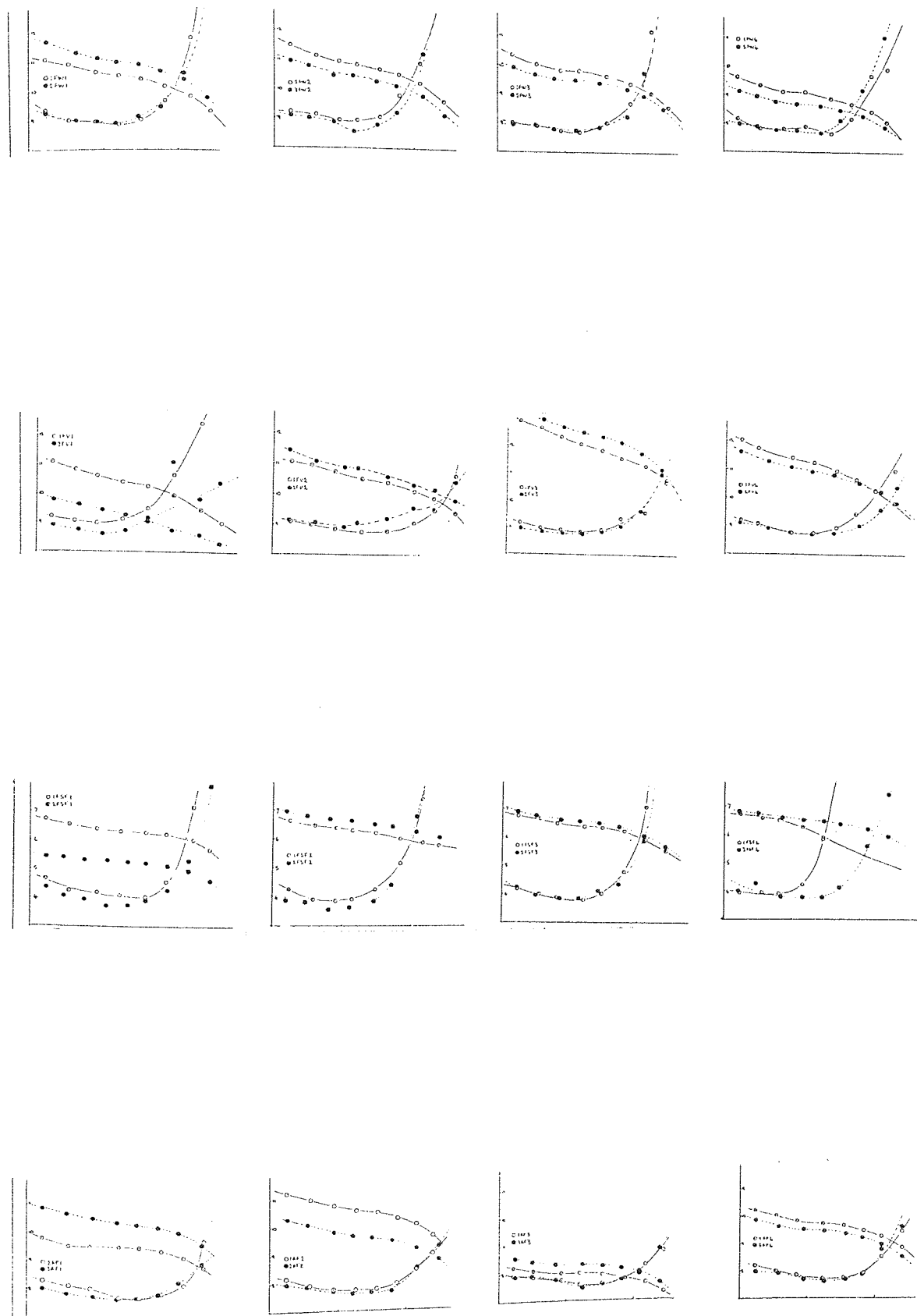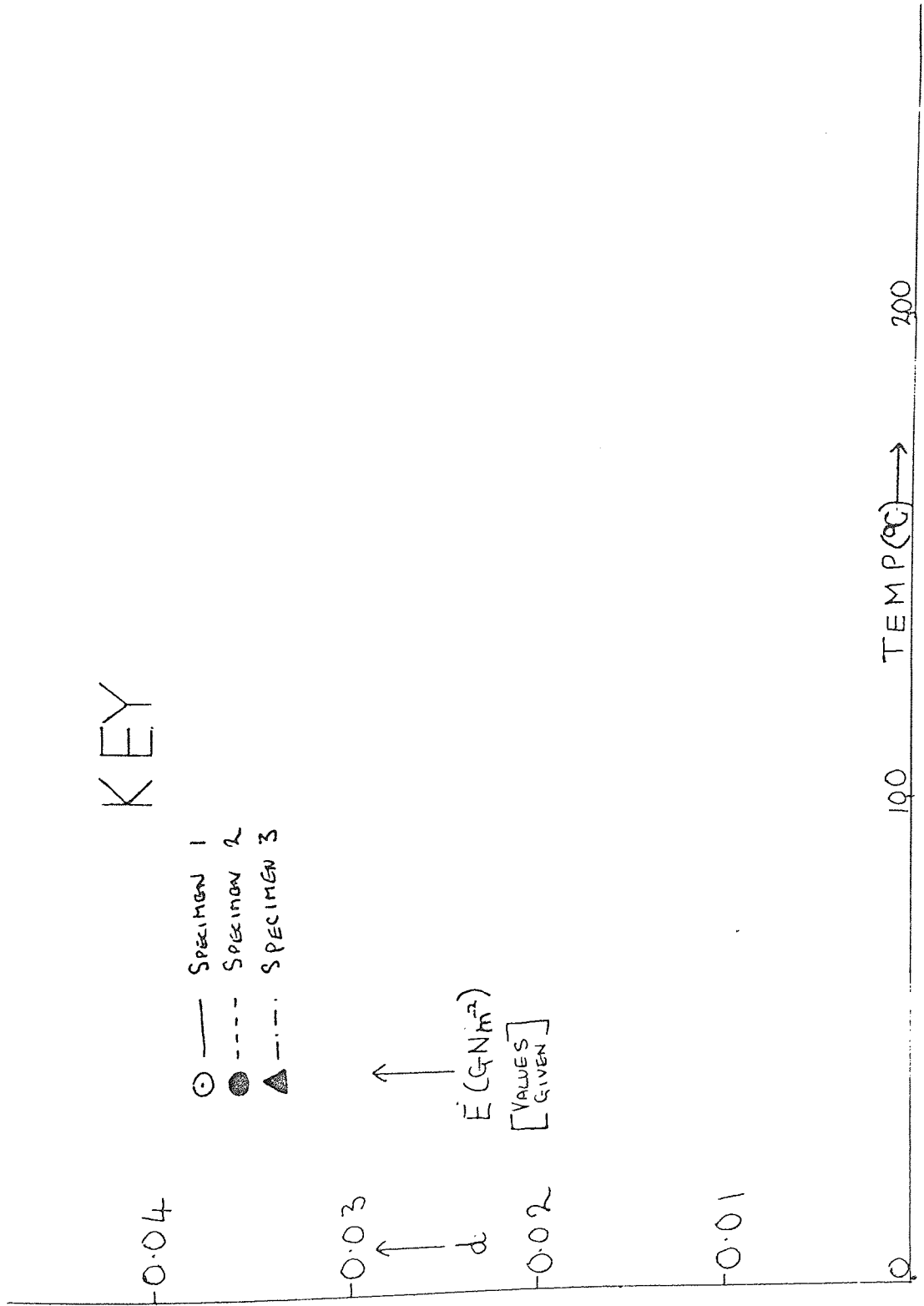
Key to figures 49,50,51 and 52.

Table 23. List of Specimen Densities

specimen reference	density		

	specimen	1	2	3
Unused pads				
Mintex M108				
1BK		1.95	1.94	1.96
4BK		1.98	1.97	2.01
8BK		2.02	1.97	1.99
9BK		2.01	2.02	2.05
10BK		1.95	1.92	1.92
11BK		1.97	2.00	1.98
12BK		1.94	2.02	1.97
13BK		1.98	1.98	1.96
14BK		2.01	2.02	2.08
15BK		1.93	1.96	1.96
16BK		2.00	2.00	1.98
18BK		1.99	2.04	2.03
Ferodo 2430				
8B+		2.46	2.45	2.73
9B+		2.60	2.56	2.55
10B+		2.53	2.47	2.38
11B+		2.51	2.47	2.52
3BK+		2.58	2.50	2.51
9BK+		2.64	2.60	2.59
10BK+		2.57	2.53	2.54
11BK+		2.59	2.56	2.70
2B		2.49	2.48	2.47
3B		2.51	2.49	2.48
4B		2.52	2.53	2.58
5B		2.58	2.55	2.53

List of Specimen Densities (continued).

specimen reference			density	
Used Pads	specimen	1	2	3
Mintex M78				
MB1		2.04	2.02	–
MB2		2.05	2.10	–
MB3		2.06	2.06	–
MB4		2.03	2.06	–
MD1		1.93	1.96	–
MD2		1.83	1.86	–
MD3		1.89	1.95	–
MD4		1.97	1.94	–
ME1		2.01	–	2.16
ME2		1.88	–	2.03
ME3		2.01	1.95	–
ME4		1.98	1.98	–
MF1		2.04	2.04	–
MF2		1.99	1.98	–
MF3		1.99	1.94	–
MF4		2.02	2.03	–
MG1		1.99	1.96	–
MG2		2.04	2.05	–
MG3		1.95	1.95	–
MG4		2.01	2.00	–
MH1		2.04	2.03	–
MH2		2.01	2.05	–
MH3		1.90	1.92	–
MH4		1.94	2.00	–

List of Specimen Densities (continued).

specimen reference density

Used Pads (cont.)	specimen	1	2	3
Mintex M108				
MA1		2.27	2.55	—
MA2		2.26	2.51	—
MA3		2.73	2.38	—
MA4		2.40	—	2.56
MB1		2.53	—	2.67
MB2		2.57	—	2.65
MB3		2.58	2.66	—
MB4		2.58	—	2.68
MC1		2.70	2.67	—
MC2		2.61	2.67	—
MC3		2.57	2.57	—
MC4		2.49	2.59	—
MSF1		1.82	1.83	—
MSF2		1.81	1.83	—
MSF3		1.77	1.82	—
MSF4		1.83	1.80	—
Ferodo 2430				
FA1		—	2.48	2.50
FA2		2.50	2.52	—
FA3		2.46	—	2.64
FA4		—	2.52	2.54
FG1		2.49	2.51	—
FG2		2.55	2.48	—
FG3		2.58	2.58	—
FG4		2.58	2.57	—

List of Specimen Densities (continued).

specimen reference			density	
Used Pads (cont.)	specimen	1	2	3
Ferodo 2430				
FM1		2.55	2.59	-
FM2		2.49	2.46	-
FM3		2.45	2.53	-
FM4		-	2.53	2.58
FP1		-	2.66	2.56
FP2		2.58	2.61	-
FP3		2.60	2.57	-
FP4		-	2.52	2.55
FU1		2.53	2.51	-
FU2		2.50	2.48	-
FU3		2.50	2.49	-
FU4		2.49	2.48	-
FV1		2.52	2.48	-
FV2		2.53	2.51	-
FV3		2.59	2.55	-
FV4		2.58	2.59	-
FW1		-	2.63	2.57
FW2		2.50	2.53	-
FW3		2.48	-	2.47
FW4		2.39	2.34	-
FSF1		2.41	2.44	-
FSF2		2.43	2.43	-
FSF3		2.44	2.40	-
FSF4				

Specimens 1,2,3 relate to the order in which the specimens are cut from the pad. Specimen 1 is from nearest the centre of the pad, then specimen 2 with specimen 3 the outermost. When testing the used pads only two pads from each sample were tested and the first figure of the complete specimen reference gives the specimen number used. Hence specimen 2FM3 is the second specimen taken from the third pad of the FM set. The squeal free specimens were denoted SF.

GRAPH 1. THE INHERENT PHASE DIFFERENCE BETWEEN THE ACCELERATION AND THE FORE SIGNAL CHANNELS

GRAPH 2 GAIN AS A FUNCTION OF FREQUENCY FOR THE AMPLIFICATION OF BOTH THE ACCELERATION AND THE FORCE SIGNAL CHANNELS.

—— ACCELERATION
---- FORCE

GAIN APPROX CONSTANT AT 300

AMPLIFICATION (GAIN)

FREQUENCY (KHz.)
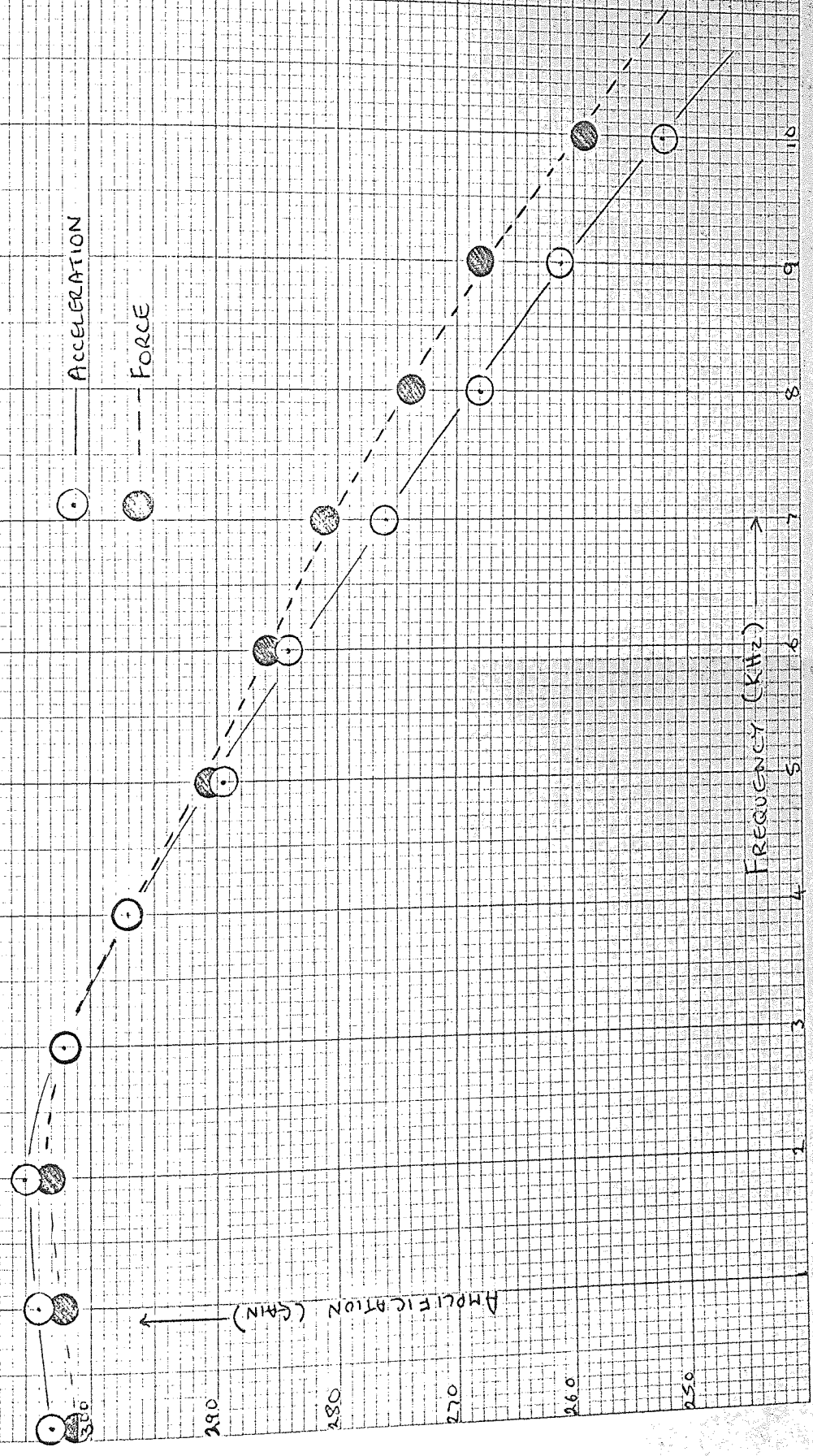
Graph 3 — The Effect of Mass Compensation And the variation with Frequency

Temperature 21°C $a_{ref} = 1\ Volt$

Average Force 260mV (Consistant with a mass of 2g)
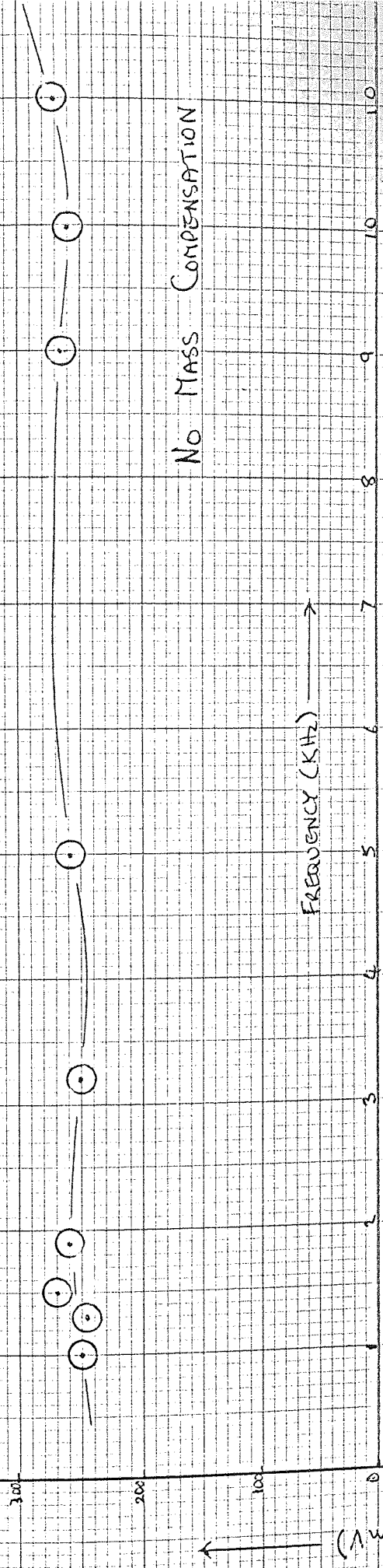
No Mass Compensation

Force (mV): 100, 200, 300

Frequency (KHz)

Temperature 21°C $a_{ref} = 1\ Volt$

Average Force 15 mV (Consistant with a mass of 0.11g)

Mass Compensation

Force (mV): 10, 20, 30

Frequency (KHz)
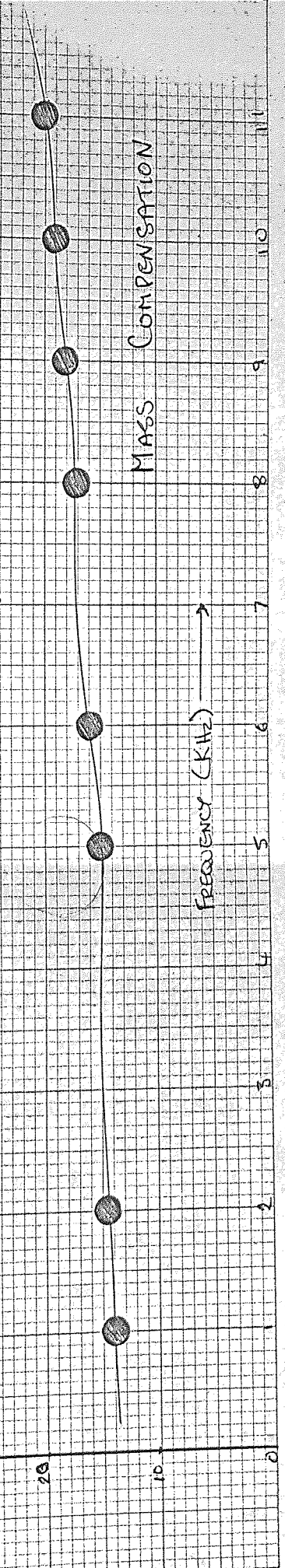
GRAPH 4   POLYPROPYLENE SPECIMEN
WITH NO ADDED WEIGHT.
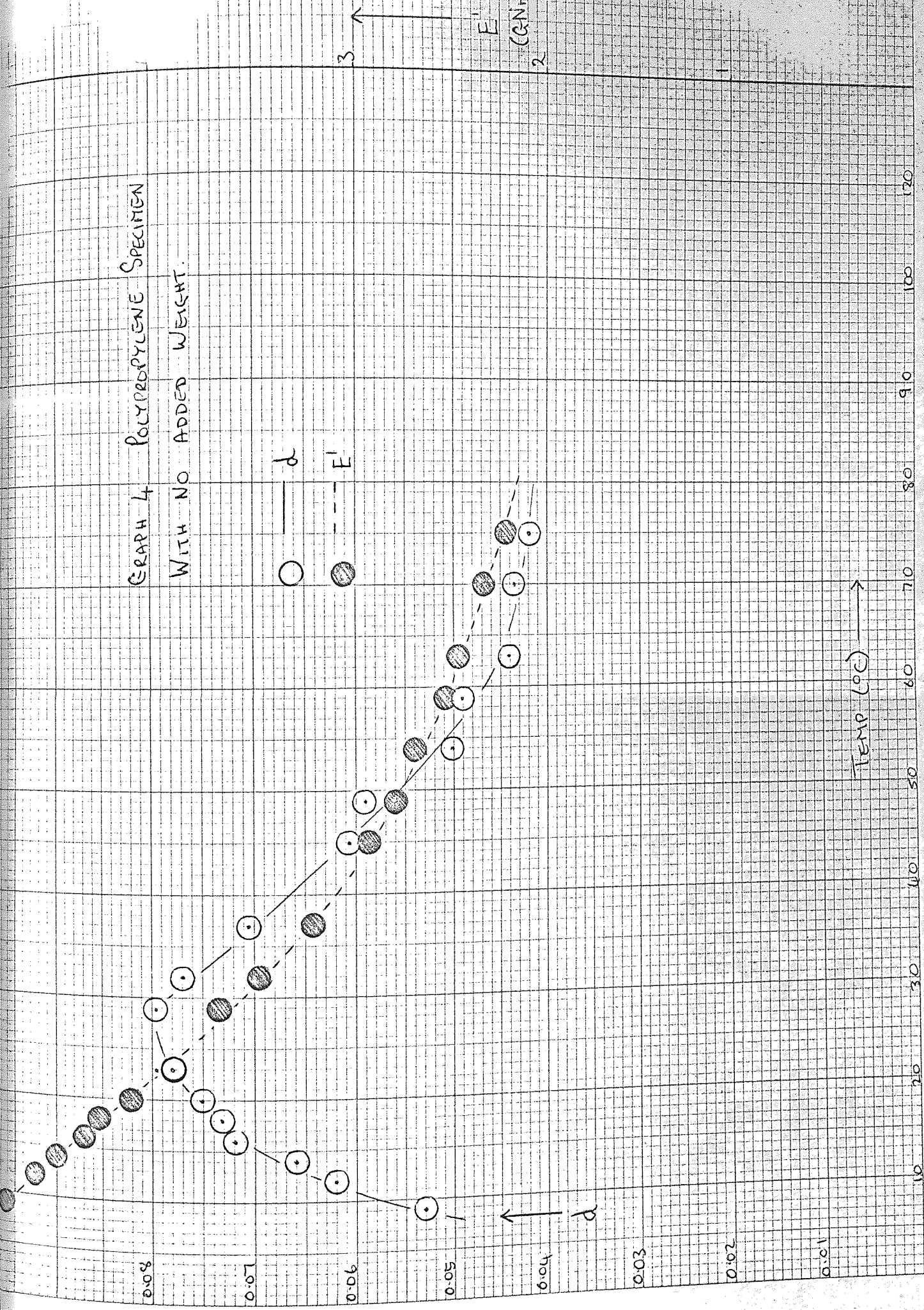
GRAPH 5. POLYPROPYLENE SPECIMEN

WITH 4.012g ADDED MASS

d ⎯⎯ d

E' ⎯ ⎯ E'

(Nm^{-2})

Temp (°C)
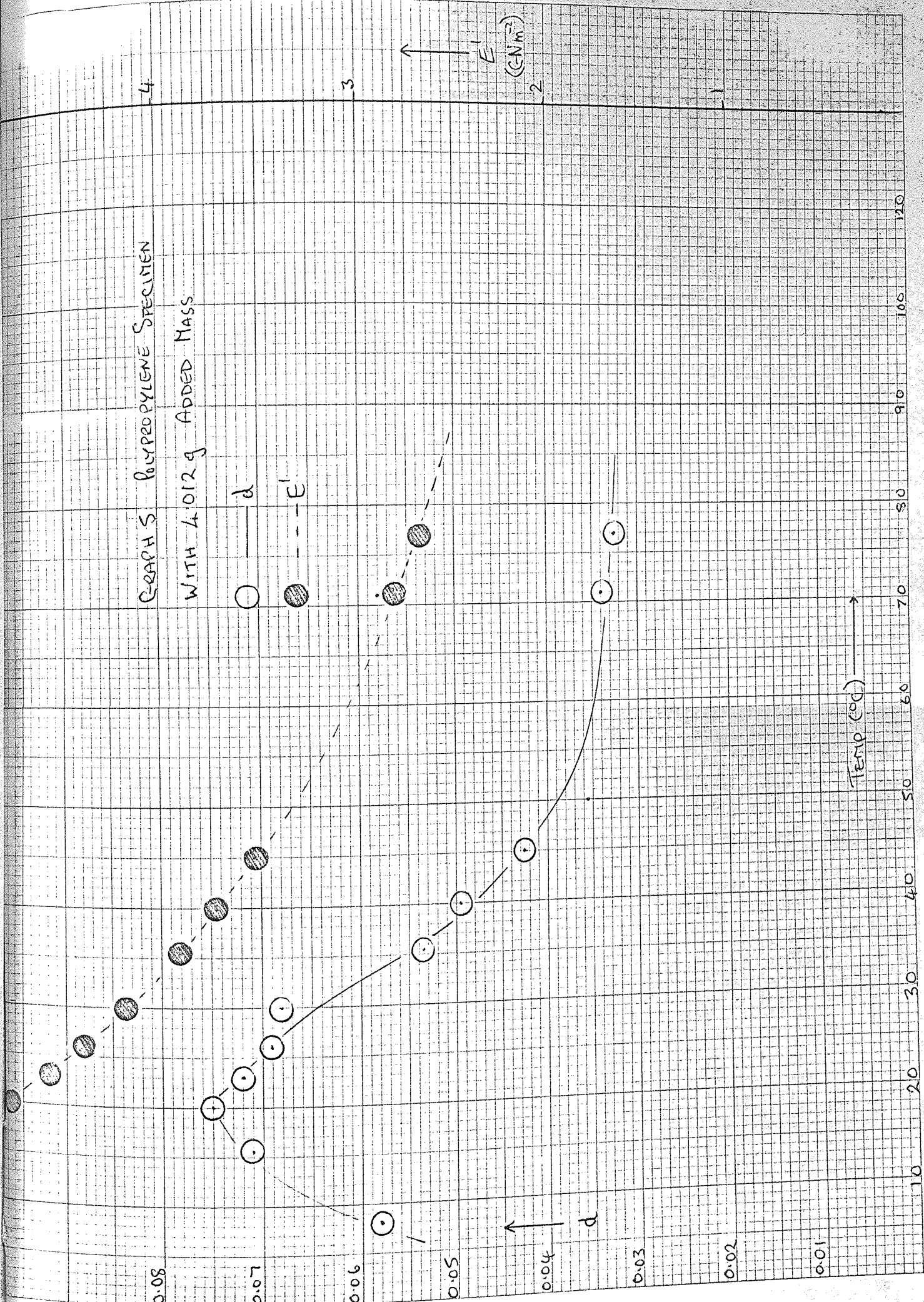
GRAPH 6 POLYPROPYLENE SPECIMEN
WITH 9.317 g ADDED MASS

d ——○——
E' --●--
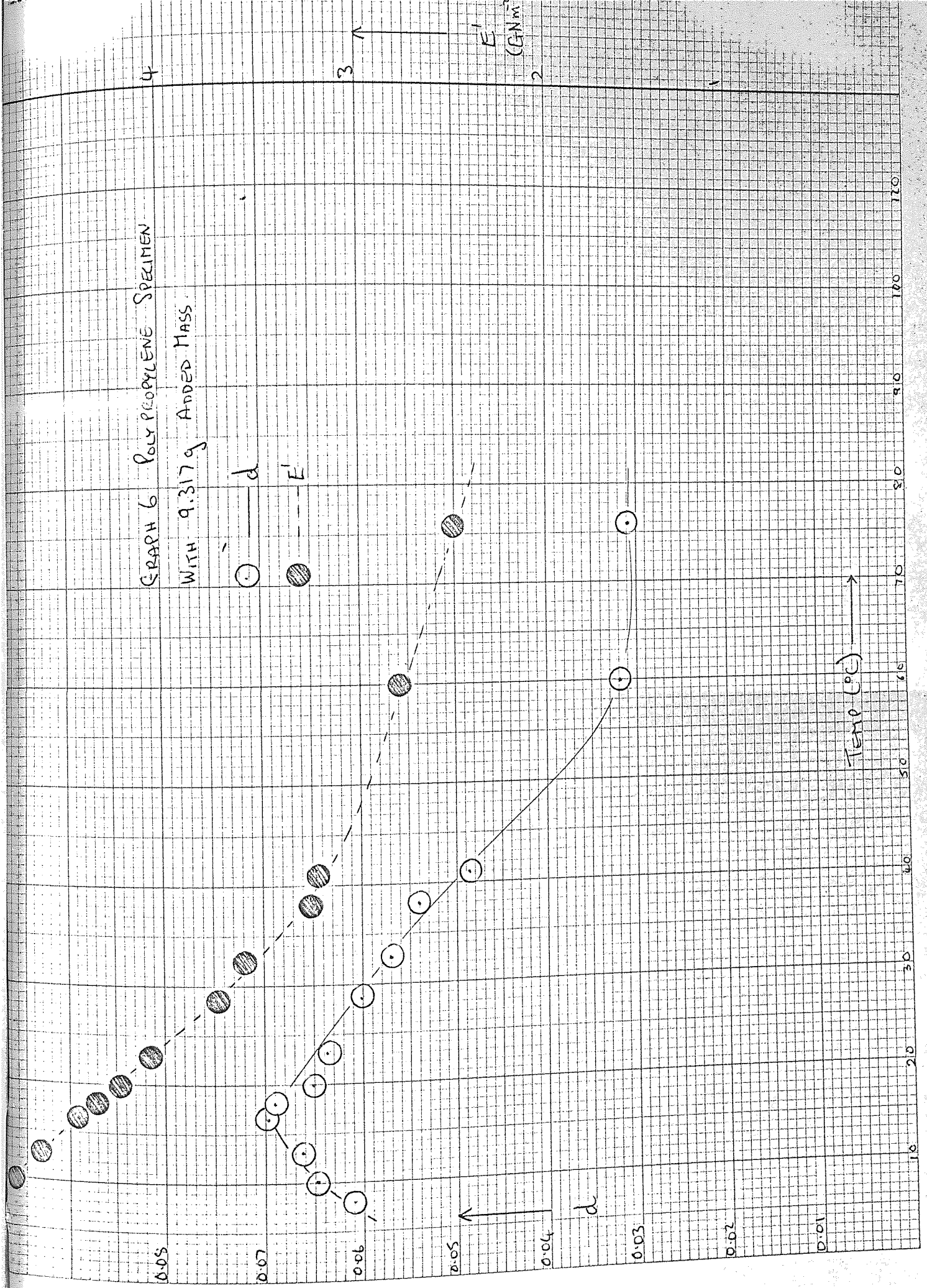
GRAPH 7 — POLYPROPYLENE SPECIMEN

WITH 20.912g ADDED MASS

d
E'
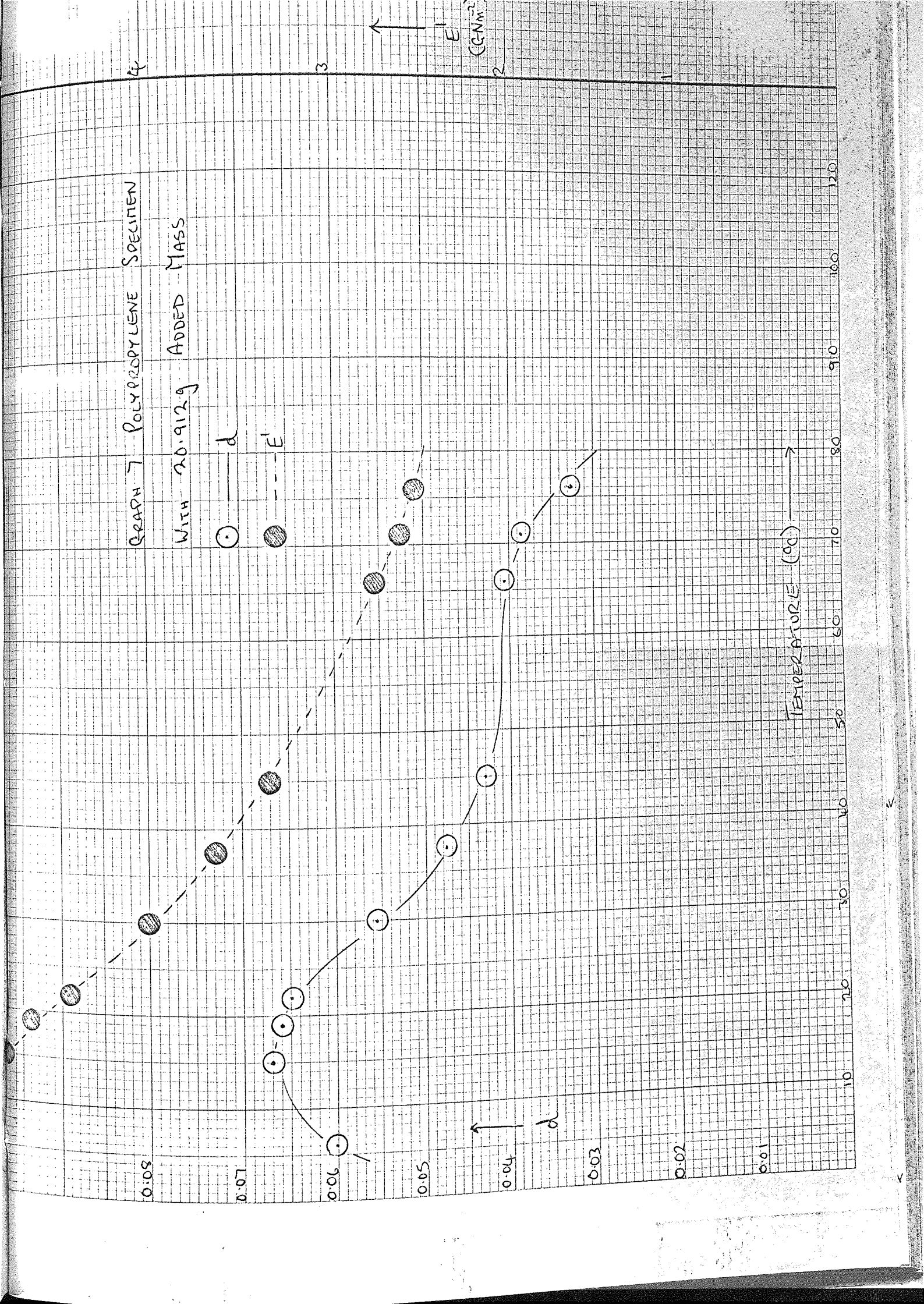
GRAPH 8   A PLOT OF FORCE
Vs FREQUENCY AT A CONSTANT ACCEL-
ERATION OF 1 VOLT FOR A 21·3cm LONG
BAR OF POLYPROPYLENE AT 21°C

FUNDAMENTAL RESONANCE

SECOND RESONANT MODE

THIRD RESONANT MODE

FOURTH RESONANT MODE

F (Volts)

Frequency (KHz)
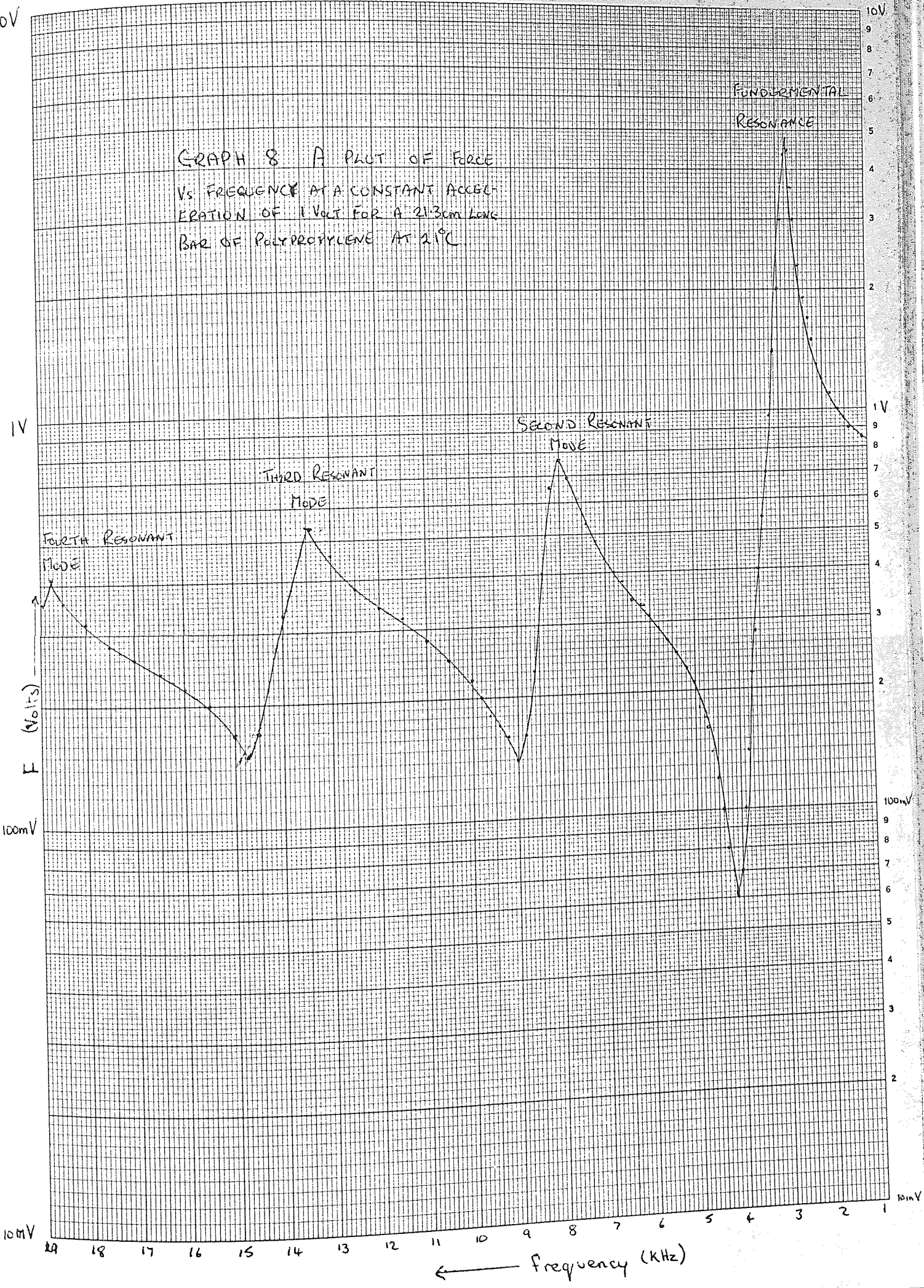
GRAPH SHOWING THE AVERAGE AND RANGE OF VALUES FOR THE DAMPING IN MINTEX 108 PADS FROM BATCH MNTX108SHD44BQ
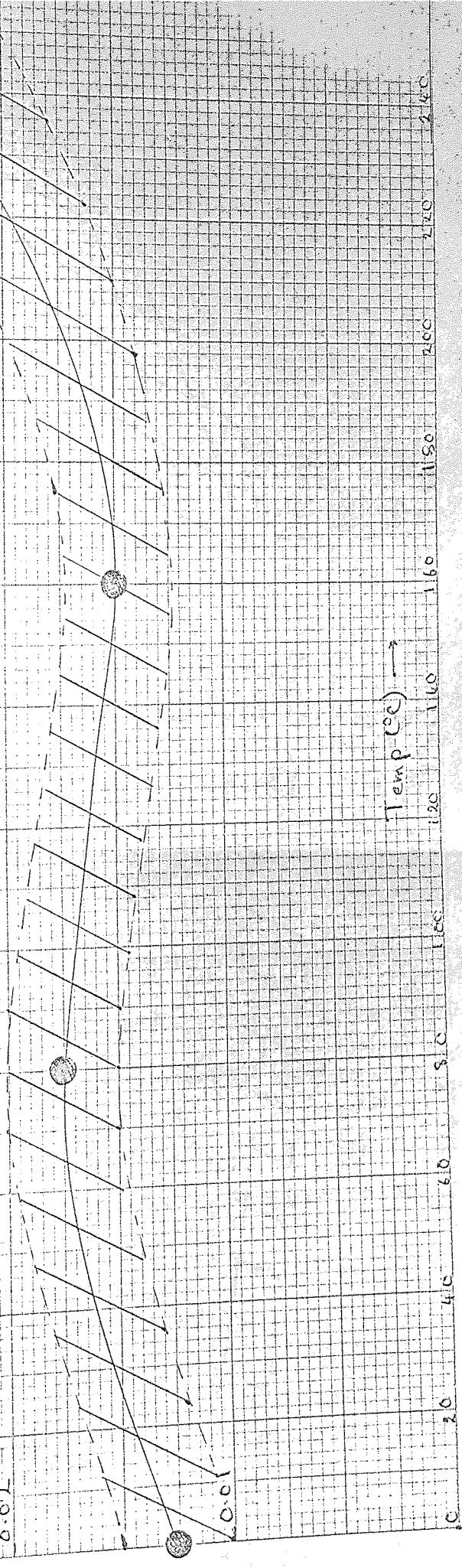
GRAPH 10 SHOWING THE AVERAGE
AND RANGE OF VALUES FOR THE
DAMPING IN FERODO 2430 PADS.

BATCH FER 2430F FF454

BATCH FER 2430F FF458

BATCH FER 2430F FF

RANGE OF VALUES FOR
ALL THREE BATCHES
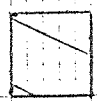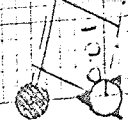
η

0.04

0.03

0.02

0.01

Temp (°C) →

20   40   60   80   100   120   140   160   180   200   220   240

Step
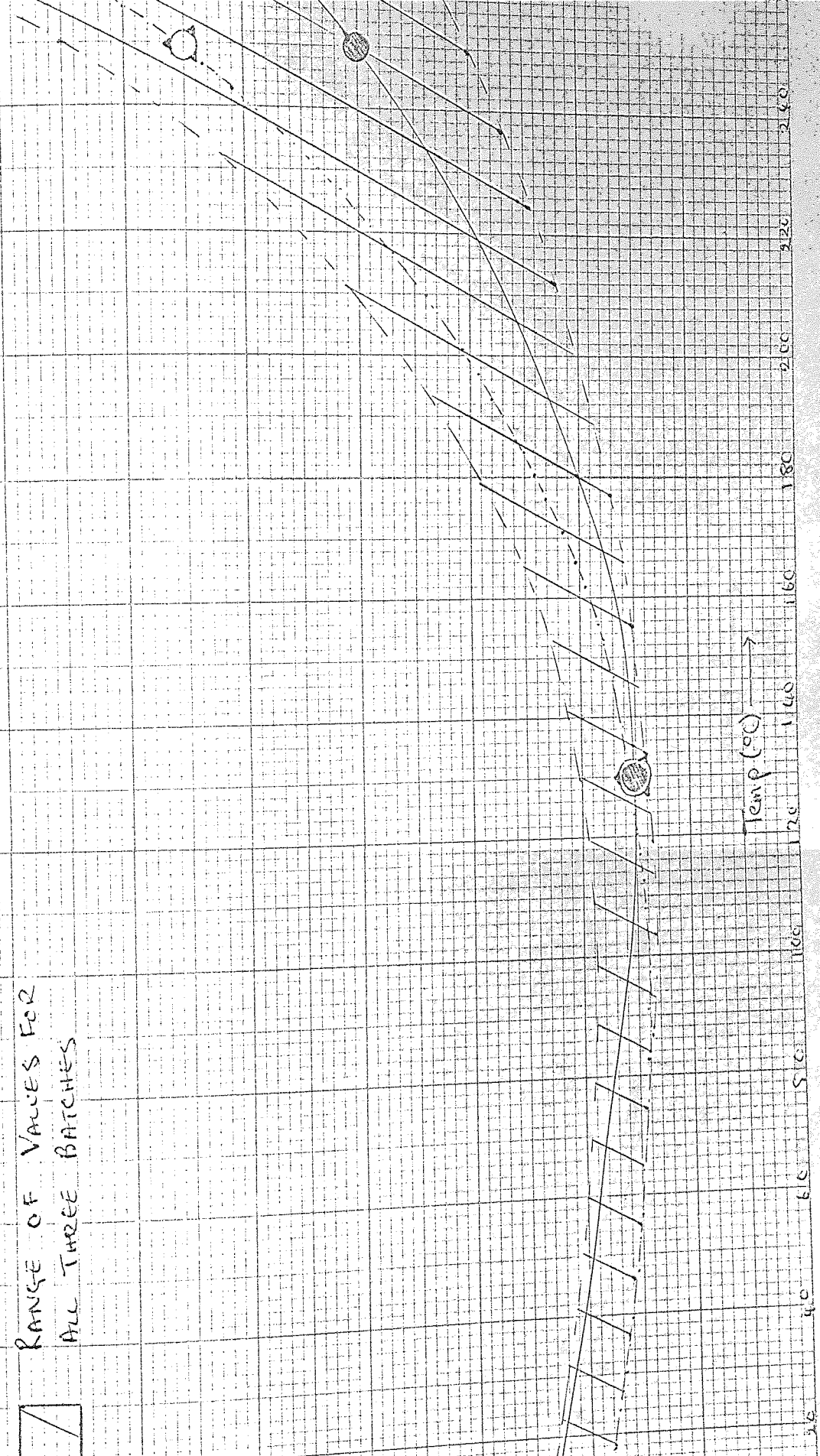
GRAPH II SHOWING THE AVERAGE
AND RANGE OF VALUES FOR THE
DAMPING IN USED FERODO 2430
PADS.

d

0.04

0.03

0.02

0.01

TEMP (°C)

0   20   40   60   80   100 120 140 160 180 200 220 240
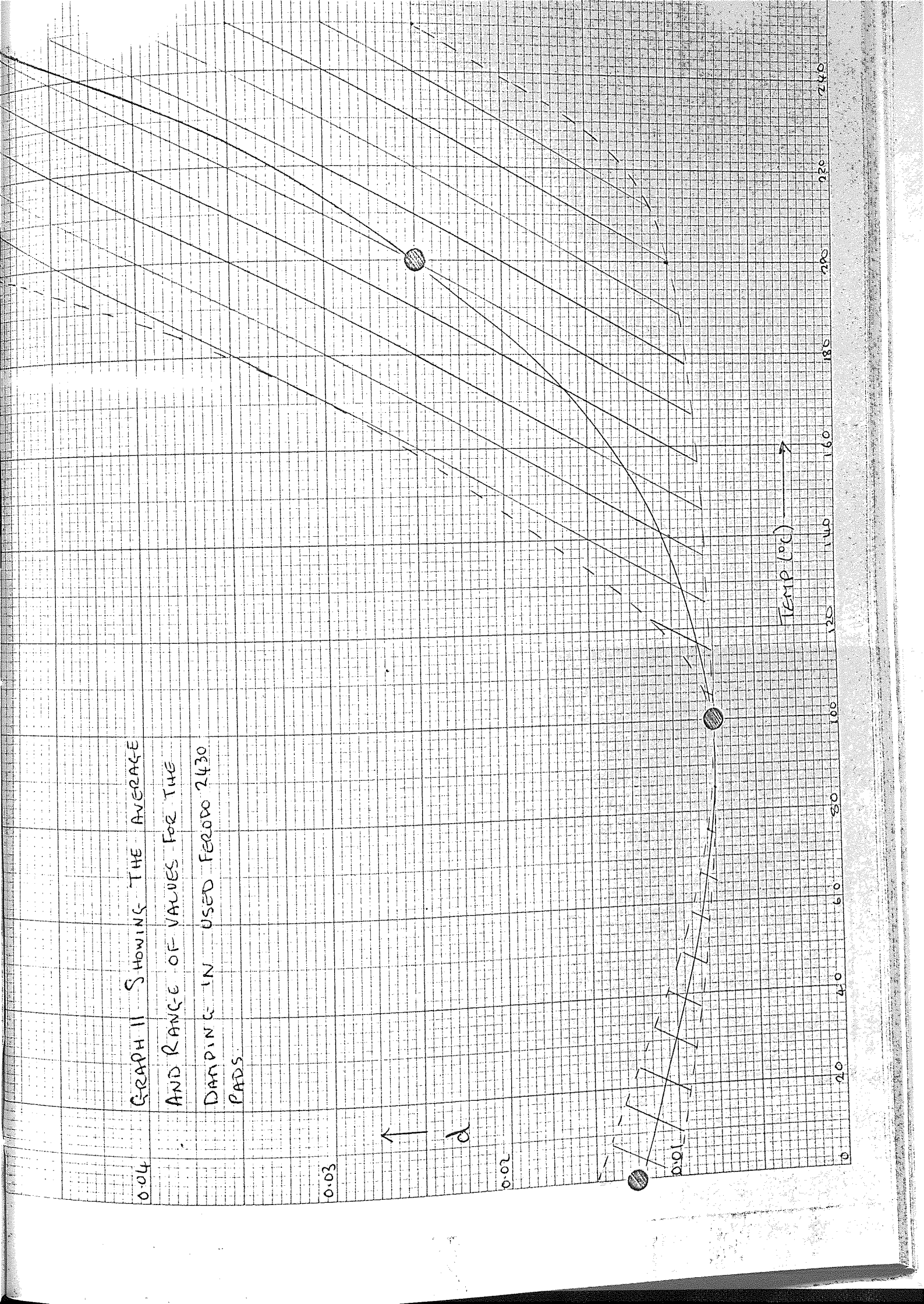
GRAPH 12 SHOWING THE AVERAGE
AND RANGE OF VALUES FOR THE
DAMPING IN USED MINTEX 108
PADS

d

0.04

0.03

0.02

0.01

20   40   60   80   100   120   140   160   180   200   220   240
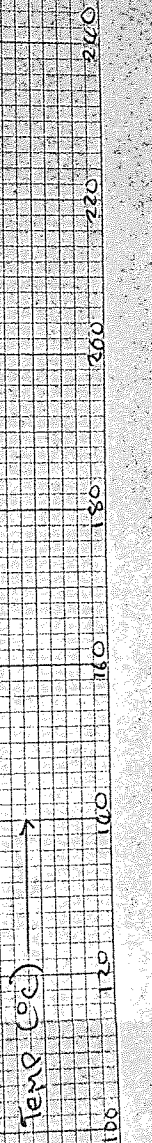
TEMP (°C)

GRAPH 13 SHOWING THE AVERAGE
AND RANGE OF VALUES FOR THE
DAMPING IN MINTEX 78 PADS
WHICH HAD BEEN USED

d

0.04

0.03

0.02

0.01

TEMP (°C)

0   20   40   60   80   100   120   140   160   180   200   220   240
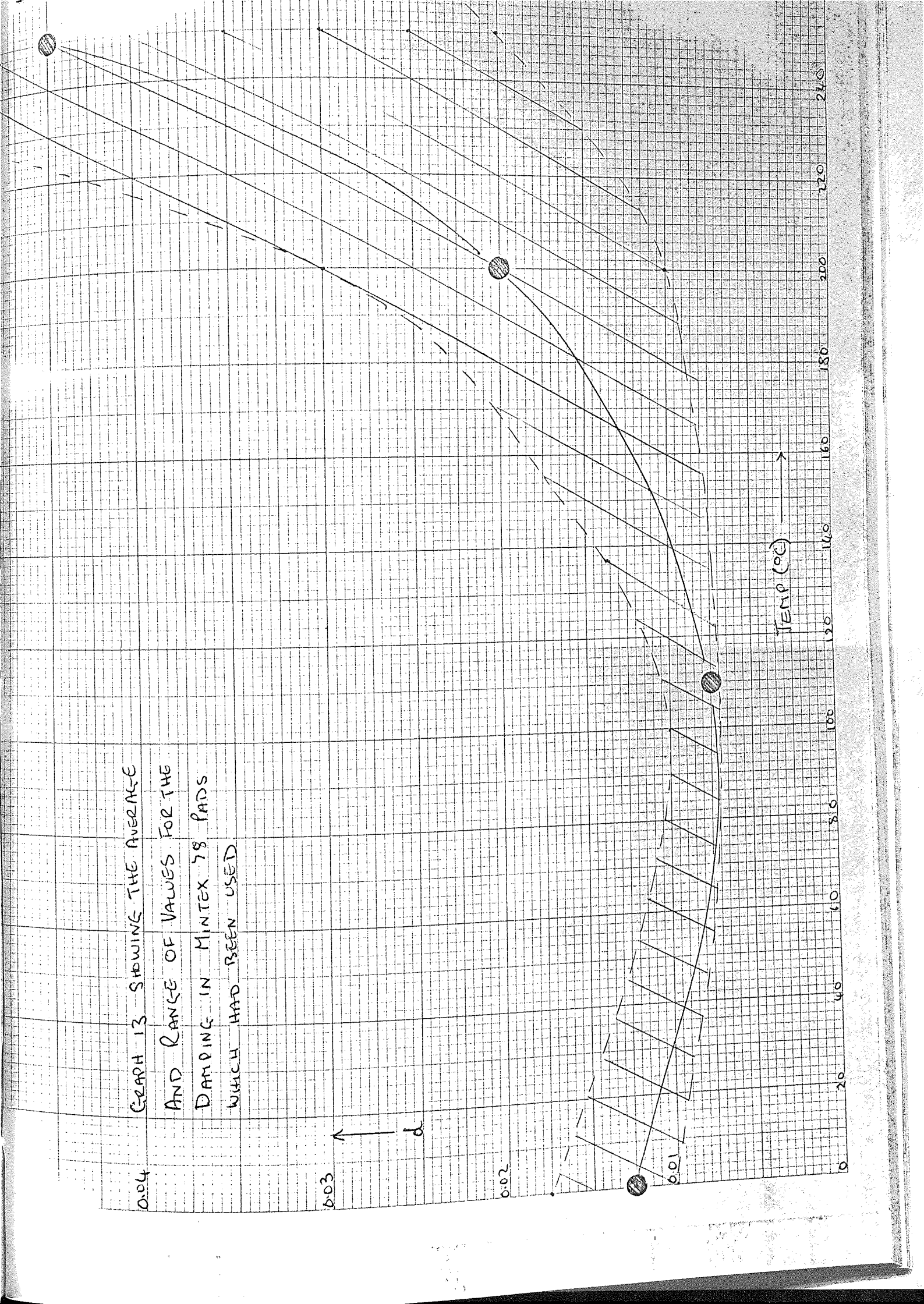
GRAPH 14 THE DAMPING PROFILES
FOR SAMPLE 9 + BK IMMERSED
IN WATER.

RETEST
AFTER } COOLING

5 MINUTES DELAY FOR STABILISATION

Temp (°C)

GRAPH 15 TIME DAMPING PROFILES
FOR SAMPLE 9 + BK IMMERSED
IN OIL-WATER SUSPENSION

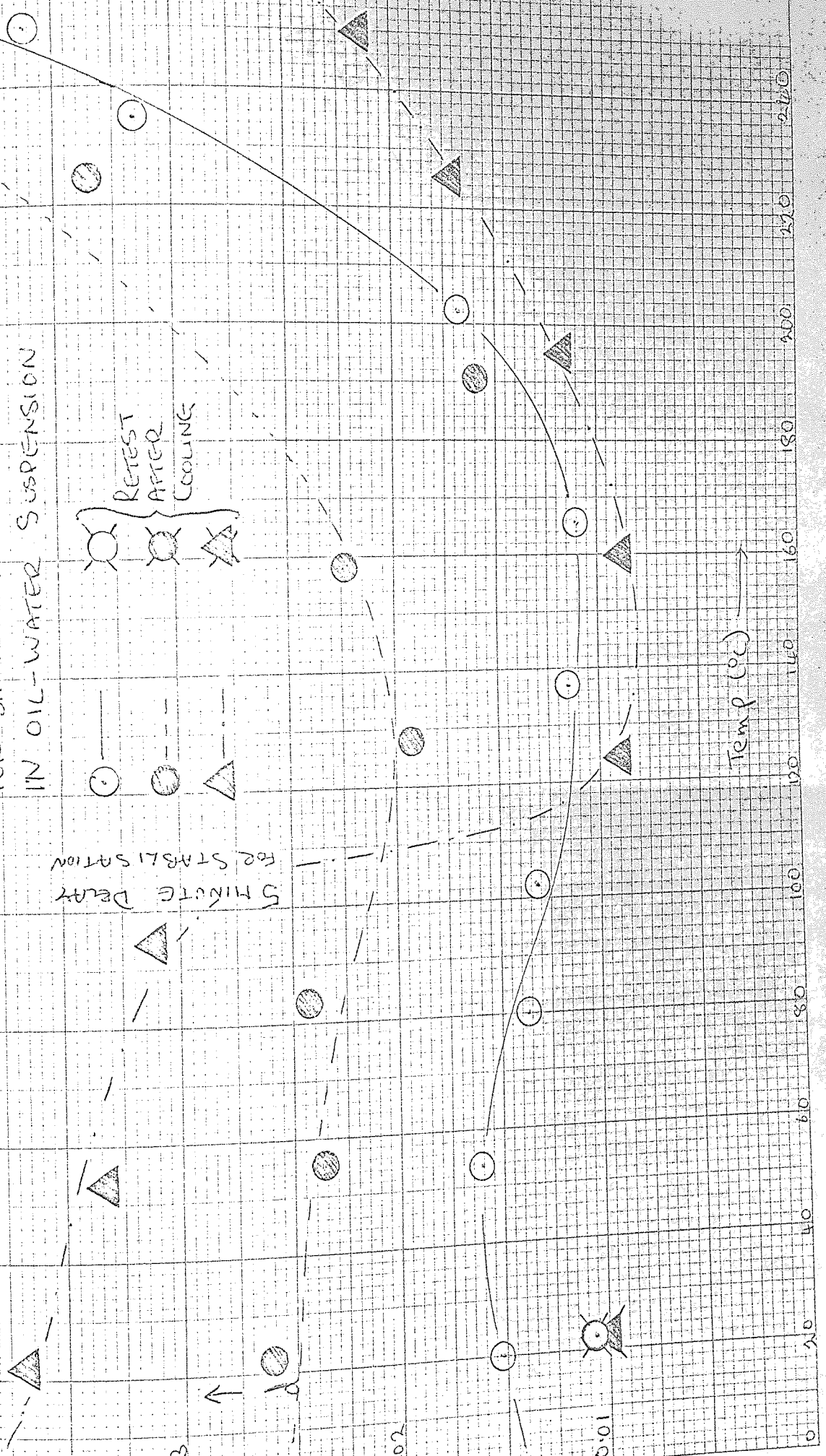RETEST
AFTER
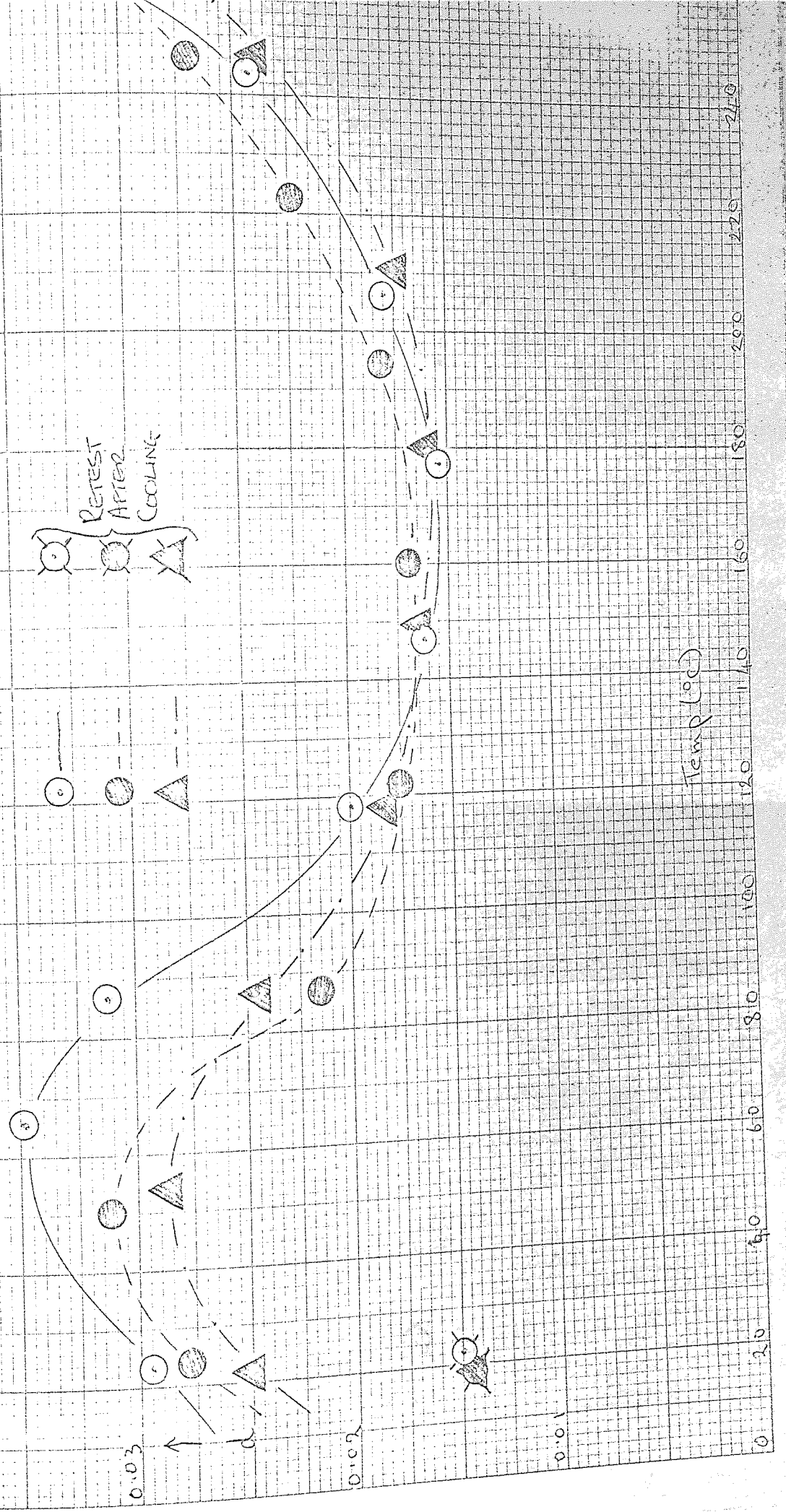COOLING

5 MINUTE DELAY
FOR STABILISATION

Temp (°C)

0.04

0.03

0.02

0.01

GRAPH 16 THE DAMPING PROFILES
FOR SAMPLE 15 BK IMMERSED IN
WATER.

GRAPH 17 THE DAMPING PROFILES
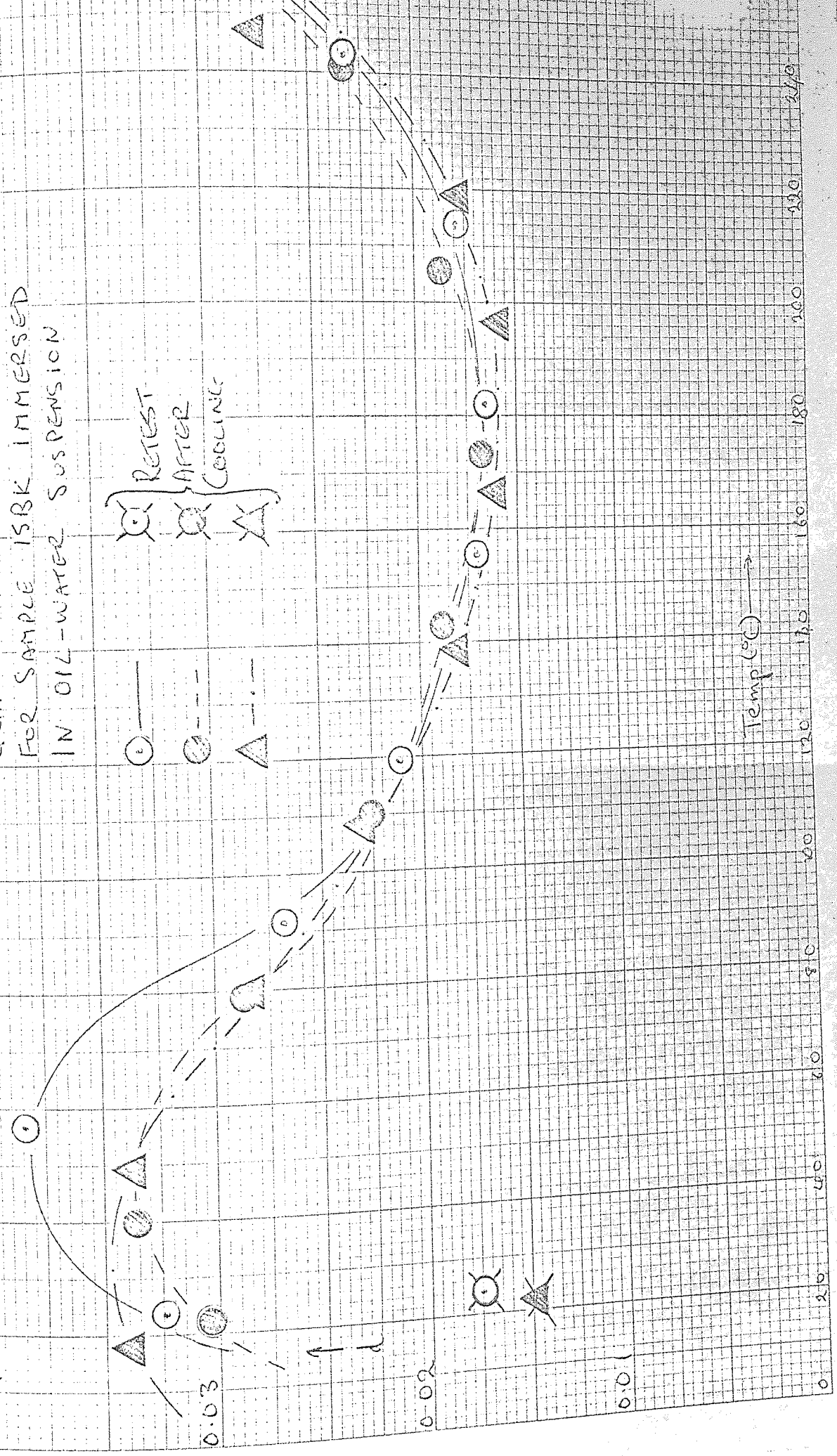FOR SAMPLE 15BK IMMERSED
IN OIL-WATER SUSPENSION

RETEST
AFTER
COOLING

Temp (°C) →

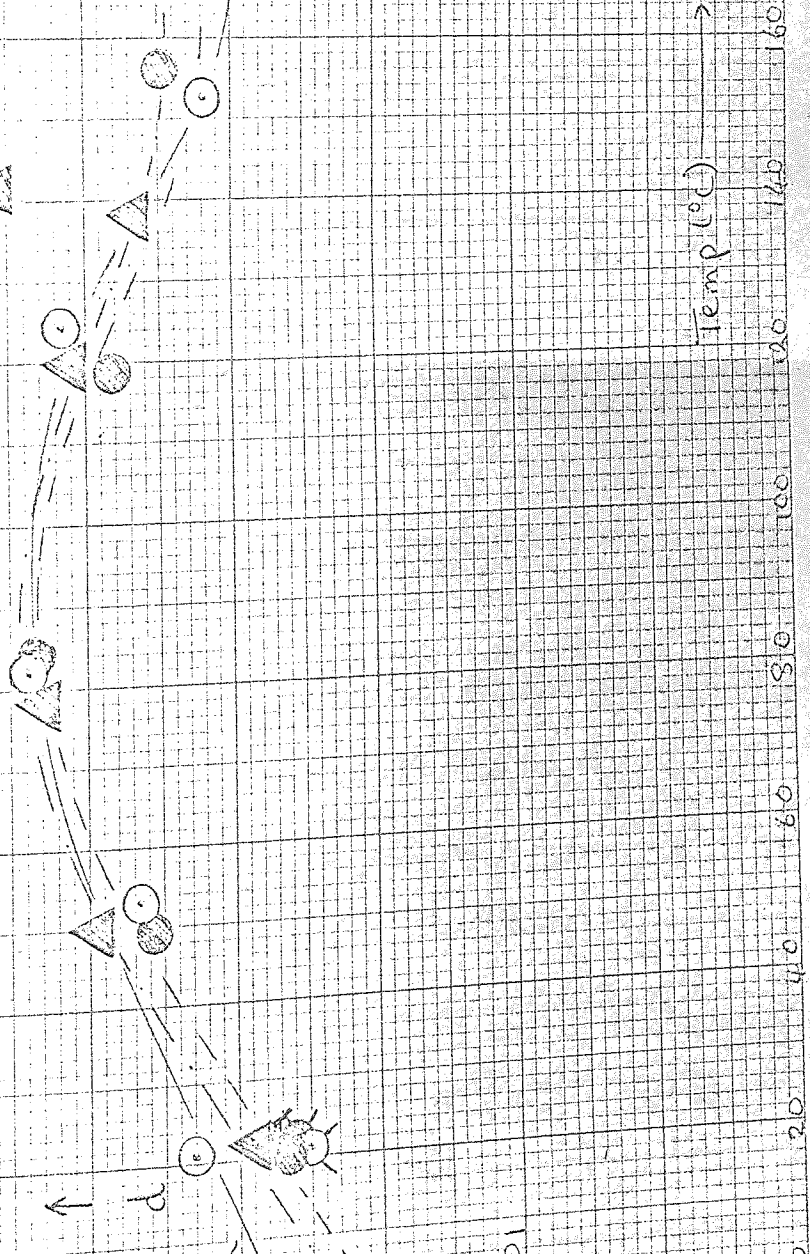GRAPH IS THE DAMPING PROFILES
FOR SAMPLE 14 BK IMMERSED
IN BRAKE FLUID.

RETEST
AFTER
COOLING

GRAPH 19 THE DAMPING PROFILES
FOR SAMPLE 11 + BK IMMERSED
IN BRAKE FLUID

RETEST
AFTER
COOLING

Temp (°C) ⟶

0.01 0.02 0.03 0.04

0 20 40 60 80 100 120 140 160 180 200 220 240
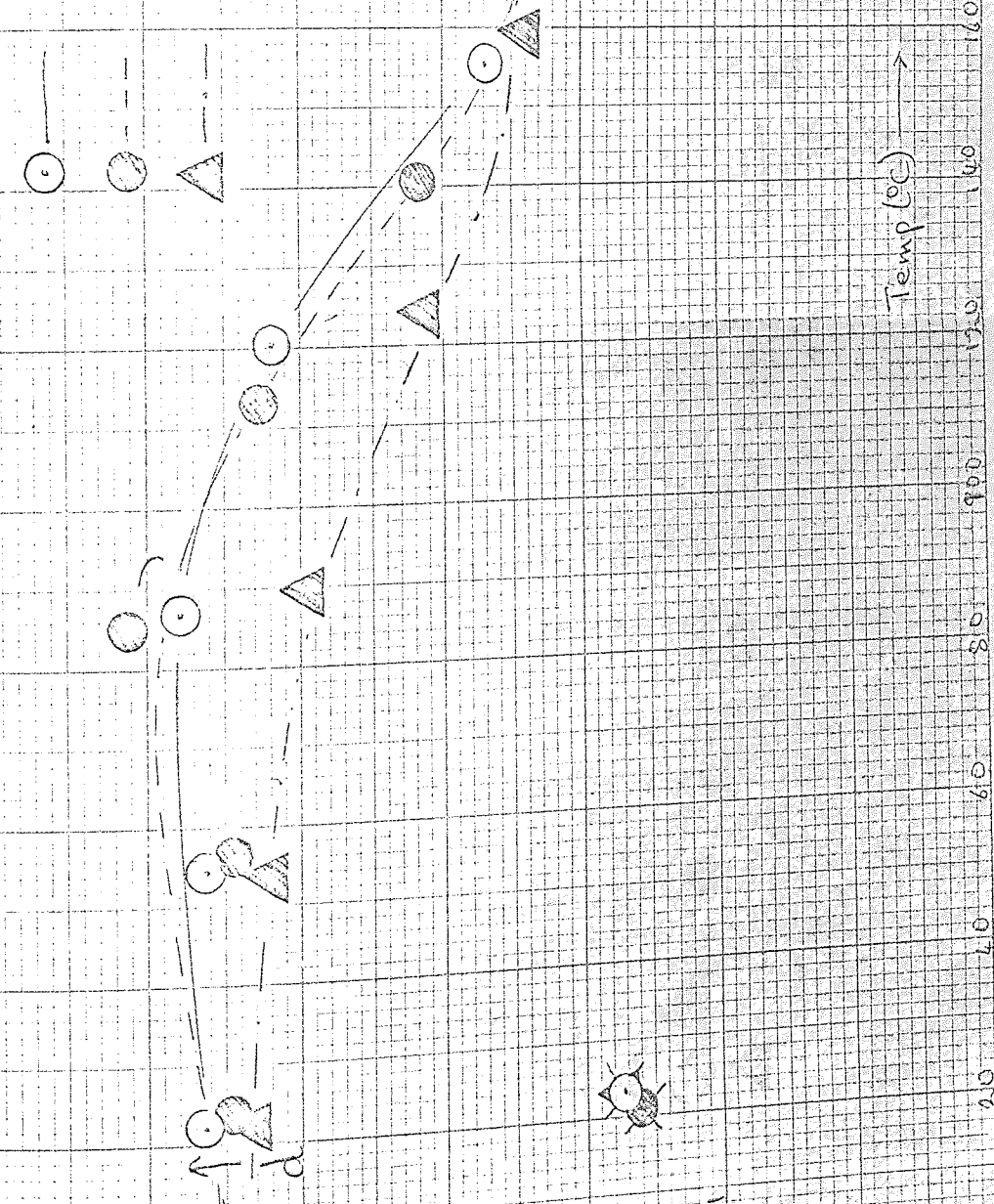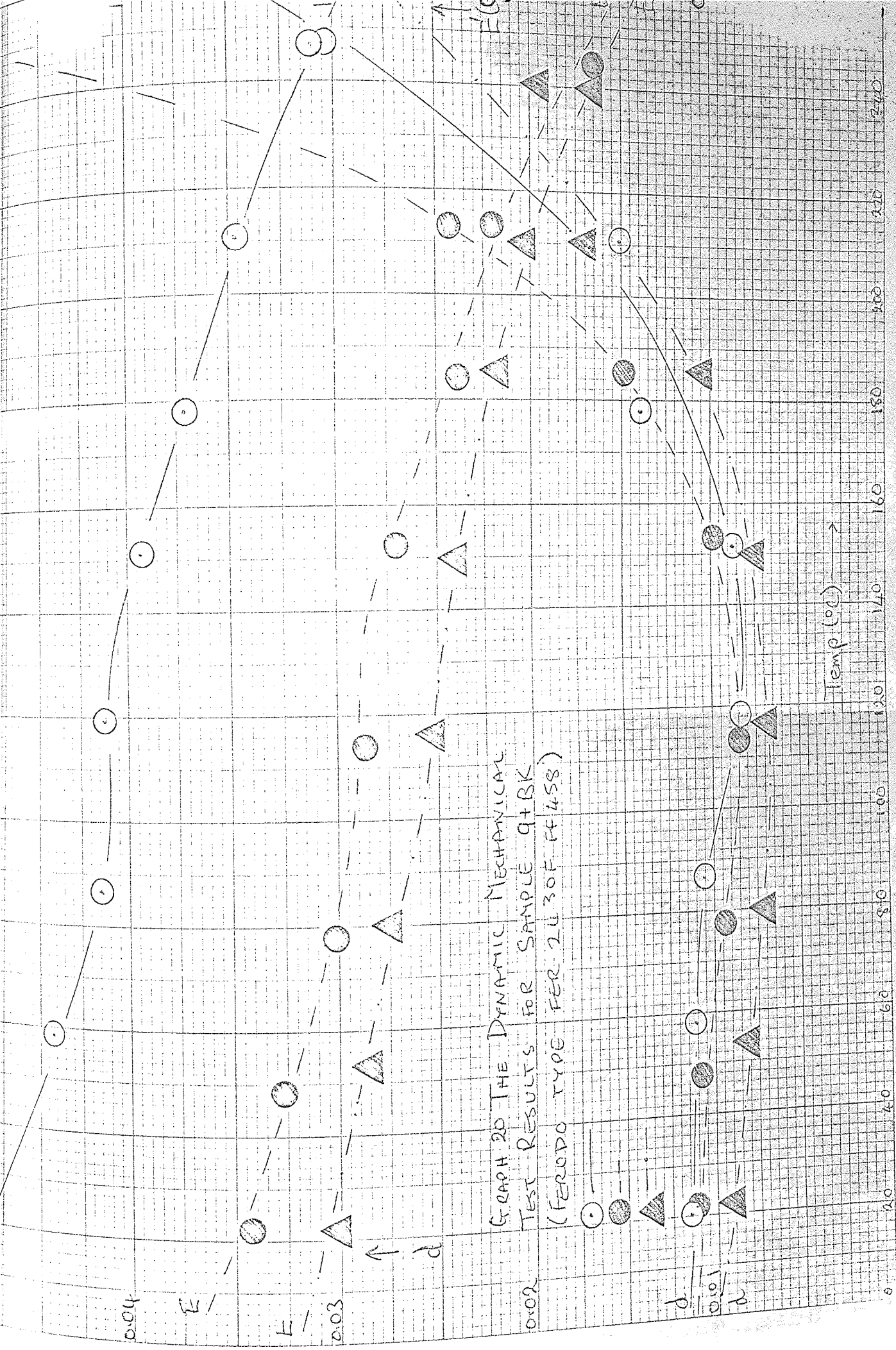
GRAPH 20 THE DYNAMIC MECHANICAL
TEST RESULTS FOR SAMPLE q+BK
(FERODO TYPE FER 24 3 OF FF458)

Temp (°C) ⟶

Graph 21 The Dynamic Mechanical Test Results for Sample 1SBK (Mintex type MNTX M108 G H D 44 BR)

$E' \left(\frac{G \cdot N}{m^2} \right)$

Temp (°C) →

GRAPH 22 THE DYNAMIC MECHANICAL
PROPERTIES OF SAMPLE 14.BK.
(MINTEX TYPE MNTX M102 G14 P4460)
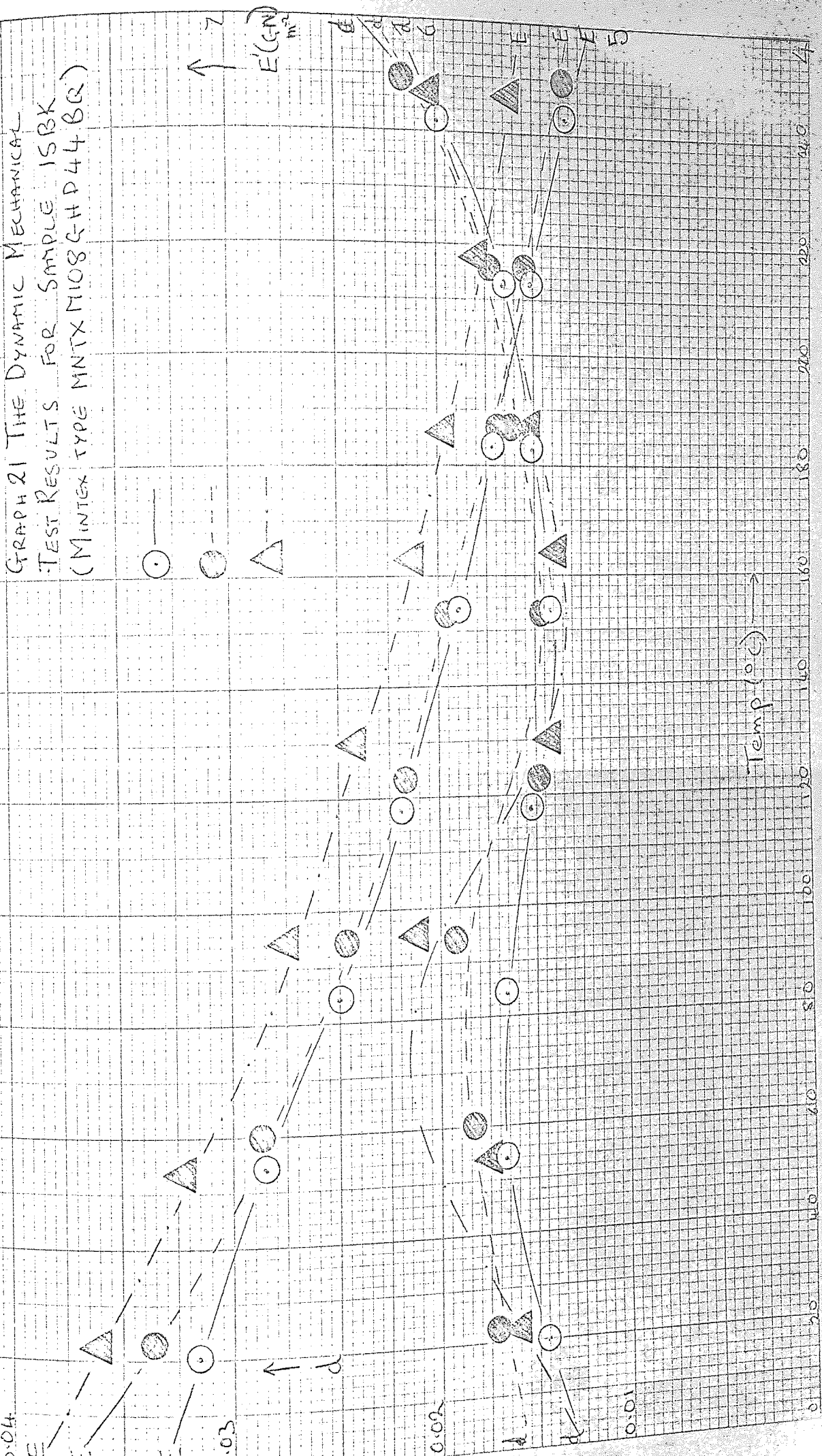
GRAPH 23 THE DYNAMIC MECHANICAL
TEST RESULTS FOR SAMPLE 11+BK
(FERODO TYPE FER 243DFFF458)

Temp (°C) →

GRAPH 24.

CURED PHENOLIC RESIN SPECIMENS

E
$(GN \, m^{-2})$

E

d

$\dfrac{d}{?}$
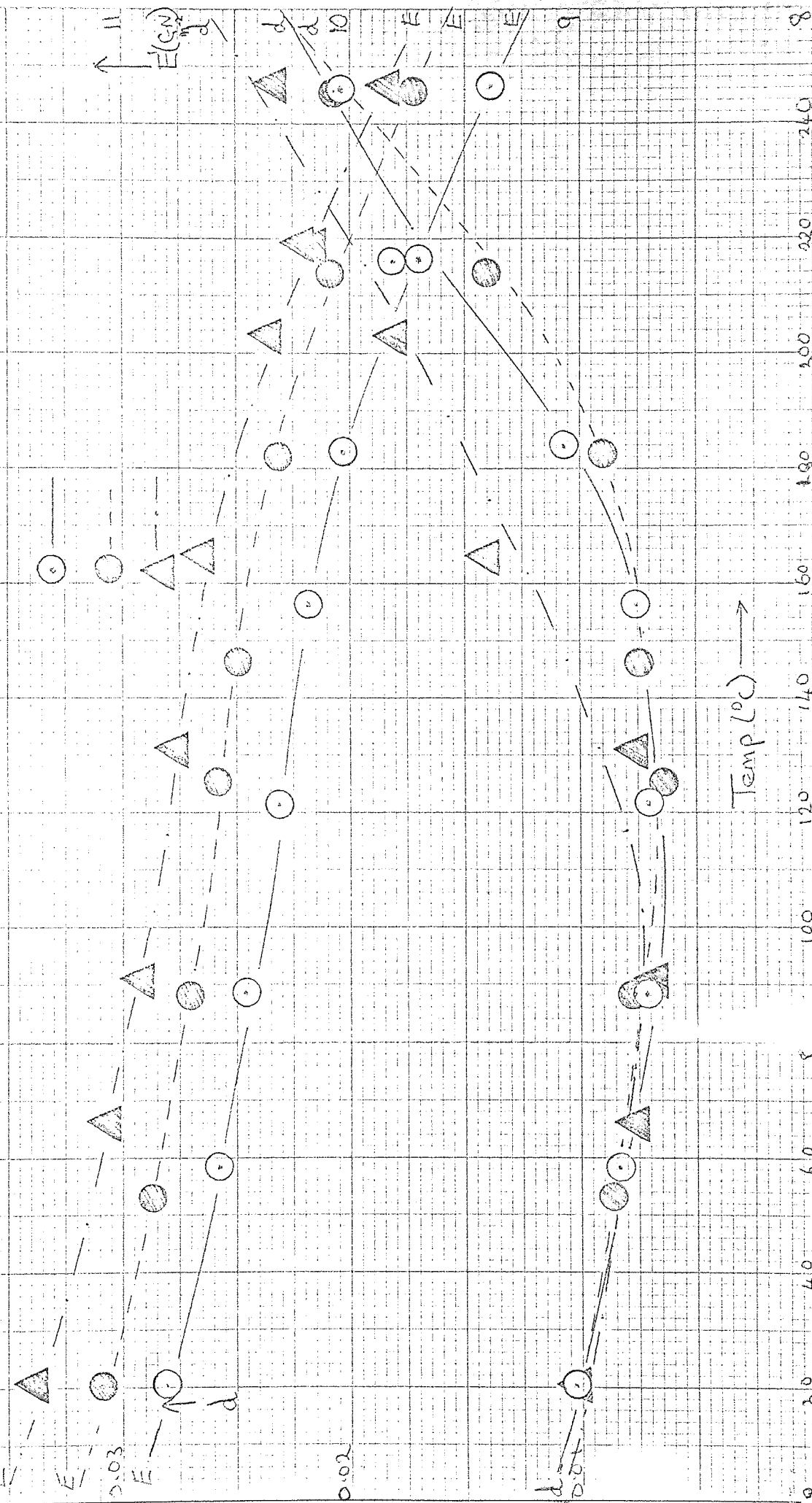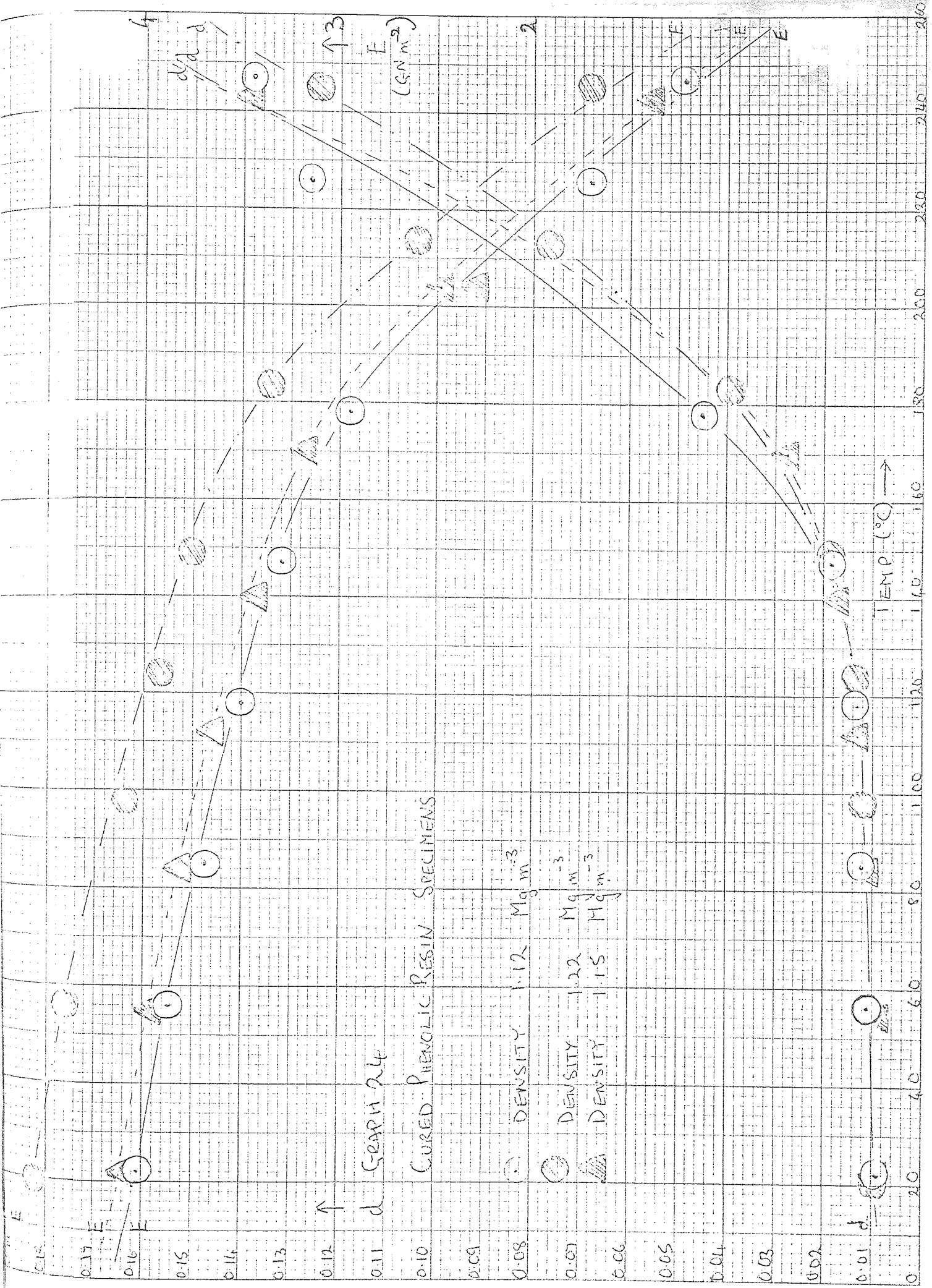
DENSITY 1.12 $Mg \, m^{-3}$

DENSITY 1.22 $Mg \, m^{-3}$

DENSITY 1.15 $Mg \, m^{-3}$

TEMP (°C)

0.17
0.16
0.15
0.14
0.13
0.12
0.11
0.10
0.09
0.08
0.07
0.06
0.05
0.04
0.03
0.02
0.01
0

20   40   60   80   100   120   140   160   180   200   220   240

GRAPH 25

CURED PHENOLIC RESIN
WITH ASBESTOS SPECIMENS

USING MULTIGRADE ASBESTOS

Density = 1.66 Mg·m⁻³ → $1.66\ \mathrm{Mg\,m^{-3}}$
Density = 1.66 Mg·m⁻³ → $1.66\ \mathrm{Mg\,m^{-3}}$
Density = 1.65 Mg·m⁻³ → $1.65\ \mathrm{Mg\,m^{-3}}$

TEMP (°C) ⟶

GRAPH 26

CURED PHENOLIC RESIN

WITH ASBESTOS SPECIMENS

(28-5% ASBESTOS)

DENSITY 1.46 Mg m^{-3}

DENSITY 1.46 Mg m^{-3}

E (GNm^{-2})
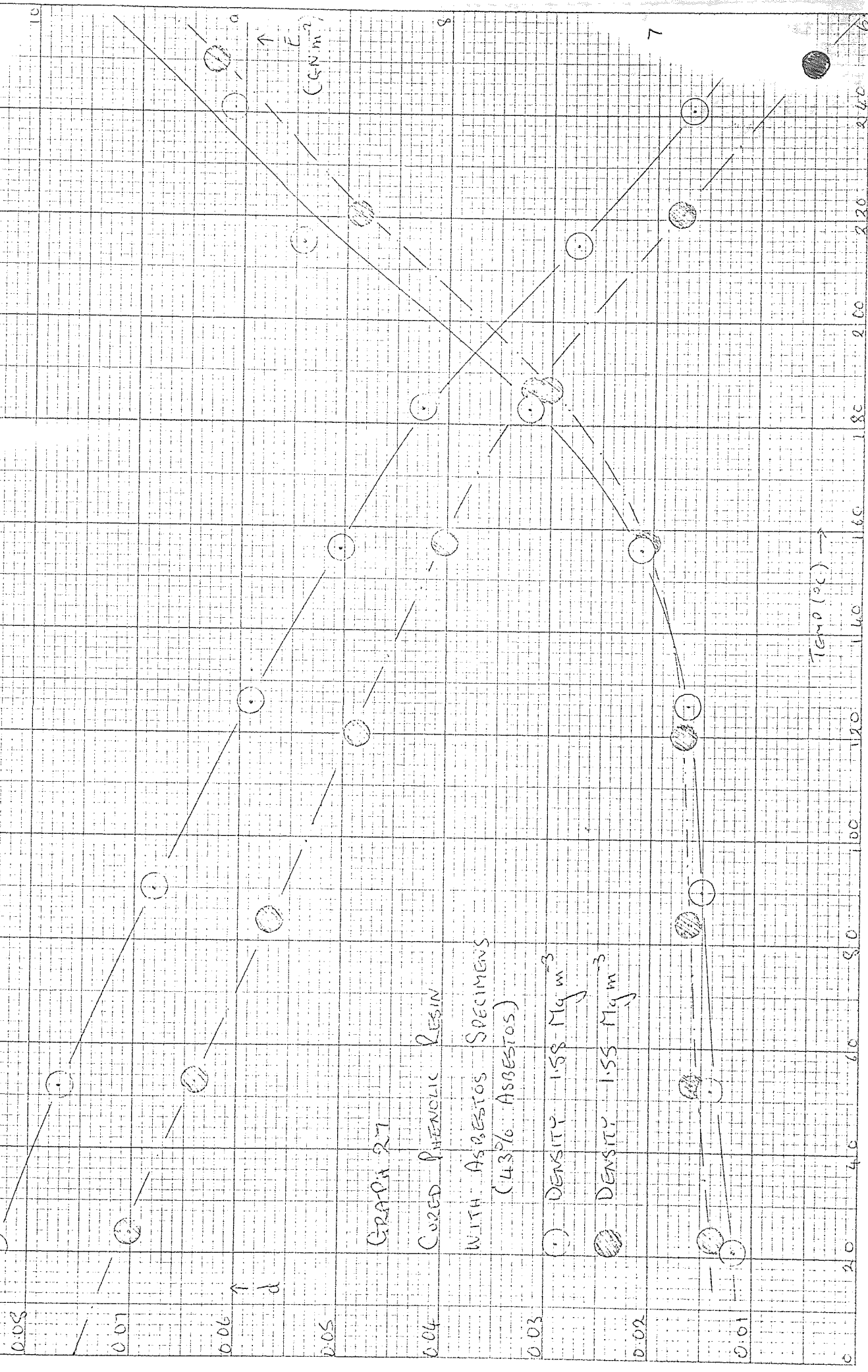
Temp (°C)

GRAPH 2

CURED PHENOLIC RESIN

WITH ASBESTOS SPECIMENS
(43% ASBESTOS)

DENSITY 1.58 Mg m⁻³

DENSITY 1.55 Mg m⁻³

GRAPH 25

CURED PHENOLIC RESIN
WITH ASBESTOS SPECIMENS
(57% ASBESTOS)

○ DENSITY 1·78 Mgm⁻³

◉ DENSITY 1·75 Mgm⁻³

Graph 29

Cured Phenolic Resin — Asbestos —

Metal Specimens

(P) Density 2.08 Mg/m³

(Q) Density 2.13 Mg/m³

Temp (°C) →

$\lambda \left(\frac{cal}{cm \cdot °C \cdot m^2}\right)$

0.01 0.02 0.03 0.04 0.05 0.06 0.07

20 40 60 80 100 120 140 160 180 200 220 240

GRAPH 30.

CURED PHENOLIC RESIN - ASBESTOS

BARYTES SPECIMENS

$\odot$ DENSITY. 1·92 $Mg\,m^{-3}$

$\odot$ DENSITY 1·90 $Mg\,m^{-3}$

E $(G N m^{-2})$

$\dfrac{dE}{dt}$

Temp (°C)

GRAPH 31

CURED PHENOLIC RESIN - ASBESTOS -

FRICTION DUST SPECIMENS

DENSITY 1·51 Mgm⁻³

DENSITY 1·50 Mgm⁻³

E (GNm^{-2})

Temp (°C) →

0·07

0·06

0·05

0·04

0·03

0·02

0·01

GRAPH 32   ANALYSIS OF PART OF A

TEST RUN BETWEEN BORTH, CARDIGANSHIRE
AND TYSELEY, BIRMINGHAM, INDICATING

THE VARIATION IN DISC TEMPERATURE.

DISC TEMP (°C)

360
340
320
300
280
260
240
220
200
180
160
140
120
100
80
60
40
20
0

46 47 48 49 50 51 52 53 54 55 56 57 58 59 60 61 62 63 64 65 66 67 68 69 70

MILES FROM BORTH

NEWTOWN

ABER MULE

LLANMULE

A 492
47 mph

A 483
41.6 mph

B 4368
34.1 mph
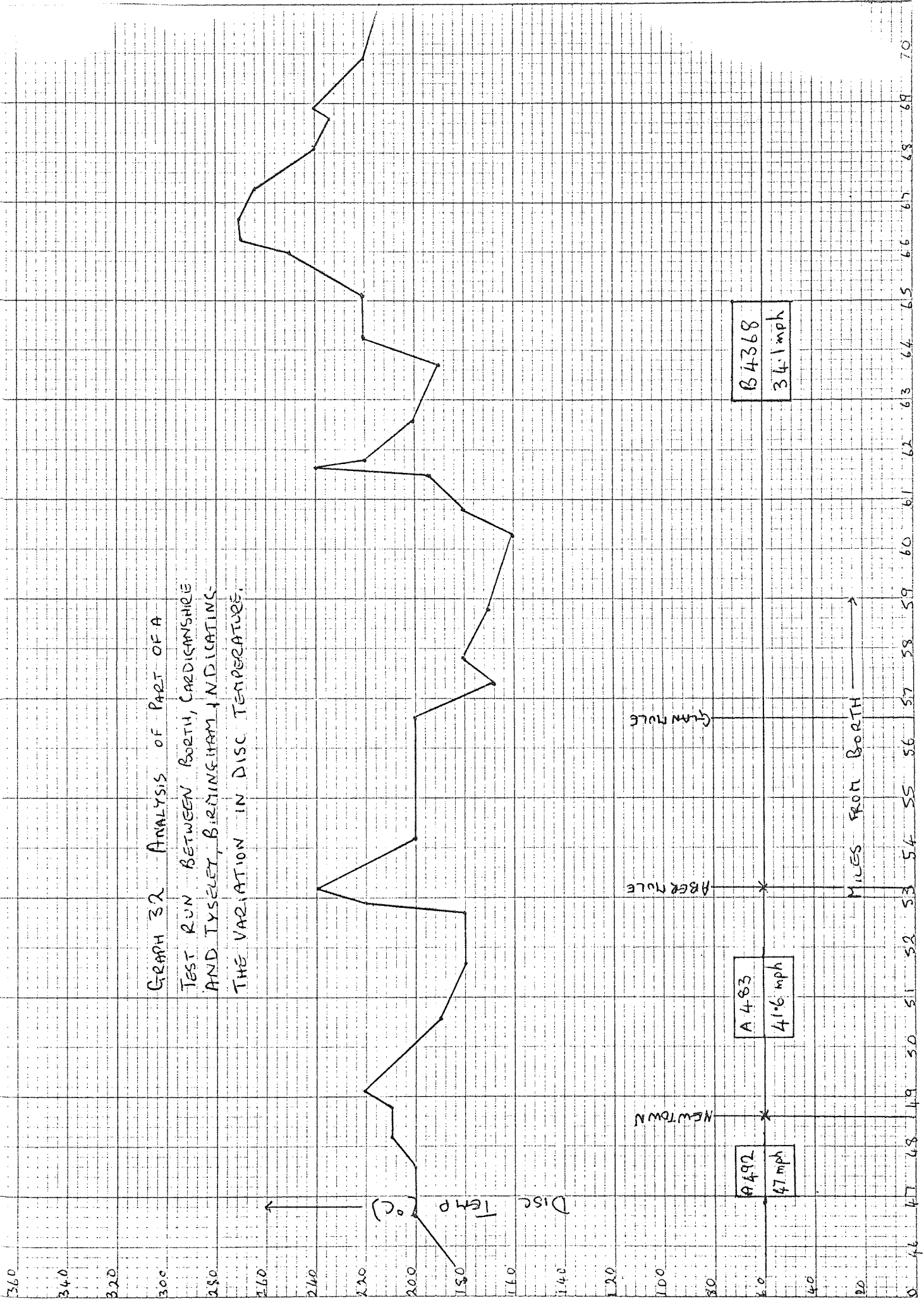
APPENDIX 3

The Dynamic Mechanical Properties of 7% Glass Filled Polypropylene

The dynamic mechanical properties of 7% w/w glass filled poly-propylene determined at high frequency could not be found in the available literature and so in order to check the accuracy of the values quoted in section 3.3.1.3. theoretical values have been determined from the literature available.

The theoretical value for the elastic component of the extensional modulus is determined by use of the law of mixtures

$$V_{pp}E'_{pp} + V_{gf}E'_{gf} = E'_{pp/gf}$$

where V_{pp} is the volume fraction of polypropylene = 0.974

V_{gf} is the volume fraction of glass fibre = 0.026

E'_{pp} is the elastic component of the extensional modulus of polypropylene = 1.7 GNm^{-2} (from ref.(70), using shock loading at 1 kHz at 20°C)

E'_{gf} is the extensional modulus of glass fibre = 74 GNm^{-2} (from ref.(95), method, frequency and temperature are not quoted but since glass is almost totally elastic conditions have little effect on the modulus value)

$E'_{pp/gf}$ is the elastic component of the extensional modulus of the polypropylene/glass fibre composite.

For a composite of polypropylene containing 7% glass fibre by weight

$$E'_{pp}/gf = 0.974 \times 1.7 + 0.026 \times 74 GNm^{-2}$$
$$= 3.68 \ GNm^{-2}$$

It is not possible to give an accurate estimate of the damping since this is extremely dependent on conditions and the nature of the polypropylene used. Factors affecting damping in this composite are;-

i) The degree of crystallinity.

ii) The manufacturing and moulding processes used.

iii) The quality of reinforcement.

The polypropylene used in the commissioning experiments was I.C.I. grade G.W.M. 22 which is the good quality, highly crystalline material with a density of 0.91 Mgm^{-3}. Much data regarding polypropylene damping is determined on less crystalline material which is not comparable. Flocke (96) gives the β peak maximum damping as 0.09 for a crystalline polypropylene (density 0.905 Mgm^{-3}) and 0.70 for an amorphous polypropylene (density 0.87 Mgm^{-3}). Heijboer (92) gives a value of 0.08 for the maximum damping of the β peak for a crystalline polypropylene giving an average for the two sources of data as 0.085. These values are determined at low frequency and so at higher frequencies higher values are expected.

The effect of adding 7% glass fibre would not be expected to alter the damping since glass has a very low damping but in practice the damping increases slightly due to imperfections in reinforcement.

In conclusion the values of damping given in table 6 will represent different positions on the β peak and not necessarily the maximum value and thus a value of about 0.085 is probably to be expected.

APPENDIX 4

Testing proceedure .

     i) Determine the value of f_n from the frequency meter at which the phasemeter is reading 90°. This value is used to calculate the elastic component of modulus.

     ii) Scan the tuner to a lower frequency at which the accelerometer signal voltage is at a minimum and adjust the oscillator amplitude control to bring this voltage to a reference value a_{ref} . Note the force signal voltage F_{max} and the frequency f_0.

     iii) From tables determine $F_{r.m.s.} = 0.707 F_{max}$.

     iv) Adjust the tuner and amplitude controls to find frequencies f_λ and f_1 above and below f_0 at which the acceleration signal is at the reference amplitude a_{ref} and the force signal is at amplitude $F_{r.m.s.}$. f_0, f_1 and f_λ are used to calculate the damping.

APPENDIX 5

Problems Encountered During Testing

Most of the problems encountered during testing have been mentioned elsewhere but table 24 is intended to bring the information together for fault finding purposes.

Table 24 Problems Encountered During Testing

Symptom	Cause	Cure
Equipment Problems		
Signal amplitude from the impedance converter on one channel falls considerably with respect to the other. The signal waveform also distorted over all frequencies	Battery in the impedance converter supplying less than 7V.	Replace battery.
Signal amplitude on one channel falls to zero.	F.E.T. transistor in the impedance converter damaged.	Replace F.E.T. transistor.
	Cable shorting signal to earth	Replace cable or repair connection.

Symptom	Cause	Cure
Signal on one or both channels superimposed on a low frequency hum.	Mains leads in close contact with signal leads.	Separate mains leads from signal leads.
Presence detected (see sect. 3.1.4.1) of spurious resonances which remain at constant frequencies.	Equipment component or joint resonating.	None unless a component has become loose and can be tightened.

Mounting Problems

Symptom	Cause	Cure
At elevated temperatures the modulus falls extremely rapidly and damping rises i.e. f_n decreases rapidly and f increases rapidly (this effect is much greater than that caused by transitions in the specimen)	Poor bond due to insufficient curing time, insufficient clamping pressure or failure to shake adhesive before use.	Rebond specimen to mounting stud.
Low value of f_n determined compared with similar specimens from the same material.	Specimen not in line with mounting stud.	Rebond specimen to mounting stud.

Symptom	Cause	Cure
Specimen Problems		
Presence detected (see sect. 3.1.4.1) of spurious resonances which appear at random frequencies.	Probably a flaw or a void in the specimen.	None, but sometimes shortening the specimen removes the problem.
Waveforms are distorted at resonance.	Harmonic distortion.	None, but sometimes shortening the specimen removes the problem.

BIBLIOGRAPHY.

1. T.P. Newcomb and R.T. Spurr, The braking of road vehicles, Chapman & Hall, Publishers.

2. R.D. Swinburn, Auto Design Engineering, November 1969 p.20.

3. R.A. Muzechuk, S.A.E. paper 670512.

4. Ferodo International Technical News.

5. R.L. Gatrell and T.P. Schreiben, S.A.E. 670511.

6. J.M. Herring, S.A.E. paper 670146.

7. M.G. Jacko et al, S.A.E. paper 680417.

8. T.P. Newcomb, Auto. Engr. 50, 1960, 288.

9. T.P. Newcomb, J. Mech. Eng. Sci., 2, (3), 1960, 167.

10. D.J.Evans and T.P. Newcomb, J.Mech. Eng. Sci.,3,(4), 1961,315.

11. F.W. Aldrich and M.G.Jacko, Berdix Technical Journal, Vol.2, No.1. Spring 1969, p.42.

12. R.T. Halstead, Paper Trade Journal, Vol.118, No.9.

13. A.A.Hodgson, "Fibrous Silicates" Lecture Series No. 4. R.I.C. 19.

14. J.R.Lynch, J. Air Poll. Cont Assn., Vol.18, 1968, p.824.

15. D. Rohrer, S.A.E. preprint, Presented at Cincinnati, Ohio, March 22, 1954.

16. M.G. Jacko, Calorimetry, p.289. Plenum Press, N.Y. 1968.

17. Cellobond, B.P. Plastics.

18. Friction Facts and Fundamentals, Rayestos-Manhattan.

19. J.A. Brydston, Plastics Materials, London, Iliffe Books Ltd. 1969.

20. N.J.L. Megson, Phenolic resin chemistry, Butterworths, 1958.

21. R.W. Martin, The Chemistry of Phenolic Resin. John Wiley, 1956.

22. R.H. White and W.T. Rust, J. Appl. Poly. Sci.,9, 777, 1964.

23. A.R. Spencer and W.M. Spurgeon, S.A.E. paper, 670081.

24. W.G. Carrol, B.Plast. Aug 1962, 414-417.

25. Carrol-Porczynski, Asbestos.

26. B.S. Gidvani, Plastics, November 1948, p. 541.

27. H. Beerer. B.Plast., May 1962, p. 146.

28. Materials Review - Friction Materials Design and Components in Engineering, June 24, 1965.

29. B.S. AU142: 1968.

30. "S.A.E. Handbook", Society of Automotive Engineers, N.T. 1966.

31. A.J. Bankman and F.H. Highley, S.A.E. Paper 670510.

32. A.E. Anderson et al, S.A.E. Paper 670079.

33. A.J. Wilson et al, The Engineer, Feb. 1968, p.317.

34. G.E. Fisher and J.C. Neerman, I and E.C. Product Research and Development, p.288.

35. R.L. Gealer and B.H. Biggers, S.A.E. Paper 670080.

36. G. Rappaport and G.C. Goldfinger, S.A.E. Paper 670514.

37. N.H. Wantrant and J.P. Bernard, S.A.E. Paper 680416.

38. A.R. Spencer et al, S.A.E. Paper 660412.

39. Lampargue, P.V., "Brake Squeak" Rpt. No 8500 B, published by The Institution of Automobile Engineers, Research and Standardisation Committee 1935.

40. H. Wogenfuhrer, Noise from Brakes, A.R.S. 1964, Vol.66, No 8, p. 217. M.I.R.A. Trans. No.15/65.

41. Chikamori, S., Mitsubishi Tech. Rev., 1968, Vol.5, No.1, p.35.

42. Yu I. Kosterir and I.I. Vasiler, Autom. Prom. 1962, No 12, p.21 M.I.R.A. Trans. 50/63.

43. H.R. Mills, I.A.E. Res.Rpt., No.9000 B, Oct. 1938.

44. H.R. Mills, I.A.E. Res. Rpt. No.9162 B, Sept. 1939.

45. Hollman, A.T.Z., March 1954, Vol. 56, No.3, pp.65-67, M.I.R.A. Trans. 16/54.

46. R. Spurr, I. Mech. E. Auto. Dir. Proc., No.1, 1961/63, pp.33, Discussion p.41.

47. R.P. Jervis and B. Mills. I. Mech. E. Vol. 178, Pt. 1, No. 32, 1963/64. p.847, Discussion p. 857.

48. S.W.E. Earles and G.B. Soar. Inst. Mech. Engrs. C101/71.

49. M.R. North, M.I.R.A. Bulletin, No. 4, 1969.

50. R.T. Spurr. Inst. Mech. Engrs. C95/71.

51. R.A.C. Fosberry and Z.Holnbecki, M.I.R.A. Rept. 1957/3.

52. R. Busford and S.B. Twiss, Pt.II, A.S.M.E., Trans. Vol.80, 1958, p.407.

53. E.J. Miller, S.A.E. Paper 690221.

54. R.A.C. Fosberry and Holnbecki, M.I.R.A. Rept., 1955/2.

55. R.A.C. Fosberry and Z. Holnbecki, M.I.R.A. Rept. 1959/4.

56. J.E. Gieck, S.A.E. Paper 650488.

57. B.R. Teitelbaum et al, S.A.E. Paper 650488.

58. Chiku et al, Journal of the Society of Automative Engineers of Japan Inc. 21,2 (1967).

59. Ferodo ITN, Squeal in drum brakes.

60. R.A.C. Fosberry and Z Holnbecki, M.I.R.A. Rept. 1961/2.

61. H.R.Mills, M.I.R.A. Bul. No. 2, 1949.

62. Mintex Technical Service Bulletin, Tech/13, July 1966.

63. R.A.C. Fosberry and Z. Honbecki, M.I.R.A. Bull. No.2, 1960, p.12.

64. Groom,1925, British Patent No. 254561.

65. R.A.C. Fosberry and Z. Holnbecki, M.I.R.A. Rept. 1957/1

66. Alexandrov and Lazurkin, Zh.Tekh. Fiz., U.S.S.R., Vol.9, 1939, p. 1249.

67. G.C. Karas and B. Warburton, British Plastics, March 1961 p.133.

68. F.R. Eirich Ed., Rheology, Theory and Applications, Academic Press, N.Y. 1956.

69. A.G. Fredrickson, Principles and Applications of Rheology, Prentice Hall Inc. 1964.

70. B.J. Lazan, Damping of Materials and Members in Structural Mechanics, Pergamon Press 1968.

71. J.D. Ferry, Viscoelastic Properties of Polymers, John Wiley & Sons, Inc., N., 1961.

72. H. Leaderman, Proposed Nomenclature for Linear Viscoelastic Behaviour, Trans. Soc. Rheology 1,213-222 1957.

73. H. Kolsky, The Mechanical Testing of High Polymers, Progress in Non-destructive Testing, Vol,2. p.29 1960.

74. P.I. Vincent, Mechanical Properties of High Polymers; Deformation, Physics of Plastics, Ed. P.D. Ritchie, Iliffe Books Ltd, London, (for the Plastics Inst.) p. 24ff.

75. L.E. Nielson, Rev Sci, Inst. Vol 22, p. 690, 1951.

76. A.R. Payne & J.R. Scott, Engineering Design with Rubber, Mclaren & Sons Ltd., London 1960, p.92.

77. L.T. Muus et al S.P.E.J., Vol 15, p. 368, 1959.

78. K.M. Sinnott. J. Appl. Phys. Vol. 29, p. 355, 1959.

79. G.W. Trayer & H.W. March. Rept. No. 334. National Advisory Committee for Aeronautics.

80. D.L. Smith et al J.Phys. E. Scientific Instr. Vol.3, p.715 1970.

81. A. Barone & A. Giacomini, Acustica Vol.4, p. 182, 1954.

82. E.B. Atkinson & R.F. Eagling, Silver Jubilee Symp. of the Plast. & Poly Group of tje S.C.I. April 1958.

83. S. Strella, A.S.T.M. Bul. (TP. 105) May 1956, p. 47.

84. S. Newman, J. Appl. Po. Sci. Vol.2, p. 333, 1959.

85. D. Bancroft & R.B. Jacobs, Rev. Sci. Instr. Vol.9 p. 279, 1958.

86. P.G. Bordoni, J. Acoust. Soc. Amer,. Vol.26, p.495, 1954.

87. J.W. Ballov & S. Silverman, J. Acoust. Soc. Amer. Vol.19, p.113 1944.

88. K.W. Hillier, Proc Phys. Sc. Vol.B64 p. 998, 1951.

89. D.G. Ivey et al, J.Appl. Phys. Vol.20, p.486, 1949.

90. A.W. Nolle & P.Sieck, J. Appl. Phys. Vol. 23, p.888, 1952.

91. G.W. Van Santen, Mechanical Vibration Philips Technical Library,
    p.23 1961.

92. J. Heijboer, Br. Polym. J. Vol.1, p.3 1969.

93. S. Haig, B.Sc. Thesis Aston.

94. G. Bowsher, Internal Rept. Girling Ltd., June 1965.

95. Oleesky & Mohr, Handbook of Reinforced Plastics, Rheinhold N.Y. 1964.

96. H.A. Flocke Kolloidzeitschrift, Vol.180, p.118, 1962.